Flexural Behavior of Reinforced-Concrete Slabs with Generalized Edge-Conditions

A PhD Thesis

Submitted in Fulfillment of the

Requirement for the Award of the Degree of

DOCTOR OF PHILOSOPHY

By

Harvinder Singh
Roll No. 90602501

Under the Supervision of

Dr. Maneek Kumar
Professor & Head,

Dr. Naveen Kwatra
Associate Professor,

Department of Civil Engineering,
Thapar University,
Patiala

DEPARTMENT OF CIVIL ENGINEERING,
THAPAR UNIVERSITY,
PATIALA-147001
PUNJAB, INDIA.

2010

CERTIFICATE

Certified that the work presented in the thesis entitled *"Flexural Behavior of Reinforced-Concrete Slabs with Generalized Edge-Conditions"* which is being submitted by *Mr. Harvinder Singh* in fulfillment of the requirement for the award of degree of Doctor of Philosophy in the Department of Civil Engineering, Thapar University Patiala, is an authentic record of the candidate's own work. This research work has been carried out by the candidate during a period from January 2007 to January 2010 in this university under our supervision. The matter presented in this thesis has not been submitted for the award of any other degree in any University.

4/5/12

Dr. Maneek Kumar
Professor,
Department of Civil Engineering,
Thapar University, Patiala (Pb).

1/5/12

Dr. Naveen Kwatra
Associate Professor,
Department of Civil Engineering,
Thapar University, Patiala (Pb).

4/5/12

Dr. Maneek Kumar
Head,
Department of Civil Engineering,
Thapar University, Patiala (Pb).

ACKNOWLEDGEMENT

Time has provided me the great opportunity to express heartful gratitude to my supervisors, Prof. (Dr.) Maneek Kumar and Dr. Naveen Kwatra. Their meticulous guidance, constructive criticism, and constant encouragement along with affectionate attitude have helped me to complete the research work and give it a shape of this thesis.

I own my deepest gratitude to Prof. (Dr.) Rafat Siddique, and Dr. Kulbir Singh for taking the keen interest in the progress of the work since its inception and helping me in improving the quality of the work at all stages.

I am deeply indebted to my Alma matter: Guru Nanak Dev Engineering College, Ludhiana for providing me all facilities as required from time to time. The cordial family atmosphere at the Department of Civil Engineering of the college has been instrumental in the smooth completion of this work. The cheerful support of all my colleagues and laboratory staff is appreciated from the bottom of my heart.

The financial help from the *All India Council for Technical Education, New Delhi* vide file no. 8023/BOR/RID/RPS-56/2007-08 dated 05/03/2008 is greatly acknowledged.

The supplementary grant from the *Consultancy & Testing Cell* of the Guru Nanak Dev Engineering College, Ludhiana for setting up a heavy testing laboratory at the department for conducting the experimental investigations vides sanction no. 166/A/Const./D.F./186 dated 6/5/2008 is also greatly appreciated and acknowledged.

It is an honor for me to express my gratitude to *M/s MRH Associates, Ludhiana* and *ACC CEMENT LTD* for providing the financial help for the purchase of material (rebars and cement respectively) during the experimental investigations. This help is greatly appreciated and acknowledged.

Finally, yet importantly, I would like to express my deep sense of gratitude, indebtedness to All, and One who remained behind the screen and has made His support available in the number of ways; in one form or another; right from day one, and without His blessing, nothing is possible to achieve....

Harvinder Singh

Harvinder Singh

ABSTRACT

Slab is the most widely used structural element. It is used almost in every type of structural system to build and/or enclose the space along with some other structural elements such as walls, columns etc. However, unlike other structural elements, a slab is highly redundant in nature due to the coupling of the internal stress resultants and consequently offers multiple load paths to the applied loading. Because of coupling of internal force-resultants, the structural behavior of the slabs is highly sensitive to the type, layout of the supporting system and/or stiffness of the supporting structural member(s). Any change in the physical parameters of the supporting systems will cause a considerable change in the moment-field induced in the slab under given loading conditions.

The moment coefficients recommended by the design code [*IS 456 (2000)* and *BS EN 1992-1 (1994)*] are applicable only for the rectangular slabs with various end-restraints and supported over the non-yielding edges on the outer four edges. But in routine design practice, number of case are encountered by the designers whereby the beam-drop and the beam-spans are restricted by architects to a level that are not sufficient to provide a non-yielding edge at the outer boundary of the slab and as such, these coefficients predict the moment-field highly on the unsafe side and produce a structurally deficient slab section.

In the present thesis, an analytical model has been developed for a rectangular slab-system resting over the non-yielding edges at its outer boundary and cast monolithic along with equally spaced internal shallow beams using the principle of the limit analysis. It can also be used for predicting the collapse load of skew slabs, design of multi-panel slabs but it must be supported over the equally spaced shallow beams along one direction and non-shallow beams at regular intervals along the other direction of the slab. The slab is subjected to an out-of-plane uniform area load acting over its entire surface thereby providing an alternative solution to the finite element based software for the analysis of the slab-system supported over the internal beams incapable of providing a non-yielding edge to the slab panels. It will supplement the design guidelines recommended by various codes which allow that any procedure can be used for designing a slab-system that satisfy the conditions of equilibrium, geometric compatibility and the requirements of strength, and serviceability stipulated by design codes. However, the proposed model can only be used to satisfy the strength criterion

enshrined in various design codes and serviceability criterion has been kept in scope for future studies. This model will also provide an alternate method to finite element procedures which is a costly, time consuming process for proportioning regular slab-systems.

The results from the proposed analytical model and the design equations are validated experimentally in the laboratory. These are also compared with the results from the well-established literature on the slab analysis and are found to be in good agreement.

The actual crack pattern at the collapse load, for the two and three-panel slabs tested in the laboratory, was found to be in good agreement with the analytical results. A non-dimensional parameter called as moment-manipulator, λ (= moment of resistance of beam/moment of resistance of beam required for the simultaneous formation of a global and a local collapse mechanism) has been proposed to distinguish the nature of the shallow beams. Test slabs designed using the λ-value less than unity failed following a global-collapse mechanism with a load factor of more than 1.40. However, these slabs show more deflection at the design load than the permissible values but selecting a highest possible value of the beam depth satisfying both the serviceability criterion as well as the *span/depth* ratio of the shallow beam can reduce the actual deflection of the slab system under the design load. It is suggested that the actual slab-beam system with shallow beams should never be proportioned with λ-value more than unity as it leads to failure of the slab in a local-collapse mechanism with a reduced load factor.

The test slabs designed for λ-value more than unity, and supported over the shallow beams failed following a local-collapse mechanism with a load factor ranging from 1.30 to 1.40, with the formation of negative yield lines near the beam-ends. At the design load, these slabs show a reduced deflection in comparison to the slabs designed for λ-value less than unity but this value of the deflection was more than permitted by the design codes. Therefore, it is suggested that the actual slab-beam system with shallow beams should never be proportioned with λ-value more than or equal to unity.

Working procedure is illustrated with the help of design examples. It is shown that with the use of shallow beam in the slab-systems, the unit cost of the material-consumption comes out to be nearly same but the beam-drop of the supporting beams along the short span of the slab-beam system reduces by about 40-50% in comparison to the slabs supported over the non-shallow (rigid) beams.

CONTENT

LIST OF TABLES

LIST OF FIGURES/GRAPHS

CHAPTER-1

OVERVIEW

1.1 INTRODUCTION

Slab is the most widely used structural element. It is used almost in every type of structural system to build and/or enclose the space along with some other structural elements such as walls, columns etc. However, unlike other structural elements, a slab is highly redundant in nature due to the coupling of the internal stress resultants and consequently offers multiple load paths to the applied loading. Because of coupling of internal force-resultants, the structural behavior of the slabs is highly sensitive to the type, layout of the supporting system and/or stiffness of the supporting structural member(s). Any change in the physical parameters of the supporting systems will cause a considerable change in the moment-field induced in the slab under given loading conditions. Removal of even a single support will lead to a considerable change in the behavior of the slab. In addition, alternation in the depth of the supporting beams cause a significant change in the moment-field in the slab panel.

Most of the available literature and the design codes fail to handle this aspect of the problem. The moment coefficients suggested by the various codes *viz*: *IS 456 (2000)* and *BS EN 1992-1(2004)* are applicable only for the rectangular slab with different aspect ratio and edge-conditions, wherein the slab panel is assumed to be supported on the non-yielding supports on its four sides. But in routine design practice, number of case are encountered by the designers whereby the beam-drop and the beam-spans are restricted by architects to a level that are not sufficient to provide non-yielding edges to the slab and as such these bending coefficients predict the moment-field highly on the unsafe side and produce a structurally deficient slab section. This design procedure may be appropriate for many situations, but in many others, it leads to wasteful overdesign or, perhaps worse, underdesigns.

The current state-of-art available for the design of reinforced concrete slabs do not satisfactorily address the problem of proportioning slabs cast monolithic with shallow-beams [*Wood (1961), Johansen (1967), Jones (1967), Jones and Wood (1967), Shukla (1973) and Park and Gamble (2000)*]. A beam that fails to provide a non-yielding edge to

the any other structural member is called as a shallow-beam otherwise it is called as a non-shallow beam. In most of the literature, design methods have been suggested based upon the results of an extensive series of tests and well-established performance record of various slab systems [*Sozen et al. (1963), Park (1968), Gamble et al. (1969), Park (1971) and Gamble (1972)*]. In these experimental investigations, most of the researchers have concentrated their work on the performance of single panel rectangular slabs resting over the non-shallow beams at their outer four edges. Slab and the supporting beams have been proportioned by distributing the total static moment; suggested by *Nichols (1914)* to the slab system. *Sozen et al. (1963)* have studied the behavior of beam supported multi-panel floors. Based upon these test results, empirical relations and some factors have been suggested for apportioning the total static moment to the slab and its supporting beams and/or column strip for the satisfactory performance. Most of the design guidelines recommended by various codes are based upon these empirical results and performance record of various slab-beam systems. Due to this, the procedure recommended by most of the codes; *ACI 318 (2008), IS 456 (2000), BS EN 1992-1 (1994) and CSA A23.3 (1994)* has number of inherent limitations in the form of assumptions, which are mandatory to be satisfied by all panels of the slab for the satisfactory performance; thereby, forcing the designers to proportion the slab-system within the domain of these limitations which sometimes fail to satisfy the architectural and other design constraints. It forces the designers to use beams with a lesser value of *span/depth*-ratio.

IS-456 (2000) offers very limited scope for the design of flat slabs supported generally without beams, over the columns with or without flared column head. The designer is forced to use either *direct design method* or *equivalent frame method.* The former method presumes a minimum of three equal rectangular panels (with a prescribed range of variation in the span and loading) to ensure that the design moments obtained from the empirical relations [mostly based upon the studies of *Gamble et.al. (1969)*] should not differ significantly from those obtained by an elastic analysis. The procedure recommended by this code for transverse distribution of moments to the middle and the column strips is identical in both methods. However, the final design using these two methods is not economical, if the column spacing is very large or load magnitude and/or variation of load in the adjacent panels of the slab is very large or when the basic prerequisite assumptions do not match with the design-constraints imposed by the field requirement/client. However, some international codes such as *CSA A23.3 (1994)* and *ACI 318 (2008)* recommend a generalized design procedure for the two-way slab systems.

The design coefficients and the procedure recommended by these codes are based upon the same empirical relations. These empirical relations have been obtained from the full scale testing of the slab panels and their subsequent satisfactory field performance.

1.2 HISTORICAL DEVELOPMENT

A slab or a plate is a two-dimensional straight (horizontal/inclined) structural member that receives the load normal to its surface and transfers the same to its supporting edges through bending, shear and twisting. Because of the coupling of these force resultants, the slabs are highly indeterminate and very sensitive to the edge-conditions. Due to a highly indeterminate nature, the rigorous elastic solutions are not available for many practically important edge-conditions. Various researchers across the globe tried their best to describe the behavior of the plates/slabs of various shapes and edge conditions for different load types. Numbers of analytical investigations are reported in the literature to describe the behavior of slabs. Most of these studies had attempted to formulate expressions based upon elastic theory of plates; boundary element method, finite element method etc, but these expressions are mathematically too cumbersome that these rarely find applications in routine design office jobs. The important milestones in historical development of the plate/slab analysis are described in this section. The observations from this study are given in *italic font* at the end of each evolution period.

Lagrange (1811) has formulated a governing differential equation for the plate bending problems in the early 1800's. The solution to these bending equations has been presented by *Navier (1820)* to the French Academy using the double-trigonometrical series for a number of loading conditions. *Navier (1820)* has also suggested a solution to the thin rectangular elastic plates supported over the non-deflecting panel boundaries.

Unknowing the earlier work of *Lagrange, Kirchoff* independently developed the differential equations for the bending of thin elastic plates in 1850. The solution to these equations was later provided by *Levy (1866)* using the 'separation of variable technique' after modifying the method suggested by *Navier*. Using the Fourier series and neglecting the Poisson's effect, *Lavoinne (1872)* provided a solution for the uniformly loaded infinitely large plate with rectangular support layout. *Grashof (1878)* suggested a solution to the basic plate equation using the polynomial approximations for the displacement function considering the Poisson's effect but failed to satisfy some important boundary conditions.

By the same time, different persons developed a number of thumb rules / empirical methods based upon the field performance studies conducted on the slabs. Patents were issued for the 'reinforced slab design' as early in 1854 based upon the concept of concrete acting as an arch and with the reinforcement in the slab acting as a tie and then in 1867, based on the caternery action of the reinforcement and concrete in the slab section just acting as a filler material.

In 1914, *Nichols* established a single criterion for the minimum total moment that must exist across the critical section of a panel to satisfy the equilibrium conditions. This paper received a lot of criticism from the building industry. The moments predicted from this method were significantly higher than the moments used in the number of successful slab designs.

It was during this period of controversy that a committee was formed by the USA government to draft the codal provisions for the design of reinforced concrete slabs. The recommendations of this committee were entirely based on the work of *Westergaard and Slatter,* who had made an extensive examination of all previous works. The first slab provisions appeared in 1921 in two parts. The first part was placed in the body of the design code and presented the design coefficients for two-way rectangular slab panels supported over the stiff beams at its outer boundary. The second part was placed in the appendix of the design code that deals with the design of the flat slabs. These slab provisions were based on the work of *Nichols* but the committee influenced by the success of early slab-construction by the use of empirical methods has recommended the total design moment in the design guidelines as low as 72% of that required by *Nichols's method*. These provisions remained unchanged for the next half-century.

During the same time, *Lewe (1921)* and *Rankine & Grashoff (1924)* suggested a new approach by conceiving the slab panel as consisting of a number of intersecting wide beams along the two orthogonal directions. They provided a solution to the complex behavior of the slab by satisfying the compatibility-conditions of these two intersecting beams. Later on, *Murcus (1930)* suggested a modified solution considering the *torsional effect* in the slab arising due to the bending of the two orthogonal strips. The results from this approximate method compare favorably well with the more accurate solutions suggested by *Kirchoff, Navier* and *Levy* based upon the elastic theory of plates.

To sum up the earlier work it can be stated that the *classical plate theory is ideally suited for the analysis of rectangular, circular shaped slabs only, and it is mathematically very cumbersome to apply in case of other shapes. Various mathematicians have worked*

out classical solutions for other different shapes, but these works are very complicated and are not of immediate use to the average designer in a routine design practice.

During the same period, some alternate concepts were also tried by a number of researchers all over the world to overcome the mathematical difficulties associated with the elastic methods. One such concept, which attracted the maximum attention, was to compute the collapse load of the slabs with different edge-conditions. As a result, *Tresca* laid the foundation of the theory of plasticity in 1868. However, this theory attracted serious attention of the researchers only after the work of *Prager, Hodge et.al.* was published in 1951. The ultimate load analysis based on such theory has indicated that the exact solution for the plates is not as difficult as appeared after establishment of the methods based upon elastic theory of plates. In general, the collapse load computed for any edge condition of the slab always lies between the two bounds-*the lower bound and the upper bound* depending upon the approach used and a rigorous solution of a particular plate should always attempt to make the computed collapse load to converge to an exact solution.

The yield line theory was innovated by a Danish engineer, *Ingerslav (1923)* based upon the earlier work of *Tresca.* It was greatly extended and advanced by *Johansen (1943).* The work in the UK by *Wood (1961)* and *Jones (1967)* brought this method into the focus of English-speaking countries.

Although considerable work has been done on this theory to predict the collapse load for different standard cases, no attempt was made to generalize this concept that should be capable to predict the collapse load for a composite system like slab-beam system; arbitrarily shaped slab panels; different loads and effect of openings in the slabs etc. Moreover, this method expects a considerable judgment and intuition from the user in finding the true collapse load and for tracing of the yield line pattern as the load predicted by this method is always an upper bound to the true value.

Considerable efforts were made by *Hillerborg (1956)* of Sweden to overcome this problem associated with the upper bound principle. He studied the previous work done by *Lagrange, Kirchoff, Navier, and Rankine et.al.* and presented a lower-bound approach to predict the collapse load of the slabs by considerably simplifying the theory of elasticity and plasticity. He suggested a procedure for reinforcing the slab in an appropriate manner to efficiently transfer the loads to the supports but in this process, considerable redistribution of moments takes place in the slab that requires the availability of adequate

rotation capacity. Therefore, he advised its users to follow the elastic moment diagram in locating the load strips as accurately as possible.

Therefore, this theory also expects its users to be highly imaginative and intuitive who should be capable of imagining the possible elastic-load-path in deciding upon the possible load-strip. Otherwise, the reinforced concrete slab will undergo a considerable redistribution of the moments and may in the process produce considerable serviceability problems like excessive cracking and displacements.

The invention of computing machines in early1950's and its subsequent availability to the research workers in early 1960 paved a new way in the development of analysis tools for the slab analysis. A number of algorithms and numerical techniques were developed for the plate analysis based upon the available analytical models derived using the elastic and plastic theories but most of these try to optimize one or other parameter influencing the plate behavior. The most significant outcome in this series was the development of finite-element approach (1960), the success of which depends much on the skillful use of computers and efficient numerical techniques. Using finite element analysis, structural systems having any complex shape and hybrid materials can be analyzed very easily in the linear as well as non-linear range of both geometrical and material behavior.

Now a day, a number of numerical techniques are available for the analysis of elastic and nonlinear continuum based upon the finite-element approach. A number of general-purpose commercial software's are available for the analysis of structural system both in linear and non-linear range of the material and geometrical behavior. Moreover, all these software are capable of handling the material as well as the geometrical non-linearity but *all of these expect a lot of precision from its users in the data preparation, interpretation of the output data along with a sufficient expertise to judge the accuracy of the output-results. Processing-time by the software may vary from few minutes to number of hours depending upon the type of problem. However, high cost of these proprietary products acts as a big hindrance in their routine applications in average design offices.*

1.3 OBJECTIVES

Keeping in mind the limitation and constraints of various theories and design guidelines available in the published literature, this thesis attempts to present an analytical model that can be used to find the moment-field induced in a slab-system cast along with generic internal beams and would supplement the strength-criterion recommended by various design codes and provide an alternate solution to the finite-element based design for the

regular slab systems meeting the constraints of the method. It has been developed using the principle of limit analysis with following aims and scope of investigations.

1.3.1 Aims of investigations

1. To develop an analytical-model for predicting the flexural behavior of the rectangular reinforced concrete slab cast monolithic along with equally spaced internal generalized beams and/or supports and resting over the non-yielding supports at the outer boundary. A generalized beam is a flexural member that can be made to behave as a rigid-edge/non-yielding edge or as a flexible-edge by a suitable selection of some beam-parameter.

2. To suggest a modified design-approach for the reinforced concrete slab cast monolithic with the equally spaced internal generalized beams and/or supports.

3. To conduct a full scale experimental testing of the slab-panels designed using the proposed approach for verification of the proposed model and subsequent interpretation.

1.3.2 Scope of the work

1. An analytical tool will be developed for a reinforced concrete rectangular slab without any openings, and subjected to the out-of-plane uniform area load over its entire top surface. This model can also be used for predicting the collapse load of skew-slabs.

2. The proposed model will predict the most probable yield line pattern at the ultimate state and the corresponding collapse load and/or the collapse moment. The effect of the punching and the shear in the slab will not be considered in the study.

3. To decide upon the beam-parameter that distinguishes the flexible-edge from the rigid-edge; *e.g.* rigid-edge as in case of the wall-supported slab and the flexible-edge, when the slab-panel deflects along with the internal support/beam(s).

4. To develop simplified design-aids for these types of reinforced concrete rectangular slabs subjected to the under uniform area load over its top face and with any number of internal panels, and aspect ratio of the slab.

5. Experimental-validation of the analytical results on the full scale testing of the slab specimens. In this part of study, reinforced concrete rectangular slab-panels supported over the non-yielding edge on all the four sides and divided into a suitable number of internal panels with in-built beams will be tested to the collapse. Number of slab-specimens to be tested will be taken as per the requirement of the model/ analytical results.

1.4 OUTLINE OF THESIS

Keeping in view the above objective, the thesis is divided into six chapters, which may broadly be grouped into the two parts. Part-1 of the thesis comprises the chapter-1 and the chapter-2; Part-2 of the thesis comprises the chapter-3 to chapter-6.

Chapter-1 deals with the historical development of various techniques used in the analysis of slabs. Thereafter the objectives of the research work are outlined. Chapter-2 presents the review of the current research in the field of the slab analysis and outlines briefly the procedure for the limit analysis of structural arrangement in general and the slab-system in particular. It also presents various techniques used for locating and tracing of the yield line pattern of a slab panel with various edge conditions subjected to the lateral loadings.

Chapter-3 describes the development of the analytical model, its assumptions and the results from the proposed analytical model.

Chapter-4 presents the results from an experimental study conducted on the full-scale slab-specimens to validate the results from the analytical model. It also describes the comparison of the results from the proposed model with the results obtained from the various analytical expressions available in the published literature.

The modified design procedure for a slab supported over the non-yielding edges at the outer boundary and cast monolithic along with the equally spaced generalized beams is presented in the Chapter-5.

Chapter-6 concludes the study. The symbols wherever have been used are explained at the place of the use itself. And all chapters of the thesis are written in a manner that reader need not to refer to the earlier chapters and the minimum information required for understanding of a concept is briefly outlined in the chapter itself.

1.5 INNOVATIVE ASPECTS OF RESEARCH

The thesis contains only the unpublished material or partially the material that has been recently presented at conferences, published in the journals by the author in different form. Therefore most of the concepts, analytical expressions and experimental results are new, fresh and unpublished.

CHAPTER-2
LITERATURE REVIEW AND LIMIT ANALYSIS

2.1 GENERAL

The main aim of structural engineer is to suggest a safe and economical structural system. Safety not only implies resistance to the external actions, but it also concentrates on the ductility and robustness of the system. The collapse of any structural system should be preceded by a perceivable deformation and in case of failure; the damage should not extend to the whole structure. A limit state is a state of impending failure beyond which a structure ceases to perform its intended function satisfactorily in term of either safety or serviceability. Accordingly, two types of limits- *limit state of collapse* and *limit state of serviceability* are proposed by most of the design codes that any structural system must fulfill for the satisfactory performance. The former limit deals with the strength, buckling, sliding/overturning etc whereas the later limit deals with the discomfort to occupancy and/or malfunction caused by the excessive deflection, cracking, and vibrations, or the loss of durability etc.

Limit Analysis is a powerful tool for modeling the structural behavior at the ultimate state and gaining an understanding of its safety. In this approach, materials with sufficient ductility are considered such that the stress redistribution required by the plastic theory can occur. Although the plain concrete is not a particularly ductile material but it can be made to behave as a sufficiently ductile material by carefully selecting material properties and proper detailing of the reinforcing steel. The ductile behavior of reinforced concrete has been demonstrated by decades of testing of large-scale concrete specimens. Moreover, the limit analysis tries to establish the ultimate limit state of a structural system by exploring the inherent reserve strength laying in the system beyond the elastic range by designing the section sufficiently ductile to enable it to behave in the rigid-perfectly-plastic range.

The first attempt in this direction dates back to the 1868, when *Tresca* laid down the foundation of the theory of plasticity. The theory of plasticity was established on the sound basis only in 1950s, when the work of *Prager, Hodge et.al.* was published in 1951 deviating radically in its approach from the theory of elasticity. The transition between the two theories was smoothened by considering the elastic-plastic behavior. However,

the complexity of the elastic-plastic analysis and the problems related to the identification of the real state of stress in a structure were remains largely of academic interest. In practice, the theories of elasticity and plasticity are used independently and with different purpose; the serviceability limit states of any structural system are checked based on the theory of elasticity whereas the design of the structural system are based upon the theory of plasticity.

The ultimate load analysis based on these theories indicates that the exact solution for the slabs/plates is not as difficult as appeared after the establishment of the elastic methods. In general, the computed collapse load of any plate with any edge conditions always lies between the two bounds- *the lower bound* and *the upper bound* depending upon the approach used. A rigorous analysis of a particular plate/slab should attempt to make the computed collapse load of the system to converge to an exact solution. These theorems of limit analysis are credited to *Gvozdev*, *Hill* and *Drucker, Greenberg and Prager*. The applications of this approach to the reinforced concrete were mainly attributed to *Thurlimann* and his students in Zurich, and to *Nielsen* and his coworkers in Denmark [*Baker (1961)*].

The yield line theory was innovated by a Danish engineer; *Ingerslev (1923)* based upon the earlier work of *Tresca.* It was greatly extended and advanced by *Johansen (1943).* The work in the UK by *R.H. Wood* and *L.L. Jones (1967)* brought this method into the focus of English-speaking countries.

Significant literature is available with regards to the analysis of the slabs supported over the non-yielding edges and /or beams at its outer boundaries. The results from the analytical as well as numerical studies are available for these types of slab panels. A brief review of the same is presented in this chapter. It also summaries the fundamentals of limit analysis of reinforced concrete slab that consists in determination of the most critical failure mechanism and the corresponding collapse load of the slabs at ultimate state.

2.2 LITERATURE REVIEW

Most of the available literature for the slab/plate analysis is well compiled in the form of books [*Timoshenko and Krieger (1959), Wood (1961), John and Wood (1967), Johansen (1967), Gallanghar and Zienkiewicz (1973), Shukla (1973), Hemp (1973), Zienkiewicz (1977), Park and Gamble (1980), Purushothaman (1984), Philip (1985) and Szilard (1985)*]. The classical work in the development of the theory of elasticity by *Lagrange, Navier and Kirchoff et.al* is well documented [*Timoshenko and Krieger (1959), Wood*

(1961), Park and Gamble (1980), Purushothaman (1984) and Szilard (1985)]. These works present a comprehensive review regarding the development of various methods for the slab analysis. Generally, the rectangular and circular slabs supported over the non-yielding supports on all the four sides were considered in their presentation subjected to the standard loads such as uniformly area load, point load and varying loads etc. *Timoshenko and Krieger (1959)* presents elastic-solutions for the analysis of plates of various standard shapes such as rectangular, circular, triangular with various edge conditions *viz:* simply supported or clamped or free or a combination of these standard constraints. *Purushothaman (1984)* provides a good coverage regarding the structural aspects of the slab behavior, its analysis and the design. He based his work on the earlier developments in the slab analysis techniques. Both elastic and plastic methods were presented in his book for the slab analysis and design. *Park and Gamble (2000)* presented the evolution of various analysis techniques for the reinforced concrete slab since 1850. The evolution of the flat slabs from the beam-supported slabs, its analysis and design and the technical basis for choosing an appropriate slab-system is well presented. He also based his work on the elastic and the plastic methods available earlier. *Szilard (1985)* and *Wood (1961)* present various numerical techniques available for the slab or plate analysis. They also give a good coverage regarding the elastic and plastic solutions for the slab of standard shapes (mainly rectangular and circular) with the simply supported or clamped and/or free edge conditions. *Johansen (1967)*-founder of the yield line theory- presents the plastic solutions of the reinforced concrete slabs having different standard shapes supported over the non-yielding edges. The yield line analysis for the flat slab is also covered in good length. *John and Wood (1967)* and *Park and Gamble (1980)* provide in sufficient details various elastic and plastic solutions for the rectangular and triangular slabs resting over the non-yielding supports. Beam-supported-slabs, forming a composite failure mechanism at collapse, are also presented in brief. *Shukla (1973)* presents the yield line solutions for reinforced concrete slabs resting over the non-yielding supports. The slabs with centric and/or eccentric openings (both rectangular and circular) are also considered. *Philip (1985)* presents various limit solutions for the circular and rectangular plates. He again considers the non-yielding supports for various types of slabs. Numerical techniques for predicting the yield line pattern for rectangular reinforced concrete slabs resting over the non-yielding supports with and without openings are well documented by *Gallanghar and Zienkiewicz (1973)*. *Hemp (1973)* has compiled the various available optimization techniques for the flexural systems and *Zienkiewicz (1977)* has compiled all

available numerical techniques forming the basis of finite element method. Plate element for the 2-D and 3-D bending analysis has been explained in good detail.

A brief review of the work done by various researchers in the field of the slab/plate analysis is presented below.

Sozon and Siess, (1963) investigated the experimental behavior of multipanel reinforced concrete slabs resting over the non-yielding supports. They considered the slabs with and without beams and verified the experimental results with those obtained from ACI codal values and suggested the modified moments being transferred to the column and the middle strip in the beamless slab. The results were found to be comparable with the theoretical figures in case of the beam-supported slabs.

Sawzuak and Winmik, (1965) formulated the mathematical model to predict the collapse load of a simply supported plate and experimentally verified the same at large deflections. The results were quite favorable. They employed the upper bound approach of the plastic analysis technique in the model development.

Gamble, Sozon and Seiss, (1969) have presented the experimental results of a two-way rectangular reinforced slabs resting over the non-yielding supports. The slab has been designed using the codal bending moment coefficients. The experimental yield line pattern and the moment field were quite similar to that used in the model development.

Corley and Jirsa, (1970) has presented the equivalent frame method for the slab analysis. In this method, the slab resting over the rigid and the flexible beam can be analyzed but there should be a minimum of three slab panels. The distribution to the middle strip and the column strip was taken from the study conducted by *Sozon and Siess, 1963.*

Islam and Park, (1971) derived a mathematical expression for the collapse load for the two-way rectangular slab resting over the rigid supports with rectangular openings. The yield line theory was used to predict the collapse load and shown that the presence of opening in the slab panel can reduce the collapse load by 20-30% depending upon the position of the opening.

Gamble W. L, (1972) in his experimental study determined the amount of moment shared by the slab panel supported over the beams. Sufficient rigid beams were used at the outer boundary of the slab panel to keep the end displacement equal to near zero. The experimental results have shown the influence of supporting beams in the slab moments. He had concluded that the moment coefficients outlined by the code are reliable only for

sufficient rigid supports and the slab moments are highly on the unsafe side for relatively less stiff beams/supports.

Jain and Kennedy, (1973) has developed the yield criterion being used in predicting the collapse load in the yield line analysis of reinforced concrete slabs. The orthotropic reinforcement was considered in the slab panel to obtain the yield criterion.

Vijayarangan B, (1973) has developed a lower bound solution for reinforced concrete slabs based upon the plastic approach. He considered the both continuous and simply supported orthotropic slabs resting over the non-yielding supports at the outer boundary. He employed the basic equilibrium equation for the slab element with a suitable yield criterion and satisfied the governing boundary conditions to arrive at the final moment field induced in the slab.

Salvadori M.G., (1979) has experimentally studied the effect of flexural and torsional stiffness of the supporting beam on the distribution of slab moments and concluded that relatively lesser stiffer beams significantly increases the moments in the slabs whereas the slab moments remains unaffected in case of a stiff supporting beam.

W. H. Dilger and A. Gali, (1981) presented the test results from an experimental study conducted on the slabs. This paper suggested various design criterion that in general liberalize several clauses of the ACI code but these had not been adopted by the ACI code.

Bauer, D. and Redwood, R.G., (1986) Authors have presented a numerical method based on the virtual work approach. The method consists of computing the yield load of a plate based on the geometry of an assumed collapse mechanism defined by means of nodes, planes and lines. In addition, it can be used for the yield line analysis of plates with complex shapes, assumed mechanisms and with any loading. Algorithms for the calculations of the work done by the external loads on the plate and the internal work dissipated along the yield lines in the assumed mechanism are also described. The features of a computer program have been outlined and a numerical example of the numerical yield line analysis of a reinforced concrete slab was given.

S. H. Simmonds and S. B. Alexander, (1987) developed a truss analogy to the edge column case and developed a complete M-V interaction diagrams that conservatively reproduced test results. The proposed model can predict the shear strength of the slab-column edge.

P. Adebar, D. Kuchma, M. P. Colins,(1990) has proposed a simple three dimensional truss model for determining the moment capacity requirement for a pile cap. They have suggested that the failure may occur in the pile cap due to the yielding of tension tie, the failure of anchorage of tension ties and the failure of compression strut or due to the excessive bearing stress over the piles or column.

Krenk S. et.al, (1993) employed the optimization technique for the plate elements to predict the reinforcement placement. The proposed finite element formulation was developed to perform the limit analysis of perfectly plastic plates using the triangular elements and linear programming. The equilibrium elements were formulated in terms of three moment components at each corner and equivalent corner forces including shear and torsion moment computations were derived in simple vector format.

Helba and Kendy, (1994) has developed a mathematical model for predicting the collapse load for skew type bridges with continuous two span slabs. They considered the skew slab with different skew angles slab resting over the steel girders placed along the span, thus forming a composite slab. The yield line theory was used for this purpose. Experimental testing was carried out to ascertain the accuracy of the model. Good agreement was shown between these two values. The results have shown that the skew angle, aspect ratio and type of connection between different elements of the composite bridge are the main factors influencing the collapse load and failure pattern.

Helba and Kendy, (1994) in their companion paper have presented a parametric study carried out by them on the skew type continuous Slab Bridge. They have taken skew angle, beam spacing, span, and number of loaded lanes and stiffness of the beams as main parameter. Results has been reported for both simply supported and two span continuous skew slabs.

Kolbjorn Saether, (1994) has used structural membrane theory for determining the bending moments induced in the flat slabs. This method improves the inherent limitations of two-dimensional frame representation of plates as recommended by ACI-318 code. The proposed method yields excellent agreement with the existing test data for the square and rectangular layouts.

Maria Anna Polak, (1996) has presented a simple method for determining the deflection in the reinforced concrete two-way slabs. Material model for reinforced concrete based upon the effective stiffness approach has been implemented in the finite-element

programs incorporating Mindlin-Plate bending elements. The uncracked concrete was treated as an isotropic elastic material and after cracking, concrete was considered as an orthotropic material. The reduced stiffness coefficients after cracking was calculated form the effective moment of inertia in both directions. Experimental testing was undertaken to validate the results obtained from the proposed model with different reinforcement ratios, boundary conditions and reinforcement orientations.

Alan Jennings, (1996) has proposed two theorems which are quite useful in establishing topologies of the yield-line mechanism likely to cause collapse of slabs (or plates). It is shown in the paper that the search amongst concave mechanisms for the most probable one to cause a collapse can use the uniqueness property that ensures that the function to be searched has no false maxima.

Ebeido and kennedy, (1996) has undertaken extensive parametric study on more than 600 prototype continuous composite steel-concrete bridge model using the finite-element analysis to obtain the influence of the slab skew and continuity on longitudinal moments in the supporting girders. This aspect was not taken into account in the bridge design as suggested in the AASHTO design manual. Girder spacing, skew angle, bridge aspect ratio, span ratio, number of lanes and girders were taken as main parameters in the study.

Armand and Marti, (1997) has reviewed the Robert Maillart's dimensioning procedure for orthogonally reinforced flat slabs that was based upon observations from a full scale testing of slabs undertaken by him in early 1909. It was shown that Maillart considerably underestimated the flexural moments acting in the flat slabs if compared with the elastic theory and if compared with the limit analysis procedures, the Maillart's designs were characterized by reasonable safety margins.

A. Thavalingam et.al, (1999) The authors has modified the method of Munro and Da Fonseca useful for numerical prediction of the yield line pattern based upon the linear programming and used a fixed, arbitrary mesh of potential yield-lines to predict the collapse load of a slab or plate. This paper describes an optimization procedure for adjusting the mesh to provide a safer estimate of the collapse load. The paper is mainly devoted to practical examples illustrating the application of the technique.

Mitchell Gohnert, (2000) The author has proposed yield-line elements which are a new type of finite element formulated for the analysis of slabs in bending. Both the elastic and inelastic theories have been developed for the analysis of slabs. However, the author has

described only the inelastic theory used to determine the collapse load of a slab. The proposed theory is an overshoot–return method which is both a simple and stable. Yield-lines and plastic rotations have been modeled by increasing the flexibility terms of the element. *Johansen* and *Kemp's* yield criterion has been adapted to permit an analysis of both isotropic and orthotropic reinforcement. The element is verified by comparison tests with experimentation and Johansen's yield line analysis. The results indicate that the proposed elements are accurate and a viable design tool

C.K. Soh et.al, (2001) described a numerical method to determine the lower-bound solution of the limit load of a rigid-perfectly plastic body obeying the von Mises yield criterion. The idea of the proposed method is to construct a smoothed linear stress field that satisfies the yield criterion everywhere in the body thereby, giving a lower bound solution. The validity of the proposed model has been demonstrated with some numerical examples. The results are quite favorable.

Denton, S.R., (2001) has proposed a procedure to postulate the yield line mechanism for the reinforced concrete slabs and described a systematic procedure for checking the compatibility of the postulated yield line mechanisms. The similarity between the proposed method and equilibrium requirements in the plane pin-jointed truss was also highlighted and an analogy between the yield-line mechanism compatibility and the statical determinacy in the pin-jointed trusses was established that could be used in postulating some yield line mechanism.

Famiyesin, O.O.R. et al. (2001) Authors has developed equations for predicting the strength of rectangular two-way spanning, reinforced concrete slabs of different edge conditions and under a uniformly distributed loading from the conventional yield line theory and the finite element method. The common material and geometrical parameters, normally associated with RC slabs have been adopted as independent variables in the equation development. The yield line equations are further calibrated with experimental data to incorporate the effect of membrane action thereby, increasing their predictive capability. The efficiency of the equations is assessed by their use for predicting known experimental results.

Valentin Quintas, (2003) has suggested a generalized yield-line method to determine the collapse load of reinforced concrete slabs. The yield line method initially proposed by *Johansen,* was modified to predict the true yield line pattern and collapse load. It was

shown that if the assumed yield line pattern is correct then it would be accompanied by the bending moments only otherwise torsional moments must be considered along with the moments acting along the assumed yield line. The former approach was called as 'normal moment method' while later as 'skew moment method'. It was suggested that if the yield line pattern is not known in advance, torsional moments must be considered to be acting along with the bending moment on the assumed yield line

Phuvoravan and Sotelino, (2005) has proposed a new finite-element analysis procedure for the nonlinear analysis of reinforced concrete slabs. The proposed element combines a four-node *Kirchhoff shell* element for concrete with the two-node *Eular* beam elements for the steel reinforcement bars. The connectivity between the reinforcement beam element and the concrete shell element was achieved by means of a rigid link and by using the transformation method for the rigid links; beam nodes were eliminated from the final mesh of the structure. The new finite element was then, verified with experimental results and it was shown that there exist a good agreement between the analysis results and the values obtained from the experimental results.

Castro, J. M. et.al (2007) has suggested an improved formula for calculating the effective slab widths in composite beams. Several 3D numerical simulations were conducted for validation of the proposed approach and it is simple to use in comparison to the guidelines recommend by various design codes.

Wust, J. and Wagner, W. (2008) have presented a new systematical algorithm to predict the initial yield-line configurations of arbitrary polygon plates and this approach can be used for optimization of plates.

Sapountzakis, E. J. and Mokos, V.G. (2008) have developed a modified method for the dynamic analysis of plates stiffened by parallel plates based upon the boundary element approach. In the paper, both free and forced damped or undamped transverse vibrations were considered and numerical examples are presented in the paper.

Sapountzakis, E. J. and Mokos, V.G. (2008) have presented a general solution for the analysis of the plates stiffened by arbitrarily placed parallel beams with deformable connections. The model permits the evaluation of the interfacial shear at the interface of the plate and beam in both directions.

Kumar, M.S et.al. (2009) have developed a model to predict the ultimate strength of the stiffened-pates with a square opening under axial and out-of-plane loads. Interaction

curves and equations has been suggested based upon the parametric studies conducted using the finite element based software.

Liu, Y and Li, R (2010) have suggested a symplectic geometry approach for accurate bending analysis of rectangular thin plates with two adjacent edges free and others clamped or simply supported. The approach suggested in the paper eliminates the predetermination of deformation function and is more reasonable than the conventional methods. Numerical results are also shown to validate the proposed approach.

Mander, T. J. et.al. (2011) have presented a modified yield line theory to estimate the overhang capacity of the full-depth concrete deck slabs accurately within 1-6% of experimental results for critical cases.

2.3 LIMIT ANALYSIS

The theorems of limit analysis derive from the application of the principle of virtual work to the rigid-perfectly plastic system. A rigid-perfectly plastic material absorbs no energy and the work done by the external forces is completely dissipated in the plastic deformations occurring at the plastic hinge and/or along the yield lines. Therefore, in any arbitrary structural system at collapse the total work done by the external and the internal forces acting in the system must disappear for any admissible virtual displacement. In other words, this principle can be stated as '*a set of real forces acting on a rigid body will be in equilibrium if the work done by these forces as they move through a set of compatible virtual displacement is equal to zero'*. In this statement, the compatible virtual displacements means all displacements that a rigid body undergoes must be consistent with the rigid body motion *i.e.* all displacement in the collapsing system are linked together through some geometric relations and there can be no change in the shape of the body during this process of deformations. The bending moment distribution in the structural system at collapse called as the *moment field* must satisfy the following three conditions in order to support a given set of an external loading [*Park (1961), Szilard (1985)*].

1. *Mechanism Conditions*: The moment field induced in the system under an applied load must approach the ultimate resisting moment of a structural member at sufficient number of sections and/or points for the structure or part of it to develop a plastic hinge and/or the yield line pattern, thereby forcing the structural system to behave as a mechanism under the applied loading.

2. *Equilibrium Conditions*: The moment field induced in the system under an applied load must represent the state of equilibrium between the internal stress resultant of the structural member and the applied loading.
3. *Yield Conditions*: The moment field induced in the structural system must nowhere be allowed to exceed the ultimate resisting moment/strength of its members.

The collapse load of any structural system is characterized by a bending moment distribution that satisfies the equilibrium and mechanism conditions along with an applicable yield criterion and there exists only one load factor at collapse that satisfies all these conditions simultaneously. The value of the load factor can be determined uniquely using the minimum and the maximum principles of the limit analysis. According to these principles, the collapse load factor for any structural system is the minimum load factor that has been obtained by fulfilling the equilibrium condition for all possible collapse mechanisms of the system, and it will be the maximum load factor if it has been calculated by considering all those bending-moment distributions that satisfy the equilibrium and yield conditions. Therefore, these two conditions will give the lower and the upper bound to the true value of the load factor of a structural system. The true value of a load factor can be achieved by satisfying all these conditions simultaneously. The value of this load factor increases or at least remains the same with the addition of any restraint, whether internal or external, in the structural system and it would reduce with the removal of restraint. This condition can be used very conveniently for predicting the collapse load of a plate-system restrained on its all the four sides by reducing it into a plate resting over the simple supports on its outer boundaries. Then, it can be suitably reinforced on its top face near the continuous outer edges to resist at least cracking moment without lowering the minimum desirable load factor.

The yield line theory postulated by *Johansen (1967)* is based on the *Minimum load Principle* or *Upper Bound Theorem* because the collapse load predicted by this principle would be either too high- an upper bound to the true value or at the most equal to the true value. In this method, an arbitrary collapse-mechanism compatible with the boundary conditions of the structural system is considered at the ultimate load in a manner that the bending moments at the plastic hinges or along the yield lines are not greater than the ultimate resisting moment of the section. However, the portion of the slab enclosed by the yield lines are not examined in routine calculations to ensure that the moments there do not exceeds the available moment capacity. The value of this bending moment will always exceed the moment capacity of the section for any incorrect and incompatible

mechanism being used in the analysis but if all possible collapse mechanisms for the structural system are examined, the mechanism giving the lowest ultimate load will give the true value of the collapse load for the structural system.

And if the bending moment distribution in any structural system has been obtained by satisfying the equilibrium and yield conditions, then the collapse load of the system will be either on the too low side – a lower bound or at the most equal to the true collapse load. The strip method of the slab design proposed by *Hillerborg (1975)* was based upon this principle. This method is known as *Maximum load Principle* or *Lower Bound Theorem.* In this method, the moment field in a structural system was selected in such a manner that the equilibrium conditions are satisfied at all points along with the requisite boundary conditions and the yield criterion is not exceeded anywhere in the structural system and consequently it always results in a safe design. Unskilled use of this method will never lead to insufficient safety against the flexural failure, but it can at worst results in a design that is unsuitable for some other reasons *e.g.* it will be too uneconomical to use or the reinforcement steel is too difficult to place with the available manpower and/or resources etc. However, the user of this method must have sufficient skill to trace the best load strips for the satisfactory performance.

2.3.1 Collapse Mechanism

Consider a reinforced concrete slab that is progressively loaded to the failure. At low load level, before the initiation of tensile cracks, the distribution of bending moments and displacement field defining the deflection of the middle plane of the slab follows the elastic plate theory. After the formation of the flexural cracks, the distribution of the moment field in the slab changes significantly due to the differential reduction in the stiffness in various segments/regions of the slab caused by the flexural and torsional cracking as well as inelastic behavior of the concrete and the reinforcement steel. With further increase in the loading, yielding of the tensile steel eventually occurs along the lines of maximum moment and the slab undergoes a large change in the curvature along the sections of yielding, with the moment there remaining practically constant at the ultimate moment of resistance of the slab section. The slab section can be said to collapse at this stage of loading when it fails to support any additional load.

A large redistribution of bending moment occurs in the slab under increasing load and it leads to the formation of lines of intense cracking in sufficient numbers at the tensile face of the slab thereby, dividing the slab into a number of interconnected segments. The

number and the shape of segments into which the slab was divided depend upon its geometry, boundary conditions, orthotropy and the type of loading. The slab at this stage of loading when it fails to support any further increase in the load is converted into the collapse mechanism.

The band of intense cracking across which the tensile steel in the slab has been yielded is represented by a single line at the center of band. All the plastic deformations in the collapsed slab are assumed to occur along this line called as yield line and it represents the line of discontinuity of the displacement field caused by infinite value of the curvature existing along the yield line. The magnitude of the plastic deformations occurring along yield lines are much greater than the elastic deformations of the slab segments enclosed between the yield lines of the collapse slab and therefore, it was reasonable to assume these segments in the elastic state of load-deformation curve and undergoing a rigid body displacement under increasing load. But for the full attainment of the ultimate load, the slab section must possess sufficient plastic rotation capacity to allow the formation of a complete yield line pattern in the slab. This can be achieved by suitably reinforcing the slab section at its tensile face.

A kinematically admissible displacement field satisfying the kinematic relations and the boundary conditions of the system controls the global deformation pattern of rigid-segments of the collapsed slab rotating about the corresponding yield line and the non-yielding edges at the outer boundary of the slab. The shape of these rigid-segments of the collapse mechanism can be derived intuitively by considering the laws of mechanics of rigid bodies and the theorems postulated by *Johansen (1967), Jennings (1996), Denton (2001), and Quintas (2003). Johansen (1967)* has postulated following two theorems for deciding the tentative shape of the rigid segments in the slab at the state of collapse.

- The yield line between two parts of a slab and their axes of rotation must intersect in a point.
- The yield line layout in the slab or the rotation axes and the rotation ratios of the various parts of rigid segments of the slab define the collapse mechanism.

2.3.2 Equilibrium of Slab-System

Any reinforced concrete slab consists of a number of interconnected segments after the formation of the complete yield line pattern at ultimate load. Each segment of the slab at collapse undergoes a rigid body displacement compatible to the boundary conditions of the slab about the yield lines and its outer non-yielding edges. After the formation of a

complete yield line pattern, the slab system starts behaving as a rigid-perfectly plastic material that absorbs no energy during deformations and the work done by the external set of forces is completely dissipated in the plastic deformations occurring along the yield lines. Therefore at ultimate state, the total work done by the external and the internal forces acting over the rigid body in equilibrium with a set of external forces must disappear for any value of a kinematically admissible virtual displacement field. This condition is used most commonly and conveniently for ensuring the equilibrium of the system at collapse *i.e.* the sum total of the work performed by the internal and the external forces acting over the body must vanish for any equilibrate system of forces.

2.3.3 Yield Condition

The yield condition/ criterion define the strength of the slab section being subjected to a general moment field. In case of a reinforced concrete slab with a uniformly placed reinforcement in the x-and y-directions, the yield criterion relates the ultimate moment of resistance per unit width of the slab along the x-axis, m_{ux} and along the y-axis, m_{uy} to the applied moment field per unit width (m_x, m_y and m_{xy}) under some external loading, when the slab section yields at ultimate load. In other words, this condition distinguishes the safe stress state from those for which a given set of reinforcement in the slab is not sufficient to support the external load.

The normal-moment yield criterion was proposed by *Johansen (1967)* and it was later on validated both experimentally as well as analytically by the number of researchers [*Morley (1965), Kwiencinski (1965), Kemp (1965), John and Wood (1967), Lenschow and Sozen (1967), Cardenas and Sozen (1973), Jain and Kennedy (1973), Holmes and Arnaouti (1973), Kowal* and *Sawczuk (1976) and Quintas (2003)*] and found this yield criterion sufficiently accurate to use within the domain of following assumptions.

1. The actual yield line formed in the slab can be replaced by a series of steps, in the x-axis and the y-axis, subjected to the moments (m_x and m_y). The torsional moment (m_{xy}) acting in these directions is assumed to be negligible.
2. Kinking of the reinforcing bars across the crack/ yield line and the biaxial stress conditions in the concrete compression zone of the slab does not influence the strength of the slab section.
3. The tensile steel along the x-axis and y-axis of the slab crossing the yield line has reached its yield strength.
4. In-plane membrane forces in the slab section are assumed negligible.

The normal-moment yield criterion [*Kemp (1965)*] requires that at any point in the slab, the normal moment per unit width of the slab, m_u due to the design moments m_x, m_y and m_{xy} should not exceed the ultimate normal resisting moment, m_{un} of the slab in that direction. This criterion should hold good at all points in the slab because the yield lines can initiate in any point and in any direction.

The ultimate moment of resistance about a yield line inclined at some angle to the reinforcing bars can assumed to be due to the components of the ultimate resisting moments along the x-axis, m_{ux} and the along y-axis, m_{uy} of the slab. Consider a slab element subjected to a general moment field along the yield line in the direction, **t** at an angle, α to the y-axis. The actual yield line is replaced by series of small steps along its length for simplification and one such triangular element is considered for the analysis purpose. The ultimate normal resisting moment acting in the n-direction along the yield line can be found from the consideration of equilibrium of the triangular element *abc* by taking moments of the components of moment, m_{ux} and moment, m_{uy} about *ab* as shown in *Figure 2.1*.

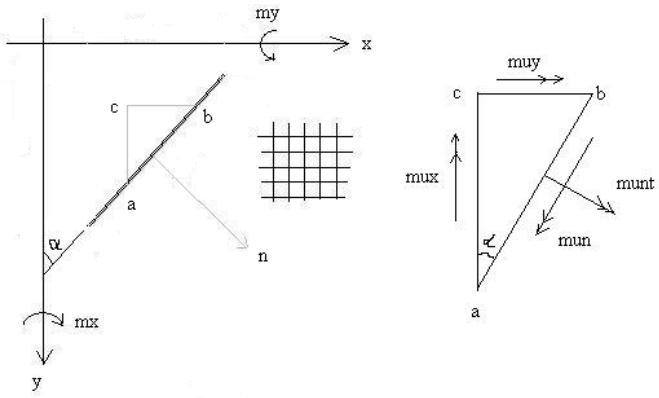

Figure 2.1: Moments acting on triangular element of reinforced concrete slab

This gives

$$m_{un}\, ab = m_{ux}\, ac \cos\alpha + m_{uy}\, bc \sin\alpha$$

Or $$m_{un} = m_{ux} \cos^2\alpha + m_{uy} \sin^2\alpha \qquad (2.1)$$

And $$m_{unt}\, ab = m_{ux}\, ac \sin\alpha + m_{uy}\, bc \cos\alpha$$

Or $$m_{unt} = (m_{ux} - m_{uy}) \sin\alpha \cos\alpha \qquad (2.2)$$

The moment per unit width of the slab, m_n and m_t and the associated torsional moment, m_{nt} due to a given moment field can be obtained by summing the components of m_x, m_y and m_{xy} in the *n* and *t*-directions using the right hand screw rule. The angle, α

between the x- and n-axis is measured clockwise from the x-axis. The equilibrium of the moments acting on the element in the n-direction requires that

$$m_n\, ab = m_x\, ac \cos\alpha + m_y\, bc \sin\alpha + 2\, m_{xy}\, bc \cos\alpha$$

Or $$m_n = m_x \cos^2\alpha + m_y \sin^2\alpha + m_{xy} \sin 2\alpha \quad (2.3)$$

Similarly, $$m_t = m_x \sin^2\alpha + m_y \cos^2\alpha - m_{xy} \sin 2\alpha \quad (2.4)$$

and $$m_{nt} = (m_x - m_y) \sin\alpha \cos\alpha - m_{xy} \cos 2\alpha \quad (2.5)$$

This yield criterion assumes that the reinforced concrete slab element reaches its strength when the normal moment, m_n due to a given moment field becomes equal to the ultimate normal resisting moment of the slab, m_{un} i.e. $m_{un} \geq m_n$

$$(m_{ux} \cos^2\alpha + m_{uy} \sin^2\alpha) \geq (m_x \cos^2\alpha + m_y \sin^2\alpha + m_{xy} \sin 2\alpha) \quad (2.6)$$

Equation (2.6), applicable for all values of α can be simplified to an easily usable form, given in equation (2.7). Dividing it through by $\cos^2\alpha$ and further simplifying, we get:

$$(m_{ux} + m_{uy} \tan^2\alpha - m_x - m_y \tan^2\alpha - 2\, m_{xy} \tan\alpha) \geq 0 \quad (2.7)$$

Left-hand side of above equation is function of 'tanα' and it represents the excess of moment, m_{un} over the moment, m_n and for this excess to be minimum:

$$\frac{\partial f(\tan\alpha)}{\partial\alpha} = \frac{\partial f(\tan\alpha) d\tan\alpha}{\partial\tan\alpha d\alpha} = \frac{\partial f(\tan\alpha)\sec^2\alpha}{\partial\tan\alpha} = 0$$

Since '$\sec^2\alpha$' cannot be zero,

$$(2\, m_{uy} \tan\alpha - 2\, m_y \tan\alpha - 2\, m_{xy}) = 0$$

$$m_{uy} = m_y + \frac{m_{xy}}{\tan\alpha} \quad (2.8)$$

And if $f(\tan\alpha)$ is to represent the minimum excess moment, then

$$\frac{\partial^2 f(\tan\alpha)}{\partial(\tan\alpha)^2} = 2\, m_{uy} - 2\, m_u \geq 0$$

or $$m_{uy} \geq m_u \quad (2.9)$$

Combining equation (2.8) and equation (2.9), we have $\frac{m_{xy}}{\tan\alpha} \geq 0$

Therefore if m_{xy} is positive, 'tanα' must be taken as positive and vice versa. Substituting equation (2.8) into equation (2.7) gives

$$m_{ux} \geq m_x + m_{xy} \tan\alpha \quad (2.10)$$

Therefore, the resisting moments can be selected from equation (2.8) and equation (2.10) for any given moment field and predefined arrangement of the reinforcing bars.

Alternatively, the yield line pattern in the slab can be imagined to follow the deformation profile of any structural member under a given loading. The positive yield lines in a uniformly reinforced concrete slab would always develop along the curve representing the maximum deflection and/or curvature produced in the slab under a given set of loading. However, the negative yield line normally develops along the non-yielding supports of the slab-system and along the curve whenever there is a sudden change in the curvature at the loaded face of the slab *e.g.* nears the beams ends, at corners of the slab, and near the columns etc. The yield line pattern, if selected following these guidelines, will be deemed to satisfy the yield criterion. Almost all yield line patterns used by different researchers have been found to satisfy this trend [*Johansen (1967), John and Wood (1967), Quintas (2003),* and *Jennings (1996)*] and it would postulate the minimum collapse load for a slab system.

2.4 SOLUTION USING ENERGY PRINCIPLE

A yield line pattern compatible with the boundary conditions of the slab is assumed at the ultimate load. A kinematically admissible displacement field will control the deformation of rigid-segments of the collapsed slab under an increasing load and these segments can be regarded as rigid bodies because the slab deformations are concentrated only along the yield lines under an increasing load. At ultimate state, the segments of the slab are in the state of equilibrium under external loading, the bending and the torsional moments along with shear forces acting along the yield lines. The equilibrium of the slab can be ensured by equating the work done by the external loading with that produced by the internal system of forces in moving through a small virtual compatible displacement field.

The reactions at non-yielding supports of the slab will not contribute to the external work as they do not undergo any displacement. The work done by the internal forces at yield lines will be due to the bending moments only because the work done by the torsional moments and the shear forces is zero when summed over the entire slab. Moreover, there will be a no relative movement between the sides of the yield line corresponding to the torsional moment and the shear forces for any value of an arbitrary displacement given to the yield line pattern of the slab. Accordingly, the bending moments in the slab will only contribute towards the internal work because of the relative rotation occurring between the two sides of the collapsed slab about the yield line.

The work done by the ultimate resisting moment per unit width of the slab, m_{un} at a yield line of length, l_o, where the relative rotation about the yield line of two segments is θ_n, can be obtained from the work equation: $-m_{un}\,\theta_n\,l_o$ as shown in *Figure 2.2.* The work done by the bending moment will be taken as negative because the direction of the rotation of the slab-segment if it is displaced in the direction of loading will be opposite to the direction of bending moment. The total work done by the resisting moments acting along the complete yield line pattern of the slab will be $-\sum m_{un}\,\theta_n\,l_o$. And for equilibrium of the system, the summation of the total work performed by the internal forces and the external force acting over the surface of the slab ($=\sum P_u\,\delta$) must vanish:

$$\sum P_u\,\delta - \sum m_{un}\,\theta_n\,l_o = 0$$

$$\text{or} \quad \sum P_u\,\delta = \sum m_{un}\,\theta_n\,l_o \qquad (2.11)$$

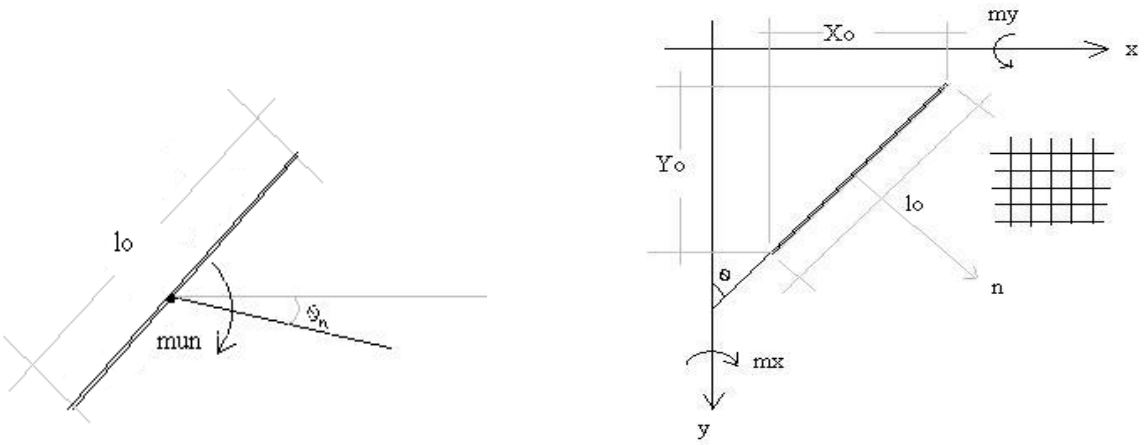

Figure 2.2: Yield line inclined to the direction of orthogonal reinforcement

However, it is a common practice to provide the reinforcing steel in the slab(s) along the two orthogonal directions, x- and y-axis. But as the yield line is free to form in any direction under the external loading (may be inclined to the reinforcing bars), it will be always better and easier to deal separately with the x-axis and y-axis components of the internal work performed by the ultimate resisting moments, m_{ux} and m_{uy}. For a yield line inclined at an angle, α to the y-axis, the ultimate resisting moment acting along the normal, m_{un} can be resolved into components along the x- and y-axis using equation (2.1). It is written below in equation (2.12).

$$\sum m_{un}\,\theta_n\,l_o = \sum (m_{ux}\cos^2\alpha + m_{uy}\sin^2\alpha)\,\theta_n\,l_o$$

$$= \sum m_{ux}\cos^2\alpha\,\theta_n\,l_o + \sum m_{uy}\sin^2\alpha\,\theta$$

$$= \sum m_{ux}\,\theta_x\,l_y + \sum m_{uy}\,\theta_y\,l_x \qquad (2.12)$$

In equation (2.12), θ_x and θ_y are the rotations of the rigid segment of the collapsed slab about the x-axis and the y-axis respectively. l_x and l_y are the projections of the yield line of length, l_o over the x-axis and the y-axis of the slab respectively. Combining equation (2.11) and equation (2.12), the equilibrium conditions of the collapsed segments of the reinforced concrete slab can be written after the formation of a complete yield line pattern at ultimate load. The final expression for this is given in equation (2.13).

$$\sum P_u \delta = \sum m_{ux} \theta_x l_y + \sum m_{uy} \theta_y l_x \qquad (2.13)$$

Equation (2.13) ensures that the collapsed-interconnected segments of the reinforced concrete slab are in equilibrium with the external loading at the ultimate state. This condition along with the applicable yield criterion and the correct collapse mechanism of the slab [*Jennings (1996), Denton (2001), Quintas (2003)*] will give the true collapse load of the slab system.

2.4 CLOSURE

A good number of elastic solutions are available in the published-literature for the slab analysis as observed from the review presented in this chapter. All of these are derived for the slab panels of some standard shapes viz: rectangular, circular etc supported either resting over the simple supports or with clamped edges or free edges and combination of these standard boundary conditions. The final expressions for the bending moments, deflections etc. are mathematically too complicated that neither these are used in routine design calculations nor these can be used to check the accuracy of the results from a finite element based software in design offices. In addition, it is very difficult and cumbersome to derive these values for other shapes, with and without openings and if the slab has been subjected to some other odd loading cases.

A similar case exists for solutions derived from the plastic methods. These methods expect its users to be highly imaginative and intuitive who should be capable of predicting the possible failure pattern of the slab system, as the load predicted from this approach is always an upper bound to the real collapse load. In case of slabs supported on internal supporting beams, no work has been reported that can handle slab-beam system in which the internal beams fail to provide the non-yielding edge to the slab. As such, the moment coefficients suggested by various design codes become ineffective for the design.

CHAPTER-3

ANALYTICAL MODELLING

3.1 GENERAL

A reinforced concrete slab progressively loaded to a failure develops a band of flexural cracks at its tensile face along the lines of maximum curvature. At low load level and before the initiation of tensile cracks, the distribution of bending moments and displacement field defining the deflection profile of the middle plane of the slab follows the elastic plate theory. After the formation of flexural cracks, this distribution of the moment field changes significantly depending upon the load level due to the reduction in the stiffness of the slab section. With further increase in the loading, a large redistribution of the moment field occurs in the slab and lines of intense cracking formed in sufficient numbers at the tensile face of the slab, thereby dividing the slab into a number of segments that leads to the formation of collapse mechanism. At this stage, yielding of the tensile steel eventually occurs along the lines of maximum moment and the slab section undergoes a large change in the curvature along the lines of yielding with the moment there remaining practically constant at the ultimate moment of resistance of the slab section. After the formation of collapse mechanism, the slab fails to support any further increase in the load and is said to be collapsed. The number and the shape of segments into which the slab was divided at the collapse depend upon its geometry, boundary conditions, orthotropy and the type of loading.

The band of this intense cracking across which the tensile steel in the slab has been yielded is represented by a single line at the center of band and all plastic rotation of the slab segments are assumed to occur along this line. This failure line is called as yield line and it represents the line of discontinuity of the displacement field caused by infinite value of the curvature existing along its length. The plastic deformation occurring along these yield lines are much greater than the elastic deformations of the slab segments enclosed between the yield lines and therefore, it was reasonable to assume these collapsed segments of the slab in the elastic state of the load-deformation curve and are undergoing only a rigid body displacement under increasing load.

After the formation of a complete yield line pattern, the slab system starts behaving as a rigid-perfectly plastic material that absorbs no energy during deformations and the work

done by the set of the external forces is completely dissipated in the plastic deformations occurring along the yield lines. Therefore at ultimate state, the total work done by the external forces and the internal forces induced in the rigid body in equilibrium with external forces must disappear for any arbitrary value of a kinematically admissible virtual displacement given to the mechanism. This condition will ensure the equilibrium of the assumed collapse mechanism of the slab at ultimate state. The collapse load predicted by using this condition would be on the higher side or at the most equal to the true value depending upon the shape of the collapse mechanism taken in the analysis. Therefore, this approach expects a considerable judgment and/or intuition and expertise from its user in finding the true collapse load and/or for tracing of the true yield line pattern of the slab system and simultaneously for ensuring a desirable factor of safety against the flexural failure.

3.2 PROBLEM

The slab is a highly redundant structural element due to the coupling of the internal moment field. Because of this, the structural behavior of the slab is greatly influenced by the stiffness of the supporting system, its position and the layout. However, the current state-of-art available for proportioning the reinforced concrete slab does not satisfactorily address the problem of designing slabs cast monolithic along with the shallow-beams. A shallow beam is a flexural member that deflects along with the slab under load and does not initiate any negative yield line pattern in the supported slab whereas the non-yielding edge and/or a internal brick wall does so at the tensile face of the slab along its length.

In most of the studies [*Sozon and Siess (1963), Gamble, Sozen and Siess (1969)*], the non-yielding edges at the outer boundaries are used to support the slab panel. Based upon the results of these experimental studies, empirical relations and some factors have been suggested for apportioning the total static moment to the slab and the supporting beams and/or the column strip for the satisfactory performance. Most of the design guidelines recommended by various codes [*ACI-318 (2008), IS 456 (2000) and CSA 23.4 (1994)*] are based upon these empirical results and the performance record of various slab-beam systems. The procedures recommended by most of these design codes have a number of inherent limitations in the form of assumptions, which are mandatory to be satisfied by all slab panels for the satisfactory performance. It forces the designers to proportion the slab-system within the domain of these limitations which sometimes fails to satisfy the architectural and some other field/design constraints.

The moment coefficients recommended by the design code [*IS 456 (2000)* and *BS EN 1992-1 (1994)*] are applicable only for the rectangular slabs with various end-restraints and supported over the non-yielding edges on the outer four edges. But in routine design practice, number of case are encountered by the designers whereby the beam-drop and the beam-spans are restricted by architects to a level that are not sufficient to provide a non-yielding edge at the outer boundary of the slab and as such, these coefficients predict the moment-field highly on the unsafe side and produce a structurally deficient slab section.

In the present chapter, an analytical model has been developed for a rectangular slab-system resting over the non-yielding edges at its outer boundary and cast monolithic along with equally spaced internal shallow beams using the principle of the limit analysis. It can also be used for predicting the collapse load of skew slabs, design of multi-panel slabs but it must be supported over the equally spaced shallow beams along one direction and non-shallow beams at regular intervals along the other direction of the slab. The slab is subjected to a out-of-plane uniform area load acting over its entire surface thereby providing an alternative solution to the finite element based software for the analysis of the slab-system supported over the internal beams incapable of providing a non-yielding edge to the slab panels. It will supplement the design guidelines recommended by various codes which allow that any procedure can be used for designing a slab-system that satisfy the conditions of equilibrium, geometric compatibility and the requirements of strength, and serviceability stipulated by design codes. However, the proposed model can only be used to satisfy the strength criterion enshrined in various design codes and serviceability criterion has been kept in scope for future studies. This model will also provide an alternate method to finite element procedures which is a costly, time consuming process for proportioning regular slab-systems satisfying assumptions given in section 3.3.

3.3 ASSUMPTIONS

It is assumed that the load-deformation response of a reinforced concrete can be idealized as a rigid-perfectly plastic at and/or near the collapse, which requires a sufficiently ductile slab section with properly anchored and uniformly distributed reinforcing steel at the tensile face of the slab. In addition to this major requirement, the analytical model has been developed with following constraints.

1. The reinforced concrete slab and the supporting beams have been cast monolithic and in case of a composite construction, the slab and the beam sections have been properly anchored to prevent the separation of two sections at ultimate load.

2. The slab is subjected to an out-of-plane uniform area load over its entire top face.
3. The slab has been divided into a number of panels with equal length using the internal generic beams running parallel to the short span of the slab system. It will represent the most common column layout in any structural system.
4. Orthotropic reinforcement has been provided at the tensile face of the slab with reinforcing steel bars placed parallel to the edges of the slab.
5. Membrane forces in the slab section have been ignored and if considered, this will only increase the post-cracking/yielding strength of the slab system.
6. Effects of slab openings, punching and shear have not been considered in the analysis.
7. Effect of kinking of the reinforcing bars across the crack / yield line and biaxial stress conditions in the concrete compression zone of slab have been ignored since these do not affect the yield criterion of reinforced concrete member/slabs.

The proposed analytical model can be used for the analysis of slab-systems only if these assumptions are satisfied.

3.4 DEVELOPMENT OF THE MODEL

The collapse load of any structural system is characterized by a bending moment distribution that satisfies the equilibrium and the mechanism conditions along with an applicable yield criterion and there exists only one load factor that satisfies all these conditions simultaneously at the collapse [*Wood (1961)*]. The value of this factor can be determined uniquely without the necessity of calculating deformations, either at collapse or at any other stage of loading, using the minimum and maximum principles of limit analysis. According to these principles, the collapse load factor for any structural system is the minimum load factor if it has been obtained by fulfilling the equilibrium condition for all possible collapse mechanisms of the system. It will represent the maximum value of the load factor if it has been calculated by considering all those bending-moment distributions that satisfy the equilibrium and the yield conditions [*Baker (1961)*]. Therefore, these two conditions will give the lower and the upper bound to the true value of the load factor that can be achieved by satisfying all these conditions simultaneously. The value of this load factor increases or at least remains the same with the addition of any restraint, whether internal or external, in the structural system at collapse and it would reduce with the removal of the restraint [*Baker (1961)*].

This condition can be used very conveniently for predicting the collapse load of a slab restrained on its all the four sides by reducing it into a slab resting over the simple

supports on its boundaries. It can suitably be reinforced later on at its top face near the outer continuous edges to resist the cracking moment without lowering the load factor.

Consider a rectangular slab of length, L_x and width, l_y divided into n-number of panels with length, l_x each. It is assumed that the rectangular slab is resting over the non-yielding supports at its outer boundary. Orthotropic reinforcement has been provided in the slab with ultimate resisting moment, m_{ux} along the long span (L_x) and m_{uy} along the short span (l_y) of the slab with orthotropy (μ); defined as ratio of ultimate resisting moment-capacity of the slab along the width, l_y and its length, L_x respectively (= m_{uy}/m_{ux}).

The ultimate negative resisting moments per unit length of the slab have been defined in terms of the ultimate positive resisting moments per unit length. The ultimate negative resisting moments along the long span, L_x of the slab is $i_x\ m_{uy}$ at the slab edges and the ultimate negative resisting moments along the short span, l_y are $i_y\ m_{ux}$ at the slab edges. The case of simple supports can be obtained by putting these *i*-values at outer boundaries of the panel as zero.

The slab was divided into a number of equally spaced panels along the long span (L_x) thereby, dividing the slab-system into a number of panels of length (l_x) each with aspect ratio (r_p). The slab has been cast monolithic along with (n-1) number of equally spaced internal shallow beams along the short span (l_y) of the slab-system with moment-capacity, m_b (= $\alpha_b\ m_{ux}\ l_x$) each. The supporting beams along the long span (L_x) of the slab were assumed adequately stiff to provide an exactly non-yielding edge to the slab. These supporting beams are also necessary to provide an adequate strength against the possible punching shear failure of the slab near the column face. The schematic diagram of the proposed analytical model has been shown in *Figure 3.1*.

The generic slab-system will behave as a one-way or as a two-way slab depending upon the strength of the internal beams cast monolithic with the slab. The slab would behave as a single panel slab of size (L_x x l_y) if the strength of the beams along the short span (l_y) of the slab were taken as zero and/or is not adequate to initiate the local collapse of the slab-panels as shown in *Figure 3.1A*. In case the internal beams are adequately stiff and/or strong as in case of the wall-supported slab-system, the slab would be transformed into a slab-system consisting of a number of smaller rectangular slabs of size (l_y x l_x) resting over the internal beams with aspect ratio, r_p (= l_y/l_x). This has been shown in *Figure 3.1B*. This happens mainly due to the formation of negative yield lines along the length of the stiff and/or strong supporting beams at collapse load. Most of the available

literature contains analytical models for these two extreme failure modes of the slab-systems [*Szilard (1961), Wood (1961), Johansen (1967), John and Wood (1967), John (1967), Shukla (1973), Park and Gamble (2000)*].

The main objective of the present investigations is to suggest an analytical model that can be used for analysis and design of slab-systems resting over the non-yielding outer boundaries and cast monolithic with internal shallow beams. It indicates the minimum strength of the internal supporting beams provided along the short span (l_y) of the slab-system at which failure mode of the slab transformed from the global-failure (large single panel slab) to the local-failure (large number of smaller rectangular slabs) at collapse thereby distinguishing the flexible-edge from the rigid (non-yielding) edge.

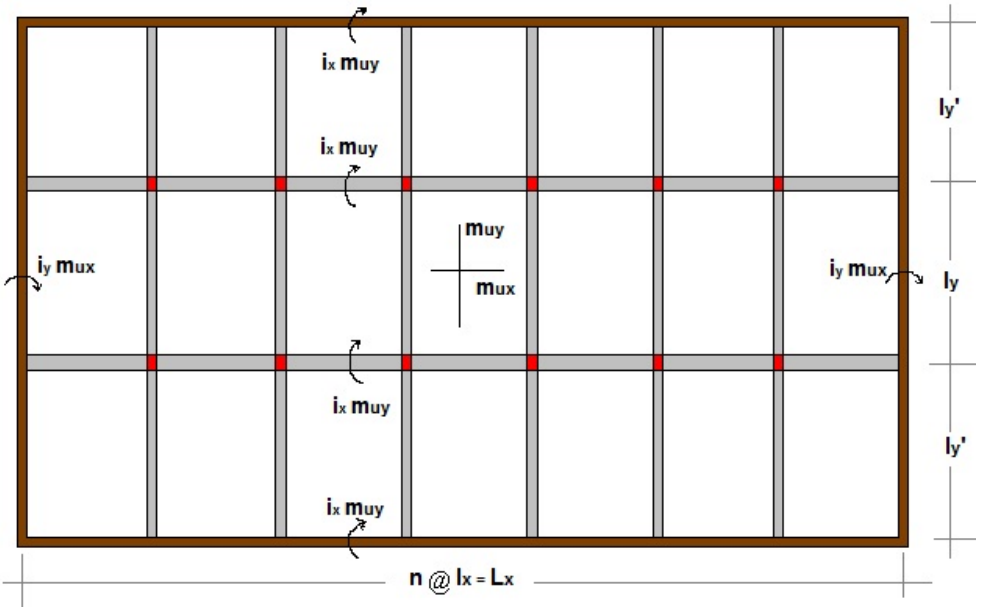

Figure 3.1: Schematic Diagram of the model

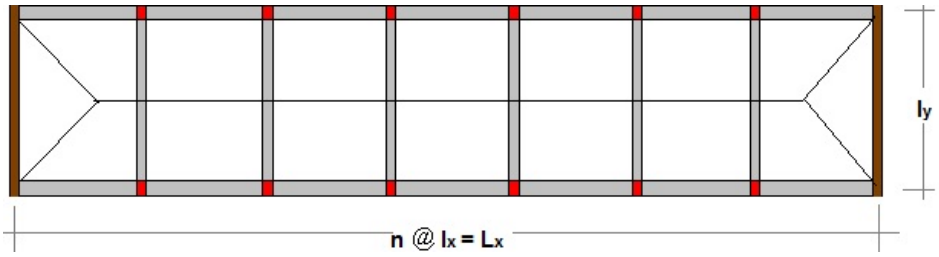

Figure 3.1A: Global Failure of a typical Middle Panel of the Slab

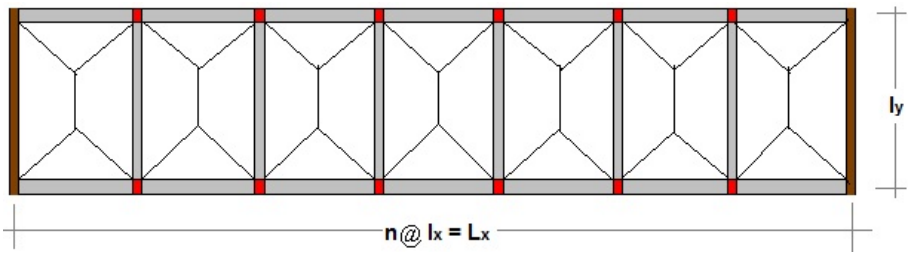

Figure 3.1B: Local Failure of a typical Middle Panel of the Slab

Shallow beam is a flexural member that deflects along with the slab and consequently, is incapable of providing a non-yielding edge to the slab under the applied loading. It will allow the yield line developed in the slab to pass through it at the point of the plastic hinge at collapse. The supporting beam maintains the compatibility conditions with respect to the displacement-field along its interface with the slab under the applied load. The depth of supporting beam must be kept less than *span/12* for a slab-system with simple edges at outer boundary otherwise it would act as a non-shallow beam and it will start producing negative yield lines along its length at the top face of the slab. This has been confirmed by an independent parametric study of a large number of rectangular slabs resting over the beams by varying their *span/depth* ratio, and studying its effect on the moment field under a uniform area load using the finite element method based software. A typical set of the results of this study have been given in section 3.8.

3.4.1 Collapse Mechanism

A reinforced concrete slab will develop a unique pattern of yield lines at the collapse load. The shape of the yield line pattern of a reinforced concrete slab depends upon the loading, its boundary conditions and the slab-constants. The development of the complete yield line pattern at ultimate state leads to the formation of collapse mechanism and at this stage, the slab fails to support any further increase in the loading. The load at this stage represents the collapse load of the slab-system.

In the present analytical modeling, the hypothesis collapse mechanism of the slab is assumed based upon the previous studies and the guidelines suggested by *Johansen (1967), Jennings (1996), Denton (2001), and Quintas (2003).* This hypothesis collapse-mechanism of the slab-system will be experimentally validated to check its accuracy and any other flaw. The results of this experimental study are given in Chapter-4.

The nature and type of the collapse-mechanism in case of a slab cast monolithic with equally spaced beams depends greatly upon its strength and stiffness in addition to other slab constants. If the internal beams are strong and stiff enough, these do not allow the yield lines developed in the slab to cross through into the adjacent panels and consequently, the slab fails with the formation of a yield line pattern, locally and simultaneously, in all panels of the slab under a uniform load acting over the entire face. At this stage, the slab-system transforms into a system consisting of a number of interconnected smaller slabs resting over the internal beams at the collapse. This type of slab failure mechanism is called as a local-collapse mechanism (see *Figure 3.3*).

Otherwise, if the failure of the slab occurs with the formation of a plastic hinge in the internal beams, simultaneously, along with the development of a yield line pattern in the slab, the failure mechanism is called as a global-collapse mechanism. In this case, all the beams allow the yield line pattern developed in the slab to pass through it at the point of the plastic hinge as shown in *Figure 3.2.* This mainly happens because of change in the curvature of the middle plane of the slab caused by the stiffness of the support-system at outer boundary of the plate and/or stiffness of the internal stiffening-beams.

Yield lines in any loaded slab always develop along the lines of maximum curvature forming in the slab and the stiffness of the support system whether external or internal is directly responsible for the formation of these lines along the line of maximum curvature in the slab. A highly stiff support or beam causes a sudden change in the curvature across its line and leads to the formation of negative yield lines along its length. A reduction in the beam-stiffness attracts the lines of maximum curvature in the slab toward the internal beams and an increase in the beam stiffness repels these lines away from the beams. At some typical value of the stiffness, line of maximum curvature start passing through the beam(s) thereby, changing the nature of the collapse mechanism from the local-collapse mechanism (highly stiff beam case) to a global-collapse mechanism (relatively flexible beam case). The strength of the slab and the internal beam(s) in general and strength available along the lines of maximum curvature in particular dictates the collapse load of the slab-beam system and there exists a coupling between the stiffness and strength of the slab-beam system. Any change in the one parameter has a significant effect on the other.

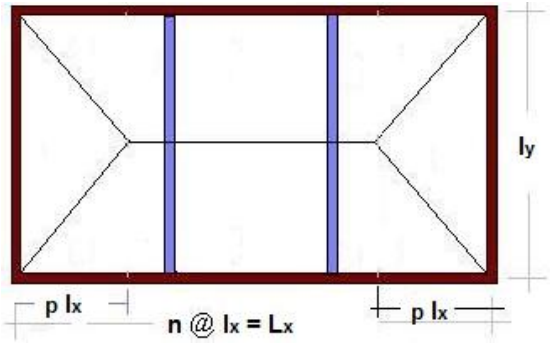

Figure 3.2: A typical *Global Collapse Mechanism*

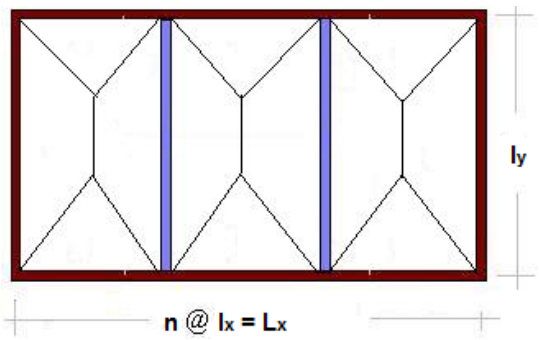

Figure 3.3: A typical *Local Collapse Mechanism*

The shape of the complete positive yield line pattern of a rectangular slab failing in the global-collapse mechanism or in the local-collapse mechanism can be derived by considering the laws of mechanics of rigid bodies and the theorems postulated by *Johansen (1967), Jennings (1996), Denton (2001), and Quintas (2003).*

3.4.2 Equilibrium and Yield Criterion

After the formation of a complete yield line pattern, the slab-beam system starts behaving as a rigid-perfectly plastic material that absorbs no energy during the deformations caused by the set of external forces and the work done by the set of these forces is completely dissipated in the plastic deformations occurring along the yield lines. Therefore at collapse, the total work done by the external and the internal forces, acting over the rigid bodies in equilibrium with the set of external forces, must disappear for any value of the kinematically admissible virtual displacement field (δ). This condition will ensure equilibrium of the hypothesis collapse mechanism of the slab-system at the ultimate state. The collapse load predicted by using this condition would be on the higher side or at the most equal to the true value depending upon the shape of the hypothesis collapse mechanism taken in the analysis. Therefore, this approach expects a considerable judgment and/or intuition and expertise from the user in finding the true collapse load and/or for tracing of the true yield line pattern of the slab and for ensuring a desirable factor of safety against the flexural failure.

The true value of the collapse load of the slab-system can be achieved either by satisfying the yield criterion at all points in the slab or by selecting a yield line pattern corresponding to the lines of maximum curvature under applied loading which always represent the true collapse-mechanism. But it will be simpler and mathematically easier to examine all possible collapse mechanisms than to check the yield criterion at all points in the slab and the collapse mechanism giving the lowest value of the load will postulate a true value of the collapse load [*Johansen (1967)*].

The equilibrium of the various segments of the collapsed slab therefore, can be ensured by equating the work done by the external surface loading in moving through a kinematically admissible displacement field in the direction of the load with that performed by the ultimate resisting moments acting along the yield lines of the assumed hypothetical collapse mechanism.

3.4.3 Solution

Consider a reinforced concrete slab failing in the global-collapse mechanism at collapse. The complete yield line pattern under the uniform area load (w) acting over the entire top surface of the slab at ultimate state is shown in *Figure 3.4*. This figure also shows the numbering scheme of various slab segments of the collapse mechanism that would be used for computing the external work performed by these segments of the slab.

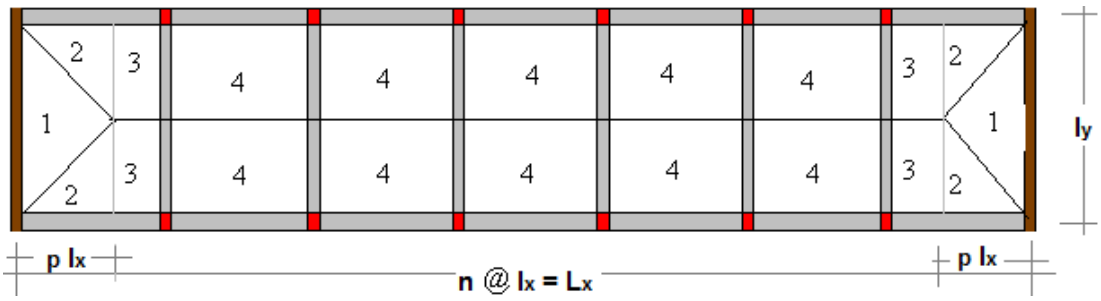

Figure 3.4: Yield line pattern of the slab failing in the Global-Collapse Mechanism

The work done by the external uniform area load of intensity (w) can be determined by multiplying the total load acting at the center of gravity of each segmental area of the collapse mechanism by a distance moved in the direction of the load due to a kinematically admissible arbitrary displacement (δ) given to the yield line pattern. The external work done by various slab segments are given below:

$$\text{Slab segment -1} = \frac{\delta\, w\, p\, r_p\, l_x^2}{6}$$

$$\text{Slab segment -2} = \frac{\delta\, w\, p\, r_p\, l_x^2}{12}$$

$$\text{Slab segment -3} = \frac{\delta\, w(1-p)\, r_p\, l_x^2}{4}$$

$$\text{Slab segment -4} = \frac{\delta\, w\, r_p\, l_x^2}{4}$$

Therefore the total external work done, EWD can be determined by summing up the individual contribution of all collapsed segments of the slab-system (see *Figure 3.4*).

$$EWD = 2\left[\frac{\delta\, w\, p\, r_p\, l_x^2}{6}\right] + 4\left[\frac{\delta\, w\, p\, r_p\, l_x^2}{12}\right] + 4\left[\frac{\delta\, w(1-p)\, r_p\, l_x^2}{4}\right] + 2(n-2)\left[\frac{\delta\, w\, r_p\, l_x^2}{4}\right]$$

$$\text{or } EWD = \frac{\delta\, w\, r_p\, l_x^2}{6}(3n - 2p) \qquad (3.1)$$

The internal work performed by the ultimate resisting moments in slab, m_{ux} and m_{uy} at the common edges of adjoining slab segments and at the plastic hinge formed at the point of maximum moment, m_b in the supporting beams can be obtained from the work-equation (2.12) *i.e.* $\sum m_{un}\, \theta_n\, l_o = \sum m_{ux}\, \theta_x\, l_y + \sum m_{uy}\, \theta_y\, l_x$.

$$\text{At edge of segment -1} = m_{ux}\, \theta_x\, l_y = m_{ux}\, l_y \frac{\delta}{p l_x} = \frac{m_{ux}\, \delta\, r_p}{p}$$

$$\text{At edge of segment - 2} = m_{uy}\,\theta_y\,p l_x = \mu\, m_{ux}\,p l_x\,\frac{\delta}{l_y/2} = \frac{2\mu\, p\delta\, m_{ux}}{r_p}$$

$$\text{At edge of segment - 3} = m_{uy}\,\theta_y\,(1-p) l_x = \mu\, m_{ux}\,(1-p) l_x\,\frac{\delta}{l_y/2} = \frac{2\mu\,(1-p)\delta\, m_{ux}}{r_p}$$

$$\text{At edge of segment - 4} = m_{uy}\,\theta_y\,l_x = \mu\, m_{ux}\,l_x\,\frac{\delta}{l_y/2} = \frac{2\mu\,\delta\, m_{ux}}{r_p}$$

$$\text{At plastic hinge of beam} = m_b\,\theta_y = m_b\,\frac{\delta}{l_y/2} = \frac{2\,m_b\,\delta}{l_y} = \frac{2\,m_b\,\delta}{r_p\,l_x}$$

Therefore total internal work done, IWD by the ultimate positive resisting moments in the slab-system acting along the yield lines of the mechanism and at the plastic hinge of the supporting beams can be determined by summing their individual contribution. This has been given in equation (3.2).

$$\text{IWD} = 2\left[\frac{m_{ux}\,\delta\, r}{r_p}\right] + 4\left[\frac{2\,\mu\, p\, m_{ux}\,\delta}{r_p}\right] + 4\left[\frac{2\,\mu\, m_{ux}(1-p)\delta}{r_p}\right] + 2(n-2)\left[\frac{2\,\mu\, m_{ux}\,\delta}{r_p}\right] + 2(n-2)\left[\frac{2m_b\delta}{r_p\,l_x}\right]$$

$$\text{or IWD} = 2\,m_{ux}\,\delta\, r\left[\frac{1}{p} + \frac{2\,\mu\, n}{r_p^2} + \frac{2\,(n-1)\alpha_b}{r_p^2}\right] \qquad (3.2)$$

In equation (3.2), $\alpha_b\left(=\dfrac{m_b}{m_{ux}\,l_x}\right)$ is the beam-strength parameter of the slab-system and r_p ($= l_y/l_x$) is aspect ratio of the slab-panel of the slab-beam system.

The internal work performed by the ultimate negative resisting moments (continuity-moments) acting along the non-yielding edges on the outer boundary of the slab-system can also be determined from the work-equation given in equation (2.12).

$$\text{Along x - axis of slab} = (2\,i_x\, m_{uy})\,n l_x\,\theta_y$$

$$\text{Along y - axis of slab} = (2\,i_y\, m_{ux})\,l_y\,\theta_x$$

$$\text{and at negative plastic hinge of beam} = 2(n-1)\,k\,m_b\,\theta_y = 2(n-1)\,k\alpha_b\,m_{ux}\,l_x\,\theta_y$$

Similarly the total internal work done, IWD by the ultimate negative resisting moments acting along the outer non-yielding edges of the slab-system can be determined by summing up their individual contribution. The final expression for the total internal work by stress-resultants induced at outer edges of the slab is given in equation 3.3.

$$= \left(2\,i_x\ \mu\, m_{ux}\right) n l_x \frac{\delta}{l_y/2} + \left(2\,i_y\ m_{ux}\right) l_y \frac{\delta}{p l_x} + 2\left(n\text{-}1\right) k\alpha_b\ m_{ux}\ l_x \frac{\delta}{l_y/2}$$

$$= \left[\mu\, m_{ux}\left(2\,i_x\right)\frac{2\,\delta\, n}{r_p}\right] + \left[m_{ux}\left(2\,i_y\right)\frac{\delta\, r_p}{p}\right] + \left[2\left(n\text{-}1\right) k\alpha_b\ m_{ux}\ \frac{2\delta}{r_p}\right]$$

$$= 2\, m_{ux}\, \delta\, r_p \left[\left(2\,i_x\right)\frac{\mu\, n}{r_p^2} + \left(2\,i_y\right)\frac{1}{2p} + 2\left(n\text{-}1\right)\frac{k\alpha_b}{r_p^2}\right] \qquad (3.3)$$

Therefore, the total internal work performed by the ultimate resisting moments in the slab at both positive and negative yield lines of the collapse mechanism and at the position of the plastic hinge in beams respectively can be obtained by adding equation (3.2) and equation (3.3). The final expression of the internal work performed by the internal system of forces in the slab-system is given in equation (3.4).

$$= 2\, m_{ux}\, \delta\, r_p \left[\frac{1}{p} + \frac{2\,\mu\, n}{r_p^2} + \left(2\,i_x\right)\frac{\mu\, n}{r_p^2} + \frac{2\left(n-1\right)\alpha_b}{r_p^2} + \frac{2\left(n-1\right) k\alpha_b}{r_p^2} + \left(2\,i_y\right)\frac{1}{2p}\right]$$

$$= 2\, m_{ux}\, \delta\, r_p \left[\left(2+2\,i_x\right)\frac{1}{2p} + \left(2+2\,i_y\right)\frac{\mu\, n}{r_p^2} + 2\left(n\text{-}1\right)\left(k+1\right)\alpha_b\ \frac{1}{r_p^2}\right]$$

$$\text{or IWD} = 2\, m_{ux}\, \delta\, r_p \left[\frac{d}{2p} + \frac{\mu\, n\, e}{r_p^2} + \frac{2\,f}{r_p^2}\right] \qquad (3.4)$$

In equation (3.4), d, e, and f are the continuity-constants of the slab-beam system that depend upon the continuity conditions at its outer boundaries and the beam-strength parameter of the slab-system. The expressions of these constants are given below:

$d = 2\left(1 + i_x\right)$;

$e = 2\left(1 + i_y\right)$;

And, $f = \alpha_b\left(n\text{-}1\right)\left(k+1\right)$

The equilibrium of the slab-beam system can be ensured by equating the work done by the external set of loading (w) with that produced by the internal moment field (m_{ux}, m_{uy} and m_b) induced in the slab-system in moving through a small virtual kinematically admissible displacement field (δ). The final expression of the slab moment, m_{ux} is given in equation (3.6). This has been obtained by equating the equation (3.1) with equation (3.4).

$$\Rightarrow \frac{\delta\, w\, r_p\, l_x^2}{6}(3n - 2p) = 2\, m_{ux}\, \delta\, r_p \left[\frac{d}{2p} + \frac{\mu\, n\, e}{r_p^2} + \frac{2f}{r_p^2}\right] \tag{3.5}$$

$$\text{or } m_{ux} = \frac{(3n - 2p)}{\left(\frac{d}{2p} + \frac{\mu\, n\, e}{r_p^2} + \frac{2f}{r_p^2}\right)} \frac{w\, l_x^2}{12} \tag{3.6}$$

Equation (3.6) has been further simplified to a more workable form in equation (3.7).

$$m_{ux} = \frac{(3n - 2p)}{\left[\frac{1}{2p} + \left(\frac{\mu\, n\, e + 2f}{d\, r_p^2}\right)\right]} \frac{w\, l_x^2}{12\, d}$$

$$\text{or} \quad m_{ux} = \frac{(3n - 2p)}{\left(\frac{1}{p} + 2\beta\right)} \frac{w\, l_x^2}{6d} \tag{3.7}$$

In equation (3.7), $\beta \left(= \frac{\mu\, n\, e + 2f}{d\, r_p^2}\right)$ is a *slab-beam parameter* of the slab-system that depends upon the aspect ratio (r_p) of the slab-panel, orthotropy (μ), number of panels (n) into which the slab-system has been divided and boundary conditions at outer edges of the slab-system in addition to the strength of internal beams.

The equation (3.7) will give the maximum value of the positive resisting moment (m_{ux}) in the slab only, if $\frac{\partial m_{ux}}{\partial p} = 0$ along with a negative value of the second derivative of the moment field (m_{ux}). This condition can be achieved by solving the quadratic expression given in the equation (3.8).

$$\frac{\frac{\partial}{\partial p}(3n - 2p)}{\frac{\partial}{\partial p}\left(\frac{d}{2p} + \frac{\mu\, n\, e}{r_p^2} + \frac{2f}{r_p^2}\right)} = \frac{(3n - 2p)}{\left(\frac{d}{2p} + \frac{\mu\, n\, e}{r_p^2} + \frac{2f}{r_p^2}\right)}$$

$$\text{or} \quad 3n - 2p = \frac{4p^2}{d}\left(\frac{d}{2p} + \frac{\mu\, n\, e}{r_p^2} + \frac{2f}{r_p^2}\right)$$

$$\text{or} \quad \left(\frac{4\mu\, n\, e}{d\, r_p^2} + \frac{8f}{d\, r_p^2}\right)p^2 + 4p - 3n = 0$$

$$\text{or} \quad 4\beta p^2 + 4p - 3n = 0 \tag{3.8}$$

The p-value defining the position of the branching point of the yield line pattern of the slab at collapse can be calculated by solving the quadratic equation given in the equation (3.8). The solution of this quadratic equation is given in equation (3.9).

$$\Rightarrow \quad p = \frac{-4 \pm \sqrt{4^2 + 4 \times 4\beta \times 3n}}{2 \times 4\beta}$$

$$\text{or} \quad p = \frac{\sqrt{1 + 3n\beta} - 1}{2\beta} \tag{3.9}$$

Equation (3.9) can be simplified into a more workable form by combining two variables of the slab-system *viz:* n and β into a single parameter called as *slab-parameter*, A ($= \sqrt{1 + 3n\beta}$). This expression is given in equation (3.10).

$$p = \frac{3n}{2}\left(\frac{A - 1}{A^2 - 1}\right) = \frac{3n}{2(A + 1)} \tag{3.10}$$

Equation (3.10) defines the exact shape of the yield line pattern for a reinforced concrete slab failing in the global-collapse mechanism. In this failure mode, the supporting beams will allow the yield line in the slab to pass through it at the point of the plastic hinge which will develop at the point of maximum moment in the supporting beams, simultaneously, along with the yield line pattern in the slab. It is interesting to note that equation (3.10) is valid whether branching point of the yield line intersect the internal beam or crosses it. This is due to the fact that the work dissipated along the single plastic hinge in case of an intersection or along two plastic hinges forming at the point of crossing in the beam will be same.

The maximum value of the positive ultimate slab moment (m_{ux}) of the slab-beam system can be obtained by substituting the p-value from equations (3.9) into equation (3.7). The final expression for the maximum value of the moment-field (m_{ux}, m_{uy}) is given in equation (3.11). This expression has been written in term of long-span (L_x) of the slab-beam system to simplify the equation which otherwise will contain one more parameter namely aspect ratio (r) of the slab-system.

$$m_{ux} = \left(\frac{3}{A + 1}\right)^2 \frac{w L_x^2}{12d}$$

$$\text{And } m_{uy} = \mu m_{ux} = \left(\frac{3}{A+1}\right)^2 \frac{\mu\, w\, L_x^2}{12d} \tag{3.11}$$

The value of the slab parameter (A) for the single panel slab with aspect ratio of unity becomes equal to two, thereby giving the slab moment (m_{ux}) that compare favorably well with the results available in the literature [*Johansen (1967)*] for the single-panel square slab with the orthotropy of unity.

Therefore, the rectangular reinforced concrete slab continuous over the non-yielding edges over its outer boundary and cast monolithic with the internal equally spaced shallow beams under a out-of-plane uniform area load (w) over its entire face can be designed using equation (3.11) for any values of internal panels (n), the orthotropy (μ), the beam-strength parameter (α_b). The value of the beam-strength parameter (α_b) of the slab-system should be selected in such a manner that the slab-beam system must fail in the global-collapse mechanism at collapse. This collapse mechanism is considered desirable in comparison to the local-collapse mechanism of the slab-beam system because of a simple detailing requirement of the reinforcement in the slab and consequently less wastage due to the absence of negative reinforcement. Slab-beam system designed in the global-failure mechanism is relatively more economical in comparison to slab designed for a local-collapse mode. In former case, there is no need to provide any reinforcement at the top face of the slab normal to the internal beams while it is mandatory to use this reinforcement in the later case as negative yield line always forms at the top face of the slab due to sudden change in the curvature across the internal stiff beams.

This condition can be checked by calculating the ultimate resisting moment of the slab-beam system failing in the local-collapse mechanism at collapse and comparing this value of the moment with that obtained from the equation (3.11). It is mathematically simple and easier to formulate expressions if the moment field is selected instead of basing expressions and calculation on the collapse load (w) of the system for comparison and interpretation of results. The slab-beam system would fail in the global-collapse mechanism only if the value of the slab moment (m_{ux}) in this failure mode is more than that obtained from the failure of the slab-beam system in the local-collapse mechanism.

The beam-system converts into a set of number of smaller isolated rectangular slabs if the internal beams are sufficient strong and/or stiff that lead to the formation of a local-collapse mechanism. These smaller slabs rest over the internal beams after the formation of the local-collapse mechanism. Thus, the slab-beam system will consist of a number (n)

of smaller isolated rectangular slabs with aspect ratio (R) at collapse. The ultimate moment (m_{ux}) of these smaller rectangular slabs is calculated in following section.

3.4.3.1: Moment Field for a single panel rectangular slab continuous at edges.

A single panel rectangular slab along with notations for the geometry and moment field required to be developed in the slab for its equilibrium under a uniform load, w is shown in *Figure 3.5*. Three unknown dimensions define the shape of the local-collapse mechanism being developed in the slab resting over the non-yielding edges at its outer boundary. Four equations required for the solution of the slab can be obtained by considering the equilibrium of each segment by taking moments about the non-yielding edge of the segment.

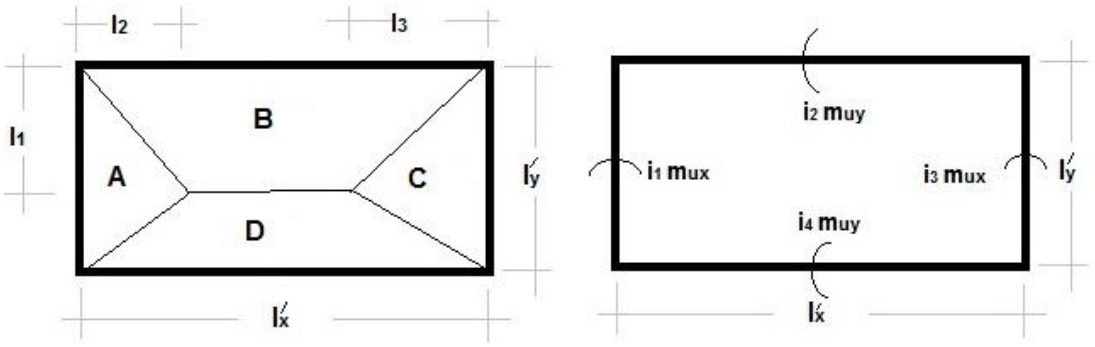

Figure 3.5: Schematic diagram of single slab continuous over edges

1) Segment-A: $(1+i_1)m^1_{ux}l^1_y = \frac{wl^1_y l^2_2}{6}$

2) Segment-B: $(1+i_2)m^1_{uy}l^1_x = \frac{wl_2l^2_1}{6} + \frac{wl_3l^2_1}{6} + \frac{w(l^1_x - l_2 - l_3)l^2_1}{6}$

3) Segment-C: $(1+i_3)m^1_{ux}l^1_y = \frac{wl^1_y l^2_3}{6}$

4) Segment-D: $(1+i_4)m^1_{uy}l^1_x = \frac{wl_2(l^1_y - l_1)^2}{6} + \frac{wl_3(l^1_y - l_1)^2}{6} + \frac{w(l^1_x - l_2 - l_3)(l^1_y - l_1)^2}{2}$

By combining the equations at serial no. 1 and 3, relationship between the parameter l_2 and l_3 can be obtained. This has been given below:

$$l_2 = l_3\sqrt{\frac{1+i_1}{1+i_3}}$$

Similarly, a relationship between the parameters l_1 and l^1_y can be obtained by combining equations at serial no. 2 and 4. This has been given below:

$$l_1 = l_y^1 \frac{\sqrt{1+i_2}}{\sqrt{1+i_2}+\sqrt{1+i_4}}$$

By substituting the values of l_1, l_2 into the equations at serial no. 2 and further simplifying this expression along with equation at serial no. 3 will give the expression for the moment, m_{uy}^1 in the slab of aspect ratio, R. This has been given below:

$$m_{uy}^1 = \frac{R^2\left[\sqrt{\left(\frac{X}{Y}\right)^2 + \frac{3\mu}{R^2}} - \left(\frac{X}{Y}\right)^2\right]^2}{\mu Y^2} \frac{w{l_y^1}^2}{6}$$

The values of constants X and Y in the above expression can be obtained from following expressions. The *i-values* define the continuity-moments at outer boundary of the slab.

$X = \sqrt{1+i_1} + \sqrt{1+i_3}$, And $Y = \sqrt{1+i_2} + \sqrt{1+_4}$

The above equation can be further simplified to a more workable expression given below:

$$m_{uy}^1 = \frac{R^2\left[\left(\frac{X}{Y}\right)\sqrt{1+\frac{3\mu}{R^2}\left(\frac{Y}{X}\right)} - \left(\frac{X}{Y}\right)^2\right]^2}{\mu Y^2} \frac{w{l_y^1}^2}{6}$$

$$m_{uy}^1 = \frac{R^2\left(\frac{X}{Y}\right)\left[\sqrt{1+\frac{3\mu}{R^2}\left(\frac{Y}{X}\right)} - 1\right]^2}{\mu Y^2} \frac{w{l_y^1}^2}{6}$$

Let $\gamma = \frac{X}{Y}$ and the slab-constant for the single panel slab, $\beta_1 = \frac{\mu^1}{R^2\gamma^2}$. By using these notations, the above equation can be further simplified.

$$m_{uy}^1 = \frac{\gamma^2\left(\sqrt{1+3\beta_1} - 1\right)^2}{X^2\beta_1} \frac{w{l_y^1}^2}{6}$$

The final expression for the slab moment, m_{uy}^1 induced under a uniform load, w in a single panel rectangular slab continuous over its outer non-yielding boundary can be written in term of the slab-parameter ($A_1 = \sqrt{1+3\beta_1}$); given in equation (3.12).

$$m_{uy}^1 = \left(\frac{A_1 - 1}{A_1 + 1}\right)\frac{w\,{l_y^1}^2}{2Y^2} \qquad (3.12)$$

In equation (3.12), the long span (l_x^1) and the short span (l_y^1) of smaller rectangular slabs should be replaced by the short span (l_y) and the panel length (l_x) of the slab-beam

system respectively in calculating its aspect ratio, R and moment capacity, m_{uy}^1. In other words, aspect ratio (R) of the smaller rectangular slab formed in the panel of the slab-beam system can be converted into the aspect ratio, r (= l_y/L_x) of the slab-beam. The modified expressions that can be used for the calculation of aspect ratio and moment capacity of these smaller rectangular slabs are given below:

$$R = \frac{l_y^1}{l_x^1} = \frac{l_x}{l_y} = \frac{l_x}{r\,L_x} = \frac{1}{n\,r}$$

And slab moment, $m_{uy}^1 = \left(\frac{A_1 - 1}{A_1 + 1}\right)\frac{w\,l_x^2}{2Y^2}$ (3.13)

Moreover, the reinforcement provided along the long span, L_x and the reinforcement provided along the short span, l_y of the slab-beam system will be the reinforcement provided along the short span, l_y^1 and the long span, l_x^1 of the smaller rectangular slabs respectively. This condition can be used to calculate the orthotropy, μ^1 of the smaller rectangular slabs from the orthotropy, μ of the main slab-beam system. The final expression for this conversion is given below:

$$\mu^1 = \frac{1}{\mu}$$

Therefore, the value of the slab-constant, β_1 and the corresponding value of the slab-parameter, A_1 ($= \sqrt{1+3\beta_1}$) for these smaller rectangular slabs can be calculated form the following expression before determining the moment, m_{uy} from equation (3.13).

$$\beta_1 = \frac{\mu^1}{R^2\gamma^2} = \frac{(nr)^2}{\mu\gamma^2}$$

The relative magnitude of the moment field given by equation (3.11) and equation (3.13) would determine the failure mode of the slab-beam system. The slab would fail in the global-collapse mechanism only if the moment capacity of the slab given by equation (3.11) is more than that predicted by equation (3.13). Otherwise, the same slab would fail following the local-collapse mechanism.

Special Case-1: *Slab-beam system with no negative reinforcement over the internal beams and the outer boundaries along its short span (l_y).*

For this case, the values of the continuity parameter (*i-values*) and the corresponding values of the parameter X and Y are simplified and these are given below.

$i_2 = i_4 = 0$

$i_1 = i_3 = i_x$

$\Rightarrow Y = 2$

$\Rightarrow X = 2\sqrt{1+i_x}$

And, $\gamma = \dfrac{X}{Y} = \dfrac{2\sqrt{1+i_x}}{2} = \sqrt{1+i_x}$, thereby giving $\beta_1 = \dfrac{(nr)^2}{\mu(1+i_x)}$

The modified value of β_1 will give a new value of the slab-parameter (A_1) for calculating the value of moment, m_{uy}^1.

$$m_{uy}^1 = \left(\frac{A_1 - 1}{A_1 + 1}\right)\frac{w\, l_x^2}{8} \tag{3.14}$$

Special Case-2: *Slab-beam system with no negative reinforcement over the internal beams and some negative reinforcement over the outer boundaries defined by* $\boldsymbol{i_x}$ *and* $\boldsymbol{i_y}$.

The moment field in the internal panels of the slab-beam system can be calculated from the equation (3.14) as there is no reinforcement over the beams (normal to the beam axis) provided along the short span (l_y) of the slab-beam system.

The moment field in the end panels of the slab-beam system can be determined from equation (3.13) by substituting the corresponding values of *i-values*. This has been given below.

$i_2 = 0$;

$i_4 = i_y$

$i_1 = i_3 = i_x$

$\Rightarrow X = 2\sqrt{1+i_x}$

$\Rightarrow Y = \sqrt{1+i_y}$

And, $\gamma = \dfrac{X}{Y} = 2\sqrt{\dfrac{1+i_x}{1+i_y}}$, thereby giving $\beta_1 = \dfrac{(nr)^2}{4\mu}\left(\dfrac{1+i_y}{1+i_x}\right)$

The modified value of β_1 will give a new value of the slab-parameter (A_1) for finding m_{uy}^1.

$$m_{uy}^1 = \left(\frac{A_1 - 1}{A_1 + 1}\right)\frac{w\, l_x^2}{2(1+i_y)} \tag{3.15}$$

Higher value of the moment field given by equations (3.14 and 3.15) in the interior and end panel of the slab-beam system respectively should be used for the comparison purpose with the moment value given by equation (3.11).

Special Case-3: *Slab-beam system with some negative reinforcement defined by parameter* $\boldsymbol{i_i}$ *over the internal beams and another set of some negative reinforcement over the outer boundaries defined by* $\boldsymbol{i_x}$ *and* $\boldsymbol{i_y}$.

The moment field in interior panels of the slab-beam system can be determined from equation (3.13) by substituting the corresponding values of *i-values*. This has been given below.

$i_2 = i_4 = i_i$

$i_1 = i_3 = i_x$

$\Rightarrow X = 2\sqrt{1+i_x}$

$\Rightarrow Y = 2\sqrt{1+i_i}$

And, $\gamma = \dfrac{X}{Y} = 2\left(\sqrt{\dfrac{1+i_x}{1+i_i}}\right)$, thereby giving $\beta_1 = \dfrac{(nr)^2}{4\mu}\left(\dfrac{1+i_i}{1+i_x}\right)$

The modified value of β_1 will give a new value of the slab-parameter (A_1) for finding m_{uy}^1.

$$m_{uy}^1 = \left(\frac{A_1 - 1}{A_1 + 1}\right)\frac{w\, l_x^2}{2(1+i_i)} \tag{3.16}$$

And, the moment field in end panels of the slab-beam system can also be determined from equation (3.13) by substituting the corresponding values of *i-values*. This has been given below.

$i_2 = i_i$

$i_4 = i_y$

$i_1 = i_3 = i_x$

$\Rightarrow X = 2\sqrt{1+i_x}$

$\Rightarrow Y = \sqrt{1+i_y} + \sqrt{1+i_i}$

And, $\gamma = \dfrac{X}{Y} = 2\left(\dfrac{\sqrt{1+i_x}}{\sqrt{1+i_i} + \sqrt{1+i_y}}\right)$, thereby giving $\beta_1 = \dfrac{(nr)^2}{\mu\gamma^2}$

The modified value of β_1 will give a new value of the slab-parameter (A_1) for finding m_{uy}^1.

$$m_{uy}^1 = \left(\frac{A_1 - 1}{A_1 + 1}\right)\frac{w\, l_x^2}{2Y^2} \tag{3.17}$$

Higher value of the moment field given by equations (3.16 and 3.17) in the interior and end panel of the slab-beam system respectively should be used for the comparison purpose with the moment value given by equation (3.11).

3.4.3.2 Strength Requirement of the Supporting-Beams

The strength requirement of the internal supporting-beams of the slab-beam system depend upon the beam-strength parameter, α_b (= $m_b/m_{ux}\, l_x$) for any given value of the slab moment capacity (m_{ux}) and the panel length (l_x) of the slab-beam system. Therefore, the strength requirement of the supporting-beams of the slab-beam system can be calculated by substituting the expression of the slab moment (m_{ux}) from the equation (3.11). This has been given in equation (3.18) in term of the slab-parameter (A).

$$m_b = \alpha_b m_{ux} l_x$$

$$m_b = \left\{\left(\frac{n}{n-1}\right)\left[\frac{\left(A^2-1\right)r^2}{3} - \mu\right]\right\} x \left[\left(\frac{3}{A+1}\right)^2 \frac{w L_x^2}{12d}\right]\frac{L_x}{n}$$

$$m_b = \left[\left(\frac{A-1}{A+1}\right)r^2 - \frac{3\mu}{(A+1)^2}\right]\frac{w L_x^3}{(n-1)4d} \qquad (3.18)$$

Therefore, the design moment field (m_{ux}, m_{uy}= μ m_{ux}, and m_b) in the laterally loaded slab-beam system can be obtained from equation (3.11) and equation (3.18) for any valid value of the slab-parameter (A). The minimum value of the slab-parameter (A) can be calculated from the equation (3.18) so that the slab-beam system must have a positive-non-zero supporting-beam moment capacity ($m_b > 0$). Otherwise the same slab-beam system would start behaving as an ordinary single panel rectangular slab. The moment field for this type of slab-beam system (with $m_b = 0$) compares favorably well with the results obtained from the well-established formulae of the slab analysis. The value of the slab-parameter (A) required for this condition can be obtained by equating expression in the equation (3.18) to a zero. The final expression for the minimum value of the slab-parameter (A) is given in equation (3.19), which depends only upon the aspect ratio (r) of the slab-beam system and its orthotropy (μ).

$$A_{min} = \sqrt{\frac{3\mu}{r^2} + 1} \qquad (3.19)$$

Therefore, the lower limit of the slab-parameter, A_{c1} can be determined by limiting the lowest value of the slab-parameter (A) to a value determined from equation (3.19). This lower limit will ensure that the slab-beam system must have supporting-beams of adequate strength to enable the slab-beam system to form a global collapse mechanism in the entire slab-system.

The final expression of the lower limit of the slab-parameter (A_{c1}) is given in equation (3.20). If the slab-system has been proportioned at value of slab-parameter (A) less than its lower limit, it will always act as a single panel slab of size L_x x l_y.

$$A_{c1} = \sqrt{\frac{3\mu}{r^2} + 1} \tag{3.20}$$

The expression in equation (3.18) can be further simplified to a more workable form by combining equation (3.20) and equation (3.18). This is given in equation (3.21).

$$m_b = \left\{ \frac{\left(A^2 - A_{c1}^2\right)}{\left(A+1\right)^2} \right\} \frac{w\ l_x^2\ L_x}{\left(n-1\right) 4d} \tag{3.21}$$

Equation (3.11) and equation (3.21) define the moment field in the rectangular slab cast monolithic with internal equally spaced shallow beams and resting over the non-yielding edges at its outer boundaries. The relative magnitude of the moment field (m_{ux}, $m_{uy} = \mu\ m_{ux}$ and m_b) defined by equation (3.11) and equation (3.13) will dictate the failure mode of the slab-beam system under a uniform area load (w) depending upon the values of the continuity constants defined through *i-values*. Different cases arising for various combinations of *i-values* are given in equations (3.14 to 3.17). Accordingly, there is a probability of a formation of following two types of collapse-mechanisms in the slab-beam system at collapse depending upon the value of the slab-parameter (A).

3.4.3.3 Global Collapse Mechanism

If the slab-beam system fails by the formation of a yield line pattern in the slab and the plastic hinge in the supporting beams simultaneously at collapse, it will lead to the formation of a *global collapse mechanism* in the slab-system. The slab will fail in this collapse mechanism only if the moment-capacity of the slab given by equation (3.11) is more than that predicted by equation (3.13). The beam-strength parameter, α_b of the slab-beam system will play a significant role in controlling the behavior of the slab under increasing load and its subsequent collapse at the ultimate state if all other slab constants are taken as constant. The schematic diagram of this failure mode is shown in *Figure 3.2*.

3.4.3.4 Local Collapse Mechanism

If the slab-beam system fails with the formation of a yield line pattern, locally and simultaneously, in all panels of the slab under the external loading and each panel of the slab behaves as isolated rectangular slabs separated by the internal shallow supporting beams, the failure mode of the slab system will be called as local-collapse mechanism.

This would happen only if the supporting beams are strong enough that do not allow the positive yield lines in the slab to cross through into the adjacent panels of the slab-beam system, thus leading to the formation of a yield line pattern, locally, in all panels of the slab-beam system at collapse load. This type of collapse mechanism will form only if the moment-capacity of the slab given by equation (3.11) is less than that predicted by the equation (3.13). The supporting beams with very high value of beam-strength parameter, α_b is required for this collapse mechanism to develop in the slab at ultimate state. The schematic diagram of this failure mode is shown in *Figure 3.3*.

3.5 CRITICAL BEAM-STRENGTH PARAMETER

It is indicated in equations (3.11 to 3.17) that the moment field (m_{ux}, m_{uy} and m_b) induced in any slab-beam system under the external load depends only on the slab-beam parameter (β) irrespective of the failure mode. The value of slab-beam parameter in turn depends mainly upon the beam-strength parameter (α_b) for a given set of slab geometrical parameters viz. aspect ratio, number of panels and orthotropy of the slab-beam system. In other words, beam-strength parameter (α_b) is the only parameter that dictates the failure mode of the slab-beam system at the collapse and the value of beam-strength parameter (α_b) at which the failure mode of the reinforced concrete slab-beam system changes from the global-collapse mechanism to the local-collapse mechanism is called as *critical beam-strength parameter* (α_{bc}). This parameter defines the minimum strength of the supporting beams that leads to the simultaneous formation of the global and local-collapse mechanism in the laterally loaded slab-beam system at collapse.

The slab-beam system would fail in the local-collapse mechanism if it has been designed with the value of beam-strength parameter (α_b) more than the critical value of the beam-strength parameter (α_{bc}). The value of the slab-parameter (A) at which the laterally loaded slab-beam system fail by the formation of the global-collapse mechanism and the local-collapse mechanism, simultaneously, at the collapse can be determined by equating the equation (3.11) and equations (3.13 to 3.17) for various cases depending upon the values of continuity parameters (i-values) at boundary of the internal panels and it will define the upper limit of the slab-parameter (A_{c2}). The upper limit of the slab-parameter (A_{c2}) will ensure that the slab-beam system would sustain the lateral load (w) in the global-collapse mechanism mode if it has been designed with the slab-parameter, $A < A_{c2}$ otherwise it will collapse in the local-collapse mechanism.

The value of the critical beam-strength parameter (α_{bc}) of the slab-beam system can be determined from a resultant equation formed after equating the expressions given by equation (3.11 to 3.17), when the value of the slab-parameter (A) in the equation, $A = \sqrt{1+3n\beta}$ approaches its upper limit (A_{c2}). At this stage, the slab-beam parameter (β) of the slab-beam system would approach its limiting value (β_c).

$$A_{c2} = \sqrt{1+3n\beta_c}$$

$$\text{or } \beta_c = \frac{A_{c2}^2 - 1}{3n} = \frac{\mu n + (n-1)\alpha_{bc}}{n^2 r^2}$$

$$\text{or } \alpha_{bc} = \left(\frac{n}{n-1}\right)\left\{\frac{\left(A_{c2}^2 - 1\right)r^2}{3} - \mu\right\} \tag{3.22}$$

Equation (3.22) can be simplified to a more workable form by combining it with equation (3.20) and the final form of the expression is given in equation (3.23).

$$\alpha_{bc} = \frac{r^2}{3}\left(\frac{n}{n-1}\right)\left[A_{c2}^2 - A_{c1}^2\right] \tag{3.23}$$

Thus, the slab-beam system would fail in the global-collapse mechanism only if the value of the slab-parameter (A) lies in the range given by the lower limit; equation (3.20) and the upper limit; defined by A_{c2}. Otherwise, it would lead to the formation of a local-collapse mechanism in the slab-beam system. Equations (3.22) or (3.23) can also be used to calculate the value of the beam-strength parameter (α_b) of the slab-beam system by substituting a suitable value of the slab-parameter, A in place of A_{c2} from the valid range of A-values.

The expressions for the upper limit of slab-parameter (A_{c2}) can be determined by equating equation (3.11) with equation (3.13). The simplified expression for A_{c2} is given in equation (3.24) for a general case of a slab-beam system with edge conditions defined through a parameters Y and d.

$$\left(\frac{3}{A_{c2}+1}\right)^2 \frac{\mu n^2 w l_x^2}{12d} = \left(\frac{A_1 - 1}{A_1 + 1}\right)\frac{w l_x^2}{2Y^2}$$

$$\text{or } A_{c2} = nY\sqrt{\frac{3\mu}{2d}\left(\frac{A_1+1}{A_1 - 1}\right)} - 1 \tag{3.24}$$

Equation (3.24) has been simplified for the special case-2 (slab-beam system having some negative steel at its outer boundary and no reinforcement over the internal beams)

of section 3.4.3.1 and it has been given in equation (3.25). This case will cover the most of the design problems for the slab-beam system with shallow beams proportioned in the global-collapse mode. In this case, no negative moment field will induce in the slab along and normal to the beam axis and according, there is no need to use negative steel for this moment field at top face of the slab.

$$A_{c2} = n\sqrt{\frac{3\mu}{4}\left(\frac{e}{d}\right)\left(\frac{A_1+1}{A_1-1}\right)} - 1 \qquad (3.25)$$

An algorithm was developed using these equations to determine the value of critical beam-strength parameter. It will generate a set of data consisting of moment coefficients (m_{ux}) against the different values of beam-strength parameter (α_b), aspect ratio of the slab ($r = l_y/L_x$) and number of panels for a predefined value of the orthotropy. Value of the beam-strength parameter is sorted out from this data against the last possible value of moment coefficient at which failure mode of the slab-beam system changes from the global-collapse mechanism to the local-collapse mechanism and this process is repeated for the predefined values of the orthotropy.

The valid values of critical beam-strength parameter of the slab-beam system resting over the simple supports at its outer boundary and without any negative reinforcement in the slab normal to the internal shallow beams that satisfies the lower and the upper limits of slab-parameter are tabulated in Table 3.1 to Table 3.6 for some selective values of the slab orthotropy. However, the equation (3.22) or the equation (3.23) can be used in practice very easily to determine the value of the critical beam-strength parameter of the slab-beam system for any desired value of the slab orthotropy and number of slab panels.

The values of critical-beam strength parameter can be determined for the value of the orthotropy required to maintain the elastic distribution of the moment field in the slab-beam system and this value of orthotropy can be obtained from equation (3.26) for a slab-beam system having internal beams of depth less than *span/20*. This equation has been derived from the regressional analysis of the bending moment coefficients suggested by Levy [*Timoshenko and Krieger (1959)*]. Charts are also prepared from a parametric study of a large number of rectangular slabs by taking depth of the beam as one of the parameter. These charts are given in Appendix-C for finding the tentative value of the orthotropy for various values of *span/depth* ratio of internal beams and aspect ratio.

$$\mu = \frac{1.2}{r} - 0.2 \qquad (3.26)$$

3.5.1 Moment-Field Manipulator (λ)

The two values of the beam-strength parameters (α_b and α_{bc}) can be expressed as a single non-dimensional parameter called as the moment-field manipulator (λ). Moment-field manipulator can be used to manipulate/trace the moment-filed in the slab-beam system at any desired strength level of the supporting beams. This non-dimensional parameter (λ) defines the ratio of the moment capacity of the supporting-beams and the moment capacity of the supporting-beams required for the simultaneous formation of a global and a local collapse mechanism in the laterally loaded slab-beam system at collapse.

The slab-beam system can be proportioned and/or analyzed for any value of λ varying from the zero to a unity. If the beam-slab system has been designed with λ-value less than unity, it must fail following the global-collapse mechanism at collapse, otherwise the same slab-beam system would collapse with the formation of a yield line pattern, locally and simultaneously, in all panels of the laterally loaded slab-beam system at the collapse load. At zero λ-value ($A = A_{c1}$), the slab-beam system would behave as a single panel slab failing in the global-collapse mechanism, whereas at the unit λ-value ($A = A_{c2}$), the same slab-system would be divided into a number of interconnected smaller slabs resting over the internal supporting-beams. The value of the slab-parameter (A) for any slab-beam system can be calculated from equation (3.27) corresponding to any arbitrarily chosen λ-value ($0< \lambda <1$) and vice versa.

$$\lambda = \frac{A^2 - A_{c1}^2}{A_{c2}^2 - A_{c1}^2} \tag{3.27}$$

Equation (3.27) has been obtained by modifying equation (3.23). The moment-field manipulator (λ) can be used very conveniently to control the participation of the slab in the load sharing between the supporting beams and the slab of the slab-beam system. At zero λ-value, the slab will behave as a single panel slab resting over the non-yielding edges at outer boundaries of the slab-beam system; whereas at λ=1, the same slab-beam system will be transformed into a system consisting of a number of smaller rectangular slabs simply resting over the internal supporting beams with discontinuous edges. The intermediate values of the moment-field manipulator (λ) in range $0 < \lambda < 1$ will predict the moment-field in the slab-beam system corresponding to some value of the slab-parameter (A) given by equation (3.27). Selecting a low value of the λ can increase the contribution of the slab in load sharing and vice versa.

If the slab has been designed with λ-value less than unity, it must fail following a global-collapse mechanism. Otherwise, the same slab would collapse with the formation of a yield line pattern, locally, in all panels of the slab-beam system at collapse load. The behavior of the supporting beams in this case will be analogous to the non-yielding beams and/or walls although it would show a little bit more deflection in comparison to the case when the same slab has been supported over the non-shallow beams. This type of beam will be termed as a shallow-rigid beam whereas the former type of the supporting beams will be called as shallow-flexible beams. In other words, the behavior of the supporting beams in slab-beam system depends entirely upon the moment-field manipulator (λ) and by selecting a suitable λ-value; the supporting beams can be made to behave as a rigid-support as well as a flexible-support. The supporting slab must be proportioned, accordingly, to carry its due share of the applied surface load.

The proposed analytical model can also be used for the analysis of a multi-panel slab-beam system in both directions. In this case, it must be ensured that the slab must be resting over the non-yielding edges at its outer boundaries. The end restraint at outer boundaries of the slab may be either a simple or a continuous in nature. Moreover for the application of the proposed analytical model, the column spacing along the orthogonal directions of the slab-beam system must be adjusted in a manner that supporting beams along one direction of the slab-beam system must behave as equally spaced shallow beams and as non-shallow beams along the other direction of the column grid. Accordingly the ratio of the column spacing along the orthogonal directions of the slab-beam system must be kept greater than 1.25 to divide the slab into a number of smaller rectangular slabs supported over the internal equally spaced shallow beams and resting over the non-shallow (non-yielding edges) at the outer boundaries of the smaller slabs [*see Figure 3.1B*].

The procedure to decide the column spacing of a two-bay multi-panel slab-beam system is illustrated in the *Chapter 5*.

3.6 SPECIAL CASES-*Slab with Discontinuous Edges at Outer Boundary and without any negative reinforcement over the internal beams:*

The ultimate positive resisting moment of a reinforced concrete rectangular slab resting over the simple and non-yielding edges at its outer boundaries and cast monolithic along with the equally spaced (n-1) number of supporting beams can be derived by a slight modification of equation (3.11).

For a slab resting the over the simple supports at the outer edges and failing in the global-collapse mechanism at ultimate state, the constants in equation (3.11) can be modified for the actual boundary conditions of the slab-system. The value of -***i***'s are zero at all outer edges of the slab-system. If the internal supporting beams along the short span (l_y) of the slab-system are also discontinuous at edges, the ***k***-value is also zero.

$\Rightarrow$ e = d = 2;

And f = (n-1) α_b

The value of the slab-constant, β simplifies to equation (3.28).

$$\beta = \frac{\mu\, n + (n-1)\alpha_b}{r_p^2} \tag{3.28}$$

The corresponding value of the slab-parameter, A ($=\sqrt{1+3n\beta}$) can be calculated from equation (3.28) to determine the slab moment (m_{ux}) form equation (3.29). This has been obtained by modifying equation (3.11).

$$m_{ux} = \left(\frac{3}{A+1}\right)^2 \frac{w\, L_x^2}{24} \tag{3.29}$$

The value of the slab-parameter (A) must lay in the range defined by its lower limit (A_{c1}) and the upper limit (A_{c2}) for the given value of A_1 (of a panel slab), given below:

$$A_{c1} = \sqrt{1+\frac{3\mu}{r^2}}$$

$$A_{c2} = n\sqrt{3\mu\left(\frac{A_1+1}{A_1-1}\right)} - 1 \tag{3.30}$$

The moment capacity required for the supporting beams of the slab-beam system resting over the simple and non-yielding outer boundaries can be obtained by modifying equation (3.21). The modified expression for the strength requirement of the supporting beams, in this case, is given in equation (3.30).

$$m_b = \left\{\frac{\left(A^2 - A_{c1}^2\right)}{(A+1)^2}\right\} \frac{w\; l_x^2\, L_x}{8(n-1)} \tag{3.31}$$

Equations (3.29) and (3.31) completely define the moment field induced in the slab-beam system with discontinuous outer edges for any arbitrarily chosen valid value of the slab-parameter (A) from the range, $A_{c1} < A < A_{c2}$ given in equation (3.30). The slab-beam system would sustain the load in the global-collapse mechanism mode only if the value of the slab-parameter (A) lies in this range. Otherwise, the same slab-beam system will be

either transformed into a single panel slab at the value of the slab-parameter, $A < A_{c1}$ or into the slab-beam system consisting of a number of interconnected smaller slabs resting over the internal supporting beams at $A > A_{c2}$. The shape of the yield line pattern of the slab-beam system can be traced by calculating the p-value from equation (3.9).

3.6.1 Slab-Parameter, $A \geq A_{c2}$

When the value of the slab-parameter (A) approaches its upper limit (A_{c2}), the supporting beam becomes strong enough to initiate the failure of the slab-beam system in the local-collapse mechanism thereby, dividing the slab-beam system into a number of smaller rectangular slabs of size (l_x x l_y) and resting over the internal supporting member (s). The moment capacity of these smaller slabs can be determined from equation (3.29) and the moment capacity of the supporting beams can be calculated from equation (3.30) by substituting the corresponding value of the slab-parameter, $A \geq A_{c2}$.

3.6.2 Slab-Parameter, $A < A_{c1}$

If the slab-beam system has been designed with the value of the slab-parameter (A) less than its lower limit, it will transform into a single panel slab of size (L_x x l_y) and simply resting over the outer non-yielding boundary of the slab-beam system. Equation (3.29) can be used to determine the moment field in the slab by substituting the corresponding value of the slab-parameter, $A < A_{c1}$. In this case, the slab-beam system behaves as a single panel slab resting over the non-yielding supports at the outer boundary.

The results from these two standard cases compare favorably well the results obtained from expressions available in the published literature [*see example 4.3.1*].

3.6.3 Moment field of a skew-slab:

The moment field (m_{ux}, m_{uy}) induced in a skew-slab supported over the non-yielding edges at its outer boundaries can be determined from the equations (3.11) or equation (3.29) by multiplying these equations by a factor $sin^2\theta$; where θ is the skew-angle of the slab [*see Annexure A*].

Table 3.1: Variation of α_{bc} with aspect ratio and orthotropy of 2-Panel Slab

μ_r	0.3	0.5	0.7	0.9	1.1	1.3	1.5	1.7	1.9	2.1
0.2	--	--	--	0.368	1.050	1.950	3.070	4.390	5.940	7.690
0.3	--	--	0.073	0.636	1.420	2.410	3.630	5.060	6.700	8.550
0.4	--	--	0.318	1.010	1.940	3.080	4.440	6.020	7.820	9.830
0.5	--	0.00	0.616	1.480	2.580	3.910	5.460	7.240	9.240	11.50
0.6	--	0.167	0.959	2.020	3.330	4.880	6.670	8.680	10.90	13.40
0.7	--	0.350	1.340	2.630	4.180	5.980	8.030	10.30	12.80	15.60
0.8	--	0.271	1.770	3.300	5.120	7.200	9.540	12.10	15.00	18.00
0.9	--	0.148	2.010	4.030	6.140	8.540	11.20	14.10	17.30	20.70
1.0	--	0.00	2.130	4.630	7.250	9.980	13.00	16.30	19.80	23.70

Table 3.2: Variation of α_{bc} with aspect ratio and orthotropy of 3-Panel Slab

μ_r	0.3	0.5	0.7	0.9	1.1	1.3	1.5	1.7	1.9	2.1
0.2	--	--	0.236	0.700	1.330	2.120	3.070	4.180	5.450	6.880
0.3	--	0.200	0.673	1.320	2.140	3.130	4.290	5.610	7.090	8.730
0.4	--	0.085	1.080	2.130	3.210	4.460	5.890	7.490	9.260	11.20
0.5	--	--	1.060	2.570	4.260	6.070	7.830	9.780	11.90	14.20
0.6	--	--	1.040	2.870	4.920	7.180	9.630	12.30	15.00	17.70
0.7	--	--	0.955	3.170	5.630	8.310	11.20	14.30	17.60	21.20
0.8	--	--	0.823	3.470	6.380	9.540	12.90	16.50	20.30	24.40
0.9	--	--	0.645	3.770	7.180	10.90	14.80	18.90	23.30	27.90
1.0	--	--	0.419	8.020	9.020	12.30	16.80	21.50	26.50	31.80

Table 3.3: Variation of α_{bc} with aspect ratio and orthotropy of 4-Panel Slab

μ_r	0.3	0.5	0.7	0.9	1.1	1.3	1.5	1.7	1.9	2.1
0.2	--	0.187	0.5770	1.120	1.810	2.650	3.650	4.760	6.030	7.450
0.3	--	0.365	1.300	2.160	3.160	4.320	5.630	7.090	8.710	10.50
0.4	--	0.224	1.520	3.000	4.670	6.480	8.220	10.10	12.20	14.40
0.5	--	0.000	1.720	3.660	5.810	8.150	10.70	13.40	16.20	19.10
0.6	--	--	1.910	4.390	7.100	10.00	13.10	16.40	19.90	23.60
0.7	--	--	2.090	5.170	8.500	12.10	15.90	19.90	24.10	28.50
0.8	--	--	2.250	6.020	10.10	14.40	18.90	23.70	28.70	33.90
0.9	--	--	2.400	6.910	11.70	16.90	22.20	27.90	33.70	39.80
1.0	--	--	2.520	7.860	13.60	19.50	25.80	32.40	39.20	46.20

Table 3.4: Variation of α_{bc} with aspect ratio and orthotropy of 5-Panel Slab

μ / r	0.3	0.5	0.7	0.9	1.1	1.3	1.5	1.7	1.9	2.1
0.2	--	0.281	0.962	1.620	2.420	3.360	4.440	5.660	7.010	8.510
0.3	--	0.010	1.160	2.490	3.990	5.640	7.360	9.060	10.90	12.90
0.4	--	--	1.220	3.090	5.160	7.390	9.800	12.40	15.10	18.00
0.5	--	--	1.200	3.730	6.480	9.430	12.60	15.90	19.40	23.00
0.6	--	--	1.100	4.400	7.950	11.70	15.70	19.90	24.30	28.80
0.7	--	--	0.919	5.100	9.560	14.30	19.20	24.40	29.80	35.30
0.8	--	--	0.655	5.830	11.30	17.10	23.10	29.40	35.80	42.60
0.9	--	--	0.309	6.580	13.20	20.10	27.40	34.80	42.60	50.50
1.0	--	--	--	7.360	15.20	23.40	32.00	40.80	49.90	59.20

Table 3.5: Variation of α_{bc} with aspect ratio and orthotropy of 6-Panel Slab

μ / r	0.3	0.5	0.7	0.9	1.1	1.3	1.5	1.7	1.9	2.1
0.2	--	0.348	1.230	2.190	3.130	4.210	5.420	6.780	8.260	9.880
0.3	--	0.118	1.540	3.15	4.920	6.850	8.940	11.20	13.60	15.80
0.4	--	--	1.830	4.170	6.710	9.430	12.30	15.40	18.60	22.00
0.5	--	--	2.080	5.310	8.780	12.50	16.30	20.40	24.60	29.10
0.6	--	--	2.290	6.580	11.10	15.90	20.90	26.20	31.60	37.20
0.7	--	--	2.470	7.960	13.80	19.80	26.10	32.70	39.50	46.50
0.8	--	--	2.610	9.460	16.70	24.20	31.90	40.00	48.30	56.80
0.9	--	--	2.710	11.10	19.80	28.90	38.30	48.00	58.00	68.30
1.0	--	--	2.780	12.80	23.80	34.10	45.30	56.80	68.70	80.70

Table 3.6: Variation of α_{bc} with aspect ratio and orthotropy of 7-Panel Slab

μ / r	0.3	0.5	0.7	0.9	1.1	1.3	1.5	1.7	1.9	2.1
0.2	--	0.137	1.170	2.350	3.680	5.160	6.560	8.080	9.720	11.50
0.3	--	--	1.330	3.250	5.350	7.610	10.00	12.60	15.30	18.20
0.4	--	--	1.370	4.250	7.330	10.60	14.10	17.60	21.50	25.50
0.5	--	--	1.280	5.330	9.620	14.10	18.90	23.80	28.90	34.20
0.6	--	--	1.080	6.500	12.20	18.20	24.40	30.80	35.50	44.30
0.7	--	--	0.743	7.750	15.10	22.70	30.60	38.80	47.20	55.80
0.8	--	--	0.283	9.080	18.20	27.80	37.60	47.10	58.10	68.70
0.9	--	--	--	10.50	21.70	33.30	45.20	57.50	70.10	82.90
1.0	--	--	--	12.00	25.50	39.40	53.60	68.30	83.20	98.50

Table 3.1 to 3.6 shows the dependence of the critical beam-strength parameter (α_{bc}) on the number of panels, aspect ratio, and orthotropy of the slab-beam system. It is indicated in these tables that orthotropy (μ) of 0.7 is the minimum value that will ensure the failure of the slab-beam system in the global-collapse mechanism for all possible values of the aspect ratios and with any number of panels. Otherwise, the slab-beam would violate the yield criterion at some points in the end panels of the slab-beam system at the value of the orthotropy less than 0.7 ($\mu < 0.7$) irrespective of the aspect ratio of the slab-beam system.

The slab-beam system acts as a two-way slab at the value of aspect ratio greater than or equal to 0.5. The value of the critical beam-strength parameter (α_{bc}) increases proportional to the value of the orthotropy and aspect ratio of the slab-beam system irrespective of the number of panels for a two-way slab system. Therefore, stronger and stronger supporting-beams are required in the two-way slab system as the shape of the slab changes from the rectangular ($r \geq 0.5$) to the square ($r = 1$) for any value of the orthotropy. And, If the supporting-beam of the slab-beam system has been proportioned with $\lambda > 1$, it would always collapse in the local-collapse mechanism irrespective of the stiffness of the supporting-beams.

The laterally loaded slab-beam system with aspect ratio less than 0.5 transfers the lateral load essentially along the shorter span of the slab. Orthotropy of the slab has very small effect on the value of critical beam-strength parameter (α_{bc}) in this range of the aspect ratio and its value goes on reducing with the increase in the orthotropy of the slab because of more predominant one-way action at low value of the slab aspect ratio ($r < 0.3$). Accordingly, low strength supporting beams are required to support the laterally loaded slabs at low values of the aspect ratio.

The value of the critical beam-strength parameter (α_{bc}) increases at a small rate with the increase in the orthotropy of the slab in range of $0.3 \leq r \leq 0.5$ as the behavior of the slab approaches the two-way action with the increase of the aspect ratio of the slab. The role of the supporting-beams becomes more predominant at the higher value of the slab aspect ratio, when the slab-system starts behaving more as a two-way slab. In this range of the aspect ratio, the beam-strength parameter (α_b) can be used very conveniently to control the load sharing between the supporting-beams and the slab. The supporting-beams can be used to provide both the strength and the stiffness to the slab-beam system. It can be stated that the function of the internal supporting beams of the slab-beam system in the global-collapse mechanism mode is more like a stiffeners rather than to just support

the slab. These beams share the lateral load along with the slab and the depth of these beams can be used to provide the strength and stiffness to the slab-beam system in accordance with the provisions of the design codes [*IS 456 (2000)*].

3.7 EFFECT OF SLAB-PARAMETERS ON THE COLLAPSE MECHANISM

The variation of the slab moment-coefficient (= m_{ux}/wL_x^2) with the slab-parameter (A) is shown in *Figure 3.6*. It indicates that the slab moment (m_{ux}) approaches its maximum value at unit value of the slab-parameter (A =1) and the minimum value of the slab moment (m_{ux}) is possible only at very large value of the slab-parameter ($A = \infty$). However, the slab-beam system would sustain the lateral load in the global-collapse mechanism mode only in the narrow range, defined by the equations (3.20) and (3.24), of a wide spectrum of the slab-parameters (A-values). Otherwise, either it would lead to the simultaneous formation of a local-collapse mechanism in all panels of the slab-system at the value of the slab-parameter, $A > A_{c2}$ [see equation (3.24)] or can results in some non-valid value of the beam strength ($m_b < 0$) at the value of the slab-parameter, $A < A_{c1}$ [see equation (3.20)].

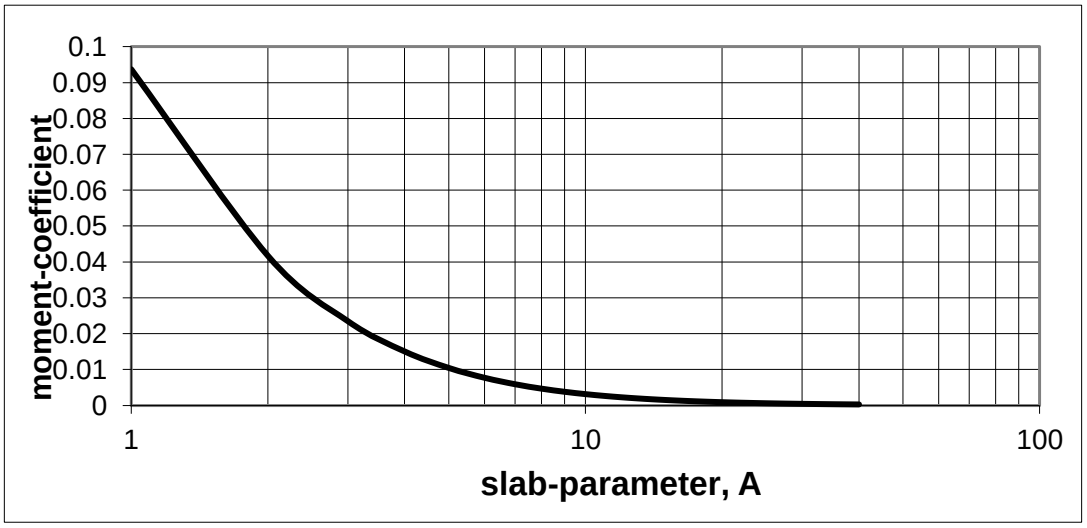

Figure 3.6: Variation of moment-coefficient (= m_{ux}/wL_x^2) with the slab-parameter (A)

The design curve shown in the *Figure 3.6* can be used to predict the design moment field induced in the single-panel slab (n = 1) with any value of the slab-parameter (A) irrespective of the lower or the upper limits prescribed by equations (3.20) and (3.24). The results predicted from the proposed model for a single-panel slab compares favorably well with the results obtained from the well-established design formulae of the yield line theory, lower bound method and elastic theory [*Johansen (1967), Jones (1967), Jones*

and Wood (1967), *Shukla (1973)*, and *Park and Gamble (2000)*] and the design coefficients recommended by design codes [*IS 456 (2000)*] [*see example 4.3.1*].

If the slab-beam system has been designed with the value of the slab-parameter more than that given by the equation (3.24), it will lead to the formation of a number of smaller rectangular slabs resting over the internal supporting-beams at collapse. In this case, the behavior of the internal supporting-beams of the slab-beam system would be analogous to the behavior of the supporting beams of any two-way slab-beam system resting over the non-yielding edge beams at collapse. The strength requirement of the supporting-beams, at this value of the slab-parameter ($A = A_{c2}$), matches favorably well with the values obtained from the design procedure recommended by the design code [*IS 456 (2000)*] [*see example 4.3.1*]. The value of the beam strength, m_b ($= \alpha_b m_{ux} l_x$) can be determined from the equation (3.30) for some valid value of the slab-parameter (A) required to form the local-collapse mechanism in the slab-beam system. Therefore, the internal supporting-beams of the slab-beam system can be made to behave similar to the non-yielding supporting beams and/or walls by the suitable selection of the slab-parameter, A ($\geq A_{c2}$). However, the rebars of the reinforced concrete rectangular slab-beam system must be detailed in a manner required for the initiation of the global-collapse mechanism under the lateral loading (w) at the collapse.

The strength requirement of the supporting-beams increases proportional to the slab-parameter (A). Higher the value of the slab-parameter, stronger the beam section must be to support the lateral load along with the slab and more it would repel the branching point of the yield line pattern away from it. When the strength of the supporting-beams approaches its upper limit (α_{bc}), it will repel the branching point of the yield line pattern to an extent that it leads to the failure of the slab-beam system in the local-collapse mechanism irrespective of the stiffness of the supporting-beams. At this value of the slab-parameter ($A = A_{c2}$), the moment field in the slab compare favorably well with the analytical results from the published literature on the slab analysis. The moment field in the slab would follow the elastic distribution, if it has been proportioned using the value of the orthotropy (μ) corresponding to the elastic theory of plates [*see example 4.3.1*].

Therefore, the purpose of using the internal supporting-beams in the slab-beam system remains only to stiffen the laterally loaded slab to enable it to satisfy the serviceability requirement of the design codes. The strength requirement of the supporting-beams of the slab-beam system can be worked out from the valid values of the slab-parameter (A). This would enable the designer to use reinforced concrete slabs with

minimum possible thickness stiffened by the equally spaced internal beams with adequate matching strength required for supporting the lateral load in the global-collapse mechanism mode and vice versa. The depth of the supporting-beams should be selected in a manner that it must satisfy the serviceability conditions of the applicable design code [*see Appendix-B*].

In brief, the slab-beam system will behave essentially as single-panel slab at zero λ-value ($A = A_{c1}$) and it will be divided into a number of smaller rectangular slabs simply resting over the supporting beams and/or stiffeners, at λ=1 ($A = A_{c2}$). The slab and the supporting-beams will share the moment field (m_{ux}, m_b and m_{uy}) for the intermediate λ-values depending upon the value of the slab-parameter (A). The slab thickness and the strength of the internal beams can be selected to match the strength requirement of the laterally loaded slab-beam system and stiffness of the beams can be used to satisfy the serviceability requirement of the design codes. At low λ-value and/or A-values, the slab-beam system would require a thick slab section with the corresponding light section of the internal beams and vice versa.

3.7.1 Effect of Orthotropy on the Beam-Strength and the Slab-Strength

The bending moment coefficients ($m_b/w L_x^3$) for the supporting beams provided along the span (l_y) of the slab-system and the slab moment coefficients ($m_{ux}/w L_x^2$) acting along the long span (L_x) of the slab-beam system are derived using the computer code developed by using the analytical equations developed in the section 3.3. The variations of these coefficients are shown in *Figures (3.7 to 3.42)* for various values of the slab orthotropy (μ) and aspect ratio (r) of the slab-beam system simply resting over the non-yielding outer boundaries. These values are plotted against the orthotropy at moment-manipulator value of 0.3, 0.5 and 0.8 to check the effect of the strength level of the supporting beams on the moment-field induced in the laterally loaded slab-beam system.

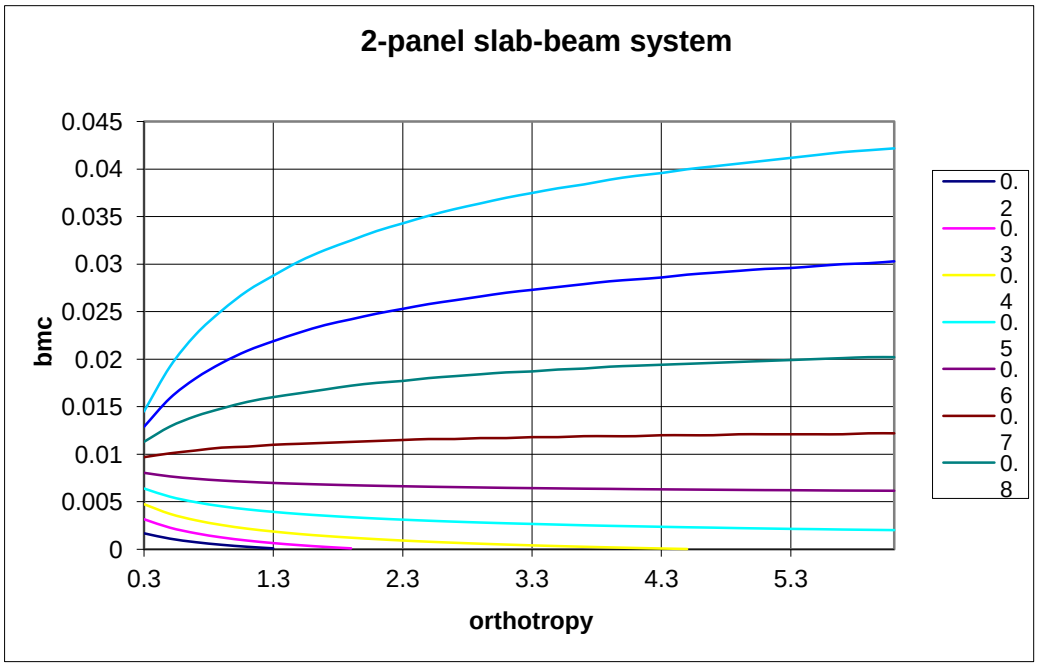

Figure 3.7: Variation of beam moment-coefficient (bmc) with the orthotropy at $\lambda = 0.3$

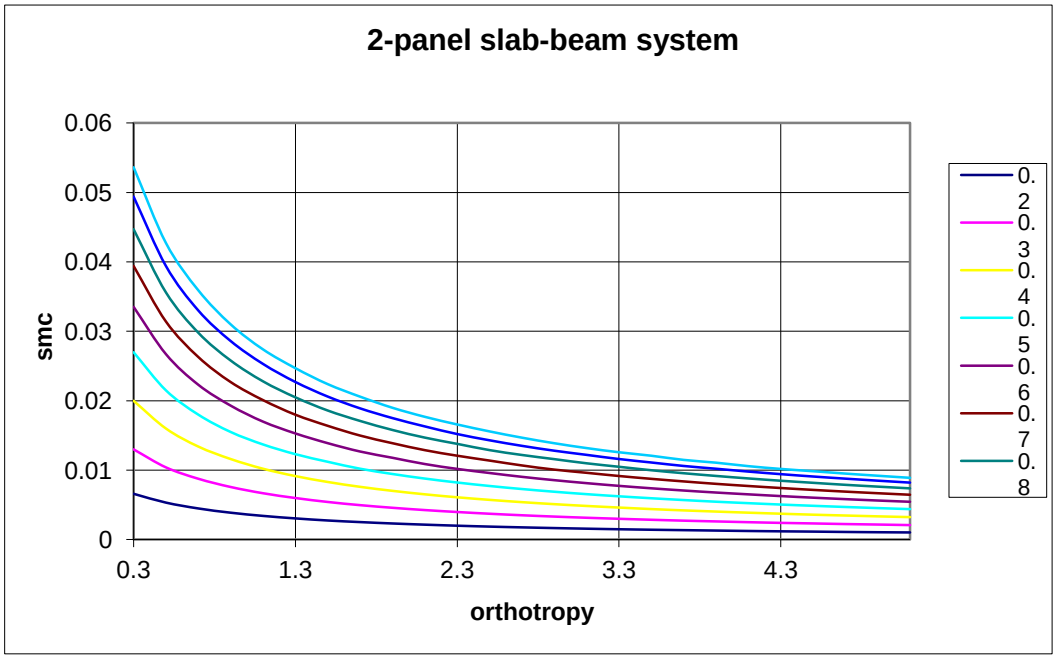

Figure 3.8: Variation of slab moment-coefficient (smc) with the orthotropy at $\lambda = 0.3$

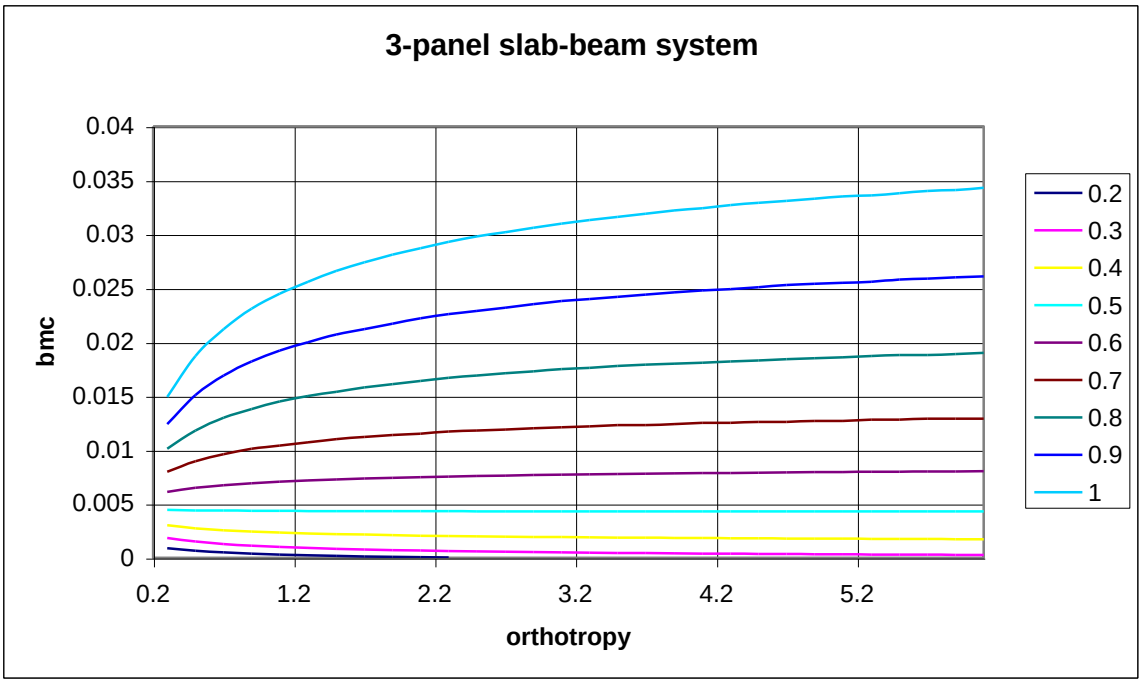

Figure 3.9: Variation of beam moment-coefficient (bmc) with the orthotropy at $\lambda = 0.3$

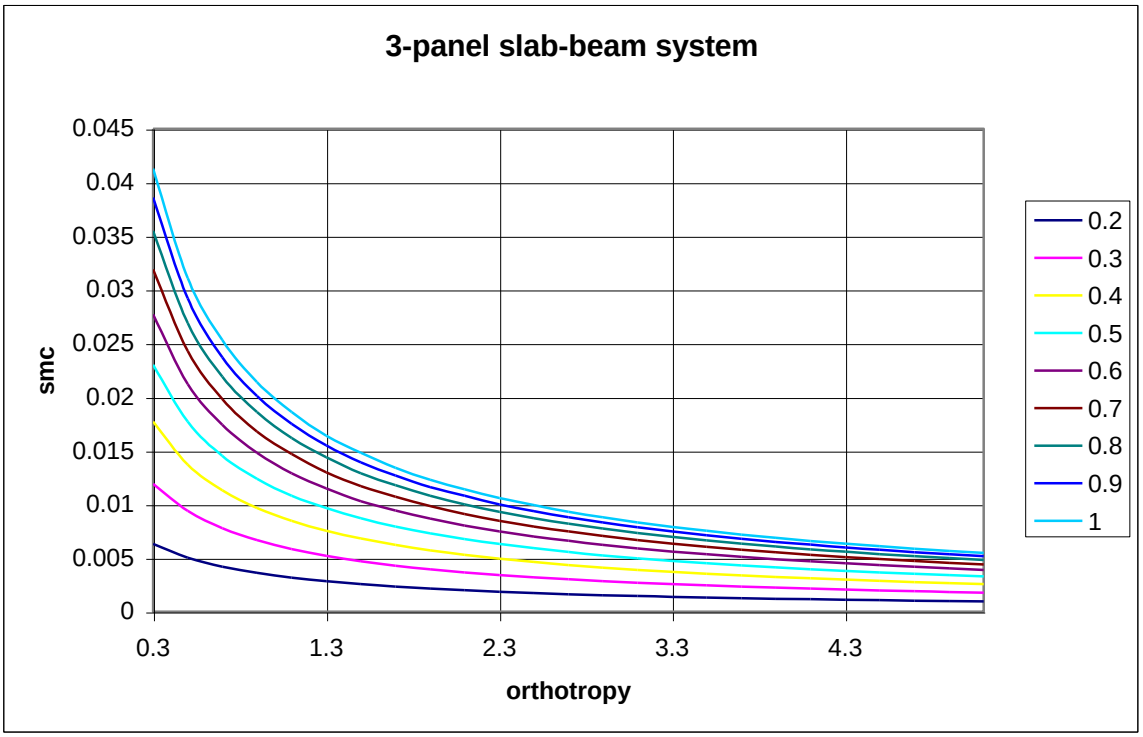

Figure 3.10: Variation of slab moment-coefficient (smc) with the orthotropy at $\lambda = 0.3$

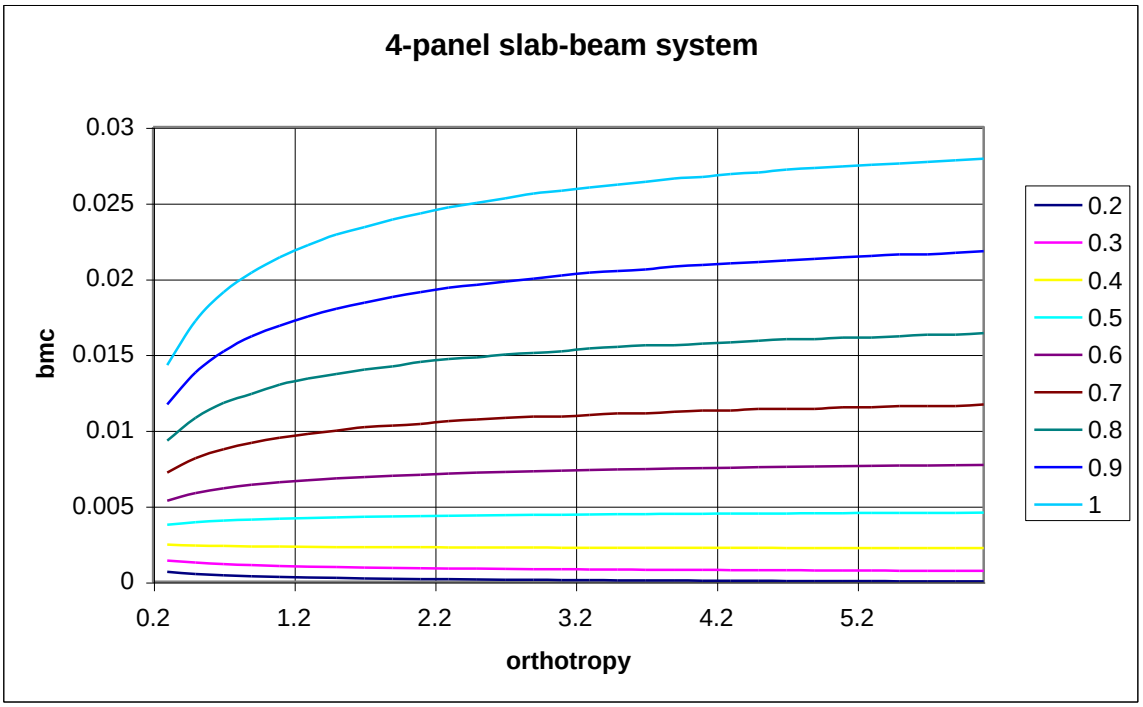

Figure 3.11: Variation of beam moment-coefficient (bmc) with the orthotropy at $\lambda = 0.3$

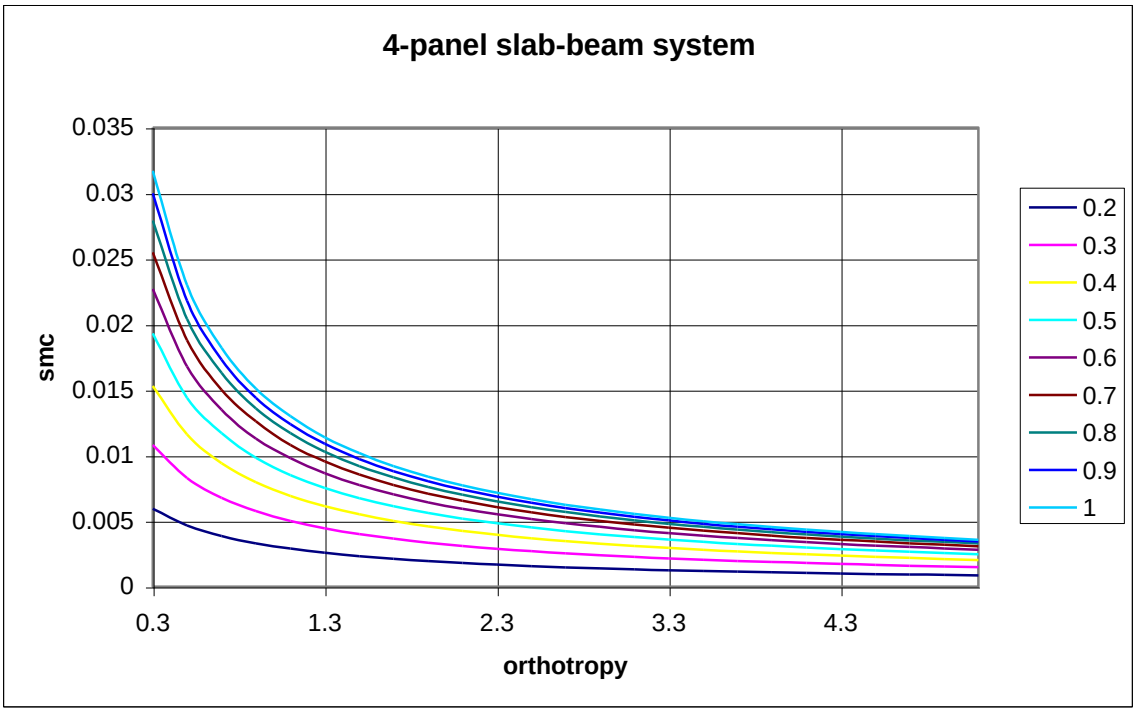

Figure 3.12: Variation of slab moment-coefficient (smc) with the orthotropy at $\lambda = 0.3$

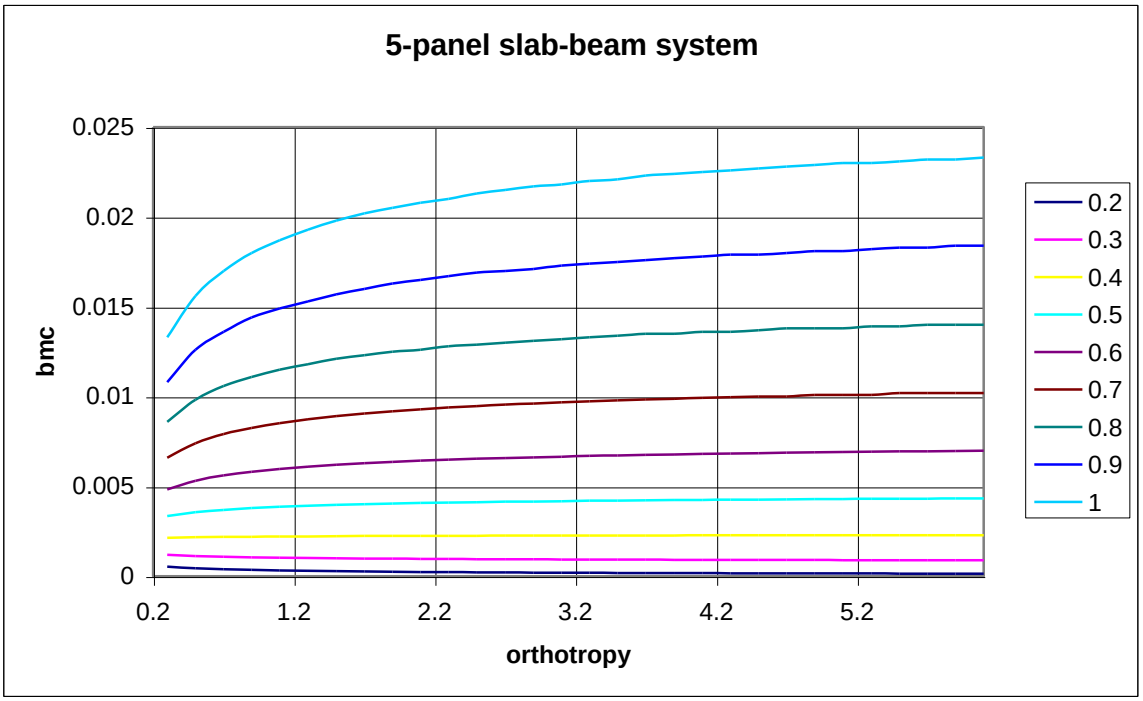

Figure 3.13: Variation of beam moment-coefficient (bmc) with the orthotropy at $\lambda = 0.3$

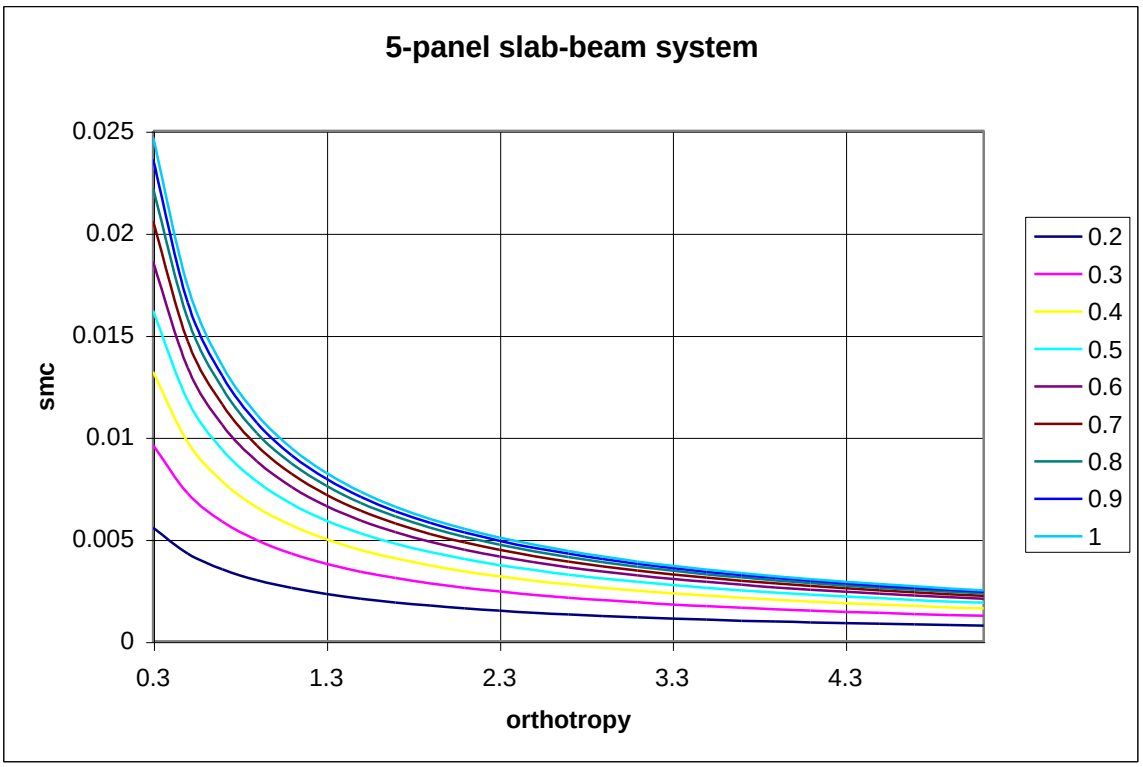

Figure 3.14: Variation of slab moment-coefficient (smc) with the orthotropy at $\lambda = 0.3$

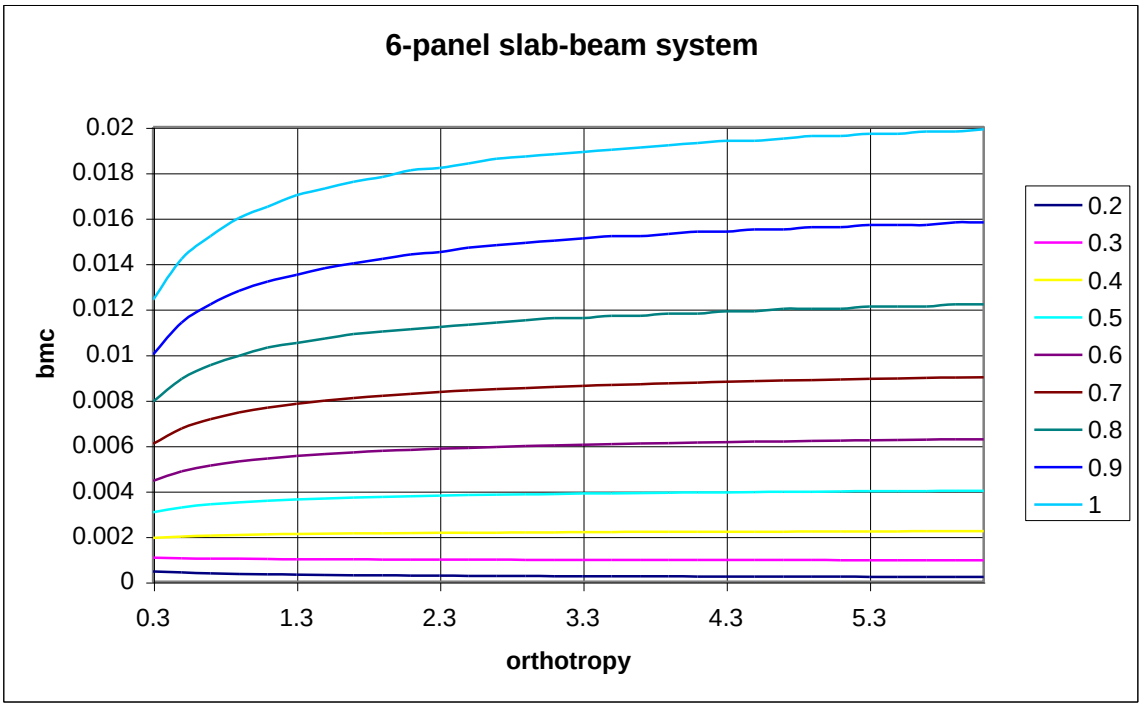

Figure 3.15: Variation of beam moment-coefficient (bmc) with the orthotropy at $\lambda = 0.3$

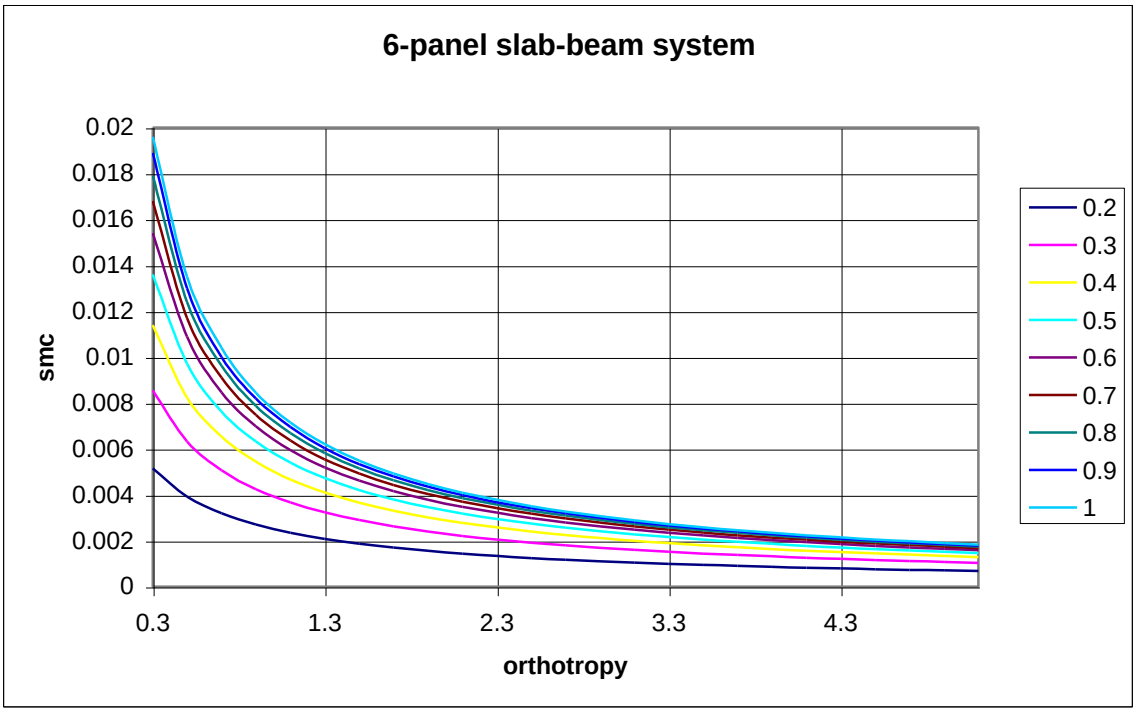

Figure 3.16: Variation of slab moment-coefficient (smc) with the orthotropy at $\lambda = 0.3$

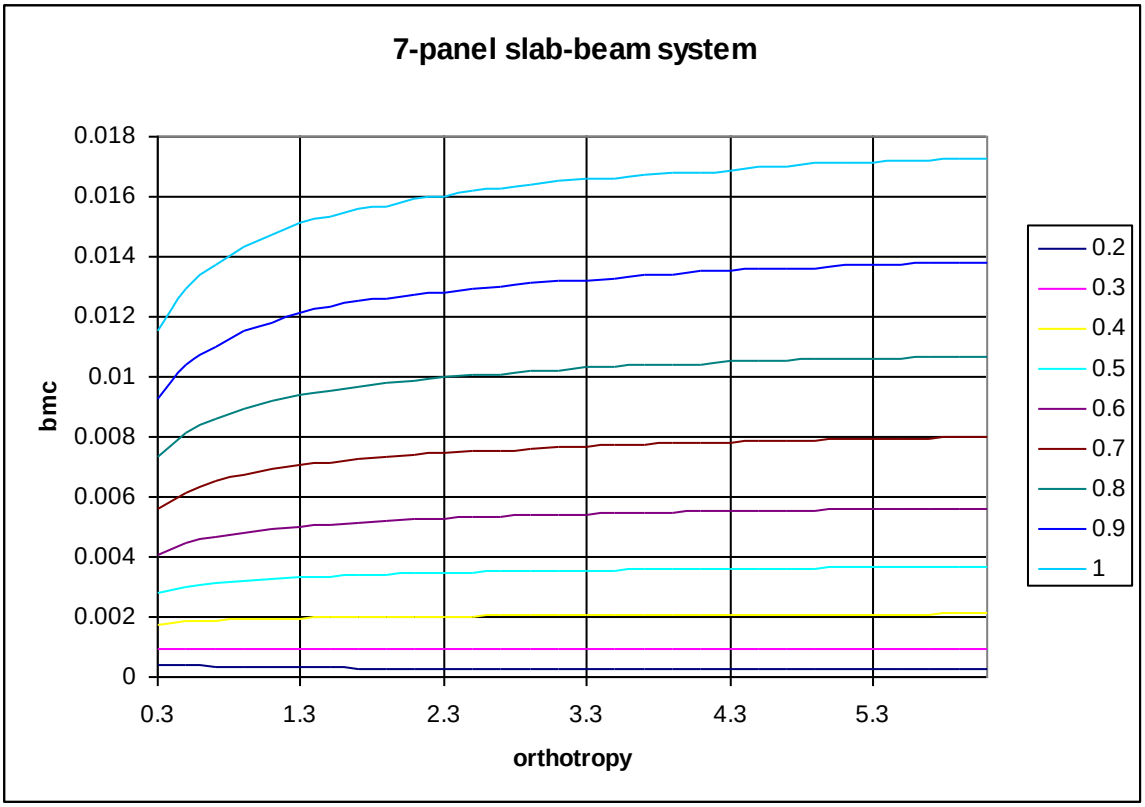

Figure 3.17: Variation of beam moment-coefficient (bmc) with the orthotropy at λ = 0.3

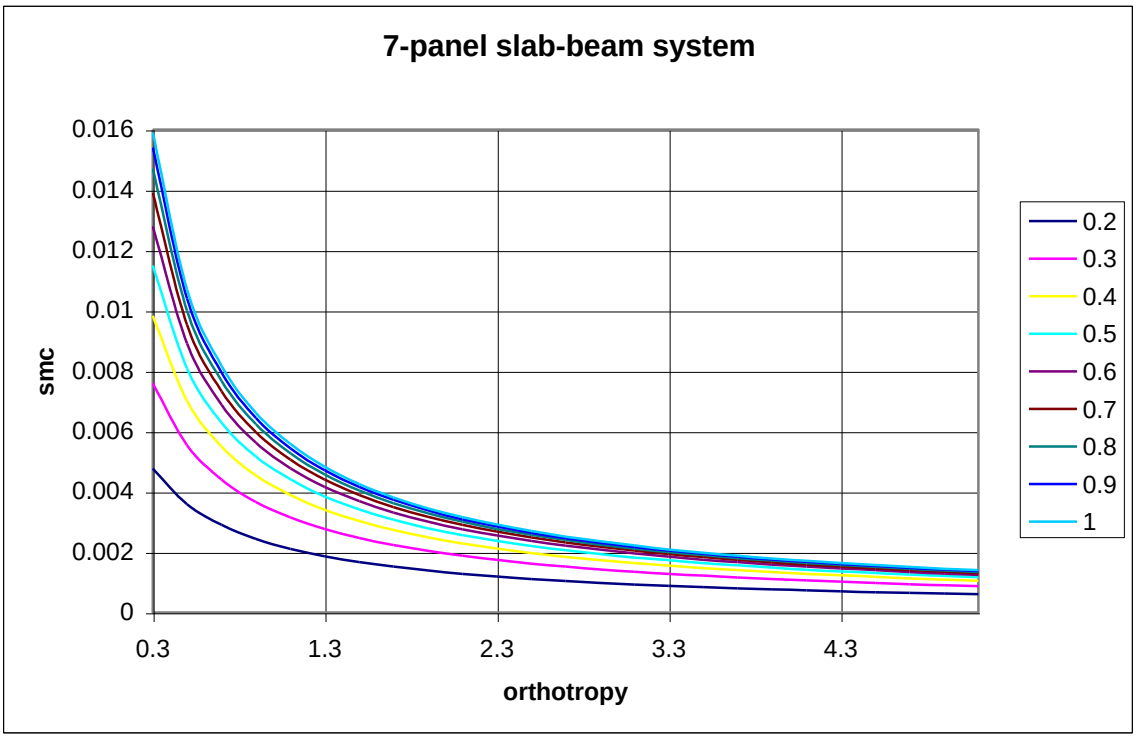

Figure 3.18: Variation of slab moment-coefficient (smc) with the orthotropy at λ = 0.3

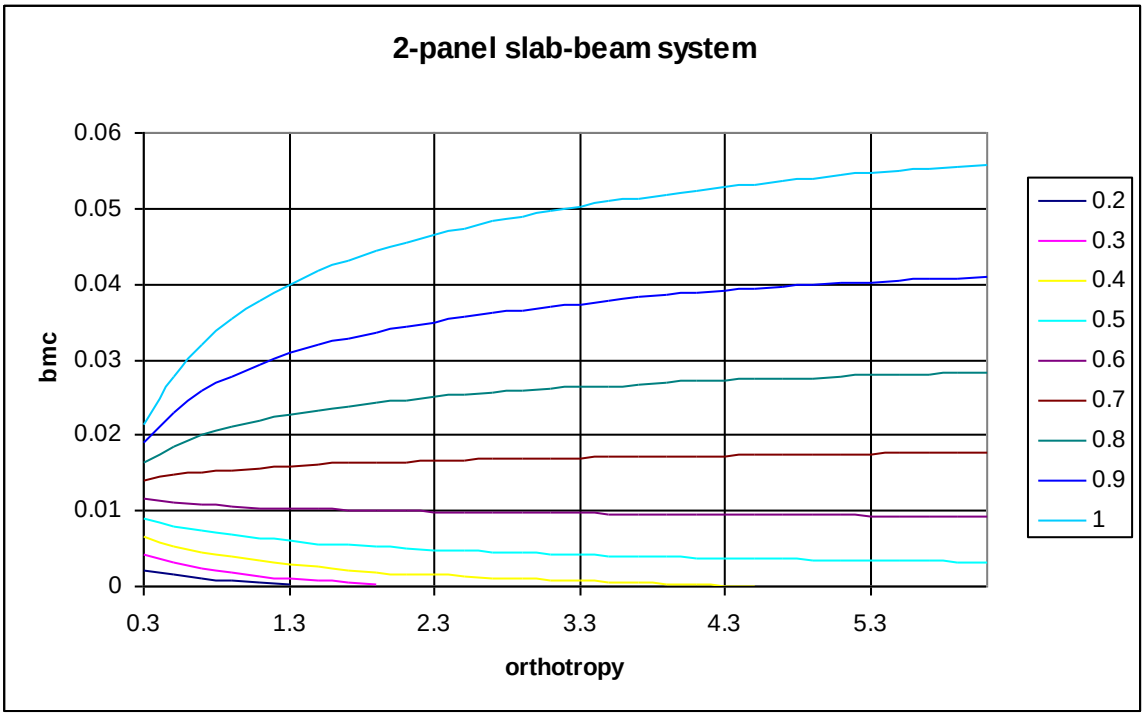

Figure 3.19: Variation of beam moment-coefficient (bmc) with the orthotropy at $\lambda = 0.5$

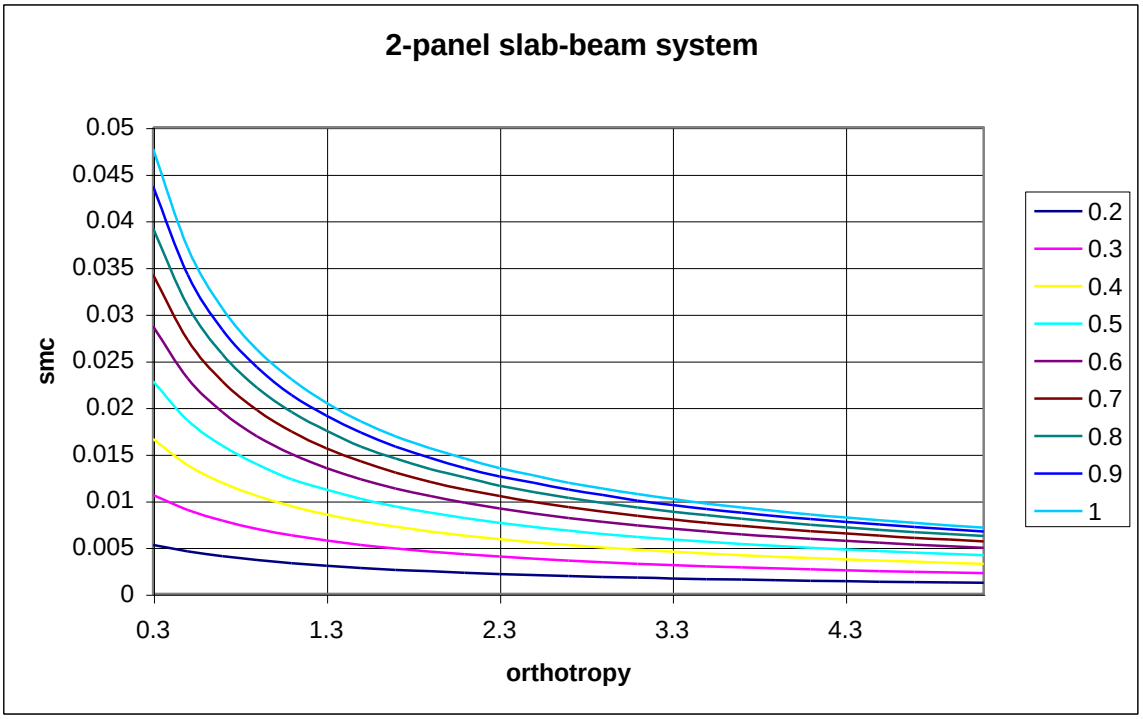

Figure 3.20: Variation of slab moment-coefficient (smc) with the orthotropy at $\lambda = 0.5$

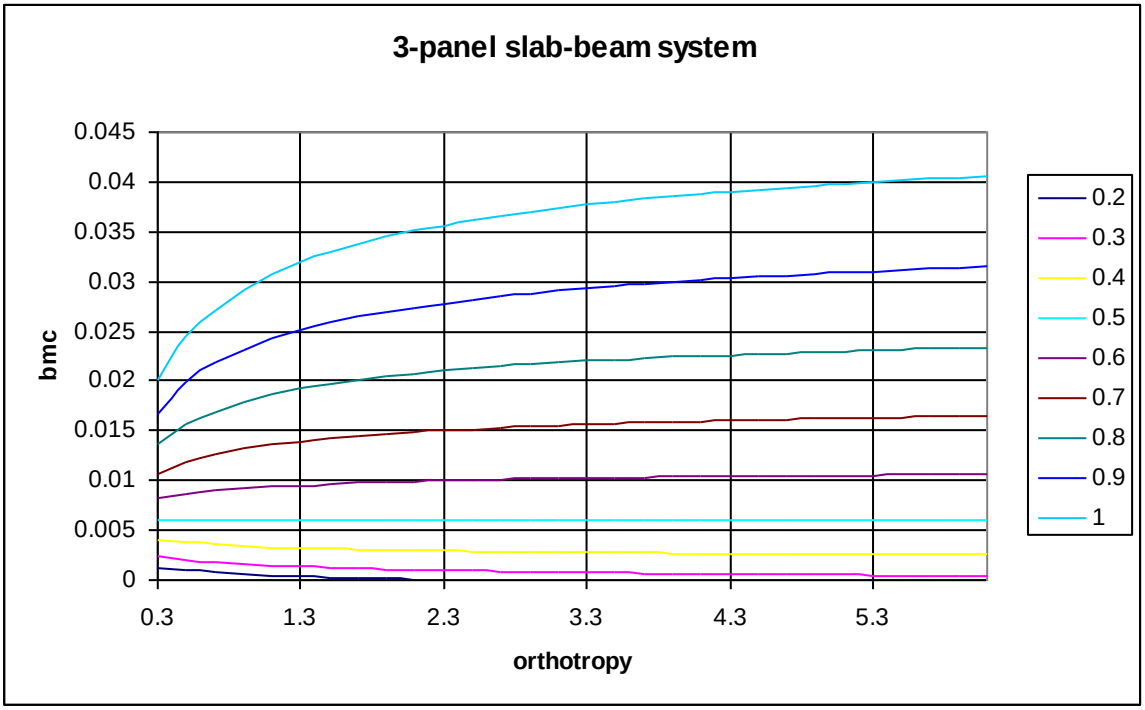

Figure 3.21: Variation of beam moment-coefficient (bmc) with the orthotropy at $\lambda = 0.5$

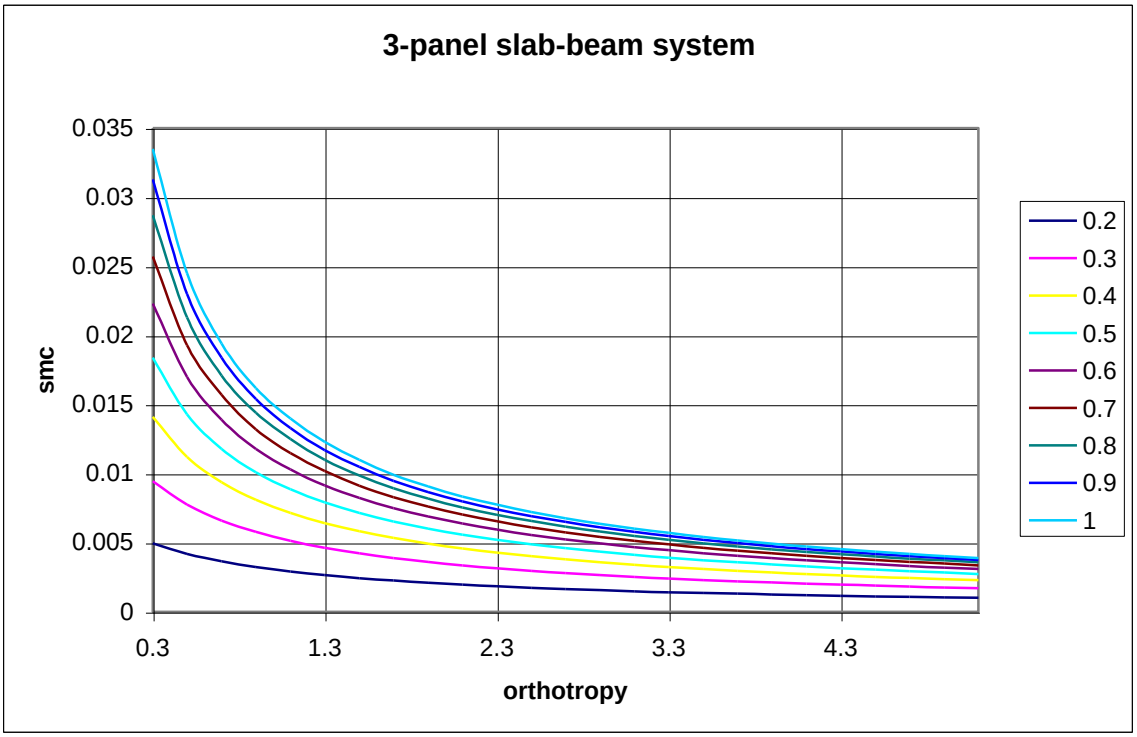

Figure 3.22: Variation of slab moment-coefficient (smc) with the orthotropy at $\lambda = 0.5$

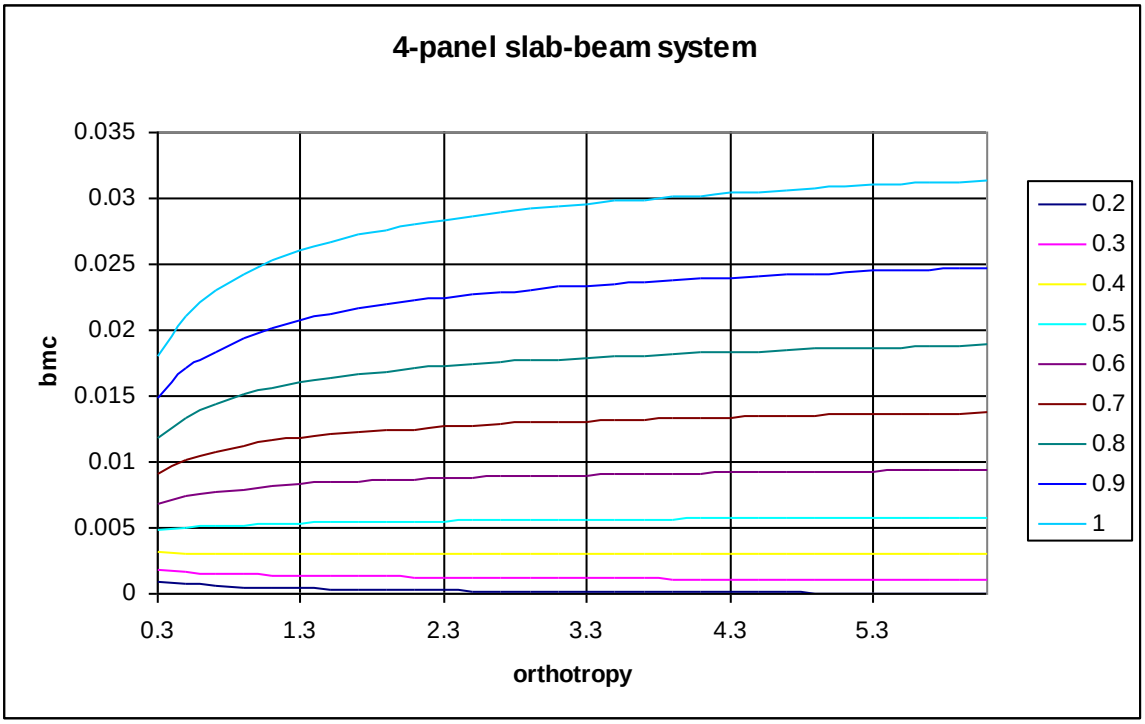

Figure 3.23: Variation of beam moment-coefficient (bmc) with the orthotropy at $\lambda = 0.5$

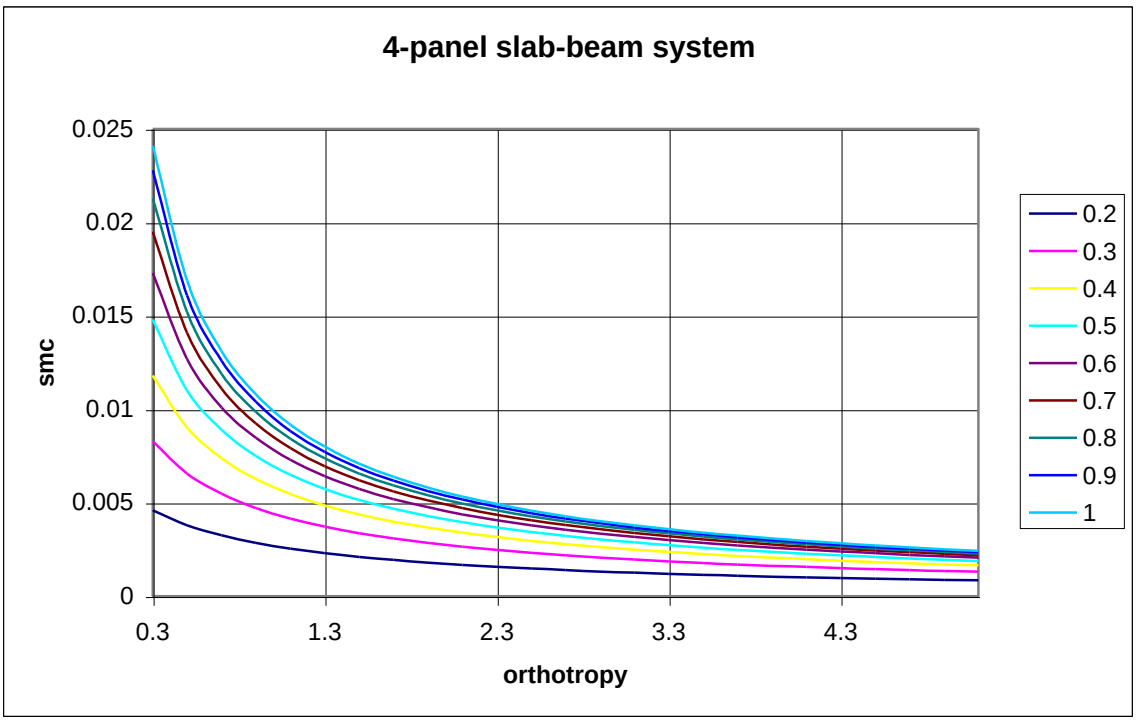

Figure 3.24: Variation of slab moment-coefficient (smc) with the orthotropy at $\lambda = 0.5$

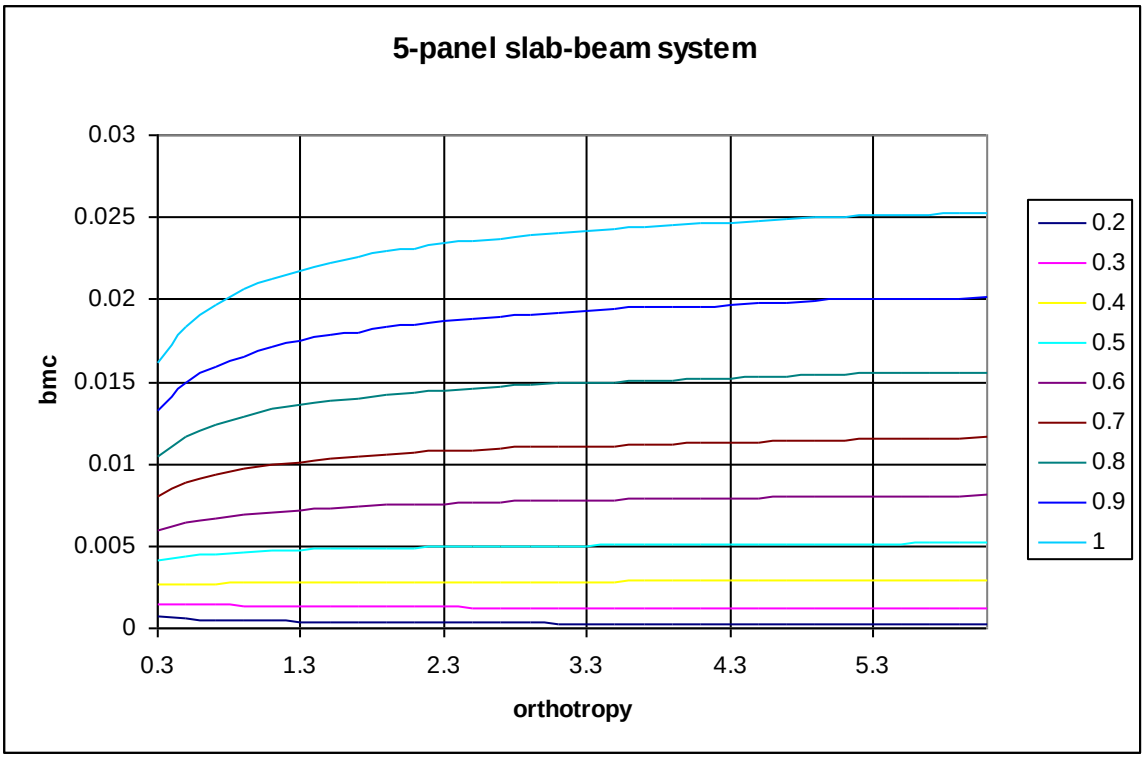

Figure 3.25: Variation of beam moment-coefficient (bmc) with the orthotropy at $\lambda = 0.5$

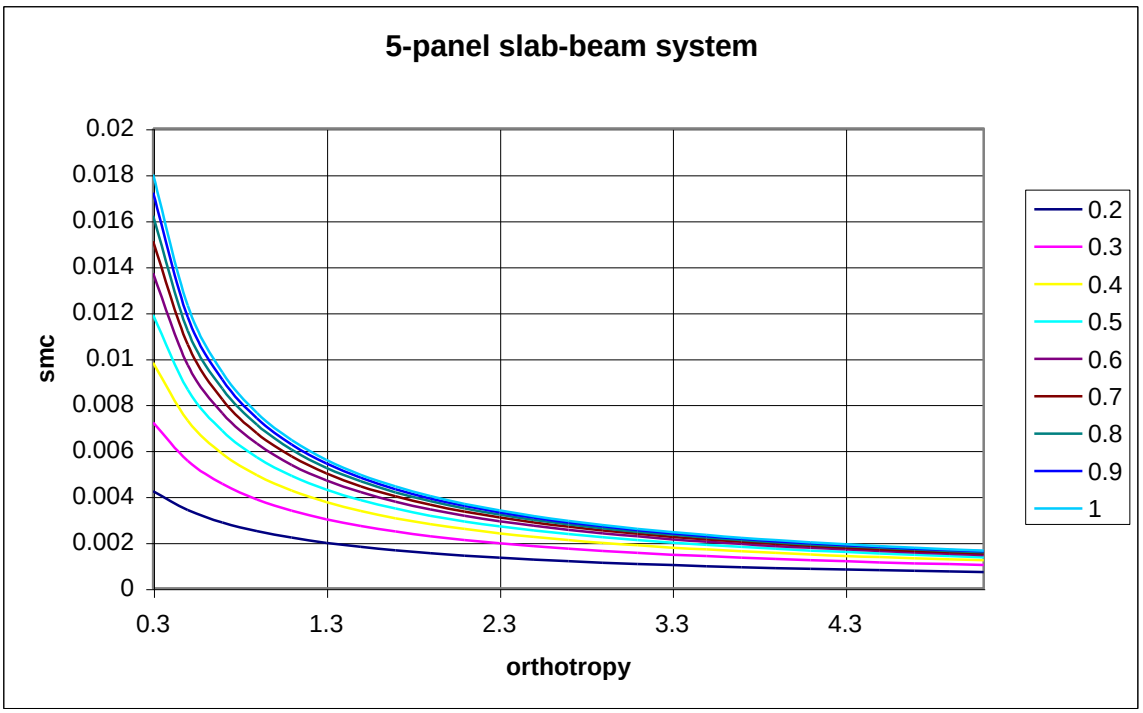

Figure 3.26: Variation of slab moment-coefficient (smc) with the orthotropy at $\lambda = 0.5$

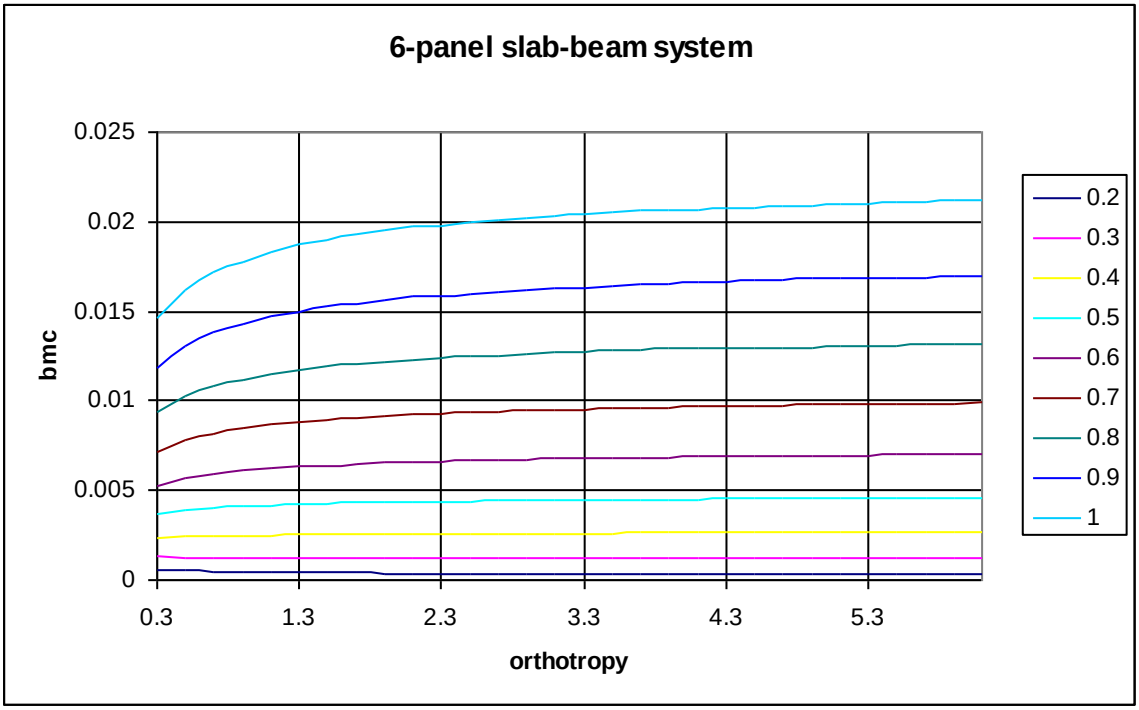

Figure 3.27: Variation of beam moment-coefficient (bmc) with the orthotropy at $\lambda = 0.5$

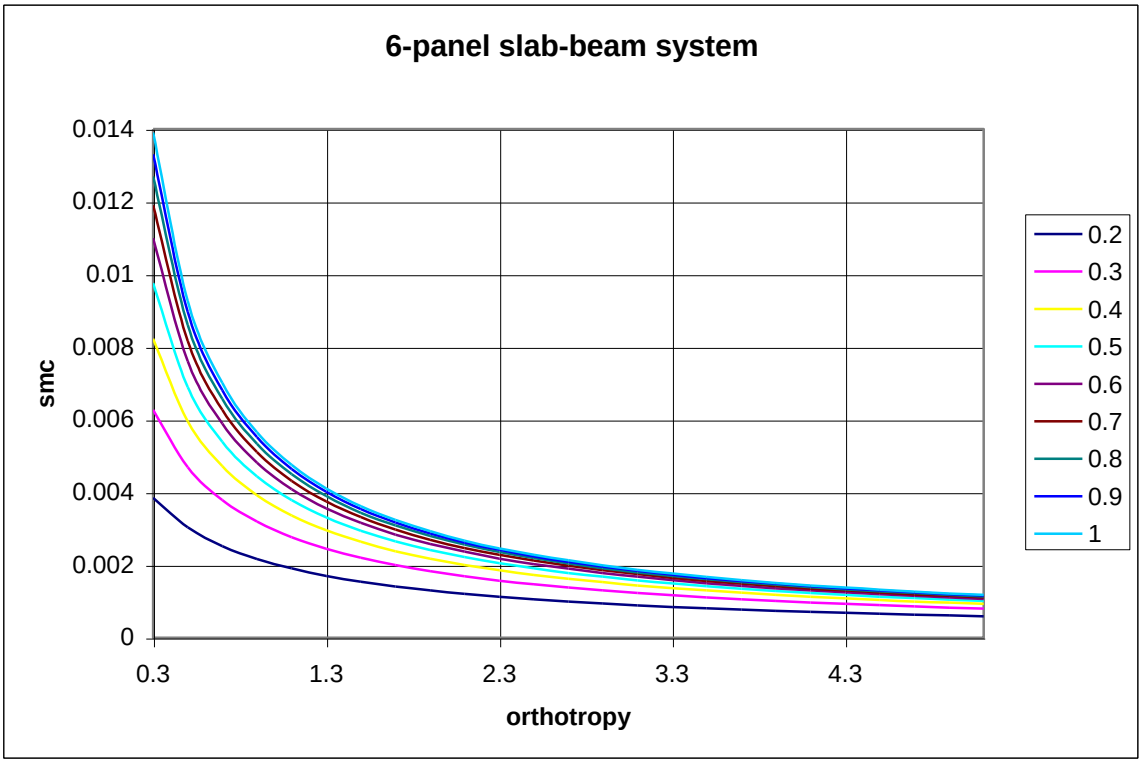

Figure 3.28: Variation of slab moment-coefficient (smc) with the orthotropy at $\lambda = 0.5$

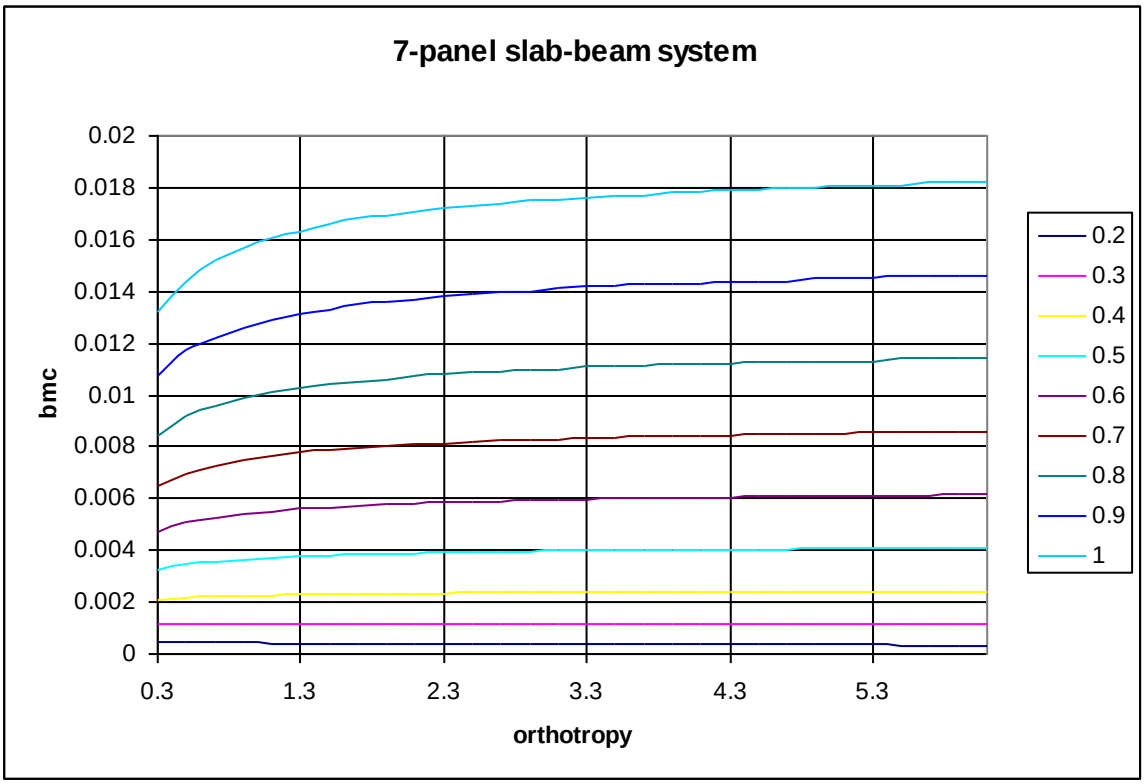

Figure 3.29: Variation of beam moment-coefficient (bmc) with the orthotropy at $\lambda = 0.5$

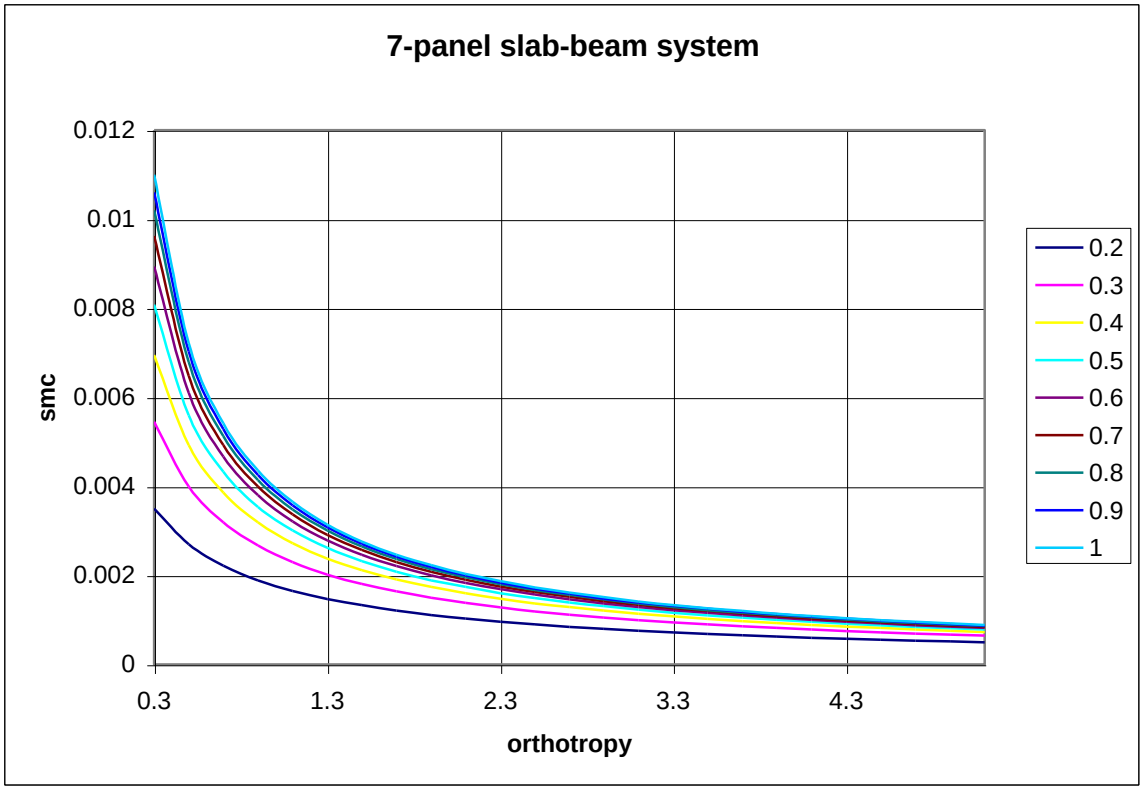

Figure 3.30: Variation of slab moment-coefficient (smc) with the orthotropy at $\lambda = 0.5$

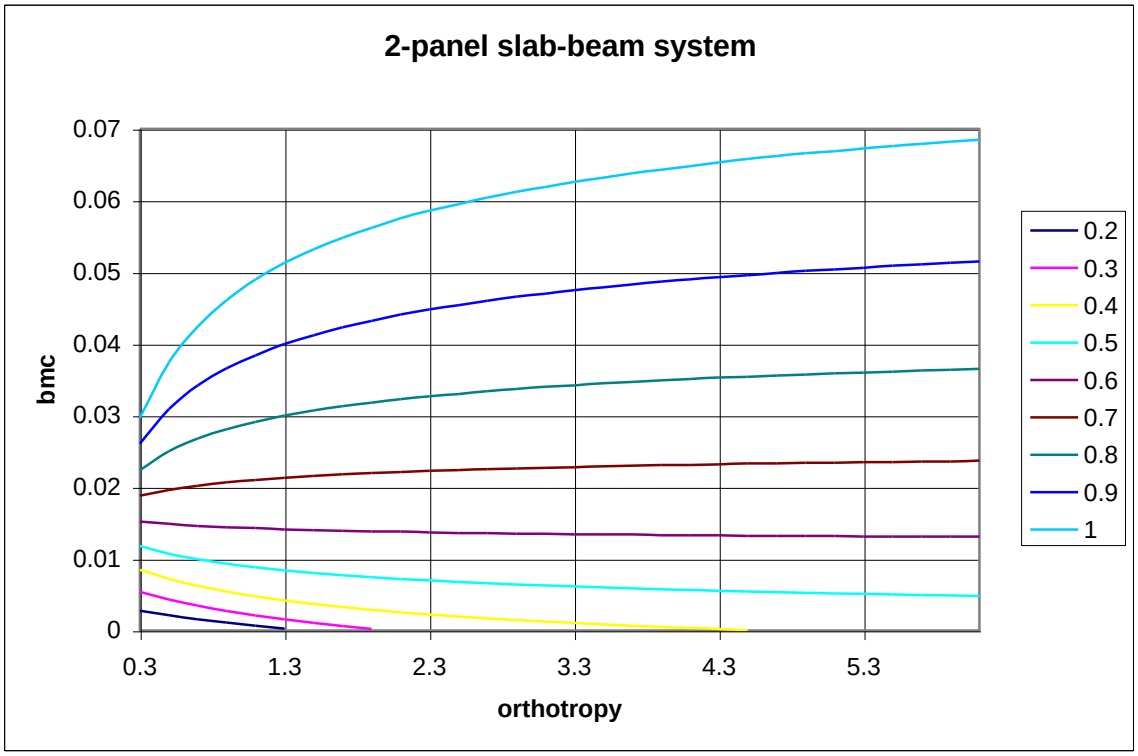

Figure 3.31: Variation of beam moment-coefficient (bmc) with the orthotropy at $\lambda = 0.8$

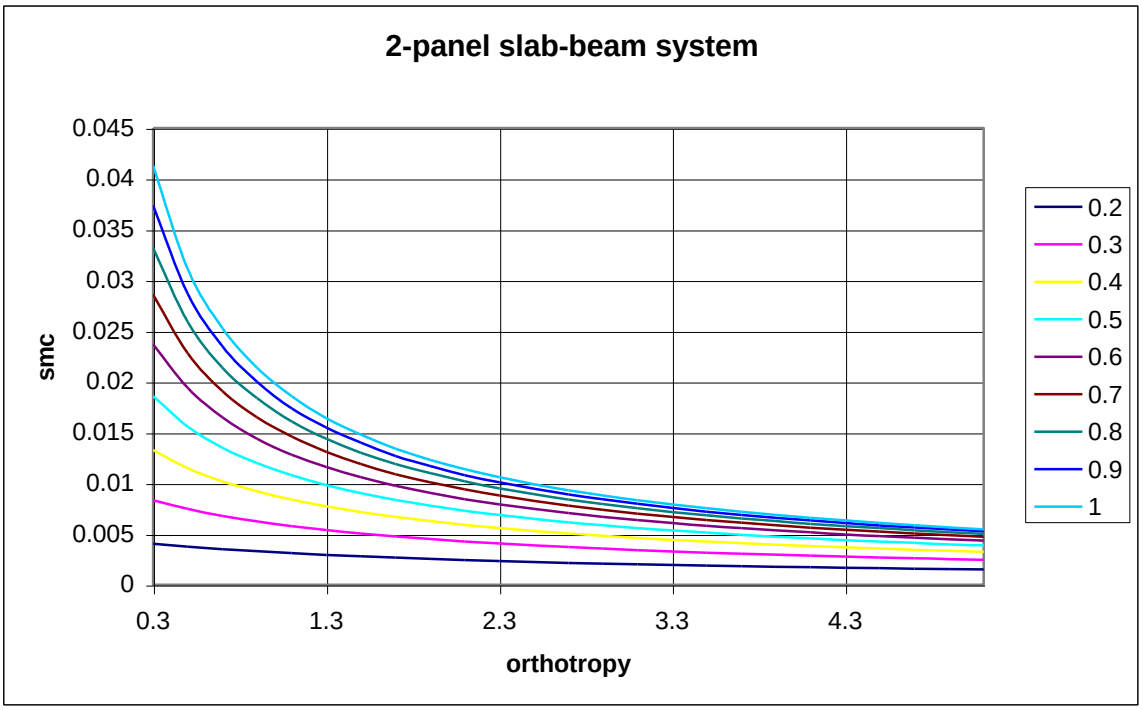

Figure 3.32: Variation of slab moment-coefficient (smc) with the orthotropy at $\lambda = 0.8$

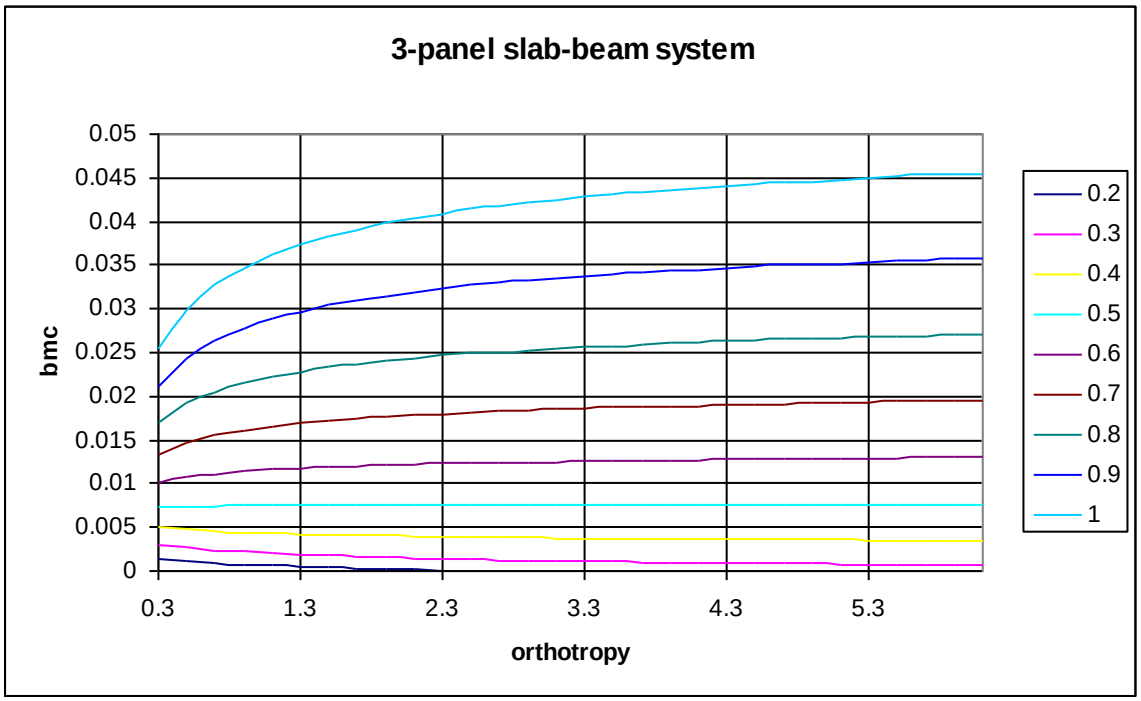

Figure 3.33: Variation of beam moment-coefficient (bmc) with the orthotropy at $\lambda = 0.8$

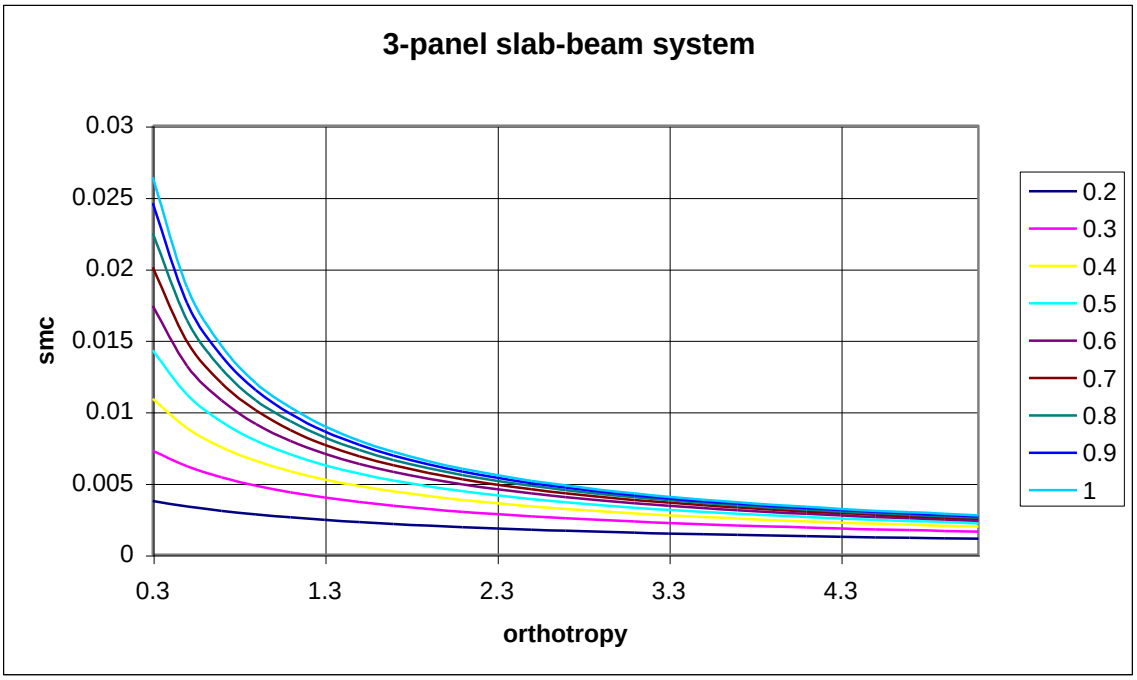

Figure 3.34: Variation of slab moment-coefficient (smc) with the orthotropy at $\lambda = 0.8$

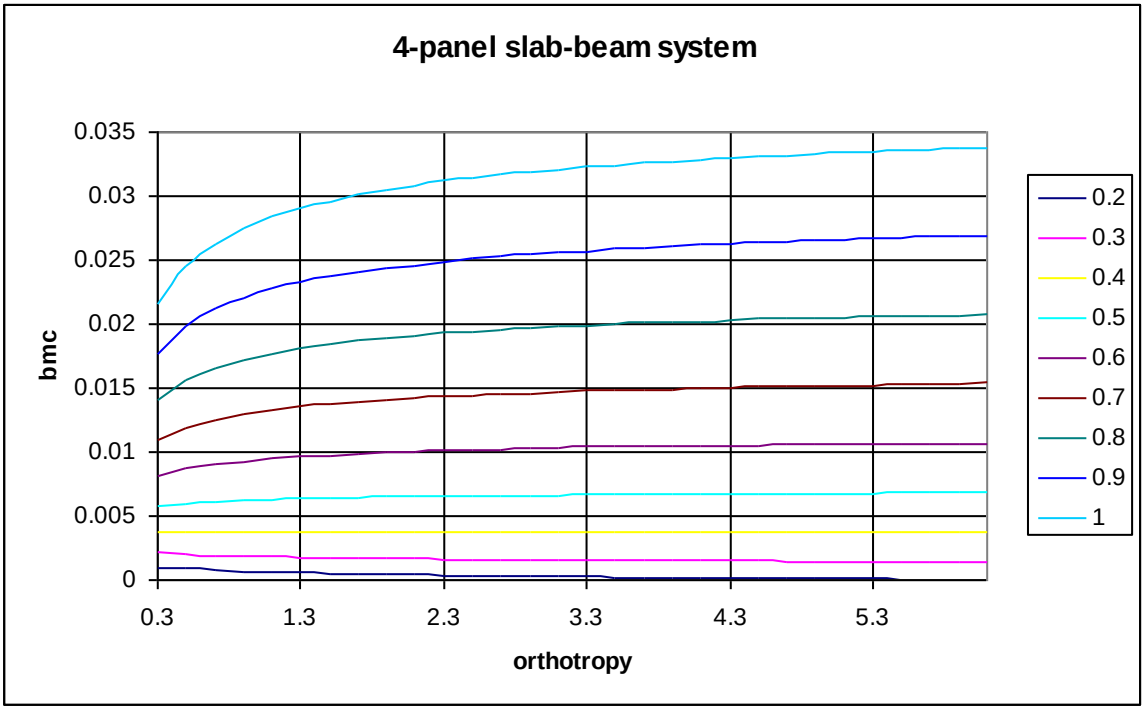

Figure 3.35: Variation of beam moment-coefficient (bmc) with the orthotropy at $\lambda = 0.8$

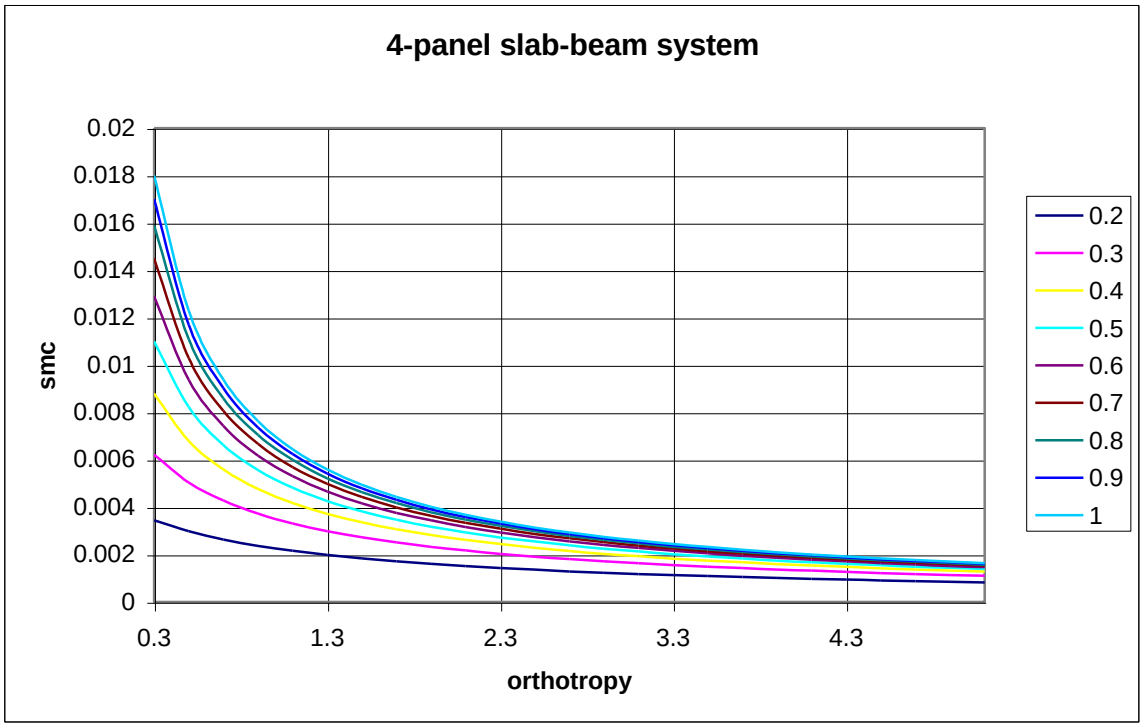

Figure 3.36: Variation of slab moment-coefficient (smc) with the orthotropy at $\lambda = 0.8$

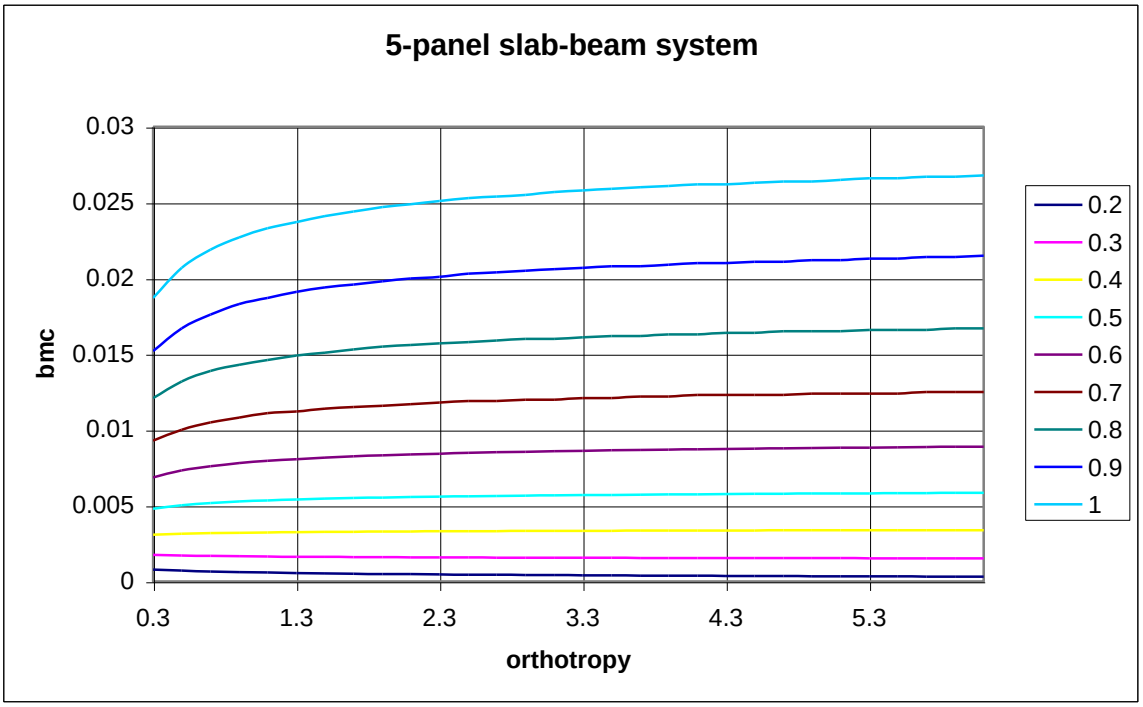

Figure 3.37: Variation of beam moment-coefficient (bmc) with the orthotropy at $\lambda = 0.8$

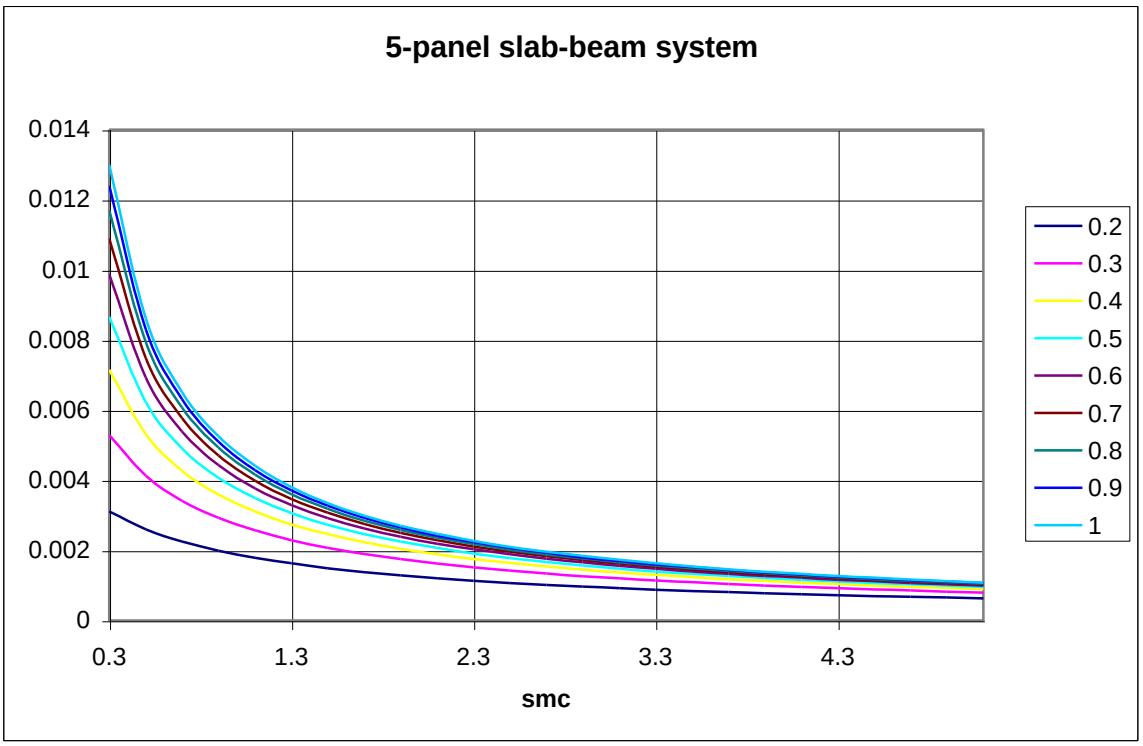

Figure 3.38: Variation of beam moment-coefficient (bmc) with the orthotropy at $\lambda = 0.8$

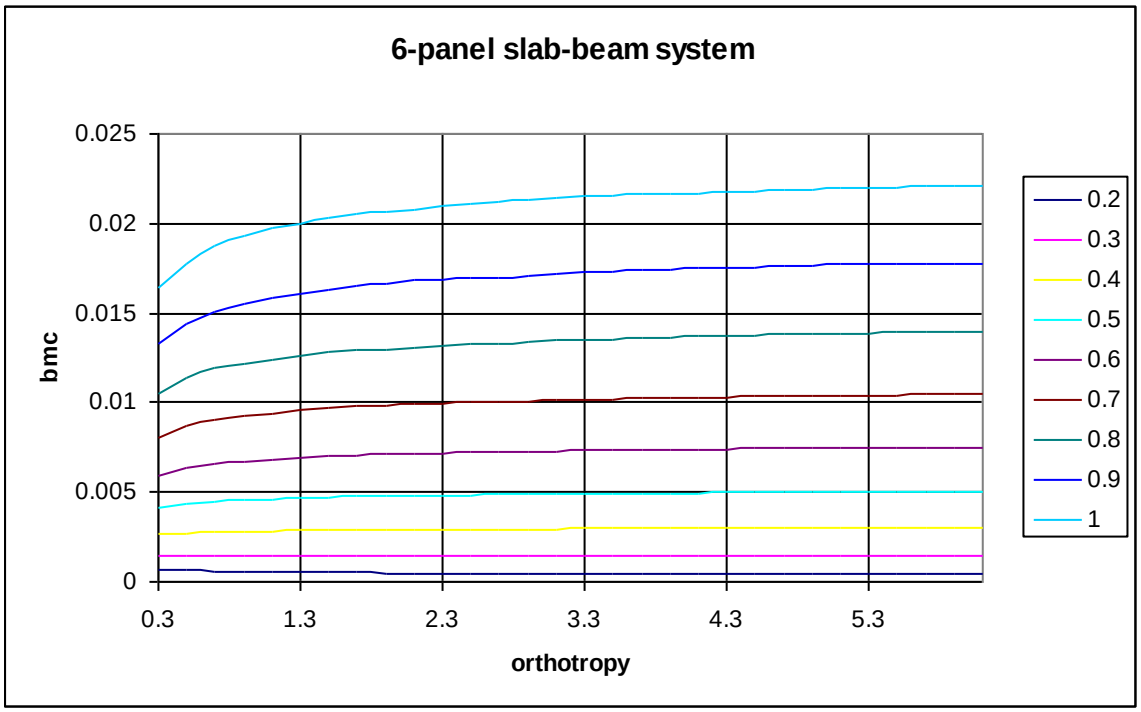

Figure 3.39: Variation of beam moment-coefficient (bmc) with the orthotropy at $\lambda = 0.8$

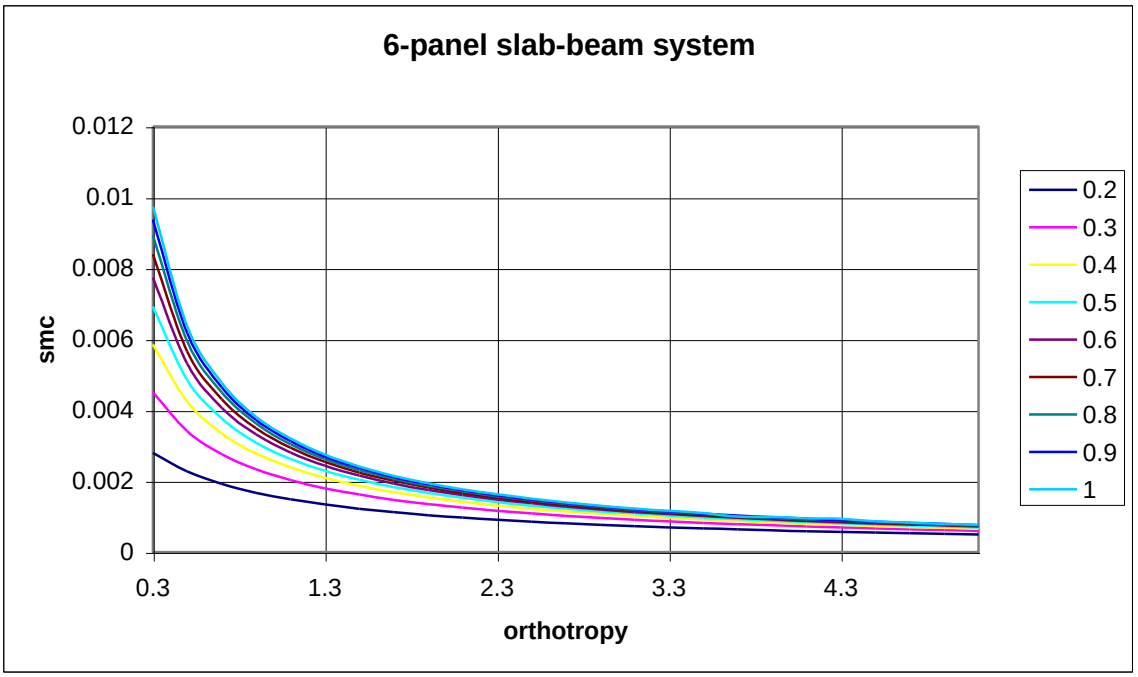

Figure 3.40: Variation of slab moment-coefficient (smc) with the orthotropy at $\lambda = 0.8$

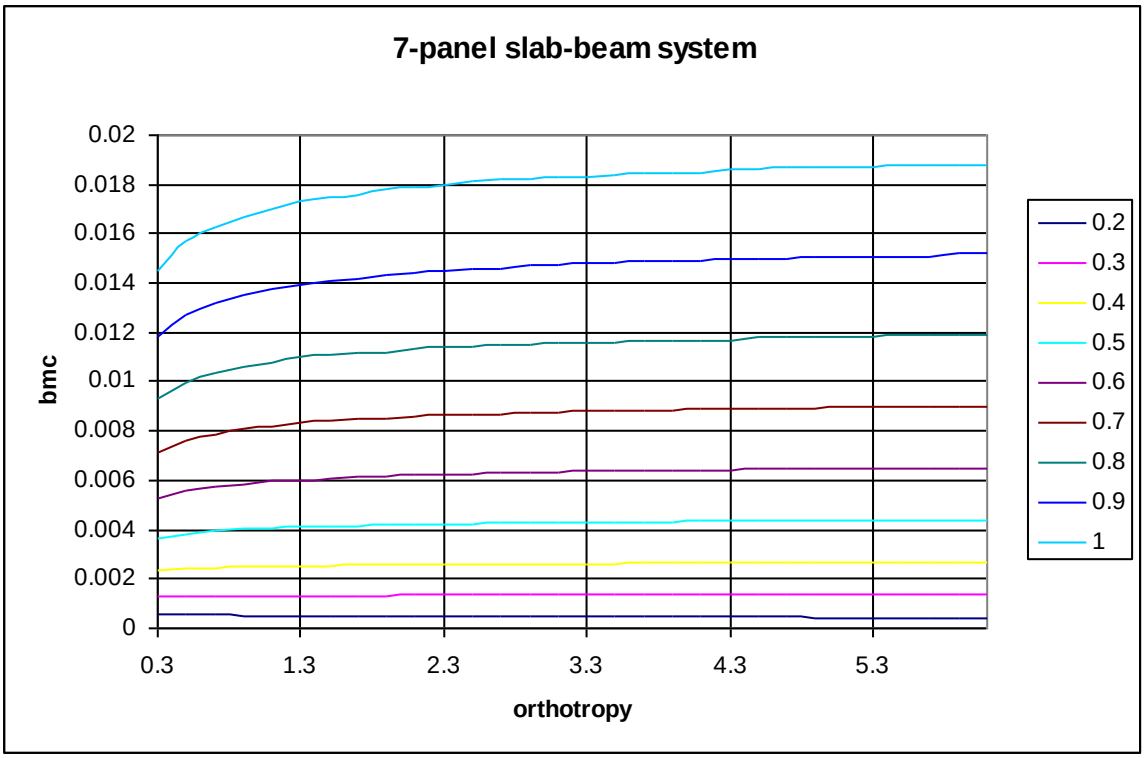

Figure 3.41: Variation of beam moment-coefficient (bmc) with the orthotropy at $\lambda = 0.8$

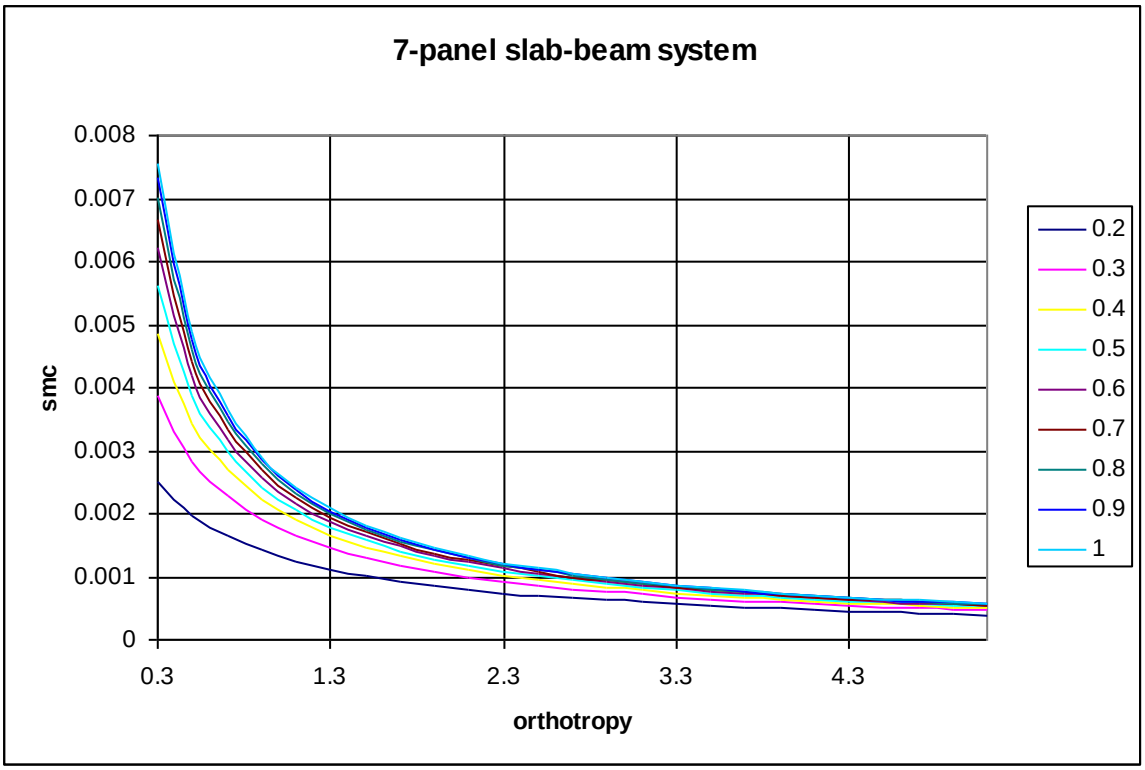

Figure 3.42: Variation of slab moment-coefficient (smc) with the orthotropy at $\lambda = 0.8$

Figures 3.7 to 3.42 indicate that the flexural strength requirement of the internal beams of the laterally loaded slab-beam system remains almost constant for the slab-beam systems with aspect ratio ($r \leq 0.5$) irrespective of the number of panels and orthotropy. When the behavior of the slab-beam system approaches the one-way action ($r \leq 0.5$), the effect of the orthotropy on the beam-strength requirement became almost negligible. At this stage, the slab-beam system transfers the external load essentially along its short span (l_y). It is therefore suggested that beams should be avoided for the slab-systems having short span less than or equal to 3.5m; however, the advantage of using internal beams (acting as stiffeners in the slab-system) should be taken into account for reducing the slab thickness for a span longer than 3.5m. The number of internal panels should be suitably decided, as it does not have much influence over the moment field.

In case of a two-way slab-beam system ($r > 0.5$), the strength requirement of the supporting beams is most affected when the orthotropy of the slab-system with four or less number of internal panels is increased form the minimum possible value to the three. Thereafter, it remains almost constant (within ±5% deviation from the mean value). If two-way slab-beam systems are designed with the value of the orthotropy less than the unity, internal beams of relatively low strength are required to support the load than the slab-system which has been reinforced with orthotropy of more than unity. It is therefore always better to use the value of the orthotropy corresponding to the elastic distribution of the moment field in the slab system. The moment field corresponding to this value of the orthotropy in the slab system will produce a most economical slab-beam section and simultaneously, it would not violate the serviceability criterion (excessive crack width etc.) of the design codes. This is because; the moment field corresponding to this value of the orthotropy will closely follows the elastic moment field in the slab and it would not poses any serviceability problem at service load. This value of the orthotropy can be obtained from the equation (3.26). These values are given in Table (3.7) for the ready reference.

Table 3.7: Value of the orthotropy for Elastic-Distribution of Moment-Field

Aspect ratio, r	0.2	0.3	0.4	0.5	0.6	0.7	0.8	0.9	1.0
Orthotropy, μ	5.80	3.80	2.80	2.20	1.80	1.51	1.30	1.13	1.00

The orthotropy plays a significant role in controlling the strength requirement of the supporting beams of slab-beam systems having four or less number of internal panels. A slight increase in the value of the orthotropy significantly increases the bending moment in the supporting beams of two-way slab-beam system ($r > 0.5$). However, the designer

cannot take the advantage of this trend because the moment field in the slab increases exponentially with the reduction in the orthotropy of the slab-beam system. The slab-beam system would behave satisfactorily under the service load only if the moment field in the slab-system does not deviate significantly from the elastic distribution, otherwise, it will start posing some serviceability problems at the service load.

It is therefore, always is a good practice to proportionate the slab-beam system with the orthotropy corresponding to the elastic-distribution of moment-field, and with as large number of internal panels as permitted by the design/architectural constraints. Because the moment field in the slab-system reduces with the increase of number of panels and attains its almost constant value after certain number of panels. The slab-beam system demands stronger and stronger beams for supporting the load as the shape of the slab-beam system changes from the rectangular ($0.3 < r < 0.9$) to the square ($r = 1$) and when the structural action of the slab system changes from the one-way to the two-way action.

3.8 EFFECT OF BEAM-DEPTH ON COLLAPSE MECHANISM

Yield lines in any loaded slab always develop along the lines of maximum curvature forming in the slab and the stiffness/depth of the support system whether external or internal is directly responsible for the formation of these lines along the line of maximum curvature in the slab. A highly stiff support and/or beam cause a sudden change in the curvature across its line and leads to the formation of negative yield lines along its length. A reduction in the beam-stiffness/depth attracts the lines of maximum curvature in the slab toward the internal beams and an increase in the beam stiffness/depth repels these lines away from the beams. At some typical value of the stiffness/depth, line of maximum curvature start passing through the beam(s) thereby, changing the nature of the collapse mechanism from the local-collapse mechanism (highly stiff beam case) to a global-collapse mechanism (relatively flexible beam case). The strength of the slab and the internal beam(s) in general and strength available along the lines of maximum curvature in particular dictates the collapse load of the slab-beam system and there exists a coupling between the stiffness and strength of the slab-beam system. Any change in the one parameter has a significant effect on the other.

All the internal beams in the slab-beam system have been assumed as shallow in nature while formulating the analytical model. A shallow beam is defined as a flexural member having a stiffness/depth that fails to provide a perfectly non-yielding edge to the slab and maintains compatibility condition with respect to the displacement field at the

interface of the supporting beam and the supported slab during loading. In other words, it will provide an elastic support to the slab and will not induce any negative moment at top face of the slab along its edges. As a result, no negative yield line pattern can develop in the slab rather the supported slab will behave as an ordinary single panel slab panel supported over the non-yielding edges at its outer boundaries and only a positive yield line pattern can develop in the slab along the lines of maximum curvature at the ultimate state.

A beam that provides an exactly non-yielding edge to the supported member is called as non-shallow beam and it always results in the development of a negative yield line along its length along with the positive yield line pattern in the slab at ultimate state. In the absence of any reinforcement for these negative yield moments, all panels of the slab will start behaving as isolated smaller rectangular slab at collapse.

To determine the effect of the beam-depth on the moment field induced in the slab, a parametric study was conducted using the finite element analysis. In this study, two panel and three panel rectangular slabs with various aspect ratios were subjected to the out-of-plane uniform area load. Only a linear-elastic analysis was performed to determine the minimum *span-depth* ratio for the supporting beams which results in the negative moment field at the top face of the slab. A typical set of the stress contours for the moment, m_x induced in the four-panel slab; discontinuous over its outer boundary with an aspect ratio, r (= 0.7117) supported over the beam with various *span-depth* ratio of 95.47, 50, 40, 30, 20, 18, 15, 14, 13, 12, 11, 10, 7.5 and 5.0 are shown in *Figures 3.43 to 3.56*. Reproducibility of the results was checked by repeating the same procedure for the two-panel slabs with aspect ratio of 0.5.

These figures clearly distinguished the *span-depth* ratios (L/d-value) of the supporting beam at which the shallow beam starts behaving as non-shallow beams. It is indicated in these figures that the supporting beams with a depth less than *span/12* act as a shallow beam and the same beam behave as a pure non-shallow beam at depth more than *span/12*. The behavior of the supporting beam at *span-depth* ratio of 10 becomes quite analogous to the brick and/or RCC wall and both initiates negative yield lines in the slab running parallel to the longitudinal edges of the supporting beams.

The results from the analysis also indicate an almost constant value of the moments for the slab and supporting beams at the *span-depth* ratio of less than 12.

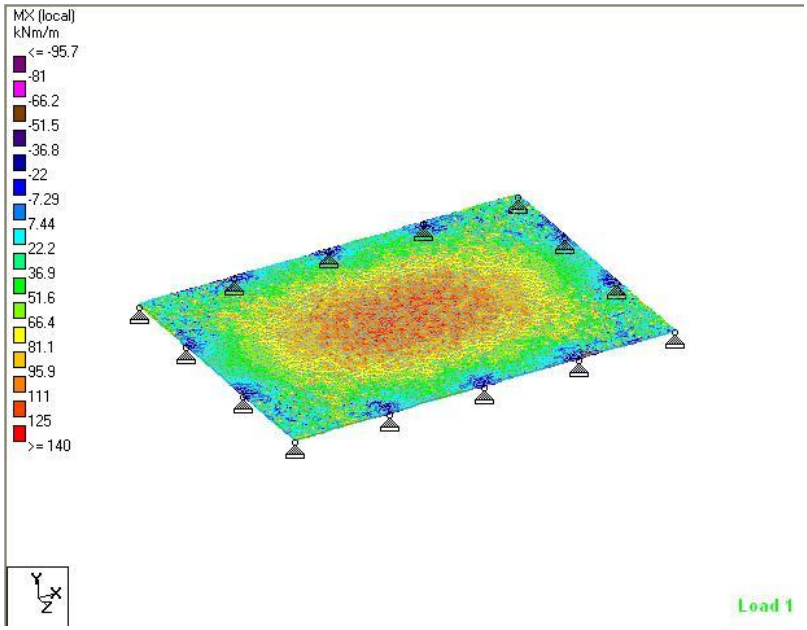

Figure 3.43: Slab with Beams having span-depth ratio = 95.47

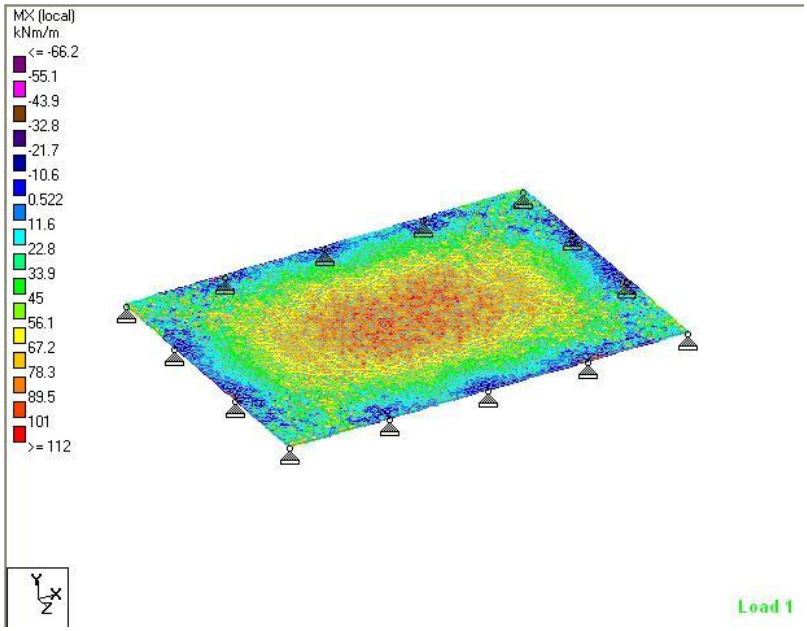

Figure 3.44: Slab with Beams having span-depth ratio = 50

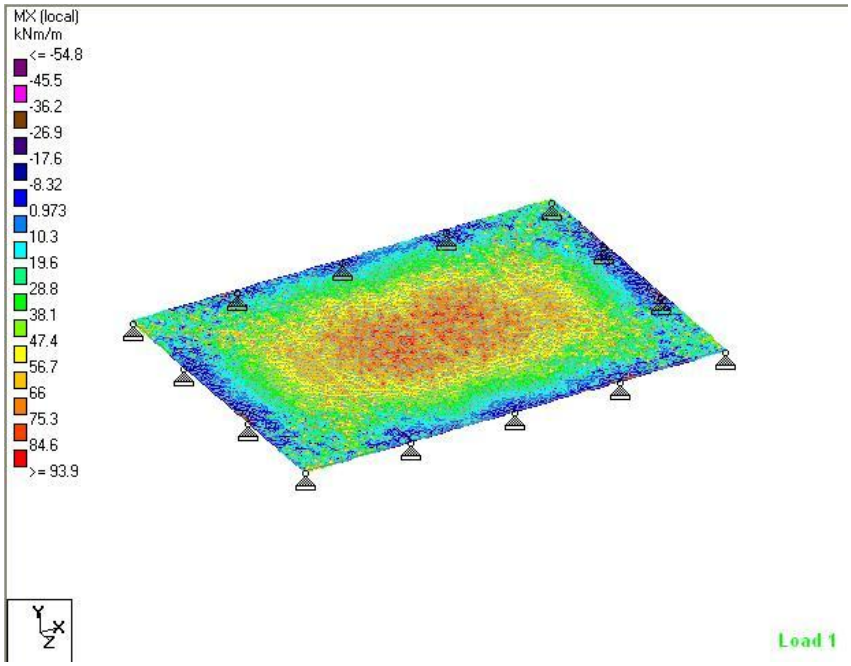

Figure 3.45: Slab with Beams having span-depth ratio = 40

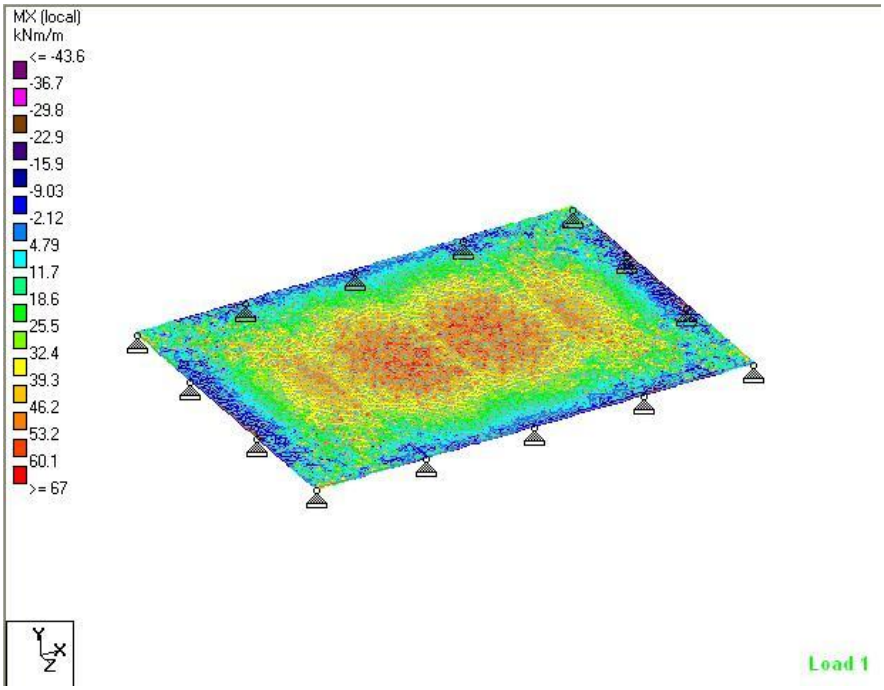

Figure 3.46: Slab with Beams having span-depth ratio = 30

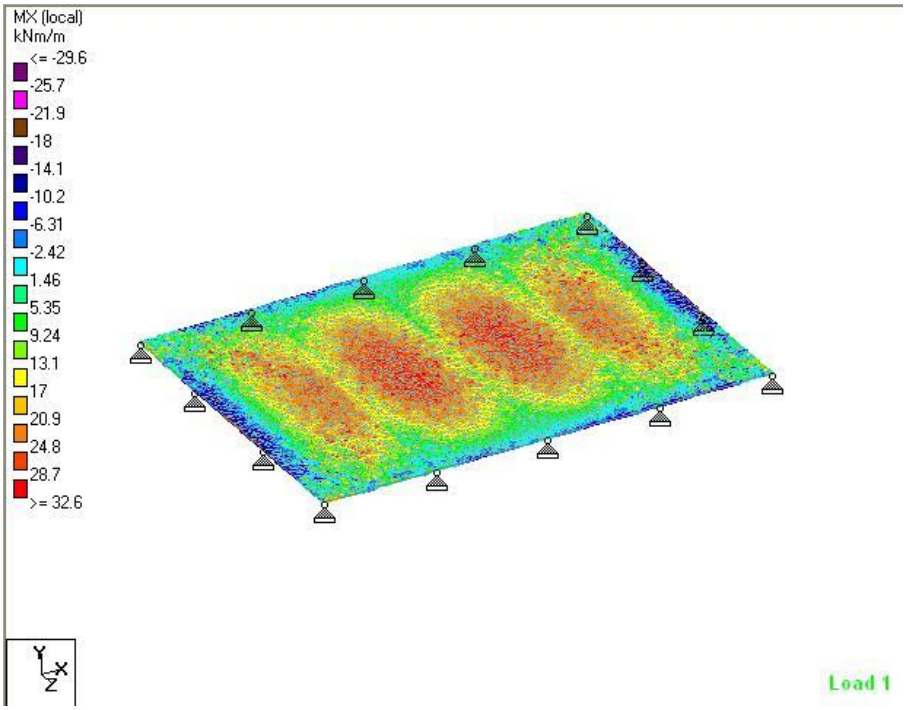

Figure 3.47: Slab with Beams having span-depth ratio = 20

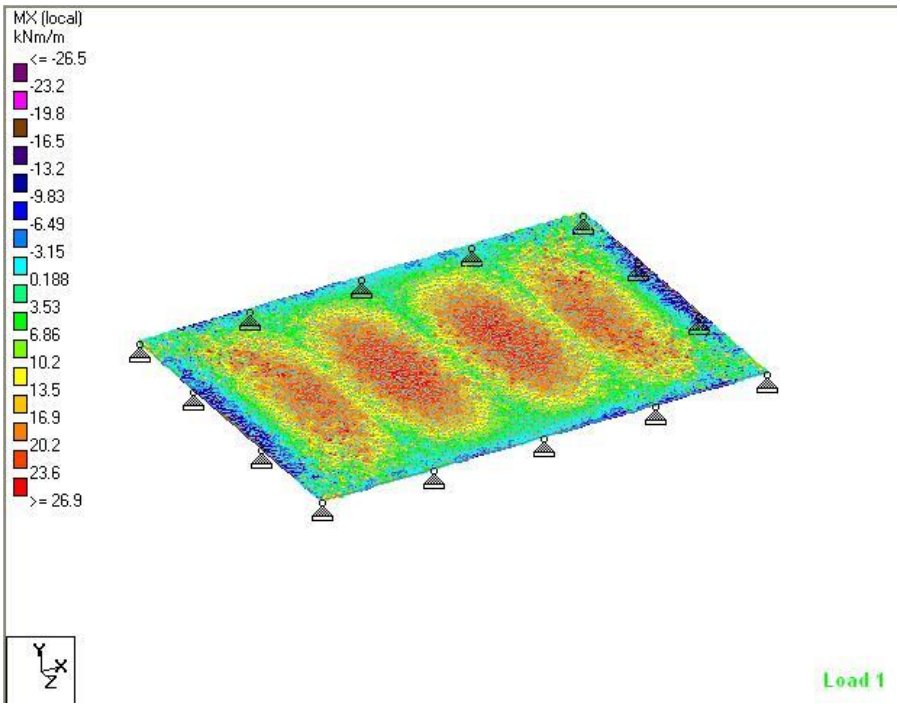

Figure 3.48: Slab with Beams having span-depth ratio = 18

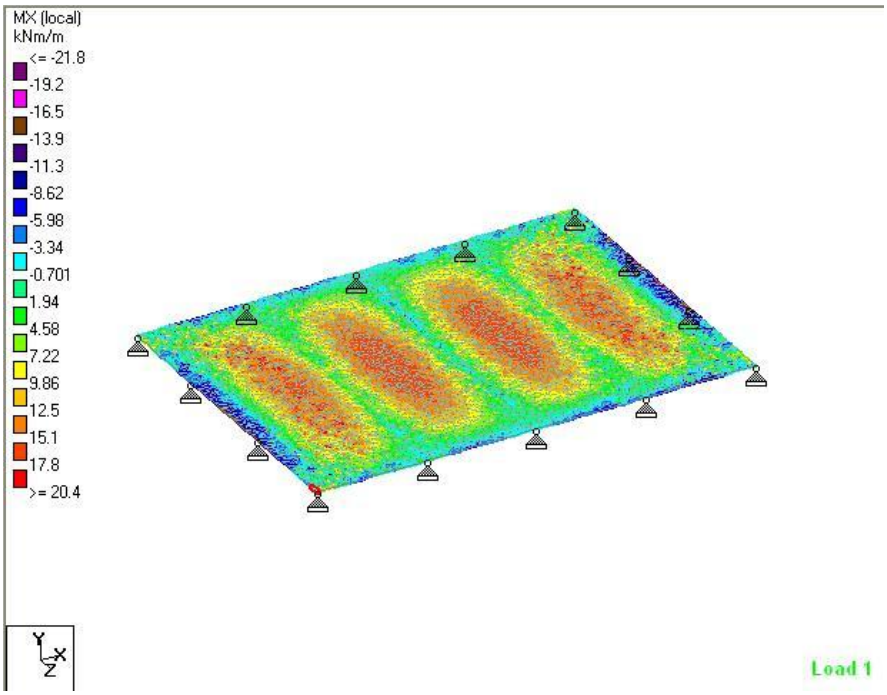

Figure 3.49: Slab with Beams having span-depth ratio = 15

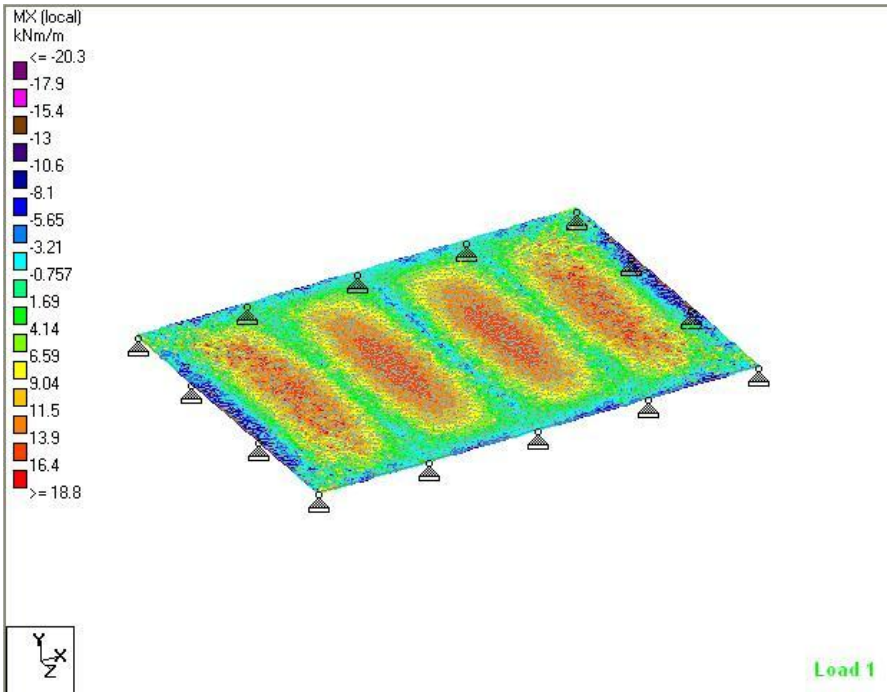

Figure 3.50: Slab with Beams having span-depth ratio = 14

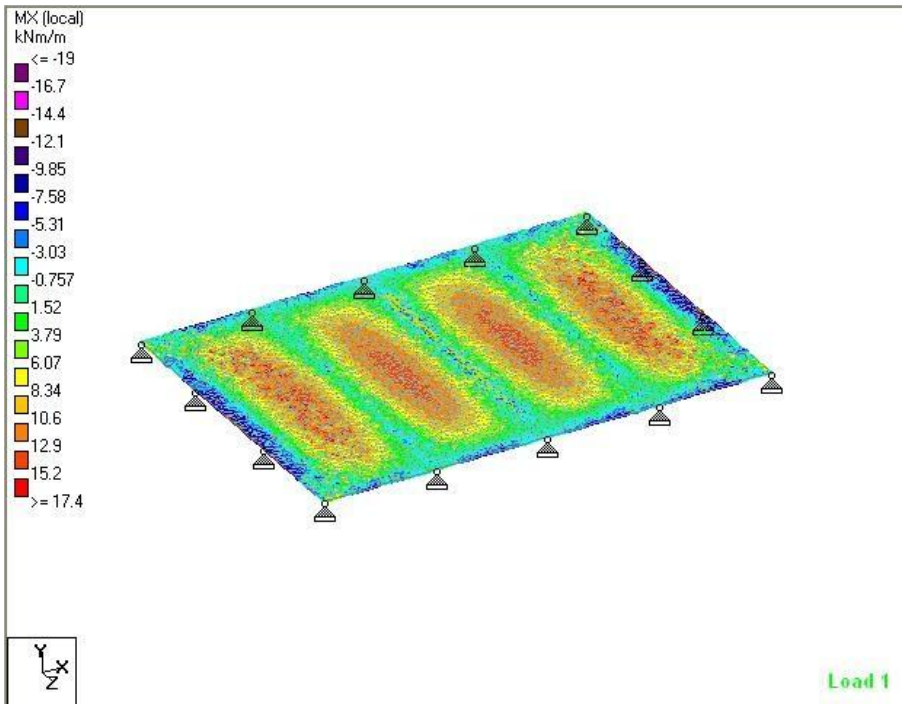

Figure 3.51: Slab with Beams having span-depth ratio = 13

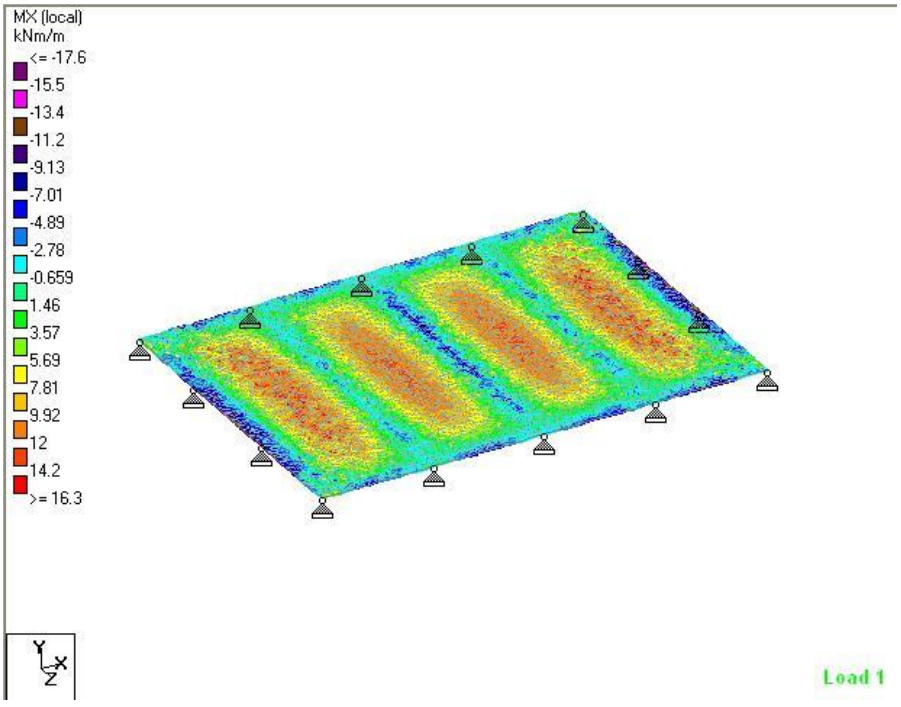

Figure 3.52: Slab with Beams having span-depth ratio = 12

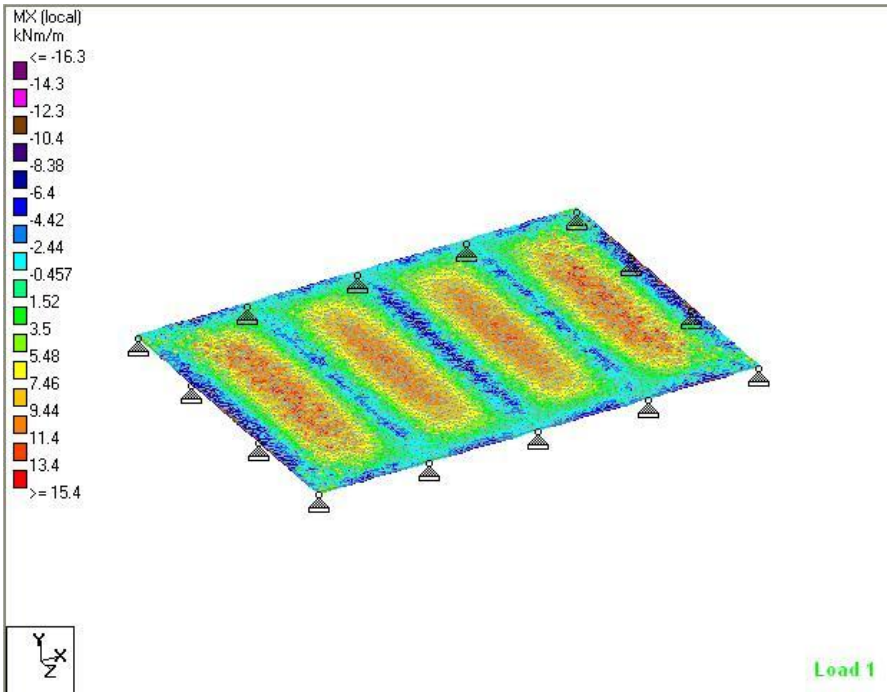

Figure 3.53: Slab with Beams having span-depth ratio = 11

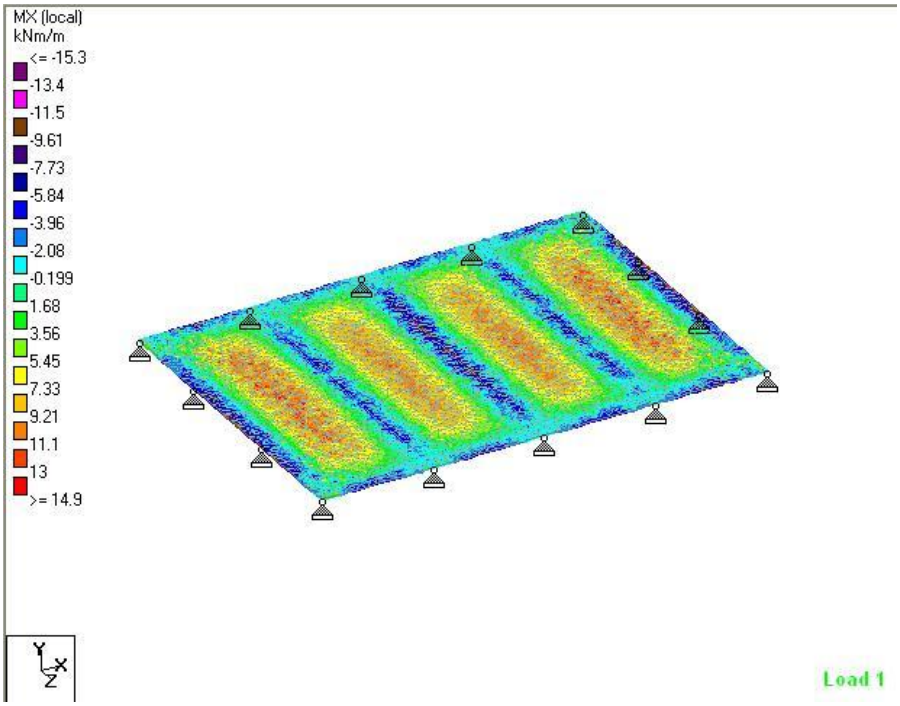

Figure 3.54: Slab with Beams having span-depth ratio = 10

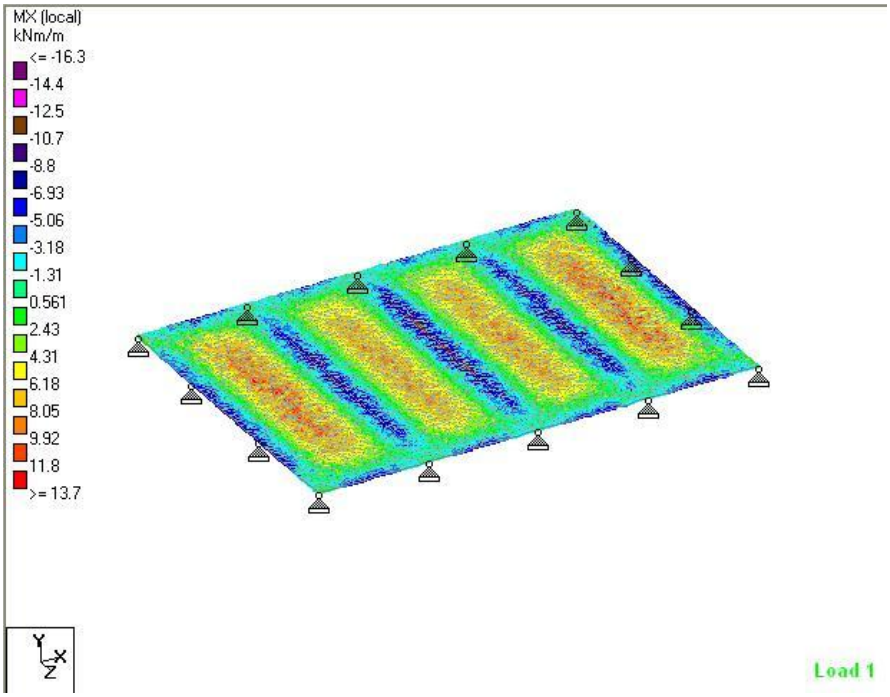

Figure 3.55: Slab with Beams having span-depth ratio = 7.5

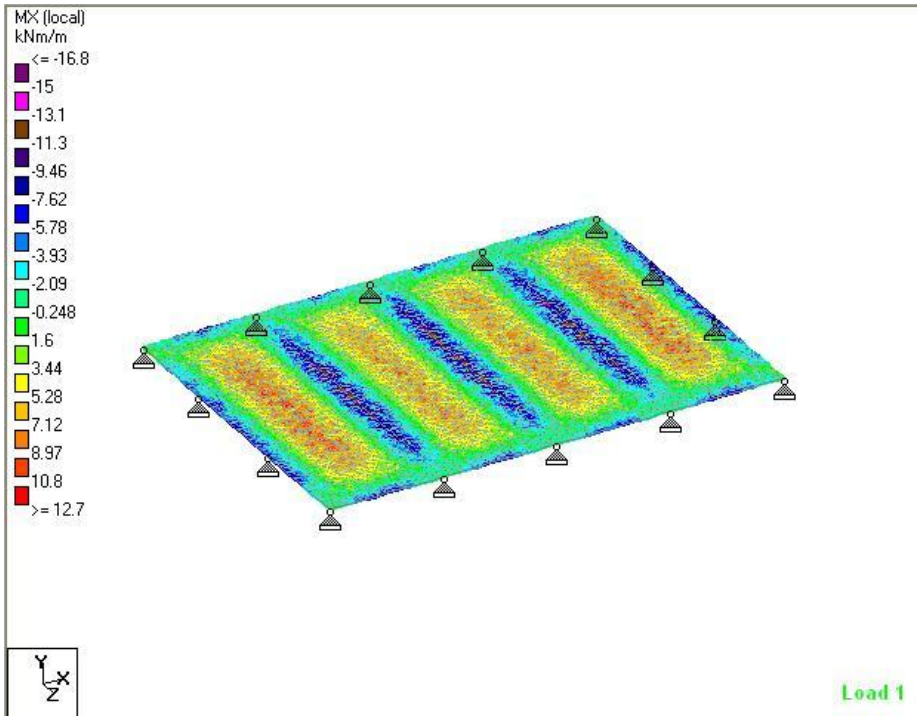

Figure 3.56: Slab with Beams having span-depth ratio = 5

3.9 CLOSURE

- An analytical model has been suggested for the analysis and design of a laterally loaded rectangular reinforced slab-beam system resting over the non-yielding edges at outer boundaries and cast monolithically using the internal equally spaced supporting beams. The results for a single-panel isotropically reinforced square slab obtained from the suggested model compares favorably well with that obtained from the well-established literature on the slab analysis. It can also be used to predict the collapse load of skew-shaped slabs by multiplying the moment field of rectangular slab by $\sin^2\theta$, where θ is the skew-angle.

- The slab-beam system can fail either globally or locally with the development of a yield line mechanism in the entire slab or in panels of the slab-beam system respectively depending upon the strength and/or stiffness of the internal supporting beams. The collapse mechanism is called as global-collapse mechanism if the slab-beam system fails globally; otherwise it is called as local-collapse mechanism.

- The strength requirement (moment field) in the slab-beam system and the nature of the failure mode can be determined by selecting a suitable value of the slab-parameter (A) whereas the stiffness of supporting beams and/or slab-system depends entirely upon the *span/depth* ratio. The *span/depth* ratio of less than 10 would always initiate a failure of the slab-system in the local-collapse mechanism and beams with *span-depth* ratio less than 12 always need some negative reinforcement in the slab (normal to the beam axis).

- The slab-beam system can sustain the load in the global-collapse mechanism mode only in the narrow range of the slab-parameters, $A_{c1} < A < A_{c2}$ thereby, allowing the designer to proportionate the slab-beam system with any suitable value of the slab-parameter from this range. The selection of this parameter will greatly control the strength requirement of the internal beams of the slab-beam system. Low strength supporting-beams will be required in the slab-beam system to support the lateral load at the low value of the slab-parameter with a corresponding heavy slab section and vice versa.

- A non-dimensional parameter called as moment-manipulator, λ ($= \alpha_b / \alpha_{bc}$) has been suggested to classify the slab-beam system based upon the failure mode of the laterally loaded slab-beam system at collapse. If the slab-system has been designed with $\lambda < 1$, it would sustain the lateral load in the global-collapse mechanism mode; whereby the supporting-beams of the slab-system can be used very effectively for controlling the load

sharing along the components of the slab-beam system. Otherwise, the same slab (with $\lambda > 1$) will support the external load in the local-collapse mechanism mode and it would be transformed into the slab-beam system consisting of a number of interconnected smaller slabs resting over the internal beams at collapse.

- The supporting beams of the slab-beam system behave as a shallow-flexible beam if these have been designed with λ-value less than unity. Otherwise, same set of supporting beams would act as shallow-rigid beams.

- The λ-value can be used very conveniently to control the participation of the slab in load sharing along with the beams of the slab-system. The slab-beam system will behave as a single panel slab at zero λ-value ($A = A_{c1}$) and it will be divided into a number of smaller rectangular slabs simply resting over the internal beams at $\lambda=1$ ($A = A_{c2}$). The supporting-beams at this λ-value or $A = A_{c2}$ behave similar to the non-yielding beams and/or walls and the slab would always fail by the formation of a local-collapse mechanism irrespective of its stiffness. The participation of the slab in the load sharing can be increased by selecting a lower value of the beam-strength parameter, α_b and vice versa.
- The value of the orthotropy should be kept as permitted by the elastic-distribution of the moment-field for the better performance of the slab-beam system under service load.

- The design moment-field in the slab-beam system cannot be minimized with respect to the orthotropy. However, selecting the lowest possible of the orthotropy as permitted by the elastic plate theory can help the designer to minimize the design moment field.

- The moment field in the slab reduces exponentially with the increase of the orthotropy irrespective of the number of panels of a two-way slab-beam system (aspect ratio more than 0.5). This rate of reduction becomes almost constant after the $\mu = 3$, and when the slab-beam system has been divided into five or more panels.

- This rate of reduction is relatively small and it becomes almost constant (within 5% of the mean value) for the slab-beam systems having aspect ratio less than 0.5, when it has been proportioned with the orthotropy of three or more irrespective of the number of panels.

- The strength requirement of the supporting beams increases, when the slab-beam system has been proportioned with higher value of the orthotropy and it become almost

constant after $\mu = 3$, and when the slab-beam system has been divided into five or more panels.

- The moment field in the slab-beam system reduces with the increase in number of internals panels. The number of panels therefore, should be selected as large as permitted by the architectural constraints and practicability at the site.

- The strength requirement of the supporting beams is insensitive to the increase and/or decrease of the orthotropy for the one-way slabs. It is therefore, suggested that the one-way slab-beam system ($r \leq 0.5$) with short span (l_y) up to the 3.5m should be designed without internal beams and the internal beams should be provided to reduce the slab thickness for higher span (over and above 3.5m).

CHAPTER-4

VALIDATION OF MODEL

4.1 GENERAL

A reinforced concrete slab progressively loaded to a failure develops a band of the flexural cracks at its tensile face along the lines of maximum curvature. At low load level and before the initiation of tensile cracks, the distribution of bending moments and displacement field defining the deflection of middle plane of the slab follows the elastic plate theory. After the formation of these cracks, the distribution of the moment field changes significantly depending upon the load level due to the differential reduction in the stiffness in various regions of the slab caused by flexural and torsional cracking, as well as inelastic behavior of concrete and reinforcement. With the further increase in the loading, yielding of the tensile steel eventually occurs along the lines of maximum moment and the slab undergoes a large change in the curvature at the sections of yielding, with the moment there remaining practically constant at the ultimate moment of resistance of the slab section. The slab can be said to be collapsed at this stage of loading, when it fails to support any additional load.

A laterally loaded reinforced concrete slab resting over the non-yielding supports on its outer boundaries and divided into panels of equal length by the internal shallow beams-a beam that deflects along with the slab under applied load, will exhibit exactly the same behavior as shown by a single panel slab with identical boundary conditions as described in the first paragraph.

If the slab-beam system has been designed with λ-value less than unity, it is expected that the slab must fail following the global collapse mechanism at the ultimate load. The same slab will collapse with the formation of the local panel-mechanism if it has been designed with a value of λ equal to or more than unity. In other words, the supporting beam will behave similar to the rigid/non-yielding beams for a slab-beam system designed with $\lambda \geq 1$; otherwise same supporting beams will start behaving as flexible beams and allows the yield-line, developed in the slab, to pass through it at the state of collapse.

The designers, thus, have a number of options to design with, depending upon the value of the moment-manipulator (λ) considered in the design. The slab will be a heavily

reinforced with massive concrete section at the small value of λ (less than unity) and it would require a light beam section having a small depth. And if the value of λ is taken as high (say 90% of α_{bc}), the slab section will be lightly reinforced with a smaller depth and the beam will become heavy in terms of the percentage tensile steel and the depth. For the intermediate value of moment-manipulator (λ) in the above range, infinite possibilities exist for proportioning a slab-beam system with given structural and/or architectural constraints.

To validate these analytical predictions, the full-scale slab panels designed using the proposed analytical model is tested experimentally on the loading-frame to collapse. The failure pattern, the collapse load and any other unexpected structural behavior of the slab specimens at the ultimate load are compared with the solution predicted from the analytical-model and the results from this experimental testing are presented in this chapter. In addition to this, the comparisons of the results from the analytical model with the results from the well-established literature on the slab analysis are also described in the present chapter.

4.2 EXPERIMETAL VALIDATION

In the present experimental investigations, three types of the reinforced concrete slabs resting over the non-yielding supports on its four outer edges are considered for full scale testing. These are divided into panels of equal length by the internal shallow and non-shallow beams. These slab specimens have been proportioned using the analytical model and design equations developed in the chapter-3. The slabs were designed to support a uniform area load of 20 kN/m^2 so that a significant number of deflection readings could be taken before its inelastic range starts and simultaneously, the slab specimens can be detailed as per the maximum rebar spacing recommended by design code. Moreover, the small size of the slabs require a lesser amount of tensile steel under a small magnitude of design load which was very difficult to detail in compliance with the design code due to non-availability of small diameter rebars. The details of test specimens are given below:

CASE-1: In this set, two-panel reinforced concrete slabs with non-yielding supports on its outer four sides were considered. These test specimens were designed with $\lambda < 1$; thereby, ensuring its failure in the global-collapse mechanism at the ultimate state and the supporting shallow beam are expected to behave as a shallow-flexible beam. This slab specimen is designated as 2PSF (two-panel shallow flexible). The detail of this slab

specimen is shown in *Figure 4.1*. The second slab specimen in this case is designed with $\lambda > 1$ and this slab specimen is expected to fail following a local-collapse mechanism with supporting shallow beam behaving similar to a rigid/non-yielding-beam. It may cause some flexural cracking at the top face of the slab along the beam edges. This slab is designated as 2PSR (two-panel shallow rigid). The detail of this slab specimen is shown in *Figure 4.2*.

CASE-2: In this set, three-panel reinforced concrete slab specimens have been designed with the non-yielding supports on its outer boundaries with $\lambda < 1$, thereby ensuring the failure of the slab specimen in the global-collapse mechanism at ultimate state and accordingly, the internal supporting shallow beams behave as shallow-flexible beams. This slab is designated as 3PSF (three-panel shallow flexible). The detail of this slab specimen is shown in *Figure 4.4*. The second slab specimen in this case is designed with $\lambda > 1$. It is expected that this slab specimen will fail following the local-collapse mechanism with the supporting shallow beams acting similar to a rigid beam. These may also cause flexural cracking at the top face of the slab along the beam edges. This slab is designated as 3PSR (three-panel shallow rigid) and is shown in *Figure 4.5*.

CASE-3: In this set, a two- and three-panel reinforced concrete slab specimens have been designed with the non-yielding supports at the outer boundaries of the slab with equally spaced internal supporting beam(s). The depth of these beams is kept sufficiently deep (non-shallow) to cause the flexural cracking at the top face of the slab along the edges of the beams (negative yield line) and both slab specimens have been designed with $\lambda > 1$. These slab specimens are expected to fail following the local-collapse mechanism with the formation of a yield line pattern, locally, in all panels of the slab at the ultimate state. The supporting beams in this case will act as rigid beams due to their significant depth ($\geq$ *span/10*). These two- and three-panel slab specimens are designated as 2PNS (two-panel non-shallow) and 3PNS (three-panel non-shallow) respectively and the details of these slab specimens are shown in *Figure 4.3* and *Figure 4.6* respectively.

4.2.1 Experimental Setup

A multipurpose reaction frame of 1000 kN rated capacity was fabricated, which can be used for the full scale testing of beams with span varying from 0.5m to 5m and one way and/or two-way slab panels with any aspect ratio under an uniform area load and/or a concentrated force applied at any point over the surface of the slab specimens (2.35m x

5m) and with any type of the edge-conditions *viz:* slab specimens supported over two and/or three sides, two panel continuous slab, fixed-edge can also be simulated with any degree of end restraint. The schematic diagram of frame is shown in *Figure 4.7.*

In the laboratory investigations, the full-scale slab specimens were loaded to a failure in the multipurpose reaction frame. The uniform area load, acting over the whole surface, was gradually applied to the top surface of the slab through a specially fabricated load distribution system. This has been shown in *Figure 4.8*. All slab specimens are assumed to be resting over the simple supports at the outer edges, with corners free to uplift during the loading. All the slab specimens were cast in M-20 concrete using the locally available materials. M-20 grade concrete mix was designed following the Indian Standard recommended guidelines. The mix proportion of concrete was found to be 1**:**1.47**:**2.5 with w/c-ratio of 0.5. The 28-day average compressive strength of the150mm concrete cubes made by these proportions was found to be 32.0 MPa (> Target strength, f_t = 27.5 MPa). The properties of reinforcement steel bars are given in Table 4.1 and the physical properties of the constituent materials of the concrete are given in Tables 4.2, 4.3 and 4.4. The details of the slab specimens are given in Table 4.5.

Table 4.1: Physical Properties of Steel Rebars (TATA Tiscon)

S. No.	Parameter*	Experimental Value
1.	Ultimate Tensile Strength	518.00 MPa
2.	Yield Strength	445.00 MPa
3.	Elongation	17%

*(Average value for various diameters used in design)

Table 4.2: Physical Properties of Cement (PPC 43 Grade)

S. No.	Parameter	Experimental Value
1.	Fineness (by 90micron sieve)	5%
2.	Standard Consistency	37%
3.	Specific gravity	3.03
4.	Compressive Strength at 7day	21.21 MPa
5.	Compressive Strength at 28day	53.00 MPa

Table 4.3: Physical Properties of Fine Aggregates

S. No.	Parameter	Experimental Value
1.	Fineness Modulus and Zone	2.626, and III
2.	Specific gravity	2.70
3.	Unit Weight (loose)	14.22 kN/m^3
4.	Unit Weight (dense)	16.77 kN/m^3

Table 4.4: Physical Properties of Coarse Aggregates

S. No.	Parameter	Experimental Value
1.	Fineness Modulus	5.82
2.	Type/size	All-in aggregate of 10mm
3.	Specific gravity	2.62
4.	Unit Weight (loose)	16.68 kN/m^3
5.	Unit Weight (dense)	17.17 kN/m^3

Table 4.5: Summary of the Key Factors of Test Slabs

Slab Type (slab size, mm)	Slab symbol	Reinforcing detail for the slab and beams				L/D-ratio for beam	λ-value	Remarks* (beam will act as……)
		Along side L_x of slab, mm c/c	Along side l_y of slab, mm c/c	Steel on tensile face of beam	Steel on the top face of beam			
Two-Panel Slab (4000 x 2350 x 75)	2PSF	10ϕ 140	10ϕ 200	3-16ϕ	3-12ϕ	15.67	0.61	Flexible-shallow
	2PSR	8ϕ 145	8ϕ 185	3-20ϕ	2-20ϕ +1-12ϕ	15.67	1.36	Rigid-shallow
	2PNS	8ϕ 145	8ϕ 185	2-16ϕ +1-12ϕ	2-12ϕ	10.00	1.83	Rigid-non shallow
Three-Panel Slab (5000 x 2350 x75)	3PSF	10ϕ 150	10ϕ 190	3-16ϕ	3-12ϕ	15.67	0.48	Flexible-shallow
	3PSR	6ϕ 120	6ϕ 150	3-20ϕ	2-20ϕ +1-12ϕ	15.67	1.73	Rigid-shallow
	3PNS	6ϕ 120	6ϕ 150	2-16ϕ +1-12ϕ	2-12ϕ	10.00	2.19	Rigid-non shallow

* If the depth of the supporting beams is kept less than *span/10*, it will act as shallow beam (See chapter-3). And it will act as flexible-shallow beam for λ<1, and as a rigid-shallow beam if λ-value is kept more than unity irrespective of its depth.

The slab specimens, designated as 2PSF and 2PSR, are two panel slabs of size 4000 x 2350 x 75mm. The slab specimens were divided into two panels by an equally spaced internal shallow beam of size 200 x 150mm with the *span/depth-ratio* of 15.67. These two slab specimens were designed using the proposed analytical model to sustain the design load of 20 kN/m^2. The details of slab specimens are given Table 4.5.

The slab specimens, designated by the symbols 3PSF and 3PSR, are three panel slabs of size 5000 x 2350 x 75mm. These slab specimens were divided into three panels by the two equally spaced internal shallow beams of size 200 x 150mm with the *span/depth*-ratio of 15.67. The reinforcement details of these two slab specimens have been given in Table 4.5 and both were designed using the proposed analytical model with λ-value less than unity (3PSF) and the second slab specimen with λ-value greater than unity (3PSR) to sustain the design load of 20 kN/m^2.

And in the third case, the slab specimens designated by the symbols 2PNS and 3PNS are two- and three-panel slabs of size 4000 x 2350 x 75mm, and 5000 x 2350 x 75mm respectively. These slabs were divided into the two and the three panels respectively by the equally spaced internal non-shallow beams of size 200 x 235mm with the *span/depth-ratio* of 10.0, thus, forcing the slab specimens to fail in the local-collapse mechanism at the ultimate state. Both the specimens were designed using the proposed analytical model with λ-value greater than unity to sustain the design load of 20 kN/m^2.

4.2.2 Casting of Test-Specimens

All test slabs were cast on the level ground with the designed mix, M20 concrete. The rebars were placed on the ground with the bottom clear cover of 15mm and the side clear cover of 25mm. The internal beams of size 200 x 150mm for the 2(3)PS-series, and 200 x 235mm for 2(3)PN-series of the test slabs were cast as a inverted-beam with the partial beam-depth projecting from the upper surface of the slab. The details of the specimens have been shown in *Figures 4.1* to *4.6*. The concrete was poured and leveled to the uniform thickness by a trowel and leveling bar, and then the rod vibrator was used for the compaction. The side shuttering was fixed at the top surface of the slab along the beam length and concrete was poured, compacted using the rod vibrator to obtain the required beam size. After casting, the slab specimens were left for the water curing for the 28 days. No reinforcement was provided at the top face of the slab near the longitudinal edges of the beams due to their shallow depth and for the non-shallow beams, it was intentionally not provided for the comparison purpose.

4.2.3 Testing of Specimens

After 28 days of water curing, the slab specimens were lifted using the gantry-crane arrangement from the casting yard to the reaction frame. The typical schematic diagrams showing the lifting-and-transferring of the two-panel slab to the reaction frame is shown in *Figure 4.10*. The bottom internal movable-beam of the reaction frame was fixed using the bolts to achieve the required size of the test slab-specimens. This beam along with the other outer lower-reaction beams of the frame will provide a non-yielding support at the outer boundary of the slab. The slab specimen supported over these non-yielding beams is shown in *Figure 4.11*.

The concentrated reaction of the hydraulic jack fixed at the upper movable reaction-girder of the frame was distributed as a uniform area load acting over the top surface of the test slab by a load-transferring arrangement. In this arrangement, 25mm diameter mild

steel balls were placed along an orthogonal grid at the uniform spacing of 50mm. The wooden planks about 25mm thick were stacked systematically over these steel balls as shown in *Figure 4.12*. These planks transfer and distribute the reaction of the transfer-girders to the grid of uniformly placed steel balls and the reaction from this grid act as a uniform area load for the test slabs.

Low value of the Young's modulus (E), flexural strength and thickness of the wooden planks, used to distribute the concentrated load from the jack, will give a near uniform pressure over the slab specimen at/or near the collapse load. At low value of the jack load, it will give a load distribution with a variation of about 10-12% (more pressure near mid-span in comparison to edges). However, this pressure becomes more and more uniform as the slab specimen deflects under the increasing concentrated jack load. However, it was ensured during loading that deflection pattern must remain axisymmetric to check that slab is deflecting evenly. The spacing of the steel balls used to transfer the load over the slab has been determined by varying the space between balls using software on assumption that these are resting over the non-yielding supports/surface thereby giving more reaction for inner supports (balls) in comparison to balls near end spans however, this reaction will become more and more even when balls/supports in interior of continuous beam/plate starts yielding (representing deflection of a slab specimen under increasing load). Low value of Young's modulus (E), flexural strength and thickness will ensure that this occurs as early as possible under increasing load.

Dial gauges with least count of 0.01mm were used to measure the vertical deflection of the slab specimens under a gradually increasing load. Three dial gauges were placed along each diagonal of the slab to check the uniformity of applied load and this will be assumed to occur if the deflection pattern of the slab is observed to be axisymmetric at all the load increments. However, the value of the central dial gauge was used to identify the collapse load. The value of the load gauge at which the vertical deflection at the lower face of the slab starts increasing at very high rate and the slab specimen fails to support any additional load is taken as the collapse load.

Manual hydraulic jack was pumped gradually to exert a uniform pressure over the top surface of the slab and this load was increased gradually in the small increments of 2-5 kN/m^2 to the full collapse load of the slab specimens. The vertical defection at the lower face of the slab was observed at each load increments in the linear range of the load-deflection curve and in the non-linear range, this value of the deflection was noted only when the dial reading becomes stable.

The bottom and the top face of the slab specimens were examined manually after each load increment to check the initiation of any possible cracking and any other unexpected behavior. The sequences of the cracking at both faces of the slab specimens was observed along with the corresponding load and dial gauge reading. These were reproduced on the paper. And the value of the load at which the slab specimen fails to carry any additional increase in the load—increase the load, the load gauge reading will increase but it will return to same initial value after some time, the value of load gauge at this stage is taken as the collapse load of the slab specimen.

4.2.4 Test Results

The development of the yield line pattern for the various slab specimens and their load-deflection curves are shown in *Figures 4.13 to 4.24*. The slabs designed for $\lambda<1$ are 2PSF and 3PSF, and these slab specimens have sustained the design load of 20 kN/m^2 without any cracking, whereas the slab specimens designed with $\lambda>1$ has developed some cracks at the top face near the ends of the supporting beams before reaching their design load. The permissible short-term deflection for the all slab specimens has been taken as 7.85mm (≈ *span/300)* based upon the serviceability criterion of the design code, IS 456 (2000). The details of the test results for all these slab specimens are given below:

4.2.4.1 Slab, 2PSF

A uniform area load was applied gradually at the top face of the slab specimen. The first flexural crack appeared at 21 kN/m^2 along the span, L_x of the slab specimen crossing the internal supporting beam at about its mid span. This crack grows in length and numbers under increasing load and the first diagonal-corner crack initiates at 24 kN/m^2. The mid-span and corner cracks grow in length and joined each other at load of 25.5 kN/m^2. The cracked slab continues to support the applied load and this band of cracks develops to a complete yield line pattern at load of about 28 kN/m^2 and then, the slab specimen failed to sustain any further increase in loading beyond 31.75 kN/m^2 with corresponding mid-span deflection of 39.38mm. This deflection reduces to 22.50mm after the release of load. The collapse load to design load ratio for this slab specimen was found to be 1.587 and it sustained the design load as predicted by the analytical model with the corresponding mid-span deflection of 20.00mm. In this case, the depth of supporting beam was kept less than *span/12*; therefore, it behaved as a shallow beam and did not produce any negative moment field along its length at top face of the slab. Accordingly, no reinforcement was provided at top face of the slab along the length of the beam. As a result, only a positive

yield line pattern was developed in the slab at ultimate state, which was found to be in good agreement with that assumed during the derivation of analytical equations. The stages of formation of the yield line pattern and the corresponding load-deflection profile of the slab specimen is shown in *Figure 4.13* and *Figure 4.14* respectively.

The deflection at the design load was found to be more than the prescribed value by the design code but selecting a suitable beam depth as per the serviceability criterion of the design code can control it. Moreover, it must be ensured that selected beam depth should be less than *span/12* to facilitate the formation of the global-collapse mechanism in the supported slab at the ultimate state.

4.2.4.2 Slab, 2PSR

The slab specimen was subjected to a uniform area load applied gradually at top face of the slab. Small cracks about 150mm in length and inclined at 30^o to the internal beam appeared at top face of the slab specimen at load of about 18 kN/m^2 and these cracks grow in numbers with increasing load as shown in *Figure 4.15*. Small diagonal cracks at bottom face of the slab initiated simultaneously from all corners of the slab specimen at load of about 21 kN/m^2. These cracks grow in length along with the formation of additional cracks parallel to the span, l_y at mid-span of both slab panels at load of 22 kN/m^2. Additional diagonal cracks formed near the ends of the internal beam with a slight increase in load. These cracks grow in length and joined each other. And this band of cracks develops to the complete positive yield line pattern at load of about 24 kN/m^2 and then, the slab specimen failed to sustain any additional load increments beyond 28 kN/m^2 with corresponding mid-span deflection of 22.84mm. This deflection reduces to 5.50mm after the release of load. The collapse load to design load ratio for this slab was found to be 1.40 and it sustained the design load as predicted by analytical equations with corresponding mid-span deflection of 12.00mm. The yield line pattern developed in the slab at ultimate state was in good agreement with that assumed during derivation of the design equation *i.e.* the slab failed following the local collapse mechanism by dividing the slab into two isolated panels. The load-deflection profile of the slab specimen is shown in *Figure 4.16*.

In this case, the depth of supporting beam was kept less than *span/12*, therefore it behaved as a shallow beam and it did not produce any negative moment field along its length at the top face of the slab. Moreover, no reinforcement was provided at the top face of the slab to take care of any negative moment field as a result, only a positive yield line

pattern was developed in the slab at ultimate state along with some negative yield lines, inclined to the beam axis, formed due to the sudden change in the curvature near ends of the supporting beam. These negative yield lines were initiated at load of about 18 kN/m^2 due to the absence of any top reinforcement in the slab specimen. Therefore, it is suggested that the slab-beam system with the shallow beams should never be proportioned with λ-value more than or equal to unity without adequate negative reinforcement near the beam-ends.

The deflection at the design load was found to be more than the prescribed value by the design code but selecting a suitable beam depth as per the serviceability criterion of the design code can control it. Moreover, it must be ensured that selected beam depth should be less than *span/12* to facilitate the formation of the global-collapse mechanism in the supported slab at the ultimate state.

4.2.4.3 Slab, 3PSF

The slab specimen was subjected to a uniform area load applied gradually at the top face of the slab specimen. The first flexural crack appeared in the slab at load of 21 kN/m^2 along the span, L_x crossing the internal supporting beams at about its mid span. This crack grows in length and numbers under the increasing load and the first diagonal-corner crack initiates at 22.5 kN/m^2. The mid-span and the corner cracks grow in length and joined each other at load of 25 kN/m^2. This cracked slab continues to support the applied load and this band of cracks develops to a complete yield line pattern at load of about 26.86 kN/m^2. Then, the slab specimen failed to sustain any additional load beyond 29 kN/m^2 with the corresponding mid-span deflection of 24.80mm and the value of this deflection reduces to 6.75mm after the release of load. The collapse load to design load ratio for the slab specimen was found to be 1.45 and it sustained the design load as predicted by the analytical equations with corresponding mid-span deflection of 12.5mm. The yield line pattern developed in the slab at the ultimate state was found to be in good agreement with that assumed in the analytical modeling. The stages of formation of the yield line pattern, and the corresponding load-deflection profile of the slab specimen is shown in *Figure 4.17* and *Figure 4.18* respectively.

In this case, the supporting beams behaved as shallow ones due to their smaller depth, being less than *span/12.* These beams did not produce any negative moment field along their length at the top face of the slab and accordingly, no reinforcement was provided at the top face. As a result, only a positive yield line pattern was developed in the slab at

ultimate state, which was found to be in good agreement with that assumed during the analytical modeling.

The deflection at the design load was found to be more than the prescribed value by the design code but selecting a suitable beam depth as per the serviceability criterion of the design code can control it. Moreover, it must be ensured that selected beam depth should be less than *span/12* to facilitate the formation of the global-collapse mechanism in the supported slab at the ultimate state.

4.2.4.4 Slab, 3PSR

The slab specimen was subjected to a uniform area load applied gradually at top face of the slab. Small cracks about 150mm in length and inclined at 44^o to the internal supporting beams appeared at the top face of the slab near the ends at load of about 19 kN/m^2 and these cracks grow in numbers (fine cracks) with increasing load as shown in *Figure 4.19*. Small diagonal cracks at the bottom face of the slab initiated simultaneously from all corners of the slab panels at load of about 21 kN/m^2. These cracks grow in length along with the formation of additional cracks parallel to the span, l_y at mid-span of both slab panels at load of 22 kN/m^2. With slight increase in the load, these cracks grow in length and joined each other. This cracked slab continues to support the applied load and this band of cracks develops to a complete positive yield line pattern at load of about 23.59 kN/m^2 and then, the slab specimen failed to sustain any additional load beyond 26 kN/m^2 with the corresponding mid-span deflection of 16.90mm and this deflection reduces to 3.70mm after the release of load. The collapse load to the design load ratio for the slab specimen was found to be 1.30 and it sustained the design load as predicted by the analytical model with corresponding mid-span deflection of 9.50mm. The yield line pattern developed in the slab at the ultimate state was found to be in good agreement with that assumed in the analytical modeling *i.e.* the slab failed following the local collapse mechanism by dividing the slab into two isolated panels. The load-deflection profile of the slab specimen is shown in *Figure 4.20.*

In this case, the depth of the supporting beams was kept as less than *span/12*, thereby forcing the supporting beams to behave as shallow beams and these beams did not produce any negative moment field along their length at the top face of the slab. No reinforcement was provided at the top face of the slab to take care of any negative moment field induced in the slab under applied load. As a result, only a positive yield line pattern was developed in the slab at ultimate state along with some negative yield lines,

formed due to a sudden change in the curvature near ends of the supporting beams. These negative yield lines were initiated due to absence of any top reinforcement in the slab at surface load of about 18 kN/m^2. Therefore, it is suggested that slab-beam system with the shallow beams should never be proportioned with λ-value more than unity without adequate negative reinforcement near the beam-ends.

The deflection at the design load was found to be more than the prescribed value by the design code but selecting a suitable beam depth as per the serviceability criterion of the design code can control it. Moreover, it must be ensured that selected beam depth should be less than *span/12* to facilitate the formation of the global-collapse mechanism in the supported slab at the ultimate state.

4.2.4.5 Slab, 2PNS

The slab specimen was subjected to a uniform area load applied gradually at top face of the slab. Small cracks about 150mm in length and inclined at 30^o to the internal beam appeared at top face of the slab at load of about 18 kN/m^2 and these cracks developed to a full-length crack along both sides of the beam at load of about 19 kN/m^2. The first flexural crack appeared at 20 kN/m^2 at bottom face of the slab along the span, l_y at mid-span of both slab panels along with small diagonal cracks initiating from all corner of the slab panels. These cracks grow in length and numbers under increasing load and joined each other at load of 22 kN/m^2. This cracked slab continues to support the applied load and this band of cracks develops to the complete positive yield line pattern at load of about 24 kN/m^2. After that, the slab specimen failed to sustain any additional load beyond a load magnitude of 25.05 kN/m^2 with a corresponding mid-span deflection of 7.11mm and the value of this deflection reduces to 2.10mm after release of the load. The collapse load to the design load ratio for this slab was found to be 1.253 and it sustained the design load as predicted by the analytical model with a corresponding mid-span deflection of 5.00mm. The yield line pattern developed in the slab as shown in *Figure 4.21* at the ultimate state was found to be in good agreement with that assumed in the analytical modeling *i.e.* the slab failed following a local collapse mechanism by dividing the slab into two isolated panels. The load-deflection profile of the slab specimen is shown in *Figure 4.22*. In this case, the depth of the supporting beam was kept as *span/10*, therefore it behaved as a non-shallow beam which produces negative moment field along its length at the top face of the slab due to change in the curvature of the supported slab under the surface loading. As no reinforcement was provided at top face of the slab to take care of

this moment field, the negative yield line was formed along the span of the beam, thereby dividing the supported slab into two isolated rectangular panels at surface load of 19 kN/m^2. Formation of these negative yield lines becomes responsible for lowering of the load factor to 1.25 but the deflection of the beam-slab system at the design load was found to be well within the limits prescribed by the design code.

4.2.4.6 Slab, 3PNS

The slab specimen was subjected to a uniform area load applied gradually at top face of the slab. Small cracks about 150mm in length and inclined at 45^o to the internal beams appeared at top face of the slab at load of about 19 kN/m^2 and these cracks grow in numbers with increasing load as shown in *Figure 4.23*. Small diagonal cracks at the bottom face of the slab initiated simultaneously from all corners of the slab at load of about 24.5 kN/m^2. These cracks grow in length along with the formation of additional cracks parallel to the span, l_y at mid-span of all slab panels at load of about 28 kN/m^2. With slight increase in the load, these cracks further grow in length and joined each other. This cracked slab continues to support the applied load and ultimately, this band of cracks develops to a complete positive yield line pattern at load of about 29 kN/m^2 and then, the slab specimen failed to sustain any additional load beyond a load magnitude of 30 kN/m^2 with a corresponding mid-span deflection of 11.20mm which reduces to 3.75mm after release of the load. The collapse load to the design load ratio for the slab specimen was found to be 1.50 and it sustained the design load as predicted by the analytical model with a corresponding mid-span deflection of 5.25mm. The yield line pattern developed in the slab at the ultimate state was found to be in good agreement with that assumed in the analytical modeling *i.e.* the slab failed following the local collapse mechanism by dividing the slab into three isolated panels separated by the internal supporting beams. The load-deflection curve of this slab is shown in *Figure 4.24*.

In this case, the depth of the supporting beams were kept as *span/10*, therefore these behaved as a non-shallow beams which produces negative moment field along their length at the top face of the slab due to sudden change in the curvature across the stiff beam used to support and divide the slab under surface loading. As no reinforcement was provided at the top face of the slab to take care of this moment field, negative yield lines were formed along the span of the beams, thereby dividing the slab into three isolated rectangular panels at surface load of 24 kN/m^2. The deflection of the slab-beam system at the design load was found to be well within limits as prescribed by the design code.

4.2.5 Interpretation of Test-Results

Slab specimens were proportioned using the analytical model suggested in the chapter-3 for a design load of 20 kN/m^2. These specimens were grouped into two classes: one that is expected to fail in the global-collapse mechanism by initiating the composite-action between the slab and the supporting beams whereas in the second group, the slab specimens have been proportioned to fail in the local-collapse mechanism. Accordingly, no reinforcement was provided to give strength against the negative yield lines expected to form at top tensile face of the slab along the length of the supporting beams. This was intentionally done to study the slab-shallow beam interaction at two extreme values of the moment-manipulator (λ) that is used to distinguish the flexible edge from the rigid edge.

It is experimentally observed that the slab specimens (2PSR, 2PNS, 3PSR and 3PNS) designed for the λ-value more than unity lead to the failure of the slab specimens in the local-panel collapse mechanism mode irrespective of the depth of the beams. These specimens have sustained the design load of 20 kN/m^2. However, some diagonal cracks appeared at top face of the slab near ends of the supporting shallow-beams due to the absence of any negative reinforcement in the slab specimens (2PSR and 3PSR) and these cracks extends along the whole length of supporting non-shallow-beams (2PNS and 3PNS). The absence of reinforcement, normal to the beam axis, at the tensile face of the slab specimens becomes responsible for lowering of the load factor in comparison to the first group of the slab specimens (2PSF and 3PSF) which has been designed for $\lambda < 1$. Therefore, it is mandatory to strengthen, suitably, the slab-beam system at the tensile face of the slab for the negative yield lines irrespective of the depth of the supporting beams if the slab-beam system has been proportioned for any value of the moment-manipulator more than unity ($\lambda > 1$).

The slab specimens (2PSF and 3PSF) designed for λ-value less than unity ensure that the slab-beam system always fails following the global-collapse mechanism and the supporting internal shallow beams allow the positive yield line developed in the slab to pass through at the point of maximum moment in the supporting beam(s) at the collapse load. These specimens have also sustained the design load of 20 kN/m^2 with the load factor of more than 1.4.

The collapse mechanism of these slab specimens compare favorably well with the hypothesis yield line pattern adopted during the design of these slab specimens, thereby validating the hypothesis collapse mechanism and the corresponding analytical model.

The summary of the test results is given in Table 4.6. It is indicated that the test slabs 2PSF and 3PSF sustained the design load with a satisfactory load factor but both slab specimens show higher deflections than permitted by the design codes at the design load. However, this deflection can be reduced by selecting a suitable depth of the shallow beams that satisfies the both serviceability criterion of the design codes as well as the *span-depth* ratio limit of the supporting beams required for the formation of global-collapse mechanism in the slab-beam system [see *Annexure B* for an example].

Table 4.6: Summary of the Test Results

Slab Type	Load, kN/m^2 at		Deflection, mm at			$\frac{\text{Collapse Load}}{\text{Design Load}}$
	Collapse	Design	Collapse	Design	Load release	
2PSF	31.75	20.00	39.38	20.00	22.50	1.587
2PSR	28.00	20.00	22.84	11.25	5.50	1.400
2PNS	25.05	20.00	7.11	5.00	7.11	1.253
3PSF	29.00	20.00	14.80	13.75	6.75	1.450
3PSR	26.00	20.00	16.90	9.50	3.70	1.300
3PNS	30.00	20.00	11.20	5.25	3.75	1.500

Test results in Table 4.6 report mid-span deflections of 20.00mm and 11.25mm for 2PSF and 2PSR slab specimens respectively produced under a design load of 20kN/m^2. This difference in the deflection in these two geometrically identical slab specimens is due to the large percentage of steel in internal beams (both total as well as tensile steel) in case of 2PSR in comparison to the slab specimen, 2PSF (about 44% higher than 2PSF) which has a significant effect of the effective stiffness (I_{eff}) in general and especially at the ultimate state when due to extensive cracking the contribution from concrete becomes very small and tensile steel in the section plays a major role in providing both stiffness and strength along with the concrete available above the neutral axis.

The crack width in 2PSF was observed to be as high as 1-2mm along the yield lines and there was excessive spalling of the concrete cover at ultimate state. This was a reason to discontinue the loading of other slab specimens after the development of a complete positive yield line pattern.

It is important to mention that the actual load factor for the slab specimens: 2PSR, 2PNS, 3PSF, 3PSR and 3PNS will be much higher than those reported in the Table 4.6 because loading of the test slabs was discontinued to minimize the damage to the dial

gauges once the visible yield line pattern was developed in the slab-system. Moreover, at this stage, the slab specimens exhibit large deflections along with spalling of the concrete cover that prohibits observation of the crack pattern; its width underneath a test slab and accordingly further increase of loading of test slab was discontinued. This fact can also be noted from Table 4.6 that shows significant inelastic deformations for the test slab, 2PSF and recoverable elastic deformations for other test specimens, thereby indicating that these slab specimens can be stressed more if experimental setup allows the observation at lower face of the slab specimens.

It is therefore recommended that use of slabs cast monolithic with internal shallow beans and designed with λ-value more than unity should be discouraged in practice because it leads to the sudden formation of the diagonal negative yield lines near the beam-ends unless the slab panel has been adequately reinforced at the top face of the slab for this negative moment field.

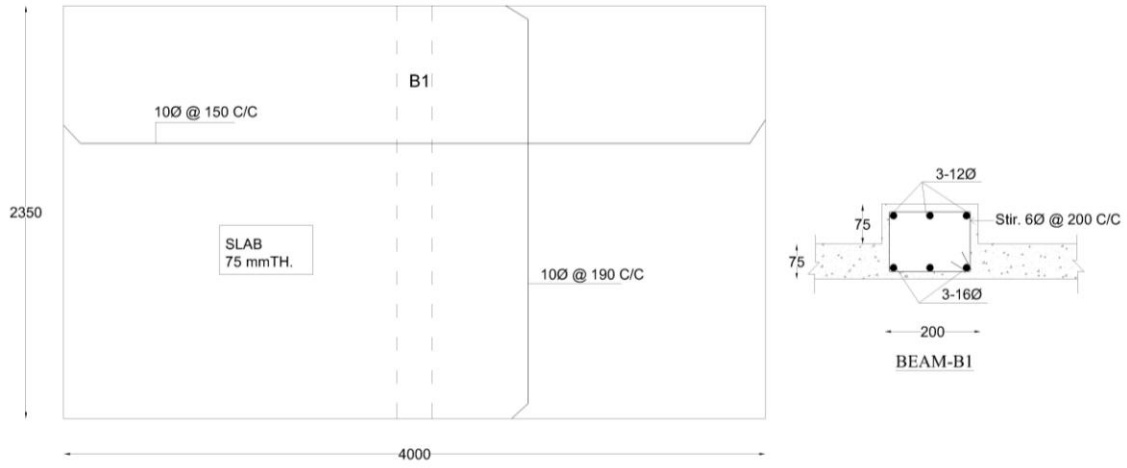

Figure 4.1: Reinforcement Detailing of Slab, 2PSF

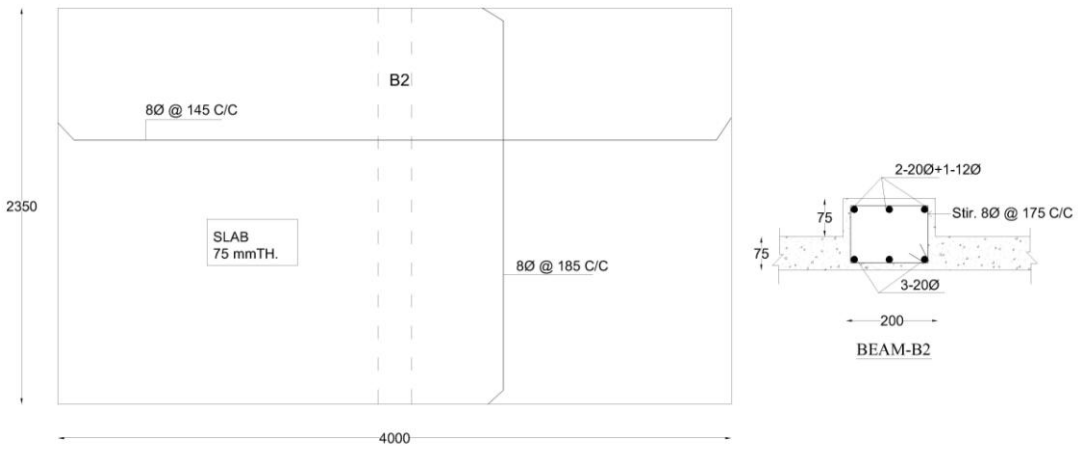

Figure 4.2: Reinforcement Detailing of Slab, 2PSR

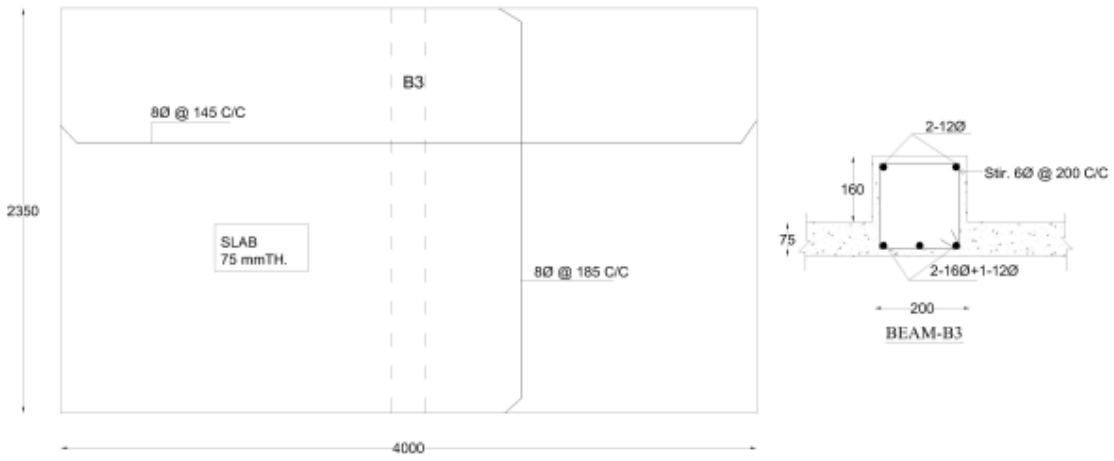

Figure 4.3: Reinforcement Detailing of Slab, 2PNS

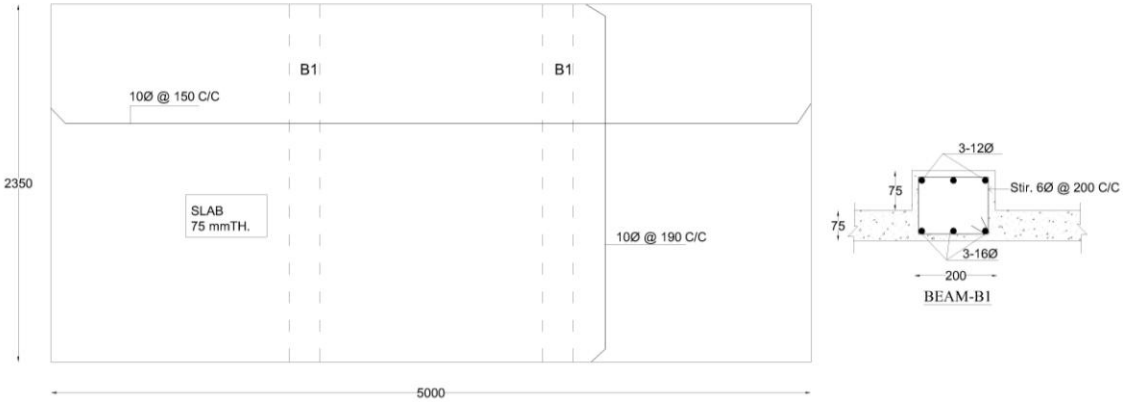

Figure 4.4: Reinforcement Detailing of Slab, 3PSF

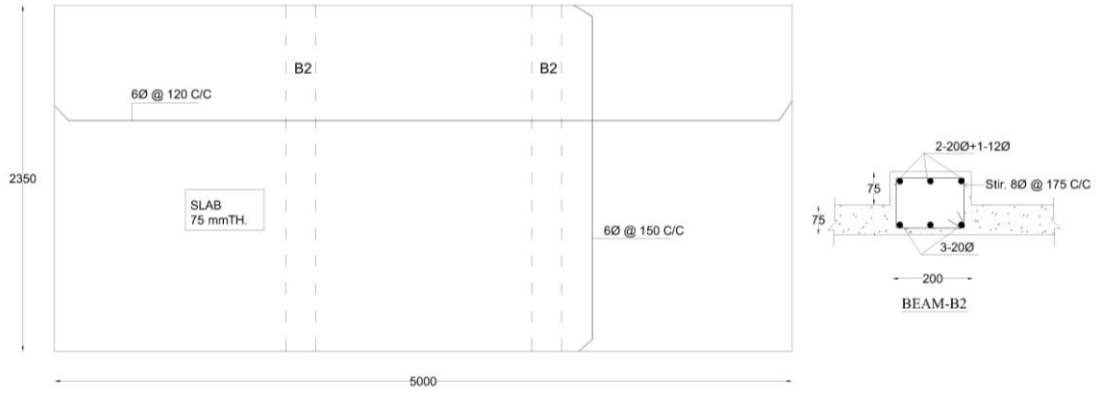

Figure 4.5: Reinforcement Detailing of Slab, 3PSR

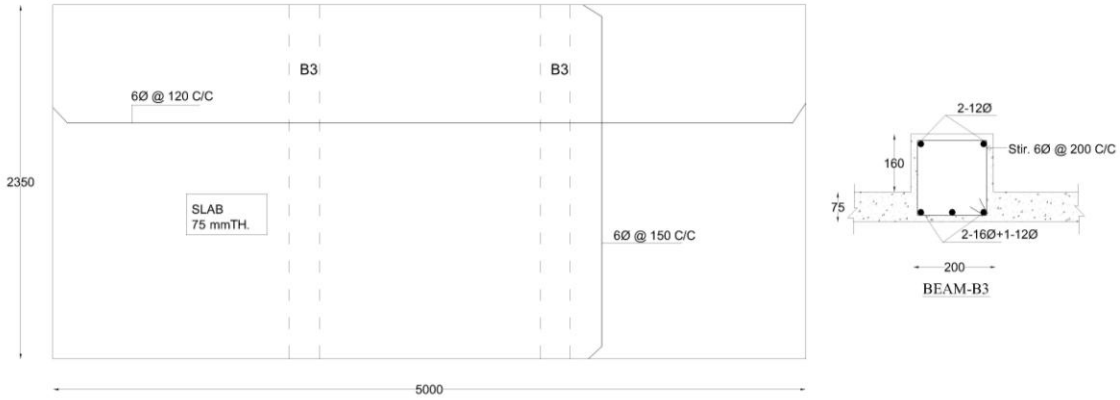

Figure 4.6: Reinforcement Detailing of Slab, 3PNR

Figure 4.7: Schematic Diagram of Multipurpose Reaction Frame

Figure 4.8A: Load Transferring/Distribution Arrangement

Figure 4.8B: Load Transferring/Distribution Arrangement

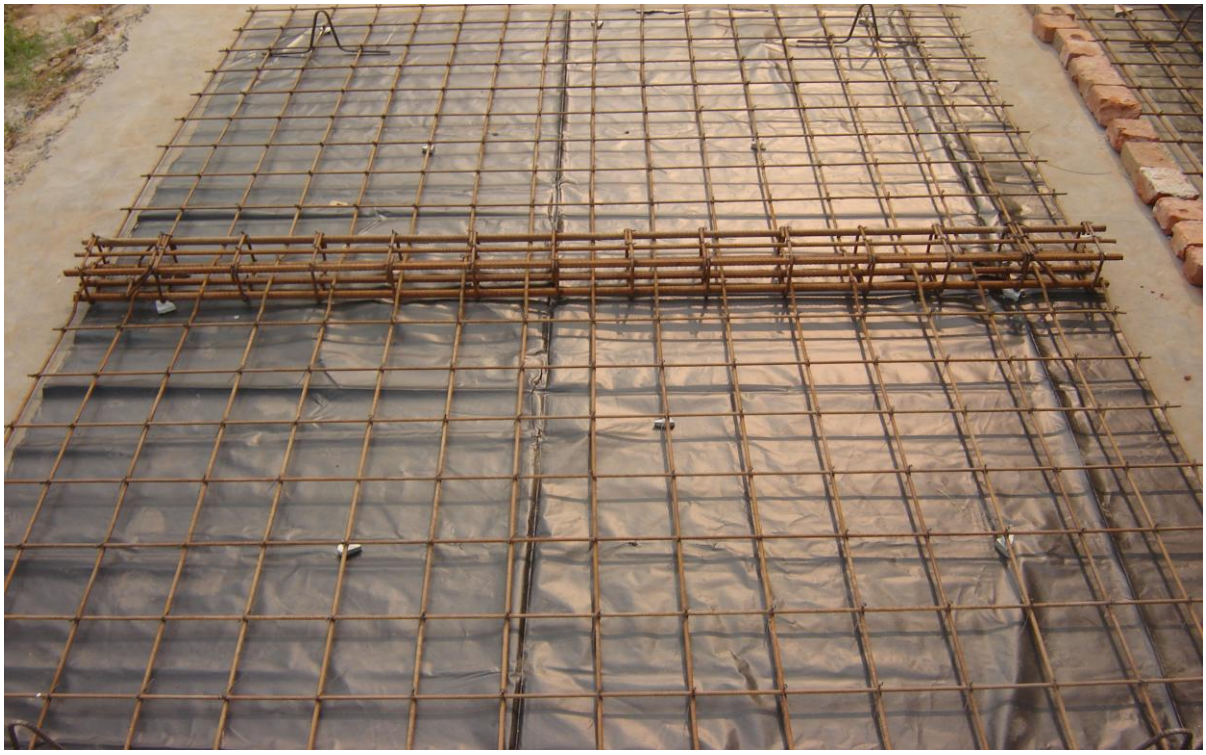

Figure 4.9: Typical Reinforcement Detailing of 2-panel Slab

Figure 4.9A: Typical Schematic Diagram showing Casting of 2-panel Slab

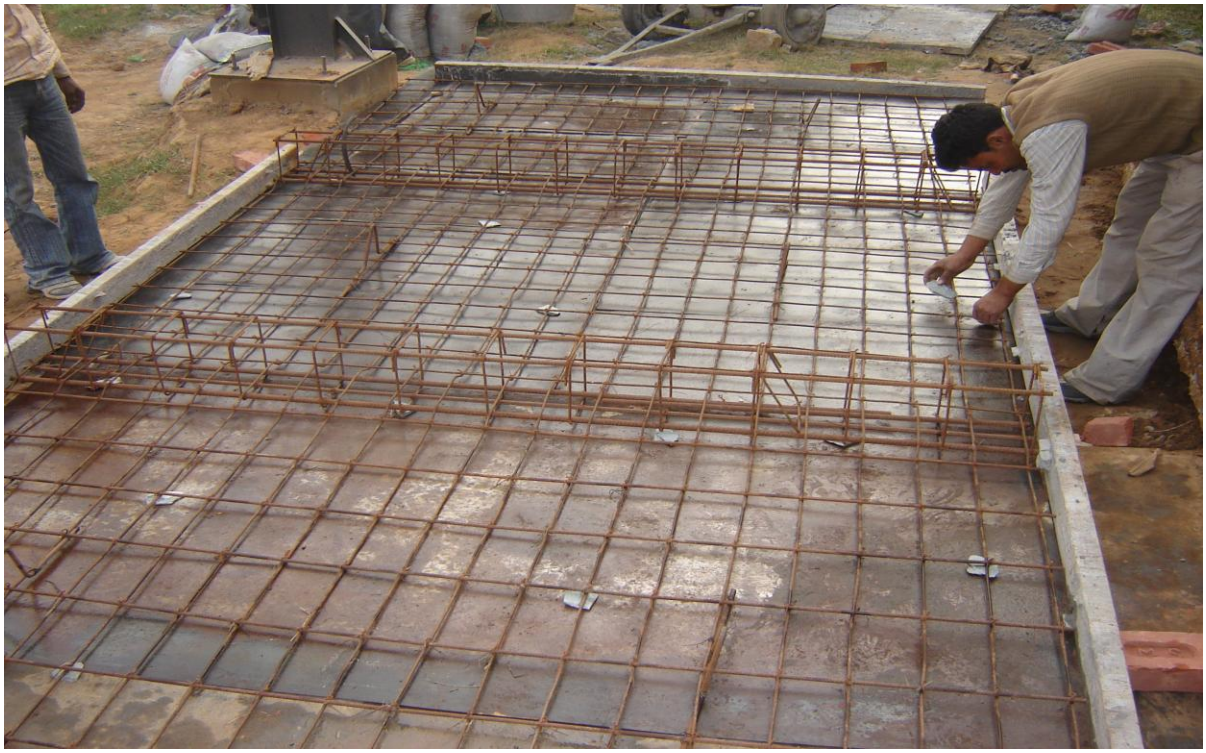

Figure 4.9B: Typical Reinforcement Detailing of 3-panel Slab

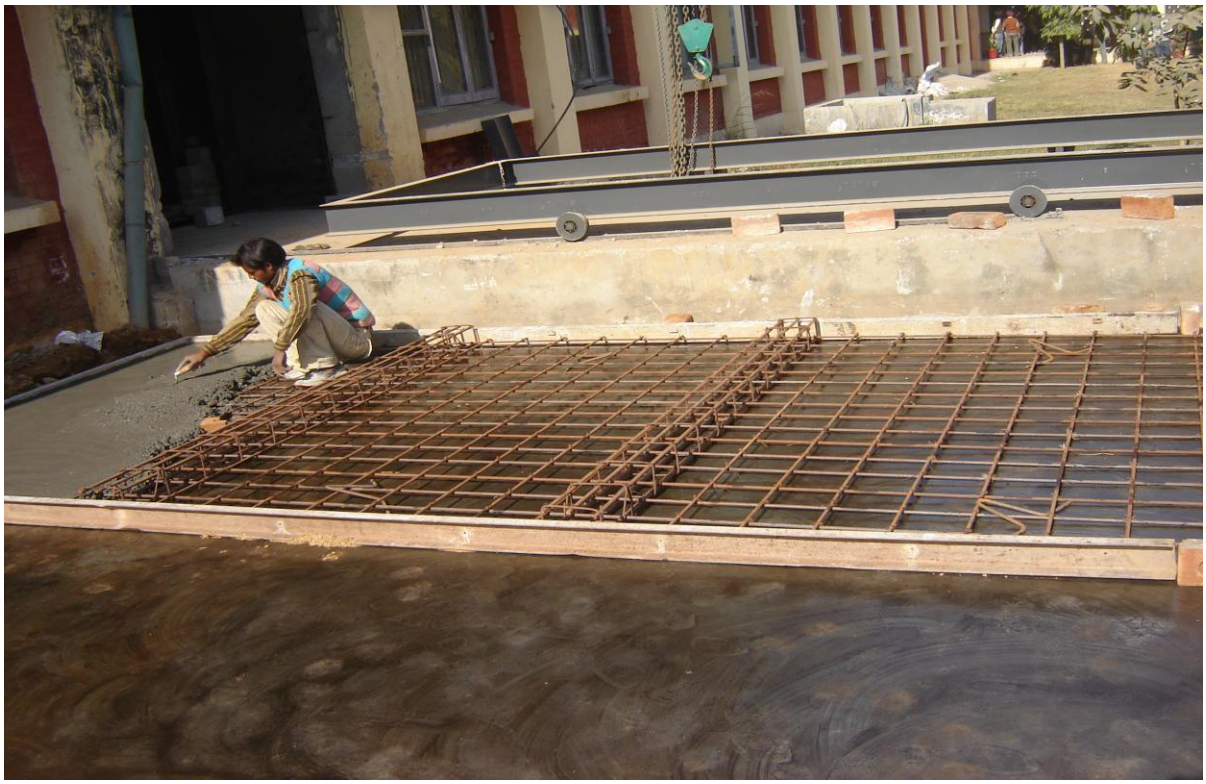

Figure 4.9C: Typical Schematic Diagram showing Casting of 3-panel Slab

Figure 4.10: Typical Schematic Diagram showing the Lifting Operation of Slab

Figure 4.10A: Typical Schematic Diagram showing the Lifting Operation of Slab

Figure 4.10B: Typical Schematic Diagram showing the Lifting Operation of Slab

Figure 4.10C: Typical Schematic Diagram showing the Transferring Operation of Slab

Figure 4.11: Typical Schematic Diagram showing the placement of Slab in Reaction Frame

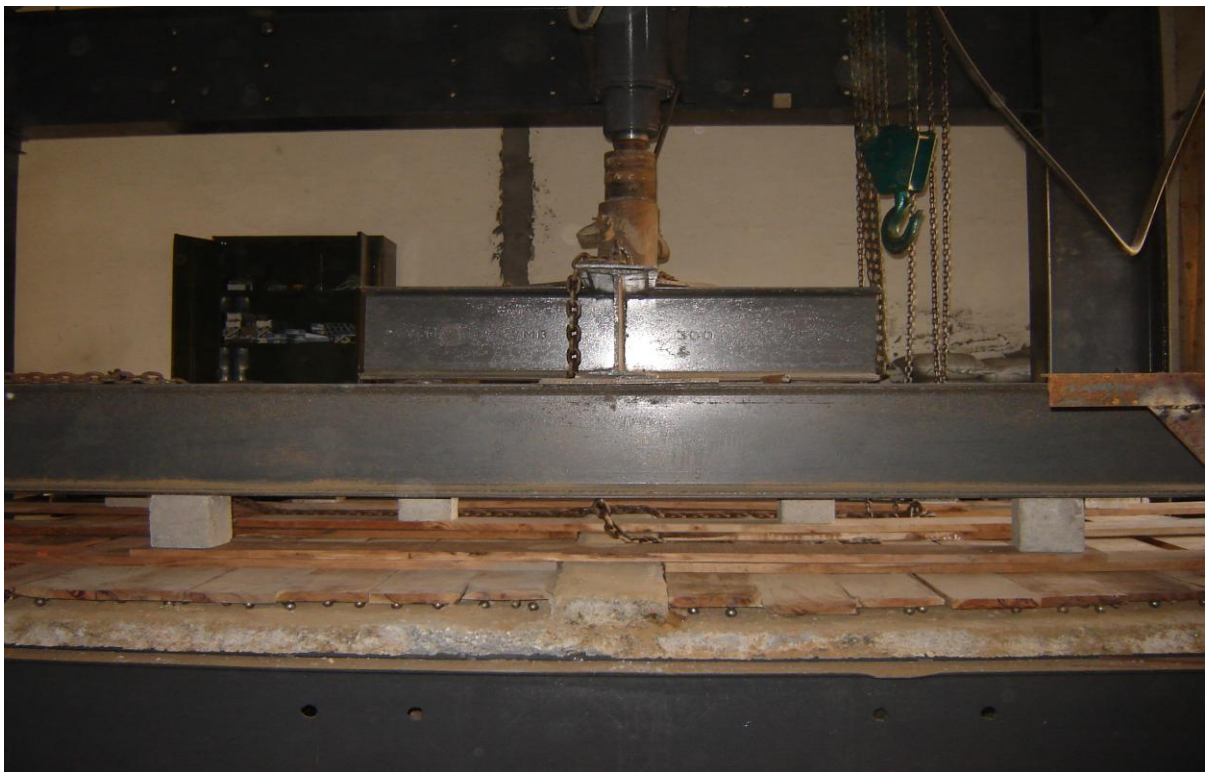

Figure 4.12: Typical Schematic Diagram showing the Load Transferring Arrangement

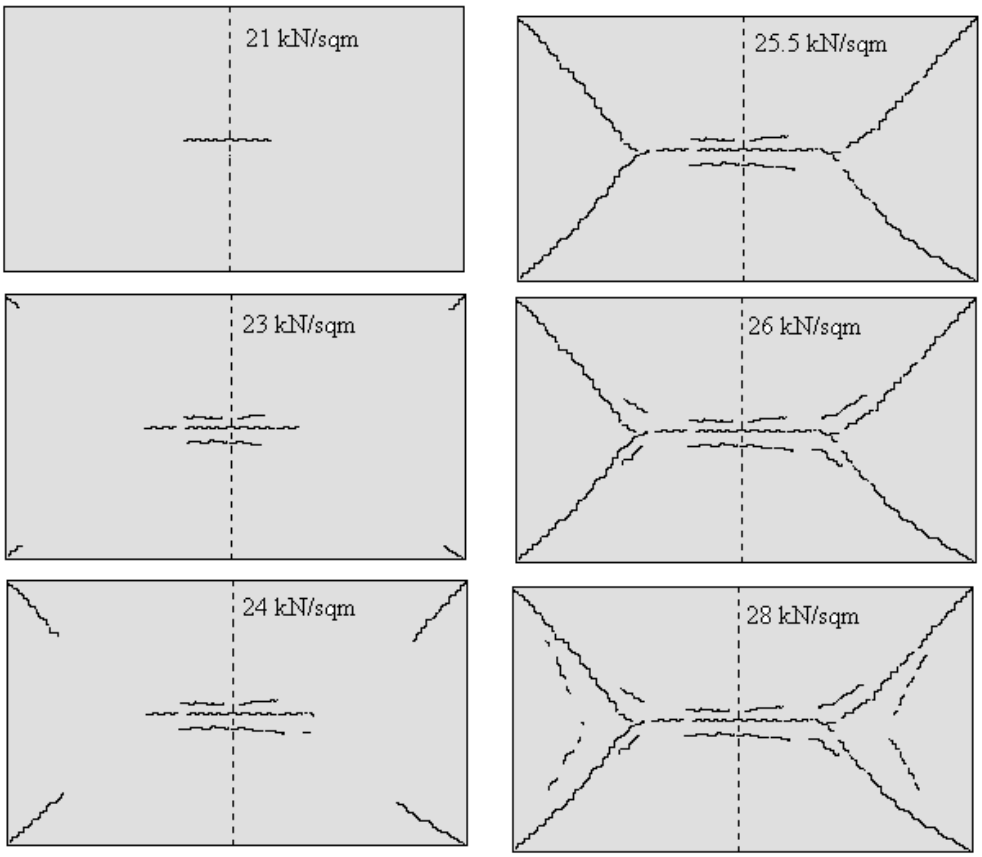

Figure4.13: Crack Formation for slab, 2PSF with λ-value less than unity
and supported over shallow internal in-built beam

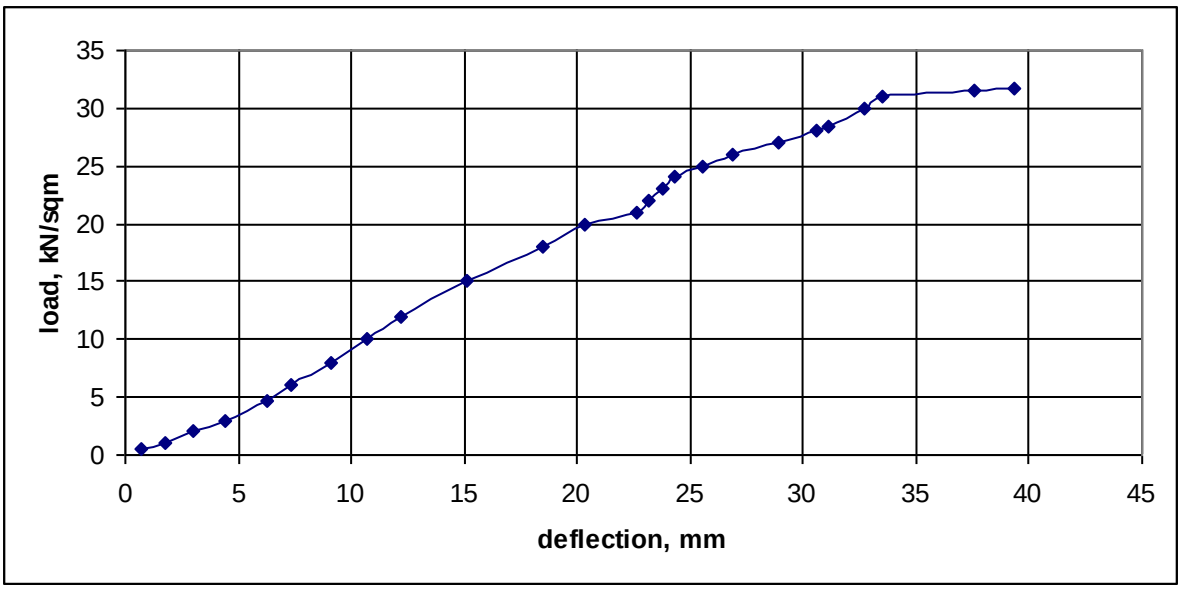

Figure 4.14: Load-deflection curve for slab, 2PSF

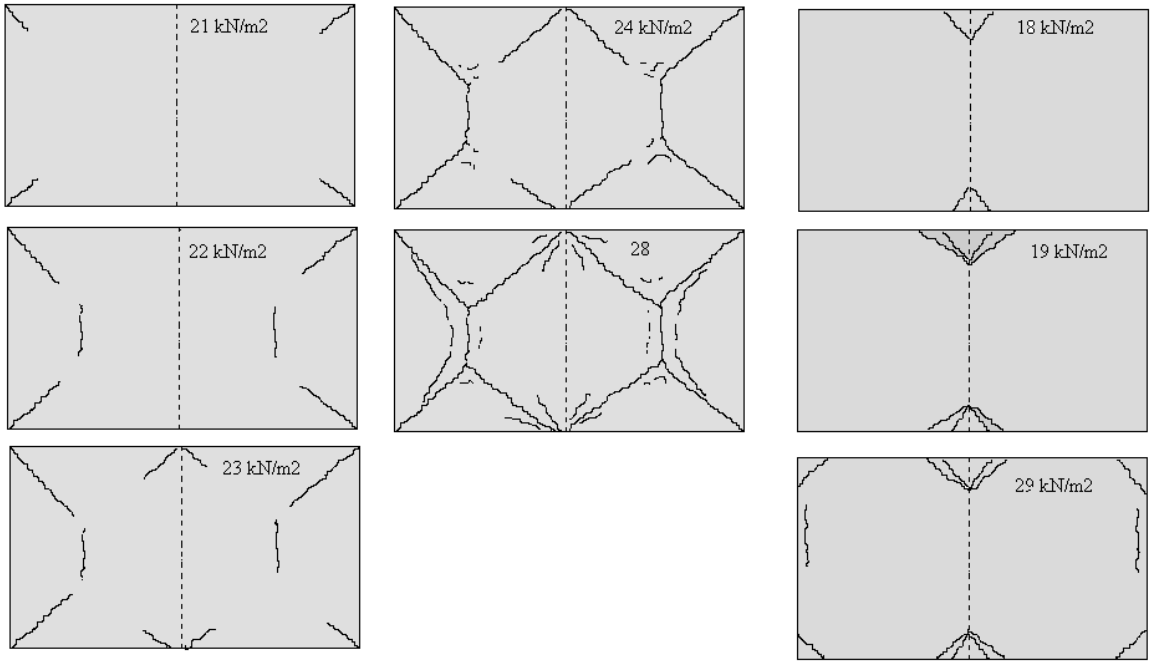

Figure 4.15: Crack Formation for 2-panel slab, 2PSR with λ-value more than unity and supported over shallow internal in-built beam

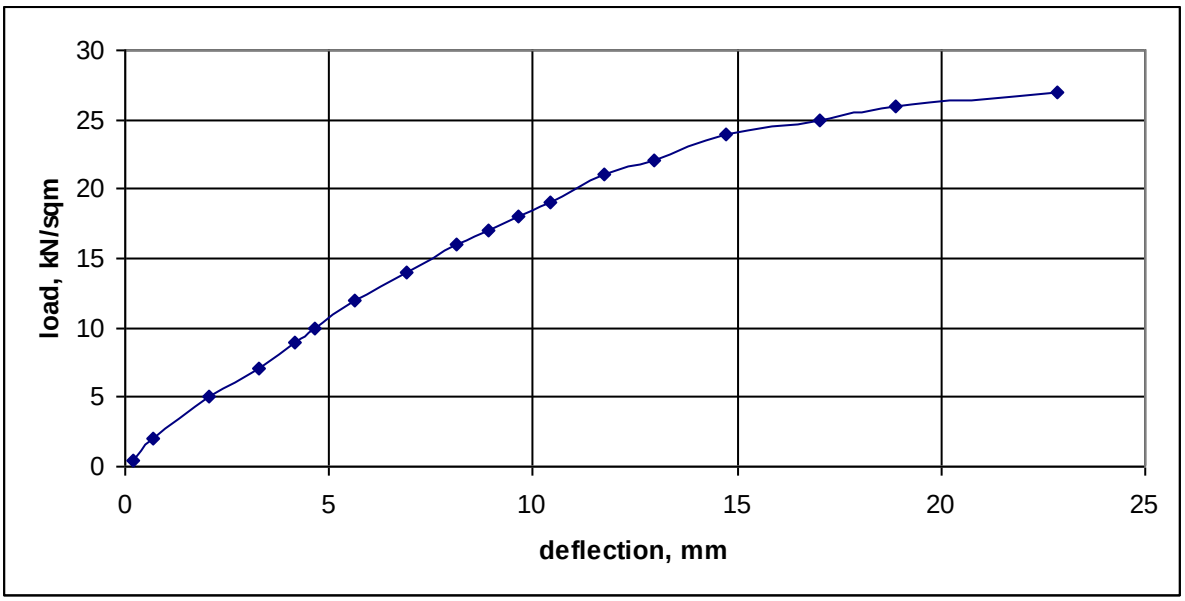

Figure 4.16: Load-deflection curve for slab, 2PSR

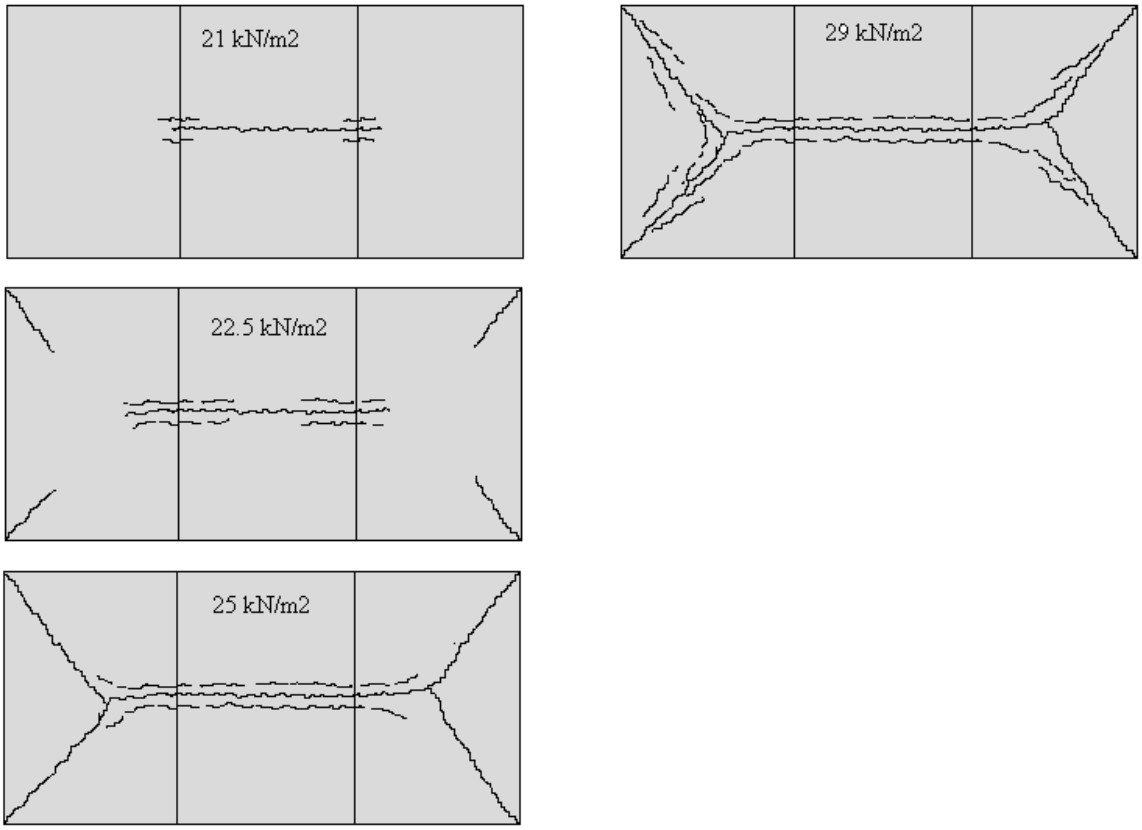

Figure 4.17: Crack Formation for 3-panel slab, 3PSF with λ-value less than unity and supported over shallow internal in-built beam

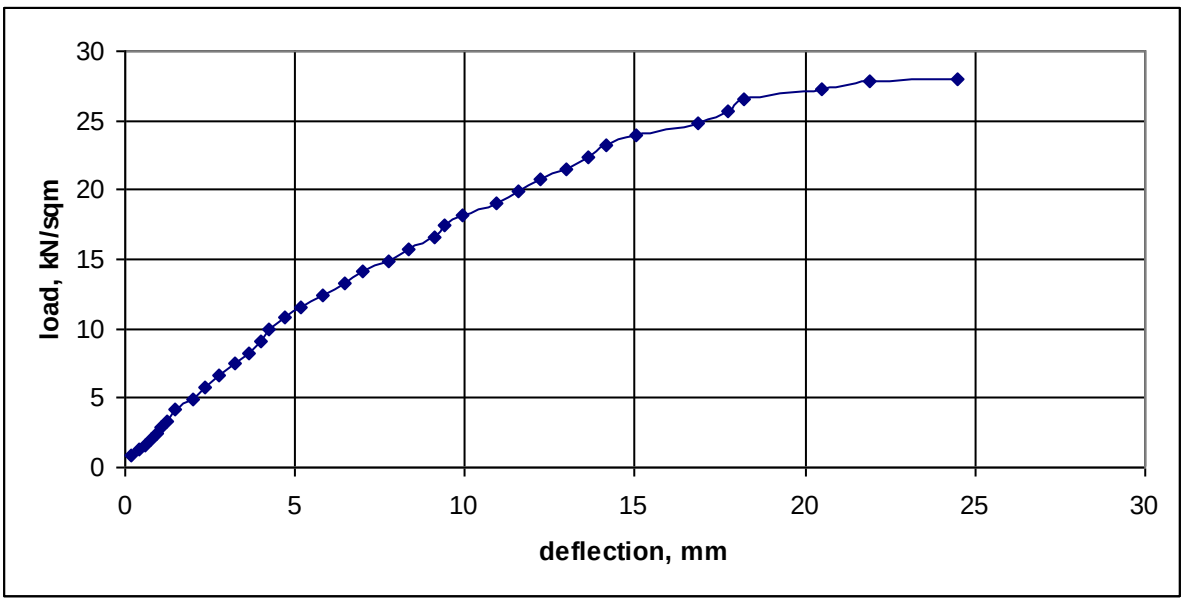

Figure 4.18: Load-deflection curve for slab, 3PSF

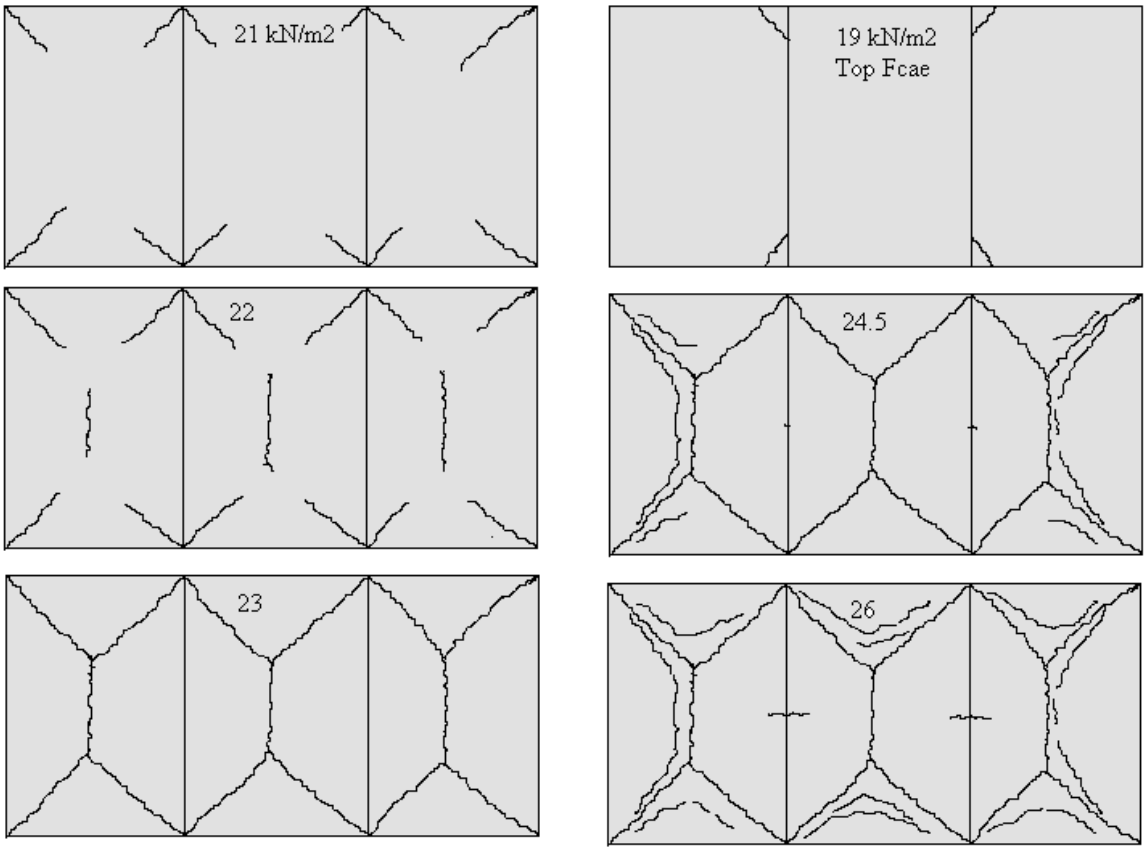

Figure 4.19: Crack Formation for 3-panel slab, 3PSR with λ-value more than unity and supported over shallow internal in-built beams

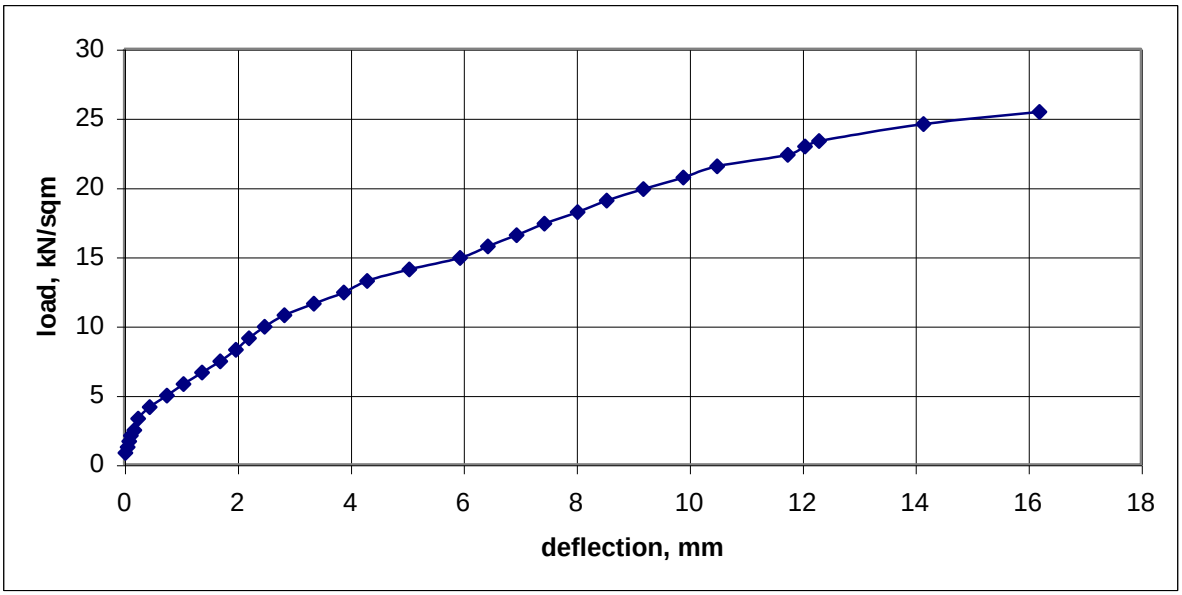

Figure 4.20: Load-deflection curve for slab, 3PSR

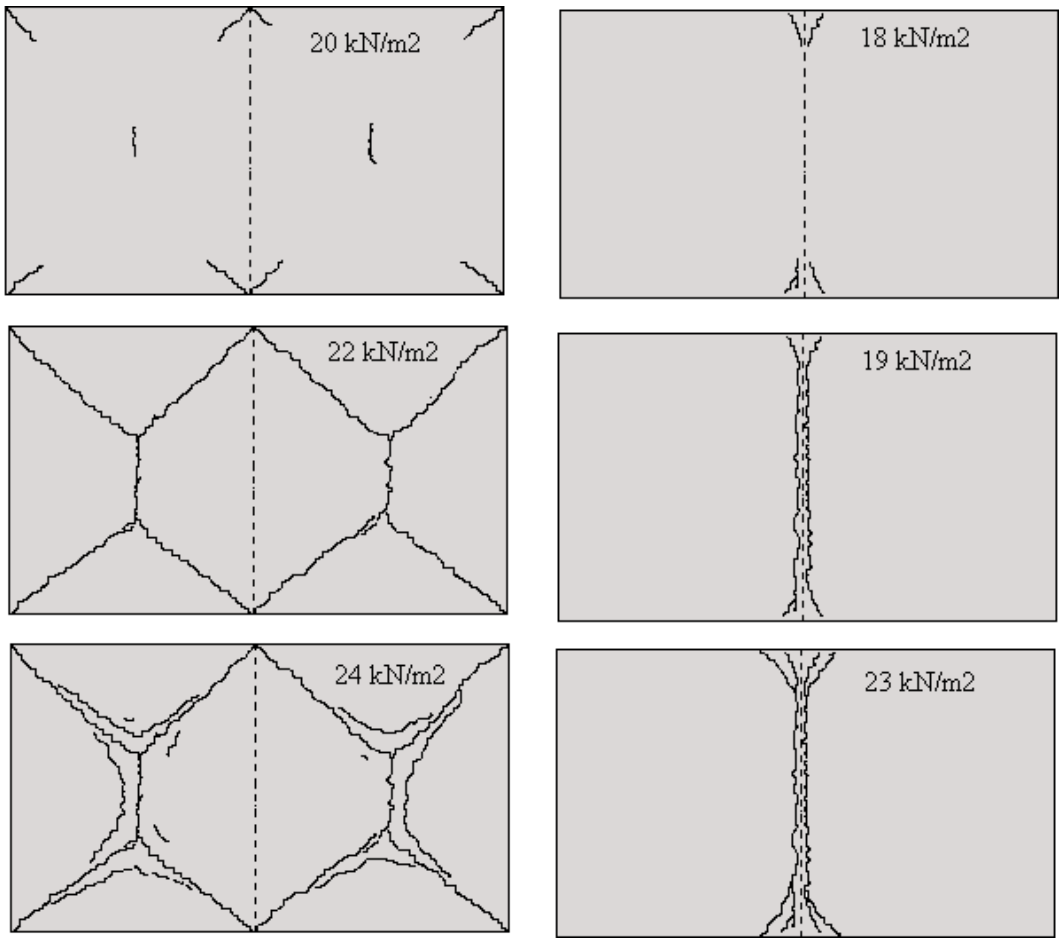

Figure 4.21: Crack Formation for 2-panel slab, 2PNS with λ-value more than unity and supported over non-shallow internal in-built beams.

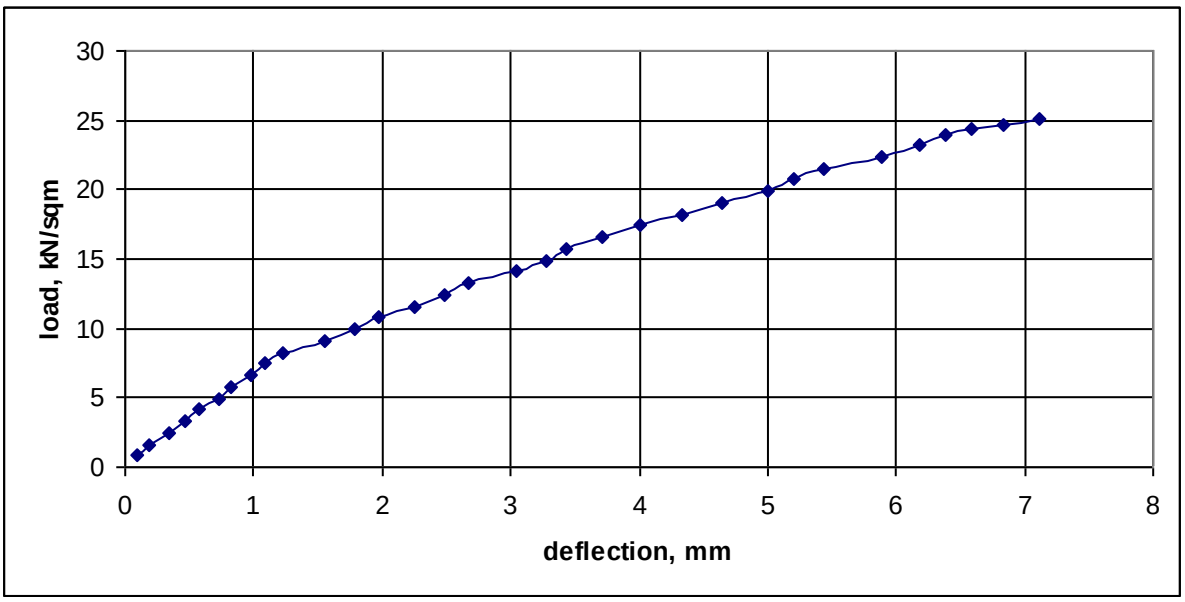

Figure 4.22: Load-deflection curve for slab, 2PNS

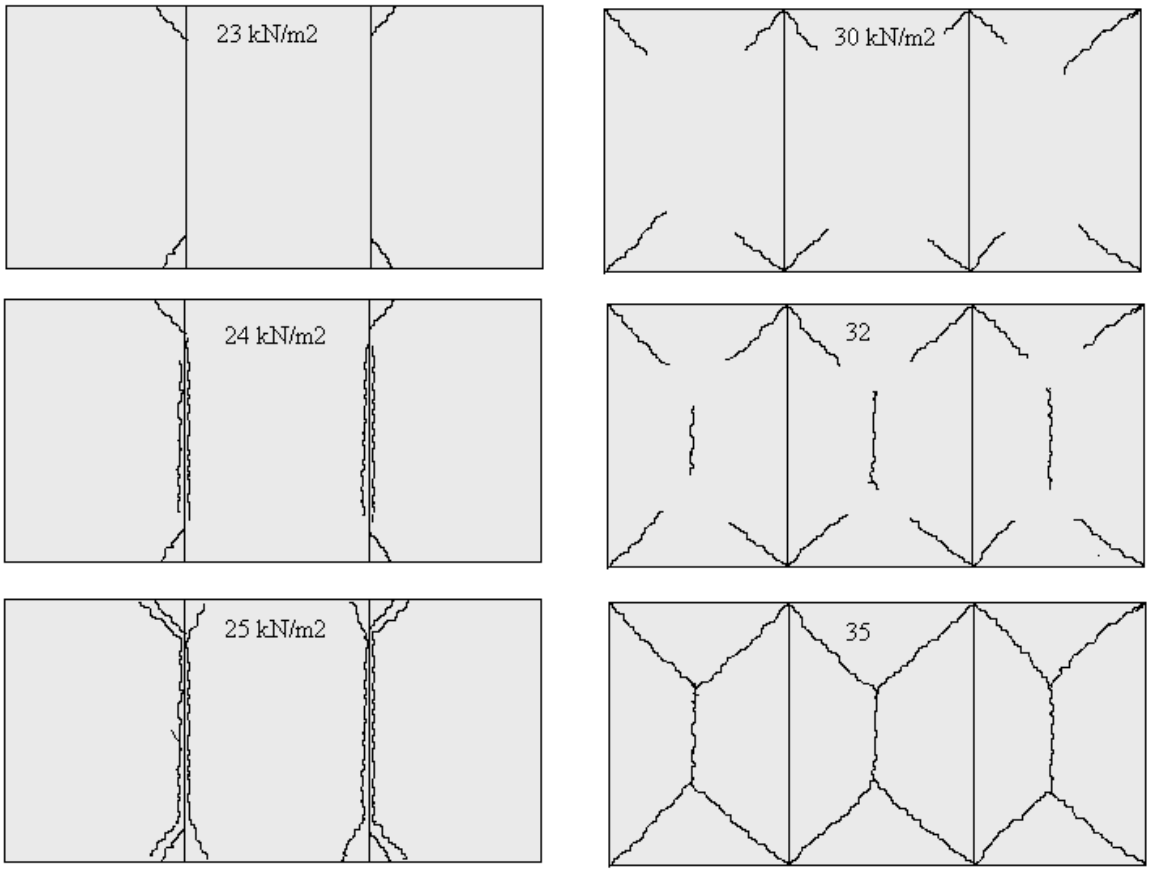

Figure 4.23: Crack Formation for 3-panel slab, 3PNS with λ-value more than unity and supported over non-shallow internal in-built beams

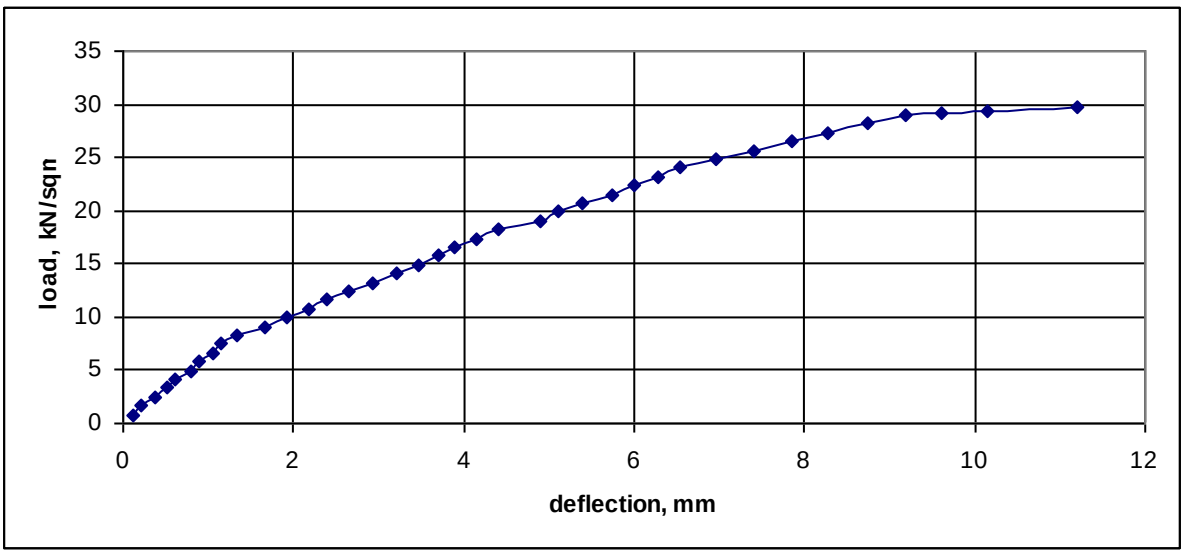

Figure 4.24: Load-deflection curve for slab, 3PNS

4.3 COMPARISON OF RESULTS FROM THE ANALYTICAL MODEL WITH THE EXPRESSIONS AVAILABLE IN THE LITERATURE

A typical single panel rectangular slab supported over the non-yielding edges on its outer boundary under a uniform area load was analyzed using the analytical model developed in the chapter 3. The results predicted by the proposed model are compared with the values obtained from the well-established literature on the yield line theory and other theories like elastic and lower bound methods to check the accuracy of the model and to illustrate its suitability for single panel rectangular slabs, when analyst analyses the slab panel at lower limit of the slab-parameter, $A \leq A_{c1}$. Examples are also shown in this section to show the applications of the proposed model in the analysis of multi-panel rectangular slab-beam system.

Example-4.3.1: *Consider a rectangular slab of size 5.0m* x *3.5m supported over the non-yielding supports on all the four sides a uniform area load of* 10 *kN/m*^{2} *applied over the entire top face of the slab. Determine the moment coefficients assuming orthotropy of slab as 1.514. The slab is discontinuous on its outer boundary.*

In this problem, number of panels, n = 1

Uniform area load, w = 10 kN/m^2

The slab length, $L_x = l_x$ = 5.0m and width, l_y = 3.5m

Therefore, the aspect ratio (r) of the slab = 3.5/5 = 0.7

CASE-1: Analysis using the proposed analytical equation [see chapter-3].

Constants e and d for a discontinuous slab = 2

Slab constant, $\beta = 1.514 / 0.7^2 = 3.0897$

The slab-parameter, $A = \sqrt{1+3\beta} = 3.204$ [= A_{c1} (= 3.204)]

Slab moment, $m_{ux} = \left(\frac{3}{A+1}\right)^2 \frac{w L_x^2}{24} = 5.303$ kNm [see Eq. (3.11)]

$\Rightarrow m_{uy} = \mu\, m_{ux} = 1.514 \times 5.303 = 8.029$ kNm

CASE-2: Analysis using the equation proposed by *John (1967), John and Wood (1967).*

John (1967), John and Wood (1967) has derived an expression (4.1) for predicting the collapse load of a rectangular slab resting over the non-yielding edges at the outer boundaries with the long span, l_x and the short span, l_y. The rectangular slab with the aspect ratio, r has been orthotropically reinforced with the coefficient of orthotropy, μ.

$$m_{ux} = \frac{w\, l_y^2}{24}\left[\sqrt{3+\mu\, r^2} - r\sqrt{\mu}\right]^2 \qquad (4.1)$$

$\Rightarrow m_{ux} = 0.0479\ w\, l_y^2 = 5.877$ kNm

And $m_{uy} = \mu\ m_{ux} = 0.0726\ w\, l_y^2 = 8.895$ kNm

CASE-3: Analysis using the equation proposed by the *Shukla (1973).*

Shukla (1973) has derived an expression (4.2) for predicting the collapse load of rectangular slabs resting over the non-yielding edges at its outer boundaries with the long span, **b** and the short span, **a**. The rectangular slab has been orthotropically reinforced with the orthotropy, μ and the continuity moments at the outer edges of the slab has been defined by i-values that can be taken as zero for the slab with simply supported end constraints.

$$m = \frac{q\, a_r^2}{24}\left[\sqrt{3+\left(\frac{a_r}{b_r}\right)^2} - \frac{a_r}{b_r}\right]^2 \qquad (4.2)$$

In equation (4.2), a_r and b_r are the reduced-span-lengths along the short and the long span of the rectangular slab respectively. The numerical values of these reduced-span-lengths can be calculated from equation (4.3) and equation (4.4).

$$a_r = \frac{2\,a}{\sqrt{1+i_2} + \sqrt{1+i_4}} \qquad (4.3)$$

$$b_r = \frac{2\,b}{\sqrt{\mu}\left(\sqrt{1+i_1} + \sqrt{1+i_3}\right)} \qquad (4.4)$$

From equations (4.3) and (4.4), the values of these reduced span lengths can be calculated for the given geometrical parameters of the slab and these values then, can be substituted in equation (4.2) to determine the moment, m.

Therefore, $a_r = 3.5$ m and $b_r = 4.0636$ m

And $m_x = 0.04797\ q\, a_r^2 = 5.877$ kNm, and $m_y = 1.514 \times 5.877 = 8.898$ kNm

CASE-4: Analysis using the equation proposed by the *Johansen (1967).*

Johansen (1967) has derived an expression for predicting the collapse load of rectangular slabs resting over the non-yielding outer edges with the long span, **b** and the short span, **a**. The rectangular slab has been orthotropically reinforced with the orthotropy, μ. The expressions for the reduced-span-lengths of the slab are similar to the equations derived

by *Shukla (1973)* and these can be calculated from equations (4.3) and (4.4). This expression is given in equation (4.5).

$$m = \frac{q\, a_r\, b_r}{8\left(1+\frac{a_r}{b_r}+\frac{b_r}{a_r}\right)} = 5.882 \text{ kNm, and } m_y = 1.514 \text{ x } 5.882 = 8.906 \text{ kNm} \quad (4.5)$$

CASE-5: Analysis using the equation proposed by the *Park and Gamble (2000).*

Park and Gamble (2000) has derived an expression for predicting the collapse load of the rectangular slabs resting over the non-yielding edges at its outer boundary with the long span, l_x and the short span, l_y. The rectangular slab with aspect ratio, r has been orthotropically reinforced with the orthotropy, μ. The final expression for computation of the collapse load is given in equation (4.6). The continuity moments at the outer edges of the slab has been defined by means of the *i-values* that can be taken as zero for the slab with simply supported end constraints.

$$w_u = \frac{6\, m_y\, \mu\, Y^2}{l_y^2\left(\frac{l_y}{l_x}\right)^2\left[\sqrt{\left(\frac{X}{Y}\right)^2+3\mu\left(\frac{l_x}{l_y}\right)^2}-\left(\frac{X}{Y}\right)\right]^2} \quad (4.6)$$

The values of constants X and Y can be calculated from equations (4.7) and (4.8).

$$X = \sqrt{1+i_1}+\sqrt{1+i_3} \quad (4.7)$$

$$\text{and } Y = \sqrt{1+i_2}+\sqrt{1+_4} \quad (4.8)$$

$\Rightarrow m_y = 0.06554\, w l_y^2 = 8.03$ kNm

And $m_x = m_y / \mu = 0.0433\, w l_y^2 = 5.303$ kNm

CASE-6: Analysis using the moment coefficients suggested by *IS 456 (2000).*

IS 456 (2000) has recommended the moment coefficients (α_x and α_y) for the design of a rectangular slabs supported over the non-yielding outer edges. These values are given in the appendix of the code for various values of the aspect ratio (= l_y/l_x) of the slab. In this expression, l_y and l_x are the long and the short span of the rectangular slab respectively. It is important to note that the design code requires that only the middle strip, which is three-fourth the width of the entire plate/slab, be reinforced. Therefore, in calculations moment field calculated using the moment coefficients has been modified to give moment

field acting over the entire width of the slab/plate by reducing it by a factor of 0.75 [*Purushothaman (1984)*]. The moment coefficients for the rectangular slab with aspect ratio of 1.43 having outer four edges as discontinuous are given below. The slab has been adequately reinforced for the torsional moments near the corners at the top face.

$m_x = 0.0862\ w l_x^2 = 10.56$ kNm acting over the middle strip. Therefore, the moment acting over the full width of the slab = 10.56 x 0.75 = 7.92 kNm

and $m_y = 0.056\ w l_x^2 = 6.86$ kNm acting over the middle strip. Therefore, the moment acting over the full width of the slab = 6.86 x 0.75 = 5.15 kNm

CASE-7: Analysis using the moment coefficients suggested by *IS 456 (2000).*

IS 456 (2000) has recommended the moment coefficients (α_x and α_y) for design of rectangular slabs simply supported over the non-yielding edges at the outer boundaries based upon the Rankine-Grashoff theory. These values are given in the appendix of the code for various values of the aspect ratio (= l_y/l_x) of the slab. In this expression, l_y and l_x are the long and the short span of the rectangular slab respectively. It is again important to note that the design code requires that only the middle strip, which is three-fourth the width of the entire plate/slab, be reinforced. Therefore, in calculations moment field calculated using the moment coefficients has been modified to give moment field acting over the entire width of the slab/plate by reducing it by a factor of 0.75 [*Purushothaman (1984)*]. The moment coefficients calculated using these coefficients for the rectangular slab are given below for an aspect ratio of 1.43.

$m_x = 0.1005\ w l_x^2 = 12.311$ kNm acting over the middle strip. Therefore, the moment acting over the full width of the slab = 12.311 x 0.75 = 9.233 kNm

and $m_y = 0.0495\ w l_x^2 = 6.064$ kNm acting over the middle strip. Therefore, the moment acting over the full width of the slab = 6.064 x 0.75 = 4.548 kNm

CASE-8: Analysis using the moment coefficients suggested by Marcus [*Purushothaman (1984)*].

Marcus recommended the moment coefficients (α_x and α_y) for design of rectangular slabs simply supported over the non-yielding outer edges based upon the Rankine-Grashoff theory after applying the applicable corrections for the torsional moments being induced in the intersecting strips of the slab. These values are suggested for various values of the aspect ratio (= l_y/l_x) of the rectangular slab. In this expression, l_y and l_x are the long and

the short span of the rectangular slab respectively. The moment coefficients and the corresponding moments for the rectangular slab are given below for an aspect ratio of 1.43.

$m_x = 0.0678\ w l_x^2 = 8.306$ kNm

And $m_y = 0.036\ w l_x^2 = 4.41$ kNm

CASE-9: Analysis using the moment coefficients from the Elastic Theory of Plates [*Timoshenko and Krieger (1959)*].

Levy recommended the moment coefficients for the design of the rectangular slabs simply supported over the non-yielding edges at outer boundaries based upon the elastic theory of plates. These values are suggested for various values of the aspect ratio (= b/a) of the rectangular slab. In this expression, **b** and **a** are the long and the short span of the rectangular slab respectively. The moment coefficients along with corresponding moments for the rectangular slab are given below for an aspect ratio of 1.43.

$m_x = 0.077\ wa^2 = 9.433$ kNm

And $m_y = 0.0504\ wa^2 = 6.174$ kNm

CASE-10: Analysis using the expression suggested by the Lower bound Analysis [*Wood (1961)*].

The bending moment distribution in the slab computed by satisfying the equilibrium conditions and the yield criterion simultaneously along with the applicable boundary constraints of the slab will predict the collapse load either on the lower side or at the most equals the true load of the slab. The final expression for collapse load of the rectangular slab computed by the lower bound method [*Wood (1961)*] is given in equation (4.9). In this expression, l_y and l_x are the short and the long span of the rectangular slab respectively.

$$w_u = \frac{8\, m_{ux}}{l_x^2}\left\{1 + \frac{l_x}{l_y} + \mu\left(\frac{l_x^2}{l_y^2}\right)\right\} \qquad (4.9)$$

$\Rightarrow m_{ux} = 0.02265\ w l_x^2 = 5.66$ kNm

And $m_y = m_{ux} \times \mu = 0.0343\ w l_x^2 = 8.57$ kNm

The comparisons of the results from different equations are tabulated in Table 4.7.

Table 4.7: Comparison of Moment Field by Different Theories

Case	Analysis Technique	Moment along short span, kNm/m	Moment along long span, kNm/m	Total static moment in slab, kNm
1	Proposed Method	8.030	5.303	54.62
2	John	8.895	5.876	60.51
3	Shukla	8.898	4.036	51.32
4	Johansen	8.906	5.882	60.58
5	Park and Gamble	8.030	5.303	54.62
6	IS 456 FED	7.920	5.150	53.47
7	IS 456 FESS	9.233	4.550	55.06
8	Marcus	8.306	4.410	51.12
9	Levy	9.443	6.174	63.92
10	Lower Bound Method	8.570	5.660	58.29

Table 4.7 shows that the analysis result predicted by the proposed analytical method for a single-panel rectangular slab compares favorably well with the results obtained from the well established equations (4.1) to (4.9) as well as the moment coefficients suggested by the design code, *IS 456 (2000)*. All these equations (4.1 to 4.8) and the moment coefficients (in case-6) of *IS 456 (2000)* have been derived by different researchers using the principles of limit analysis for a rectangular slabs resting over the non-yielding edges at the outer boundaries.

It is to be noted that the equations (4.1 to 4.8) available in the literature are quite complicated and substitutive in nature. Considerable mathematical substitutions are required in determining the collapse load/ moment field of any rectangular single panel slab and additional efforts are required for determining the support reactions induced at the outer boundary of the slab panel under the applied load. Whereas, the equations suggested by the proposed method are simple to apply and define the exact shape of the yield line pattern of the slab in the routine flow of calculations that can be used for determining the support reactions and the same set of equations is applicable for the both single as well as multi-panel slab supported over the non-yielding edges at the outer boundary. Moreover, it can be used to check randomly the results of a finite-element based software. The multi-panel slab can be proportioned at any arbitrary value of the beam strength level. This has been illustrated in the examples below:

Example-4.3.2: *Consider a typical slab of size 9.0m* x *3.0m supported the over non-yielding supports on all the four sides under a uniform area load of 10 kN/m^2. The slab is divided into three panels of 3.0 m each. Study the effect of varying* λ*-value on the slab*

moment field assuming orthotropy of the slab as 0.7. The slab is discontinuous over its outer boundary and there is no negative reinforcement over the internal beams.

In above problem, number of panels, n = 3

Uniform area load, w = 10 kN/m^2

The slab length, L_x = 9m and width, l_y = 3m

Aspect ratio, r of the slab = 3/9 = 0.333

And the panel length, l_x = 9/3 = 3m

Orthotropy, $\mu = 0.7$ [given]

The lower limit of the slab-parameter, $A_{c1} = 4.461$ [from equation (3.30)]

The upper limit of the slab-parameter, $A_{c2} = 5.928$ [from equation (3.30)]

The value of critical beam-strength parameter of the slab-beam system can be determined from equation (3.23), $\alpha_{bc} = 0.846$

The moment field for the slab ($m_{ux,}$ m_{uy}) and the supporting shallow-beams (m_b) can be calculated from the equations (3.29) and (3.31) for the various assumed values of the moment-manipulator (λ). These values are tabulated in Table 4.8.

The total static moment induced in the slab-beam system under a given surface load is compared at various value of the moment-manipulator (λ) with the total static moment suggested by *Nichols (1914).*

Table 4.8: Typical Analysis Results for Three-Panel Rectangular Slab

λ-value	**0.2**	**0.4**	**0.6**	**0.8**	**1.0**
m_{ux}, kNm/m	9.06	8.16	7.44	6.84	6.33
m_{uy}, kNm/m	6.34	5.72	5.21	4.78	4.43
m_b, kNm	4.60	8.30	11.33	13.89	16.10
Total static moment, kNm	109.75	107.20	105.25	103.70	102.39
Nichols's static moment, kNm	101.25	101.25	101.25	101.25	101.25

It is indicated in Table 4.8 that with increase in the λ-value, the magnitude of the moment field in the slab reduces with a corresponding increase in the moment of the supporting beam and vice versa. In addition, the value of the total static moment in the panel of the slab goes on reducing with increase of the λ-value. This trend is in conformity with the test results reported by various researchers [*Sozen and Siess (1963)*; *Hatcher, Sozen and Siess (1965)*; *Hatcher, Sozen and Siess (1969)*; *Jirsa, Sozen and Siess (1966); Vanderbilt, Sozen and Siess (1969)*]. Therefore, the structural designer can choose any moment-set for the design purpose, keeping in mind any architectural and/or any other design constraint. If there is any constraint of a low ceiling height, equally spaced

internal supporting shallow-beams with minimum bending-moment can be selected (*e.g.* low λ-value) with a corresponding heavy slab section to sustain the ultimate load.

The total static moment induced in the slab-system matches favorably well with that suggested by *Nichols (1914).* This trend is also in conformity with the moment coefficients and design procedure for the design of slabs recommended by various design codes [*IS 456 (2000), BS EN 1992-1 (2004)*].

Example 4.3.3: *Consider a typical slab of size 20.12m* x *14.32m resting over the non-yielding supports at the outer boundaries and subjected to uniform area load of 10 kN/m^2. The slab is divided into four panels of 5.03m each. Determine the moment field in the slab-beam system assuming orthotropy of the slab as 1.482 and compare the results from the finite element analysis. The slab is discontinuous over its outer boundary and there is no negative reinforcement over the internal beams.*

In the given problem, number of panels, n = 4

Uniform area load, w = 10 kN/m^2

Length of the slab, L_x = 20.12m and the slab width, l_y = 14.32m.

Therefore, aspect ratio of the slab, r = 20.12/14.32 = 0.7135

And the panel length, l_x = 5.03m

Orthotropy, μ = 1.482 [given]

The lower limit of the slab-parameter, A_{c1} = 3.1198 [from equation (3.30)]

The upper limit of the slab-parameter, A_{c2} = 9.763 [from equation (3.30)]

The analytical model developed in chapter 3 of the thesis is used to find the moment-field induced in the slab-beam system. It can be proportioned for any value of the slab-parameter (A) form its valid range defined by the equations (3.29) and (3.31). The moment-field in the slab is given in Table 4.9.

Table 4.9: Variation of the moment-field with the slab-parameter (results from the proposed model)

λ-value	0	0.2	0.4	0.6	0.8	1.0
Slab moment, m_{ux}, kNm/m	89.14	39.73	26.07	19.53	15.67	13.10
Beam moment, m_b, kNm	0.00	773.90	1015.76	1141.60	1221.00	1276.00

In order to validate the proposed design procedure, finite-element based software was used to compare the results given in Table 4.9. In the numerical study, a four panel rectangular slab-beam system was subjected to an out-of-plane uniform area load of intensity, 10 kN/m^2. Only a linear-elastic analysis was performed to determine the moment field induced in the slab-beam system under the given load because the moment-

field determined by considering the true collapse-mechanism, equilibrium conditions along with the applicable yield criterion would always predict a true solution and results in this case would be identical with those calculated from the lower-bound analysis. The depth of the beams in the slab-beam system is taken arbitrarily from a set of number of beam-depths examined in the finite element analysis.

The moment field predicted from the numerical model is given in Table 4.10 along with the corresponding depth of the supporting beams. The finite model of the slab-beam system along with the stress contours of moment (m_x), deflection profile and the beam moment diagram at various *span/depth* ratios are given in *Figures (4.25 to 4.41).*

Table 4.10: Variation of the moment-field with the beam-depth (results from the FEM model)

λ-value	0	0.2	0.4	0.6	0.8	1.0
Span/depth ratio of the beam	30.00	25.00	20.79	17.31	14.41	12.00
Slab moment, m_{ux}, kNm/m	93.07	47.19	35.20	25.40	19.40	15.27
Beam moment, m_b, kNm	0.00	765.0	930.0	1067.0	1168.0	1232.0

It is indicated in the Table 4.9 that moments in the internal beams reduce with the reduction in the value of moment manipulator (λ). Accordingly, supporting beams of comparatively smaller depths are required to provide the requisite flexural strength to the slab-beam system at low λ-values and vice versa. Alternatively, the tensile steel in the beams can be reduced to provide a matching strength to the moment demand of the slab-beam system.

Table 4.10 tabulates the maximum value of moments induced in the slab-beam system under a lateral load of 10kN/m^2 along with the corresponding depth of the internal beams. The position of the maximum moment in the slab and the internal beams is found to be identical in the analytical model and numerical simulation carried out using the finite element software and these occurred along the line of hypothetical collapse mechanism. It is indicated in Tables 4.9 and 4.10 that the moment field in the slab-beam system compare favorably well with the results obtained from the finite element analysis. The moment field in both these cases follows exactly the values recommended by the design code [*IS 456 (2000)*] for the rectangular slab with discontinuous edges on all four sides.

The proposed design equation is simple to use and it can be used for proportioning the slab-beam system for any arbitrarily chosen value of the slab constant as per the field/design constraints. The thickness of the slab and the internal beams can be provided to suit the design constraints *vis-à-vis* beam-drop restriction, long spans etc by selecting a

suitable value of the slab-parameter (A). Most importantly, the proposed method can be used very conveniently to economize the slab-beam system in case of slabs requiring minimum tensile steel to satisfy the design code with regards to maximum/minimum rebar spacing. In such situations, designer can opt for suitable rebar spacing as per design code requirement and beams can be proportioned to meet the balance strength demand of the slab-beam system. Moreover, it will define the shape of collapse mechanism of the slab-beam system in routine flow of calculations thereby saving a considerable amount of time that is otherwise get used in determination of the support reactions etc from some other supplementary formulae.

Figures (4.25 to 4.41) indicate that the moment in the slab reduce with the increase of the value of depth of the internal beams and attains a minimum values at the beam depth calculated from the *span/12*. The negative moment field also starts inducing in the slab, when the depth of supporting beams approaches this value (*span/12)*. The non-shallower (stiff) beams attract more loads in comparison to the shallow beams. Accordingly, the supporting beams with depth equal to or more than *span/12* requires more flexural strength in comparison to the shallow beams for same set of the geometrical layout of the slab-beam system and the external applied load. The behavior of the supporting beams, at this depth, becomes analogous to the slab-system supported over the internal walls and/or non-yielding beams.

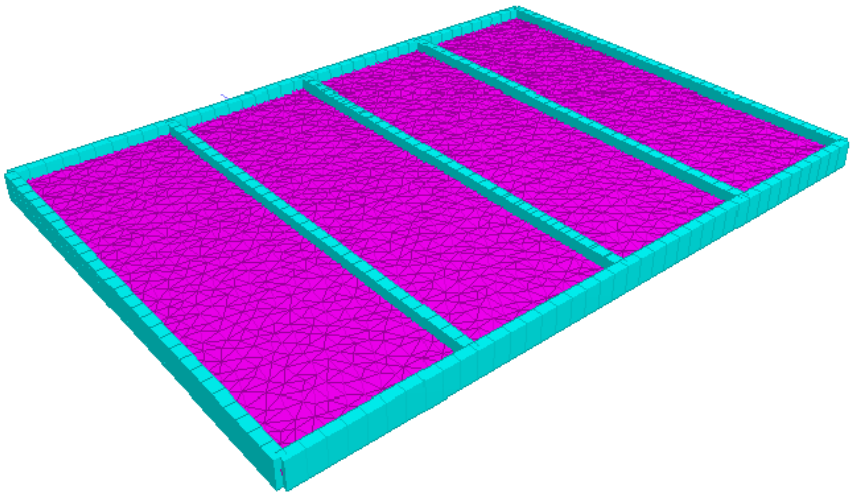

Figure 4.25: Finite element model showing the meshing of the slab-beam system

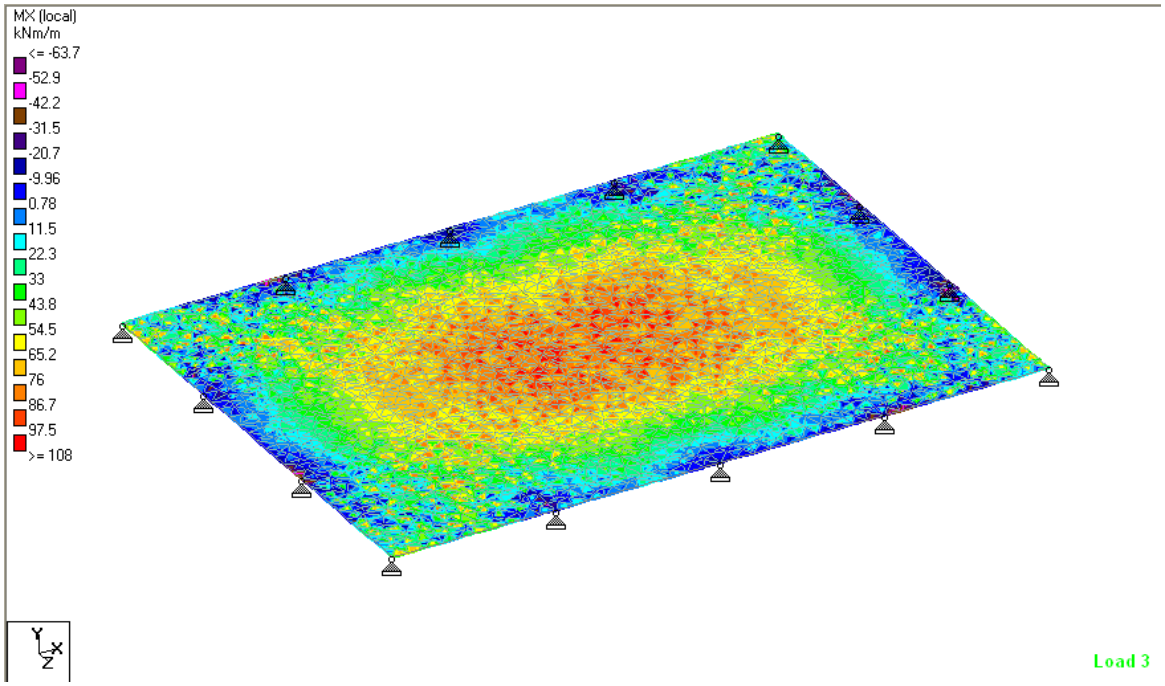

Figure 4.26: Stress contour of moment (m_x) at *span/depth* ratio of 47.733

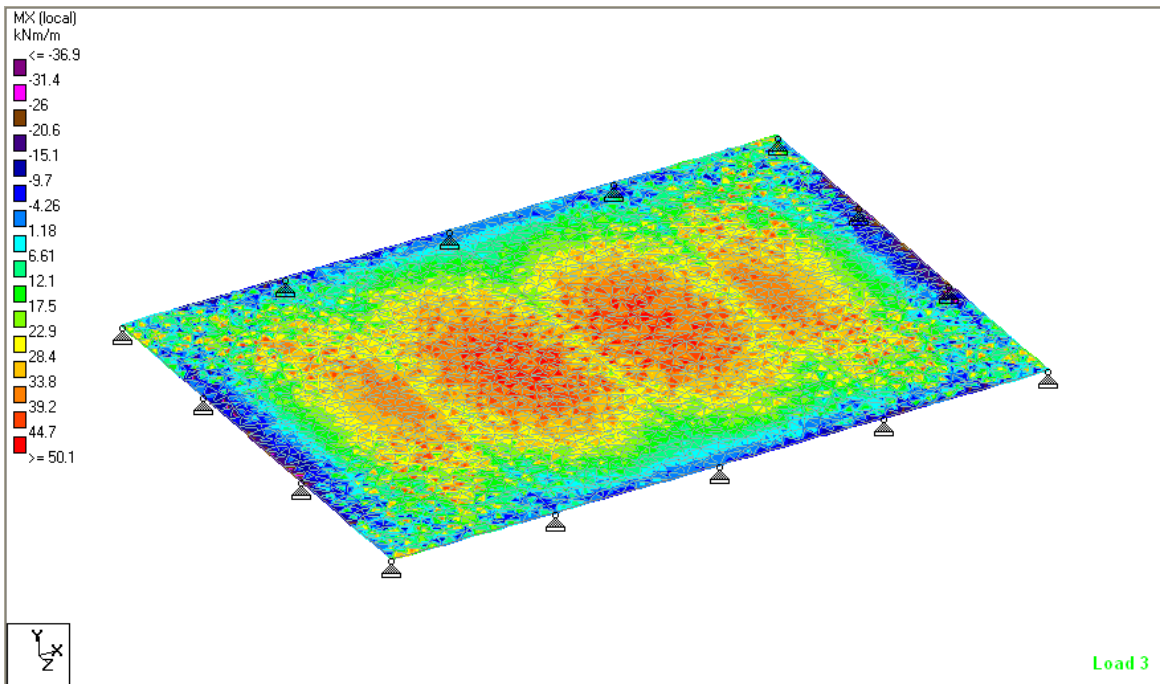

Figure 4.27: Stress contour of moment (m_x) at *span/depth* ratio of 25

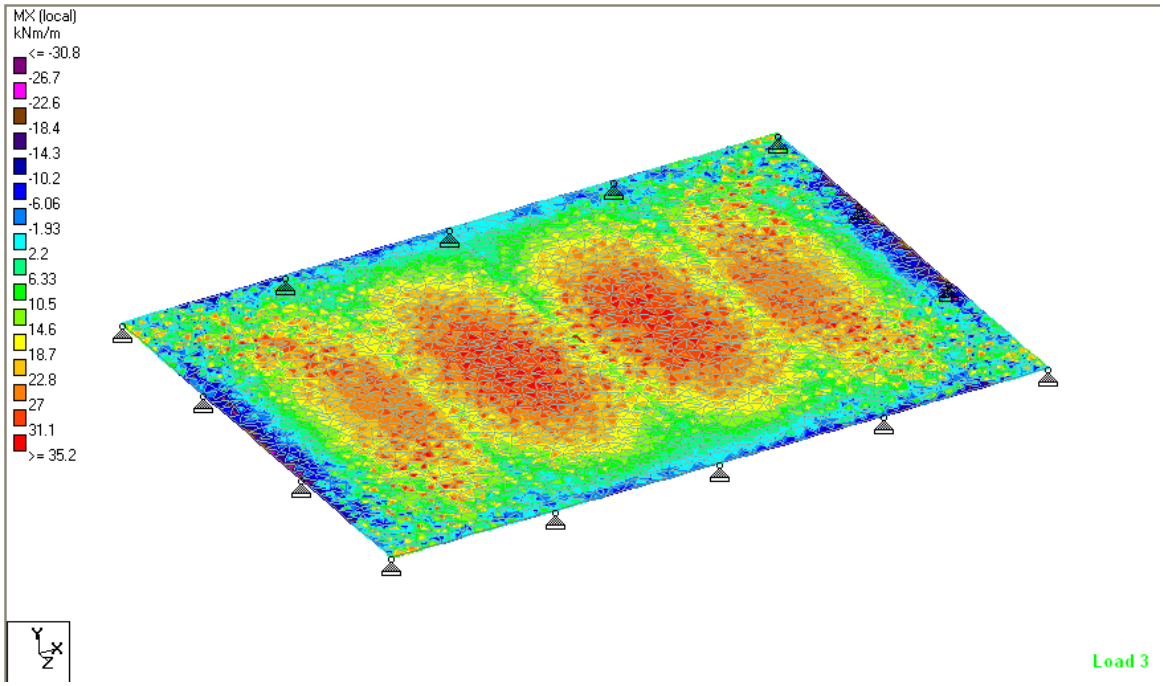

Figure 4.28: Stress contour of moment (m_x) at *span/depth* ratio of 20.79

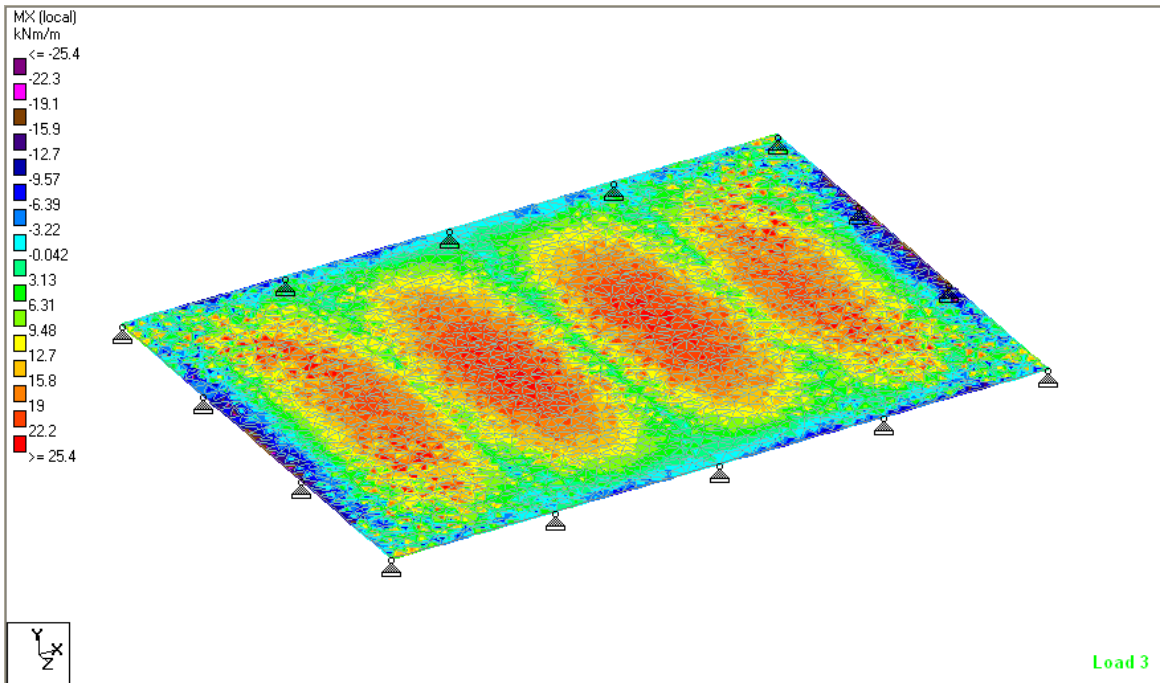

Figure 4.29: Stress contour of moment (m_x) at *span/depth* ratio of 17.31

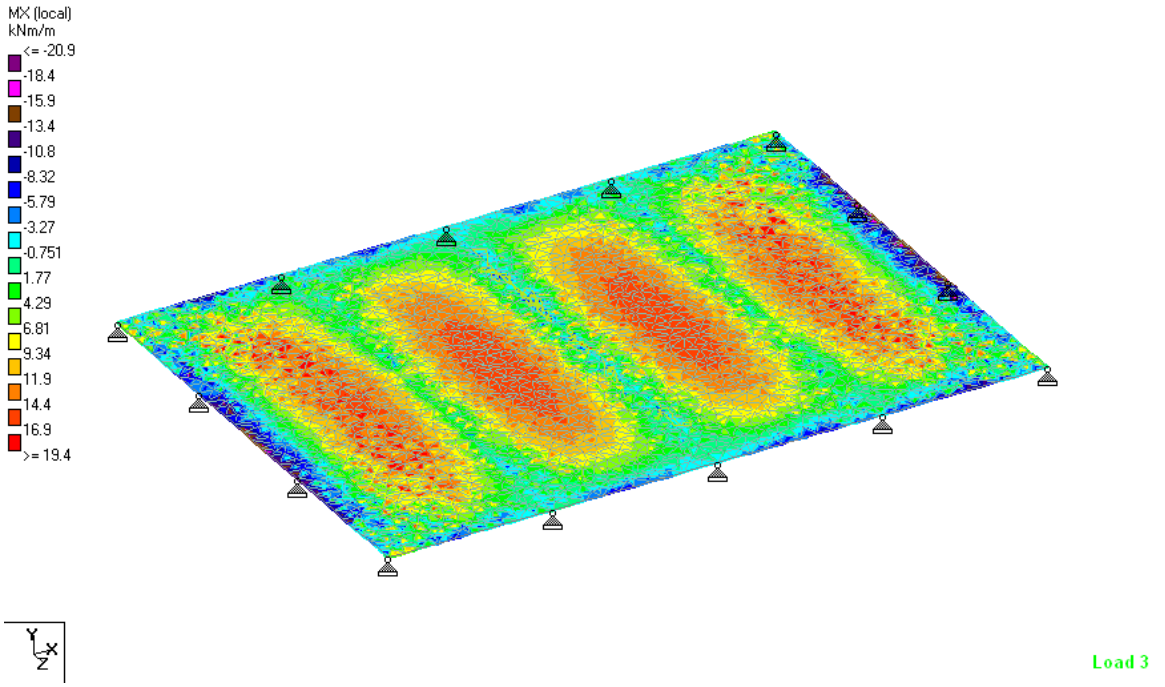

Figure 4.30: Stress contour of moment (m_x) at *span/depth* ratio of 14.41

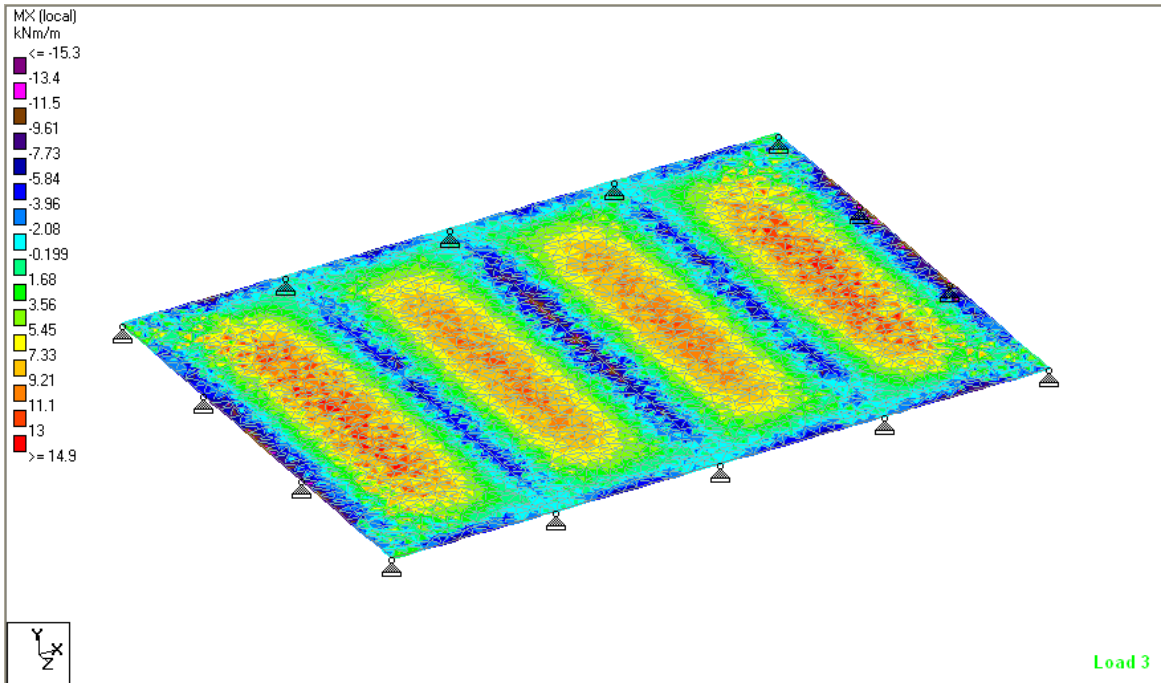

Figure 4.31: Stress contour of moment (m_x) at *span/depth* ratio of 12.0

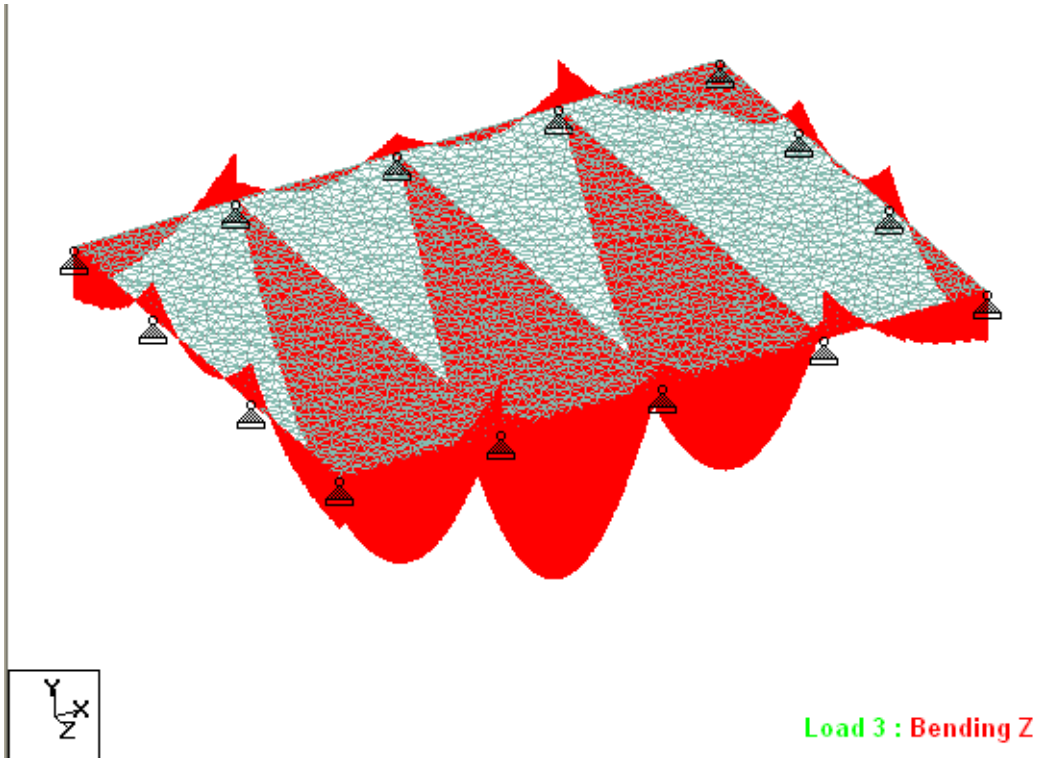

Figure 4.32: Typical bending moment diagram of supporting beams at *span/depth* ratio of 17.31

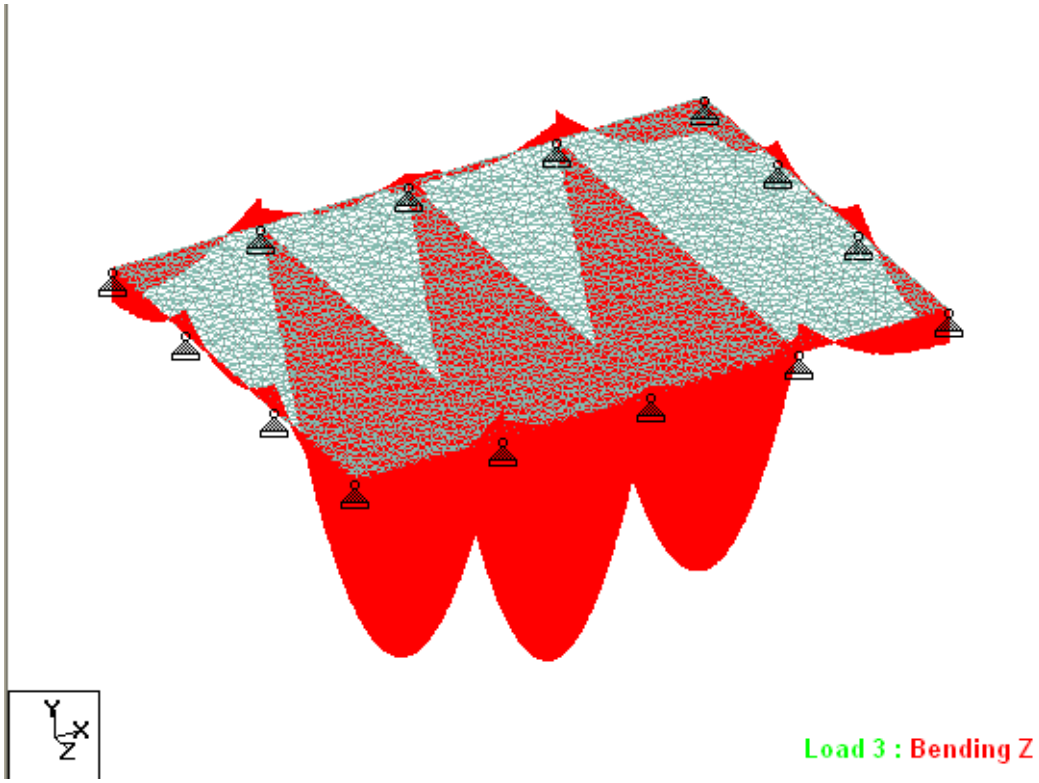

Figure 4.33: Typical bending moment diagram of supporting beams at *span/depth* ratio of 12.0

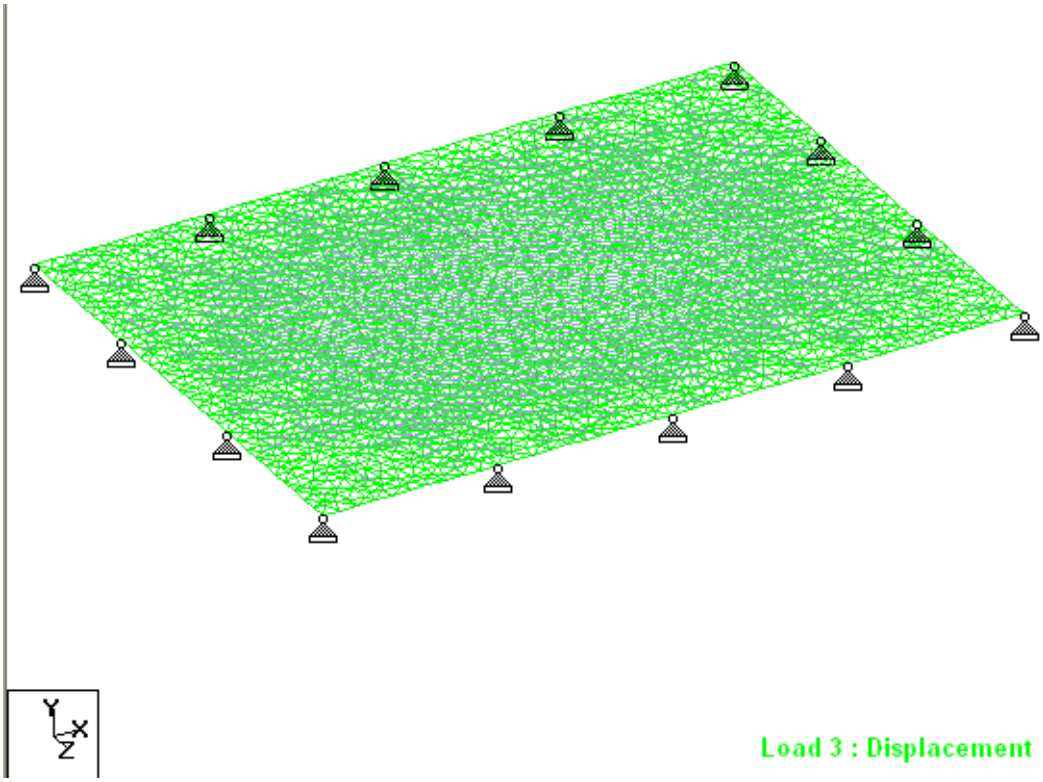

Figure 4.34: Deflection profile of the slab-beam system at *span/depth* ratio of 17.31

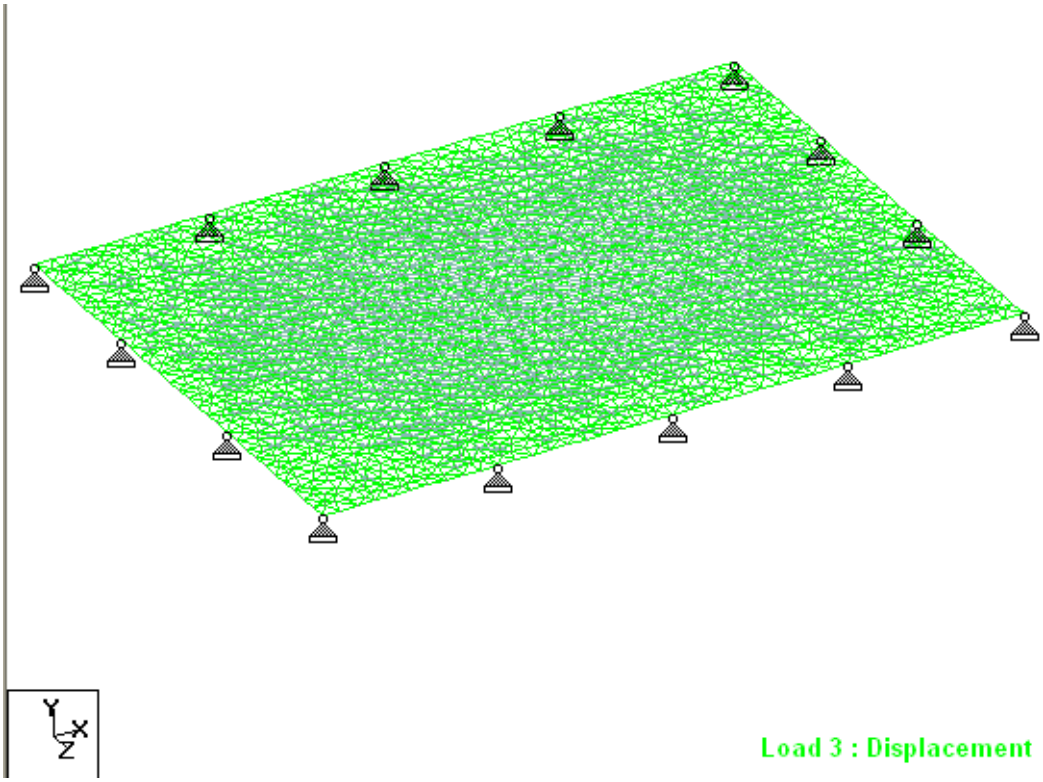

Figure 4.35: Deflection profile of the slab-beam system at *span/depth* ratio of 14.41

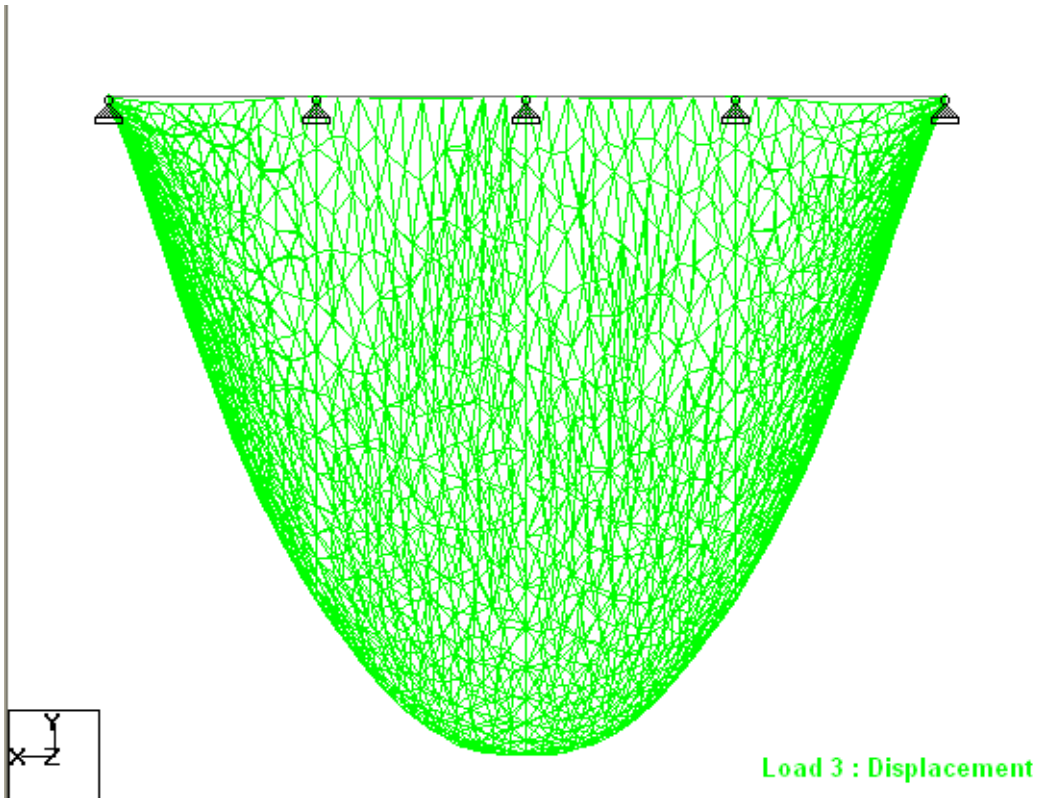

Figure 4.36: Deflection profile of the slab-beam system at *span/depth* ratio of 25.0

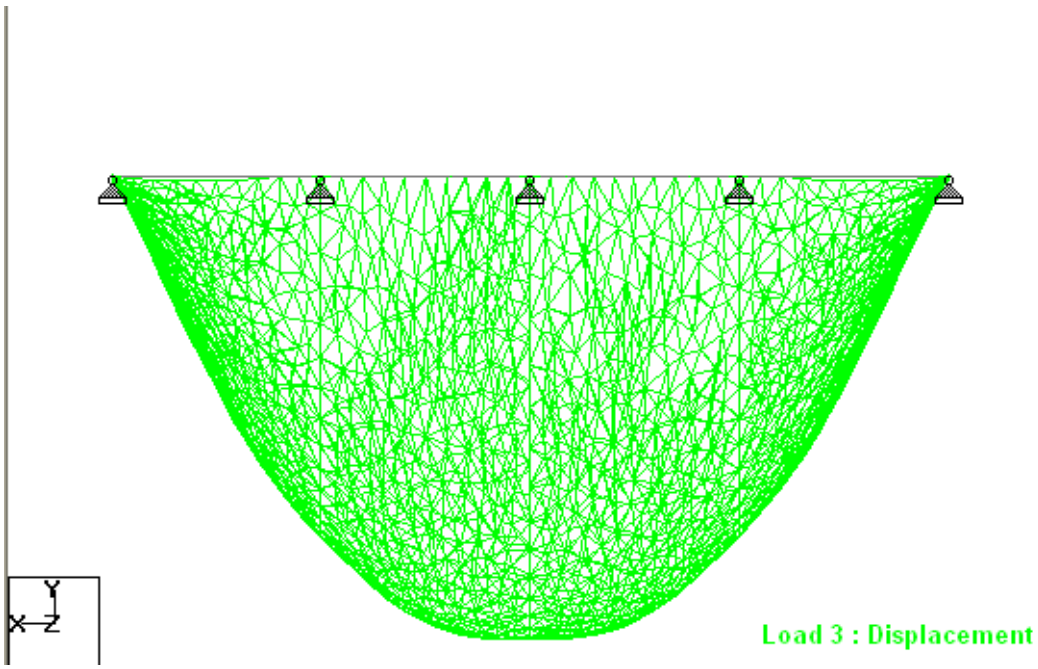

Figure 4.37: Deflection profile of the slab-beam system at *span/depth* ratio of 20.79

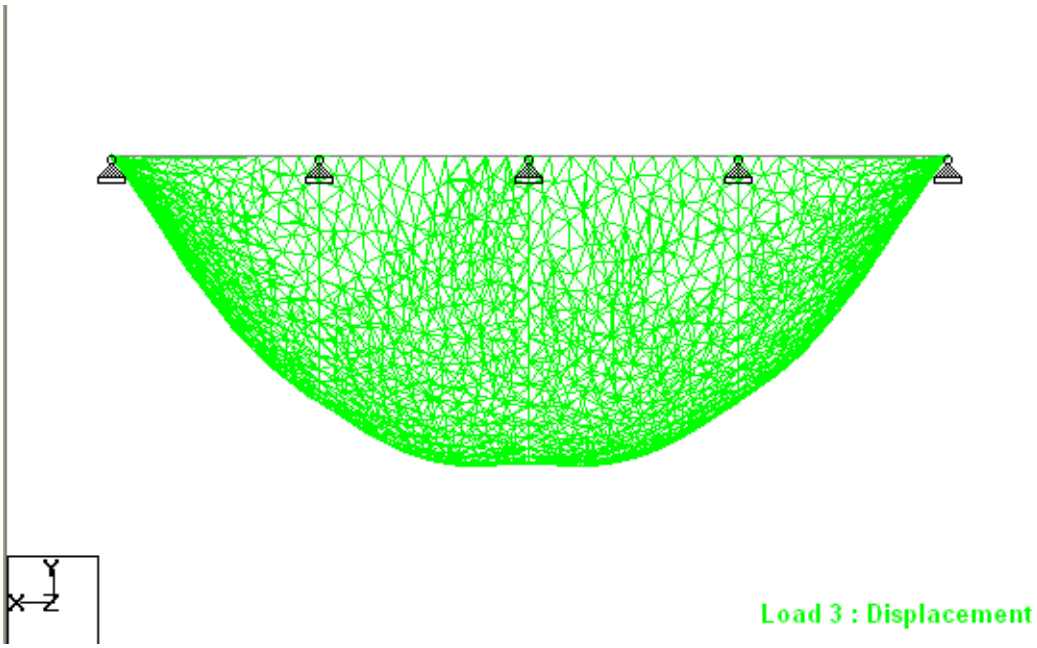

Figure 4.38: Deflection profile of the slab-beam system at *span/depth* ratio of 17.31

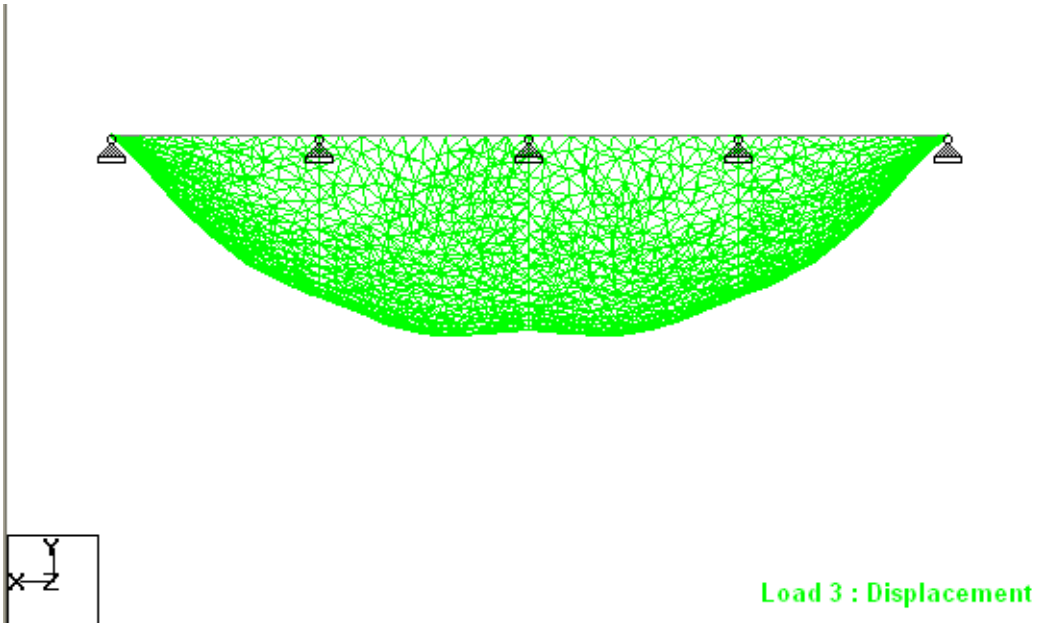

Figure 4.39: Deflection profile of the slab-beam system at *span/depth* ratio of 14.41

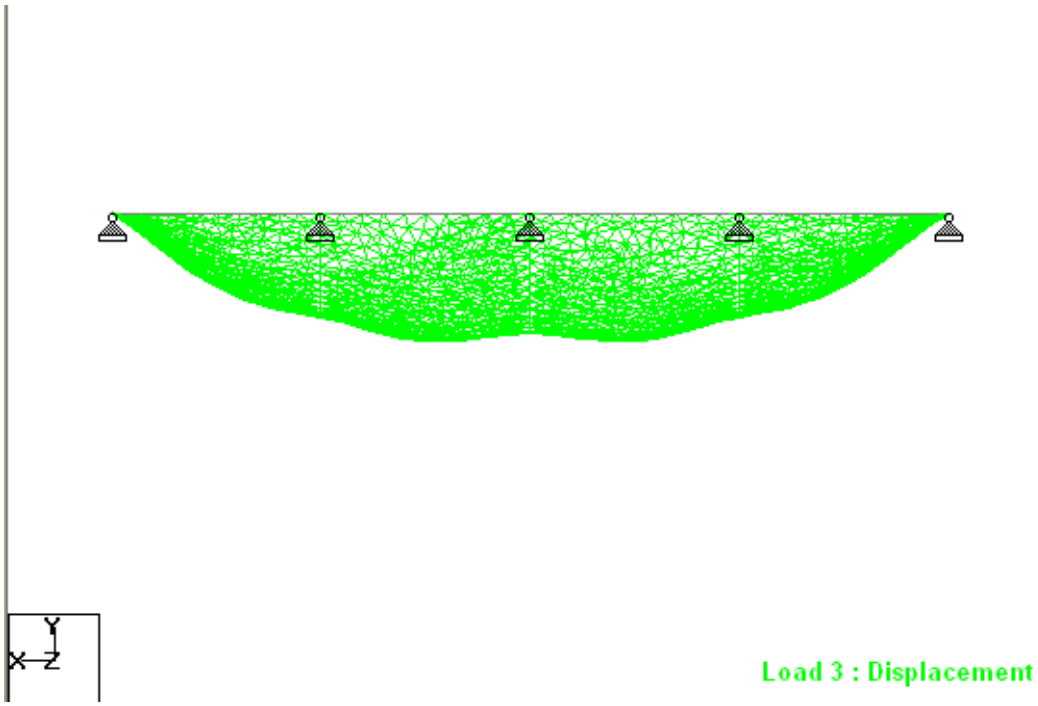

Figure 4.40: Deflection profile of the slab-beam system at *span/depth* ratio of 12.0

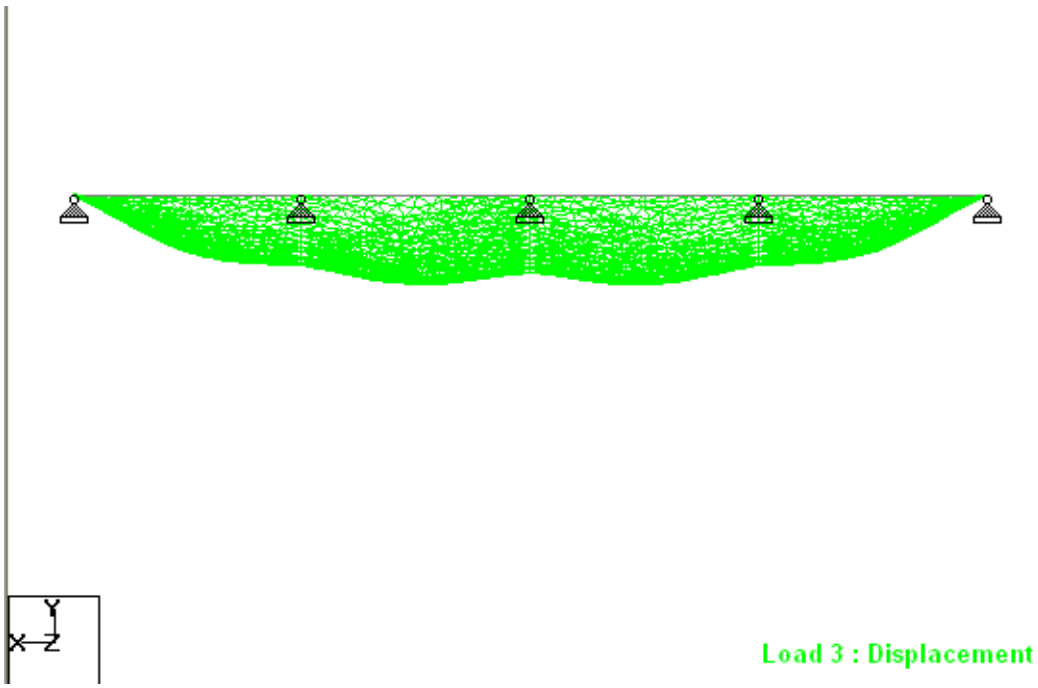

Figure 4.41: Deflection profile of the slab-beam system at *span/depth* ratio of 10.0

4.4 CLOSURE

- A beam with a depth less than *span/12* will not initiate any negative yield-line along its length at the top face of slab and is classified as a shallow beam. These supporting beams can be further classified into two categories viz. shallow-flexible beams and shallow-rigid beams. A beam that leads to the failure of slab in the global-collapse mechanism is classified as shallow-flexible beam whereas the beam that causes the failure of slab with the formation of a collapse mechanism, locally and simultaneously, in all panels of the slab is classified as a shallow-rigid beam.

- A non-dimensional parameter called as the moment-manipulator, λ (= moment of resistance of beam/moment of resistance of beam required for the simultaneous formation of global and local collapse mechanism) has been proposed to distinguish the nature of the internal shallow beams. If the slab has been designed with $\lambda < 1$, it will always fail following a global-collapse mechanism; otherwise, the same slab will fail in the local-collapse mechanism irrespective of the beam-depth. In this failure mode, the supporting beams will not allow the yield lines to cross over into the adjacent panels of the slab and the slab-beam system will fail with the formation of a yield line pattern, locally, in all panels of the slab at the ultimate state of collapse.

- The results from the analytical model compares favorably well with the results obtained from the well-established formulae of the limit analysis.

- Actual crack pattern, at the collapse load, for the two and three-panel slabs tested in the laboratory were found to be in good agreement with that predicted from the design equations and confirm the hypothetical collapse mechanism of the slab-beam system.

- The test slabs designed for λ-value less than unity and with the beam depth less than *span/10* failed following a global-collapse mechanism with a load factor of more than 1.40. However, these slabs show more deflection at the design load than the permissible values but selecting a suitable beam depth satisfying both the serviceability criterion as well as the *span/depth* ratio of the shallow beam can reduce the actual deflection of the slab-beam system under the design load. Therefore, it is recommended to use highest possible value of the depth of the supporting shallow beams that satisfies serviceability criterion of the design codes, and simultaneously, facilitates the formation of a global-collapse mechanism in the slab at the ultimate state.

- The test slabs designed for λ-value more than unity and supported over the shallow beams failed following a local-collapse mechanism with a load factor ranging from 1.30 to 1.40 with the formation of negative yield lines near the beam-ends. At the design load, these slabs show a reduced deflection in comparison to the slabs designed for λ-value less than unity but this value of the deflection was more than permitted by the design codes.

- It is suggested that the actual slab-beam system with shallow beams should never be proportioned with λ-value more than or equal to unity. Moreover, it is recommended to use the highest possible value of the depth of the shallow supporting beams that satisfies the serviceability criterion of the design codes and facilitates the formation of the global-collapse mechanism in the slab-beam system at ultimate state.

CHAPTER-5

MODIFIED DESIGN-APPROACH FOR RC SLAB

5.1 GENERAL

Slabs are the most widely used structural element. These are used almost in every type of structural system to build and/or enclose the space along with other structural elements as walls; columns etc. Unlike other structural elements, it is a highly redundant element due to the coupling of the internal stress resultants and offers multiple load paths to the applied loading. However, the structural behavior of the slabs is very sensitive to the type, layout of the supporting system and/or stiffness of the supporting structural member(s). Any change in the physical parameters of these supporting systems causes a considerable change in the moment-field induced in the slab under given loading conditions.

Various researchers across the globe tried their best to describe the behavior of the slabs of various shapes, for different load types. Numbers of test results [*Park (1968), Gamble et al. (1969), Park (1971), Gamble (1972), and Sozen et al. (1963)*] are reported in the literature and design methods have been suggested based upon the results of these extensive series of tests and well-established performance record of various slab systems. Empirical relations and some factors have been suggested for apportioning the total static moment to the slab and its supporting beams and/or the column strip for the satisfactory performance. These relations and factors formed the basis for the design guidelines recommended by various design codes [*ACI 318 (2008), CSA 23.4 (1994), IS 456 (2000)* and *BS EN 1992-1 (2008)*]. These guidelines have a number of inherent limitations in the form of assumptions, which are mandatory to be satisfied by all slab panels for the satisfactory performance. Thus, it forces the designers to use supporting beams with lesser value of the *span/depth*-ratio.

However, in routine design practice, numbers of case are encountered by designers whereby the beam-drop and beams spans are restricted by architects to a level that are not sufficient to provide a non-yielding edge to the slab. Alternatively, due to provisions for some mechanical services, beams of relatively lesser depth are required to support the slab and as such, these coefficients predict the moment-field highly on unsafe side and produce a structurally deficient slab section. The moment coefficients recommended by various design guidelines are applicable only if the slab panel(s) are resting over the non-

yielding supporting system at the outer boundary of the slab-system. This design procedure may be appropriate for many situations, but in many others, it leads to wasteful overdesign or, perhaps worse, underdesign.

In the present chapter, a design procedure has been developed and recommended for proportioning the reinforced concrete rectangular slab cast monolithic along with equally spaced shallow beams and resting over the non-yielding supports at its outer boundaries. The proposed procedure can also be used for the multi-panel slabs but it must be supported over the equally spaced shallow beams along one direction and the non-shallow beams at regular intervals along the other direction of the slab-beam system. The slab should be subjected to out-of-plane uniform area load over its entire top face.

5.2 SLAB BEHAVIOR

A reinforced concrete slab resting over the simple non-yielding supports on its outer boundaries will develop a band of flexural cracks at its tensile face along the lines of maximum curvature, if progressively loaded to the failure. At low load level before the initiation of the tensile cracks, the distribution of the bending moments and displacement field defining the deflection of middle plane of the slab follows the elastic plate theory. After the formation of cracks, this distribution of the moment field changes significantly due to the differential reduction in the stiffness of the slab caused by the flexural and torsional cracking, as well as inelastic behavior of concrete and reinforcement. With the further increase in loading, yielding of the tensile steel eventually occurs along the lines of maximum moment and the slab section undergoes a large change in the curvature along the sections of the yielding, with the moment there remaining practically constant at the ultimate moment of resistance of the slab. The slab can be said to ‘collapse’ at this stage of loading, when it fails to support any additional load and it develops a unique pattern of the yield lines at collapse load. The shape of the yield line pattern of the slab will depend upon the loading, its boundary conditions and slab-constants.

A reinforced concrete slab cast monolithic along with the equally spaced shallow beams and resting over the simple non-yielding supports on its outer boundaries will develop either one of following collapse mechanisms at ultimate state:

1. The plastic hinge will form in all supporting beams, simultaneously, along with the development of the yield line pattern in the slab and these beams allow the yield line in the slab to pass through it at the point of the formation of plastic hinge in the beam. This type of the slab failure-mode is called as a global-collapse mechanism.

2. Alternatively, the supporting beams will not allow the yield line to pass through it and the yield line pattern develops locally in all panels of the slab and all panels of the slab start behaving as separate entities; isolated from each other by the internal beams. This type of failure-mode is called as a local-collapse mechanism.

The actual failure-mode of the slab-beam system depends upon the relative magnitude of the moment-field induced in the slab under the applied loading and the ultimate moment resisting capacity of the slab. The slab will fail in the global-collapse mechanism only if the moment-capacity of the slab in this failure mode is more than that required for the local-collapse mechanism and vice versa.

Therefore, the designer has a full control over the behavior of the shallow beam-supported slab of the slab-beam system. A slab cast monolithic along with the internal beams and with given end-constraints at it outer boundaries can be forced to fail in the global-collapse mechanism or in the local-collapse mechanism by selecting an appropriate value of the slab-parameter (A) or the moment-manipulator (λ). In other words, the behavior of the supporting beams in the slab-beam system depends entirely upon the λ-value and by selecting a suitable λ-value; the supporting beams can be made to behave as a rigid-support whereby the slab behaves similar to a slab resting over the non-yielding edges as well as a flexible-support. The supporting slab must be proportioned accordingly to carry its due share of the applied surface load.

5.3 DESIGN APPROACH

Most of the design codes allow that slab-systems may be designed by any procedure satisfying the conditions of equilibrium and geometric compatibility, and the code requirements of strength and serviceability. The principle of limit analysis can be used very conveniently to ensure the conditions of equilibrium and geometric compatibility in the slab-beam system at collapse and asses the strength requirement of the system. Because the collapse load of any structural system is always characterized by a bending moment distribution that satisfies the equilibrium and the mechanism conditions along with an applicable yield criterion and there exists only one load factor that satisfies all these conditions simultaneously at the collapse [*Wood (1961)*]. The value of this factor can be determined uniquely without the necessity of calculating deformations, either at collapse or at any other stage of loading, using the minimum and maximum principles of limit analysis. According to these principles, the collapse load factor for any structural system is the minimum load factor if it has been obtained by fulfilling the equilibrium

condition for all possible collapse mechanisms of the system. It represents the maximum value of the load factor if it has been calculated by considering all those bending-moment distributions that satisfy the equilibrium and the yield conditions [*Baker (1961)*]. Therefore, these two conditions will always give the lower and the upper bound to the true value of the load factor that can be achieved by satisfying all these conditions simultaneously. The value of this load factor increases or at least remains the same with the addition of any restraint, whether internal or external, in the structural system at collapse and it would reduce with the removal of the restraint [*Baker (1961)*].

This condition can be used very conveniently for proportioning a slab-system restrained on all the four sides by reducing it into a slab resting over the simple supports on its boundaries. It can suitably be reinforced, later on, at its top face near the outer continuous edges to resist the cracking moment without lowering the load factor.

The analytical model has been developed in *Chapter 3* using this approach and can be used for the analysis and design of the reinforced concrete slab cast monolithic along with the equally spaced shallow beams and resting over the non-yielding supports on its outer boundaries as well as a multi-bay- multi-panel slab beam system. However, in the later case, it must be ensured that the slab must be resting over the non-yielding edges at its outer boundaries. The end restraint at outer boundaries of the slab may be either simple or continuous.

In the application of the proposed analytical model for a multi-bay-multi-panel slab system, the column spacing along the orthogonal directions of the slab-beam system must be adjusted in a manner that the supporting beams along one direction should behave as equally spaced shallow beams and as non-shallow beams along the other direction of the column grid. And accordingly, the ratio of the column spacing along the orthogonal directions of the slab-beam system must be greater than 1.25 to divide the slab-system into a number of smaller rectangular slabs supported over the internal equally spaced shallow beams and resting over the non-shallow (non-yielding edges) at outer boundaries in each bay of the system.

The slab is divided into number of panels with equal length (l_x) keeping in mind the architectural and/or any other design constraints. The number of panels and the size of the slab (aspect ratio) will fix the value of critical beam-strength parameter, α_{bc} for the slab-system for a predefined value of the orthotropy. It is indicated in *Chapter 3* that the value of the critical beam-strength parameter (α_{bc}) for any slab-beam system depends upon the

orthotropy of the slab in addition to the number of panels and the aspect ratio of the slab. Equations (3.22 and 3.23) can be used to calculate the value of the critical beam-strength parameter of the slab-beam system. However, it is always better to provide a slab-beam system designed for an elastic distribution of the moment field for the sake of economy as it always results in a relatively more economical section [see chapter 3, *Wood (1961)*]. Accordingly, a design procedure is developed for the laterally loaded slab-beam system being proportioned for an elastically distributed moment field. However, it can be used for the slab-beam system being proportioned for any other value of the orthotropy but in such cases, the serviceability criterion of applicable design codes must be strictly adhered to keep the crack-widths within allowable limits.

For simplicity and its subsequent use in the analysis and design of the slab-beam systems, the two values of the beam-strength parameters are expressed as a single non-dimensional parameter called as moment-manipulator, λ ($= \alpha_b/\alpha_{bc}$). Then, a suitable value of the moment-manipulator, λ is selected that will decide the behavior of the slab-beam system at the collapse. If the slab has been designed with λ-value less than unity, it must fail following the global-collapse mechanism. Otherwise, the same slab-beam system would collapse with the formation of a yield line pattern locally in all panels of the slab at collapse load and in this case, the behavior of the supporting beams will be quite similar to the rigid beams although it would show a little bit more deflection in comparison to the non-shallow beams. These types of beam are termed as a shallow-rigid beam whereas the former types of beams are called as a shallow-flexible beam. The slab supported over the shallow-rigid beams will show a comparatively lesser value of the deflection at a given load level in comparison to the shallow-flexible beams but this value of the deflection will be more in comparison to the rigid beams. Therefore, it is suggested to use highest possible value of the beam depth that would, simultaneously, facilitates the formation of the global collapse mechanism in the slab-beam system as well as meets the serviceability requirement of the design codes.

Based upon the continuity-conditions at the outer edges of the slab-beam system, the slab-constants; *d, e* and *f* are determined to calculate the slab-parameter (A). It must be ensued that the value of slab-parameter (A) must lie within the range defined by the equations (3.20 and 3.24) for the slab to initiate the composite-action between the slab and the supporting beams at the collapse. This can indirectly be controlled by deciding the value of the moment-manipulator (λ) and using this value of the λ in determination of

the slab-parameter (A) from equation (3.27). The design moment field in the slab-beam system can be determined from the equations (3.11, and 3.21) applicable for a rectangular reinforced concrete slab cast monolithic with the internal equally spaced shallow beams and supported over non-yielding edges at outer boundaries.

Alternatively, in order to make the design procedure similar to that recommended by the design code, *IS 456 (2000)*, the design equations derived in the chapeter-3 can be modified to calculate the moments being shared between the slab (middle-strip as per the code) and the supporting beams (column-strip as per the code) depending upon the slab-constants. The detail of this modified procedure is given below:

The sum total of the moment field (m_{ux}, $m_{uy,}$ and m_b) induced in the panel of the shallow-beam supported slab at collapse is given in equation (5.1). This total moment acting in the panel of the slab-system is called as the panel-static moment, PSM.

$$\mathrm{PSM} = \mathrm{m_b} + \mathrm{m_{ux}} \mathrm{l_x} + \mathrm{m_{uy}} \mathrm{l_y} \tag{5.1}$$

Equation (5.1) can be further simplified by replacing the moment-field by their expressions. This is given in equation (5.2).

$$\mathrm{PSM} = \left(1 + \alpha_b + \mu\, \mathrm{n\, r}\right) \mathrm{m_{ux}} \frac{\mathrm{L_x}}{\mathrm{n}} \tag{5.2}$$

In equation (5.2), m_{ux} is the bending moment acting along span, L_x of the slab-beam system. The panel-static moment (PSM) in any slab-beam system, initially, is an unknown factor as it depends upon the internal moment-field induced in the slab-system under uniform load (w) acting over the entire top face. However, it can very easily be calibrated with the known design parameters of the slab-beam system viz: uniform area load (w), the short span (l_y), and the long span (L_x). All these known parameters of the slab-beam system can be expressed as a Nichol's moment, NM given in Eq. (5.3). Most of the design codes [*ACI 318 (2008), IS 456 (2000)* and *CSA 23.4 (1994)*] use Nichol's moment acting in the panel of the slab-beam system for calculating the middle-strip and the column-strip moments of the slab-systems.

$$\mathrm{NM} = \frac{\mathrm{w\, l_x\, l_y^2}}{8} \tag{5.3}$$

Nichol's moment can be further simplified and is given in equation (5.4).

$$\mathrm{NM} = \left(\frac{\mathrm{r}^2}{8\,\mathrm{n}}\right) \mathrm{w\, L_x^3} \tag{5.4}$$

By combining equation (5.2) and equation (5.4), a non-dimensional factor, k can be obtained to convert the Nichol's moment (NM) to the panel-static moment (PSM) of the slab-beam system. The final expression for this factor is given in equation (5.6).

$$k = \frac{PSM}{NM} = \frac{8}{r^2}\left(1 + \alpha_b + \mu n r\right)\frac{m_{ux}}{w L_x^2} \tag{5.5}$$

$$k = \frac{8 c_x}{r^2}\left(1 + \alpha_b + \mu n r\right) \tag{5.6}$$

In equation (5.6), c_x is the slab moment coefficient acting along the long span (L_x) of the slab-system. The PSM of the slab can be divided in ratio of 1**:** α_b**:** μnr to calculate the slab moment, m_{ux} acting over the length l_x; the beam moment, m_b and the slab moment, m_{uy} acting over the length l_y of the slab respectively. The expression of k-factor, defined as the ratio of the PSM and the NM in the panel of the slab, is given in equation (5.6) and its values are tabulated in Tables 5.2 to 5.8 for various aspect ratios of the slab-beam system and λ-values. These values are determined for an orthotropy required to maintain elastic distribution of the moment field in the slab-system.

Otherwise, the equation (5.5) can be simplified to a generalized expression given in equation (5.7) that can be used for the analysis of the slab-beam system with any arbitrary value of the orthotropy by substituting the value of the moment coefficient (c_x) from the equation (3.29). The generalized expression for the k-factor is given in equation (5.7).

$$k = \frac{3}{\left[r\left(A+1\right)\right]^2}\left(1 + \alpha_b + \mu n r\right) \tag{5.7}$$

In equation (5.7), a suitable value of the slab-parameter (A) is selected from the valid range defined in the equations (3.20 and 3.22) to calculate the k-factor. Equation (5.7) can be made more workable by mutual interchanging various terms as given in equation (5.8). The k-factor, given in the equation (5.7), can be further simplified to the participation factor (q) that depends upon the slab-parameter (A) only. The expression of the participation factor is given in equation (5.8) and the variation of this factor (q) with the slab-parameter (A) is plotted in *Figure 5.1*.

$$q = \frac{k r^2}{\left(1 + \alpha_b + \mu n r\right)} = \left\{\frac{3}{\left(A+1\right)^2}\right\} \tag{5.8}$$

The rectangular slab resting over the simple supports at its outer boundary and cast monolithic with equally spaced internal shallow beams can therefore, be designed either

for an elastically distributed moment field using Tables 5.1 to 5.8 or for any arbitrary value of the orthotropy for various aspect ratios of the slab and λ-values by distributing the PSM in ratio of 1:α_b: μnr under a uniform area load (w) acting at the top face of the slab.

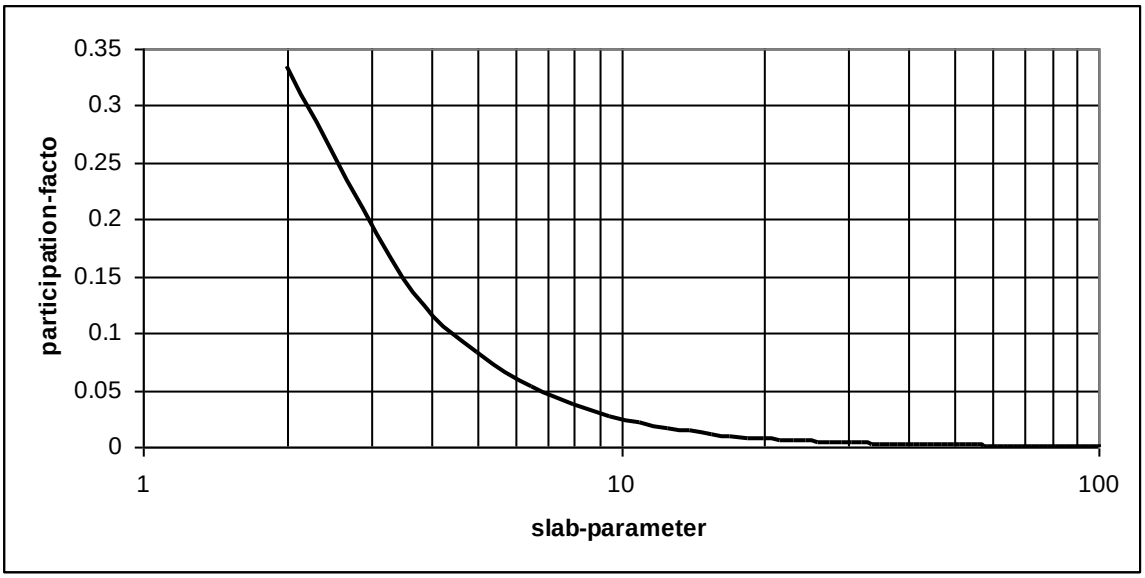

Figure 5.1: Variation of participation-factor against different values of slab-parameter

And for a column supported slab-beam system, the column spacing along the two orthogonal directions of the grid is selected in a manner that the beams along the short span (l_y) of the slab-beam system must behave as shallow beams and along the other direction, the supporting beams must be able to provide a non-deflecting edge to the slab. This can be ensured by selecting the ratio of the column spacing along the orthogonal directions of the slab greater than 1.25 [see *Figure 3.1*]. The procedure to calculate the column spacing of the slab-beam system is illustrated in the section 5.5.

Alternatively, the equations (3.11 and 3.21) along with the equations (3.20 and 3.24) can be used for proportioning a slab-beam system with the internal equally spaced shallow beams and resting over the non-yielding supports on its outer boundaries. Using these equations, the slab-beam system can be designed for any value of the orthotropy and the continuity-conditions at outer boundaries. However, it is always better to provide a slab-beam system being designed for an elastic distribution of the moment field because it will give a relatively more economical section [*Wood (1961)*] and the slab-beam system will not pose any serviceability problem at service load. The thickness of the slab and the internal beams can be provided to suit the design constraints vis-à-vis beam-drop restriction, long spans etc and serviceability criterion of the design codes by selecting a suitable value of the slab-parameter (A). Most importantly, the proposed method can very

intuitively be used to economize the slab-beam system in cases designer has to use some minimum tensile steel in the slab panels of the slab-system to satisfy the requirement of a design code with regards to the maximum /minimum rebar spacing. In such situations, designer can opt for some suitable rebar spacing as per design code requirement and beams of the slab-beam system can be proportioned to meet the balance strength demand of the slab-system by selecting a suitable value of the moment-manipulator/ slab-parameter (A) in the range defined by its lower and upper limits.

5.4 DESIGN PROCEDURE

The laterally loaded slab-beam system can be designed using the any one of the following approaches or it can quickly be used to check the accuracy of finite element models.

5.4.1 Analytical Procedure

The slab-beam system can be designed by following the procedural steps enumerated below:

1. Decide the column spacing in a manner that the supporting beams along the one direction of the column-grid must be capable of providing a flexible edge to the slab and along the other direction; the beams must be sufficiently stiff to provide the non-yielding support to the slab. The supporting beams provide a flexible-edge only, if the depth of these beams is kept less than the *span/12* and *span/15* for simple and continuous outer boundary of the slab-system respectively. The side of the slab-system along the flexible-edge will be the short span (l_y) and the side along the stiff beams will be the long span (L_x) of the slab-beam system [see *Figure 3.1*].
2. Calculate the aspect ratio, r (= l_y/L_x) of the slab-beam system.
3. Decide upon the number of panels (n) of equal length along the long span (L_x) of the slab-beam system. The number of panels should be kept as large as permitted by the architectural constrains.
4. Decide upon the orthotropy of the slab-system. The value of the orthotropy should be taken as permitted by the elastic plate theory [see equation (3.26) and appendix-C].
5. Calculate the lower limit (A_{c1}) of the slab-beam system from equation (3.20).
6. Calculate the upper limit (A_{c2}) of the slab-beam system from equation (3.24).
7. Decide upon the value of the moment-manipulator (λ) and then, calculate the corresponding value of the slab-parameter (A) from the equation (3.27).

8. Determine the moment-field (m_{ux}, $m_{uy} = \mu\ m_{ux}$, and m_b) in the slab-beam system using the equations (3.11 and 3.21).

5.4.2 Proportioning of the slab-beam system using the design-chart

The laterally loaded slab-beam system can be designed for an elastic distribution of the moment-field by following the procedural steps enumerated below:

1. Decide the column spacing in a manner that the supporting beams along the one direction of the column-grid must be capable of providing a flexible edge to the supported slab and along the other direction; the beams must be sufficiently stiff to provide the non-yielding support to the slab. For a flexible-edge, the depth of these beams should be kept less than the *span/12* and *span/15* for simple and continuous outer boundary of the slab-system respectively. The side of the slab-system along the flexible-edge will be the short span (l_y) and the side along the rigid beams will be the long span (L_x) of the slab-beam system [see *Figure 3.1*].
2. Calculate the aspect ratio, r (= l_y/L_x) of the slab-beam system.
3. Decide upon the number of panels (n) of equal length along the long span (L_x) of the slab-beam system.
4. Decide upon the orthotropy of the slab-system. The value of the orthotropy should be taken as permitted by the elastic theory [see equation (3.26) and appendix-C].
5. Calculate the lower limit (A_{c1}) of the slab-beam system from equation (3.20).
6. Calculate the upper limit (A_{c2}) of the slab-beam system from equation (3.24).
7. Determine the value of the critical beam-strength parameter from equation (3.23).
8. Select any suitable value of the slab-parameter (A) from the valid range defined by the steps (5) and (6).
9. Determine the value of the participation factor (q) from the design chart given in the *Figure 5.1*.
10. Knowing the value of the participation factor (q), calculate the value of the k-factor from the equation (5.8).
11. Calculate the Nichol's moment (NM) from equation (5.3).
12. Calculate the panel-static moment (PSM) of the slab-beam system from the Nichol's moment (NM) by multiplying it with the k-factor.
13. The panel-static moment (PSM) of the slab can be divided in ratio of 1**:** α_b**:** μnr to calculate the slab moment, m_{ux} acting over the length (l_x); the beam-moment, m_b and the slab moment, m_{uy} acting over the length (l_y) of the slab respectively.

14. Convert these slab moments to moment per unit width of the slab by dividing these values by the corresponding side of the slab.

5.5 ILLUSTRATIVE EXAMPLES

To assist in the understanding of procedural steps of the design procedure and their comparison with the results from well-established literature on the slab analysis are illustrated in following examples.

Example 5.5.1: *Consider a typical slab of size 20.12m* x *14.32m continuous over the non-yielding supports at the outer boundaries and subjected to uniform area load of 10 kN/m^2. The slab is divided into four panels of 5.03m each. Determine the moment field in the slab-beam system assuming orthotropy of the slab as 1.482. Take the continuity constant at the outer boundaries and internal beams of the slab-system as 4/3.*

In above problem, number of panels, n = 4

Uniform area load, w = 10 kN/m^2

The slab length, L_x = 20.12m and width, l_y = 14.32m

$\therefore$ Aspect ratio, r of the slab-system = 14.32/20.12 = 0.7135

The panel length of the slab-system, l_x = 5.03m

The *i-values* at various edges of the slab-beam system = 4/3 [given]

Orthotropy, μ = 1.482 [given]

The lower limit of the slab-parameter, A_{c1} = 3.1198 [from equation (3.20)]

The upper limit of the slab-parameter, $A_{c2} = nY\sqrt{\frac{3\mu}{2d}\left(\frac{A_1-1}{A_1+1}\right)}-1$ [from equation (3.24)]

In above equation, values of parameter d, Y and A_1 are calculated as below:

d = 2 (1 + i_x) = 4.667

$Y = \sqrt{1+i_i} + \sqrt{1+i_y} = 3.055$

$X = 2\sqrt{1+i_x} = 3.055$

$\gamma = \frac{X}{Y} = 1$

$\beta_1 = \frac{(nr)^2}{\mu\gamma^2} = 5.496$

$A_1 = \sqrt{1+3\beta_1}$ =4.182

Therefore, the value of the upper limit of the slab-parameter, A_{c2} = 9.763

The value of bending-moments for the slab (m_x, m_y) and the supporting shallow-beams (m_b) at value of the moment-manipulator (λ) of 0.8 is tabulated below. The corresponding value of the slab-parameter (A) can be calculated from equation (3.27) and is found to be 8.843. Using this value of the slab-parameter (A), the moment field in the slab can be determined using the equation (3.11).

Table 5.1: Typical Analysis Results 4-Panel Slab Supported over Shallow-Flexible Beam

λ-Value	m_x, kNm/m		m_y, kNm/m		m_b, kNm	
	+ve value	-ve value	+ve value	-ve value	+ve value	-ve value
0.8	6.71	8.95	9.95	13.27	523.14	697.53

It is important to note that the total-static moment in the slab-beam system calculated from the proposed model and that calculated from the finite-element analysis comes out to be same. The total-static moment in the slab-beam system considered in this example is calculated as 4309.60 kNm and this value compare fairly well with the total static moment for the slab-beam system that is discontinues over its outer boundary and without any negative steel over its internal beams [*see example 4.3.3*], where the total static moment for the slab-beam system comes out to be 4310.83 kNm and for the same system, when it was analyzed using a finite-element based software comes out as 4310.90 kNm; thereby satisfying the Nicholas' hypothesis of minimum static moment existing in a slab.

The slab-beam system can be proportioned for this moment field with the condition that the depth of the supporting beam must be kept less than *span/12* to achieve the composite slab-beam action in the global collapse mechanism.

Example-5.5.2: *There is a proposal to construct* a *reinforced concrete slab over a plan area of 25m* x *15m. Assuming an elastic distribution of moment-field in the slab, suggest a suitable slab-beam system and determine a design moment field for the proposed slab-beam system subjected to a uniform area load of 11 kN/m^2.*

Assuming that 15m length of the plan area is divided into 3 bays of 5m each and the length along 25m length of the area is divided into 'n' number of equally spaced bays. In order to maintain the ratio of column spacing along the two orthogonal directions equal to 1.25 (minimum) or more, the value of 'n' must be taken equal to 4. Therefore, the given plan is divided into 3 bays of 5m each along 15m length and 4 bays of 6.25m each along the 25m length of the area.

The 3-span beam along 15m length can be made to behave as a non-shallow beam by selecting the depth of the beam more than or at the most equal to *span/10* (= 0.5m). By keeping the same depth of the beam along the other direction of the grid will give

span/depth ratio of 12.5 (>12) and therefore, these beams will behave as shallow beams. Moreover, the designer has an option to select any suitable value of the beam depth, depending upon the architectural constraint etc., satisfying the serviceability criterion of the applicable design guidelines and the *span/depth* ratio of the shallow beams along 6.25m lengths. Therefore, the master slab of size 25m x 15m will consists of four number smaller three-panel rectangular slabs of size 15m x 6.25m each, supported over the internal shallow-beams, and resting over the non-yielding edges on the outer boundaries. Then, these smaller slabs can be designed for any set of the moment field for a predefined value of λ.

In this case, number of panels, n = 3 and the slab is subjected to a uniform area load, w = 11 kN/m$^{2.}$ The slab length, L_x = 15m and width, l_y = 6.25m with a corresponding value of the aspect ratio, r = 6.25/15 = 0.41667

The panel length of the slab-system, l_x = 5.0m

The *i-values* at various edges of the slab-beam system = 0 [assumed]

Orthotropy, μ = 2.65 [from equation (3.26)]

The lower limit of the slab-parameter, A_{c1} = 6.84 [from equation (3.20)]

The upper limit of the slab-parameter, A_{c2} = 15.94 [from equation (3.24)]

In above equation, a value of the parameter A_1 was calculated as 1.664 for β_1 of 0.5896. Equation (3.23) will give the critical beam-strength parameter of the slab-system as 18.

The value of the slab-parameter (A) can be calculated from equation (3.27) for any assumed value of moment-manipulator (λ) and its lower limit (A_{c1}) and upper limit (A_{c2}). The value of moment-manipulator (λ) in the present example is taken as 0.6.

Slab-parameter (A) for λ-value of 0.6 = 13.08 [from equation (3.27)]

k-factor for λ-value of 0.6 = 1.316 [from equation (5.7)]

$$\text{Nichol's moment} = \frac{10 \text{ x } 5 \text{ x } 6.25^2}{8} = 268.55 \text{ kNm}$$

Therefore, PSM = 1.316 x 268.55 = 353.49 kNm and this can be divided in the ratio of 1:α_b: μnr (= 1: 10.8: 3.31) to determine the slab moment, m_{ux} (= 4.678 kNm/m), beam moment, m_b (= 252.66 kNm) and the slab moment, m_{uy} (= 12.389 kNm/m) respectively.

The slab can suitably be reinforced at the top face along the length of 3-span non-shallow beam to control the flexural cracking due to a sudden change in curvature of the slab under loading and it always results in a safe design due to the increase in the load factor of the proposed slab-beam system at collapse. However, any alternation in the failure mode of the slab-beam system after placement of the negative steel along the non-

yielding boundaries must be checked and it must be ensured that it always fail by the formation of the global-collapse mechanism at collapse.

Example-5.5.3: *Consider a typical square slab of side 9.14m each. The slab is supported over the non-yielding supports and is discontinuous on all the four sides. It is subjected to uniform area load of 11 kN/m^2. The slab is divided into three panels of 3.05m each. Assuming an elastic distribution of moments in the slab, determine the design moment field*

In the given problem, number of panels, n = 3

Uniform area load, w = 10 kN/m^2

Length of the slab, L_x = 9.15m and the slab width, l_y = 9.15m.

Therefore, aspect ratio of the slab, r = 1 and panel length, l_x = 3.05m

Value of the orthotropy of the slab required for the elastic distribution of moment field can be calculated from the equation (3.26).

Orthotropy, $\mu = 1$ [from equation (3.26)]

The lower limit of the slab-parameter, $A_{c1} = 2.0$ [from equation (3.20)]

The upper limit of the slab-parameter, $A_{c2} = 5.2915$ [from equation (3.24)]

Suppose, we are proportioning the slab-beam system at $\lambda = 0.6$. The value of the slab-parameter corresponding to this value of the moment-manipulator is 4.289.

Case-1- Design using the analytical equations: Equation (3.11) and equation (3.21) can be used to calculate the slab moments and the supporting beam moment. These are given below after substituting the corresponding values in the formulae.

$$m_{ux} = \left(\frac{3}{4.289+1}\right)^2 \frac{10 \text{ x } 9.15^2}{24} = 11.223 \text{ kNm}$$

$$m_b = \left\{\frac{1^2 \text{ x } \left(4.289^2 - 2^2\right)}{(4.289+1)^2 (3-1)}\right\} \frac{10 \text{ x } 9.15^3}{8} = 246.389 \text{ kNm}$$

Case-2- Design using the design-chart:

Using the lower and the upper limit of slab-parameter, the value of the critical beam-strength parameter can be calculated from the equation (3.23).

Therefore, beam-strength parameter (α_b) at $\lambda = 0.6 = 0.6 \text{ x } 12 = 7.2$

The participation-factor (q) = 0.10724 [from equation (5.8) or Figure (5.1)]

And $k = \frac{q}{r^2}\left(1 + \alpha_b + \mu \text{ n r}\right) = 1.20109$

$$\text{Nichols moment} = \frac{10 \text{ x } 3.05 \text{ x } 9.15^2}{8} = 319.19 \text{ kNm}$$

The panel-static moment (PSM) = 1.20109 x 319.19 = 383.34 kNm

The PSM can be distributed in ratio of 1**:** 7.2**:** 3 to determine the slab moment, m_{ux} (= 11.22 kNm/m), the beam moment, m_b (= 246.46 kNm) and the slab moment, m_{uy} (= 11.22 kNm/m) respectively.

Example 5.5.4: *Consider a typical slab of size 20.12m* x *14.32m resting over the non-yielding supports at the outer boundaries and subjected to uniform area load of 10 kN/m*^{2}*. The slab is divided into four panels of 5.03m each. Determine the moment field in the slab-beam system assuming orthotropy of the slab as 1.482. The slab is discontinuous over its outer boundary and there is no negative reinforcement over the internal beams.*

CASE-1-Design of slab-beam system using the proposed procedure:

In the given problem, number of panels, n = 4

Uniform area load, w = 10 kN/m^2

Length of the slab, L_x = 20.12m and the slab width, l_y = 14.32m.

Therefore, aspect ratio of the slab, r = 20.12/14.32 = 0.7135

And the panel length, l_x = 5.03m

Orthotropy, μ = 1.482 [given]

The lower limit of the slab-parameter, A_{c1} = 3.1198 [from equation (3.30)]

The upper limit of the slab-parameter, A_{c2} = 9.763 [from equation (3.30)]

The analytical model developed in chapter 3 of the thesis is used to find the moment-field induced in the slab-beam system. It can be proportioned for any value of the slab-parameter (A) form the valid range of its lower and upper limits; defined by the equations (3.29) and (3.31). The moment-field in the slab is given in Table 5.2.

Table 5.2: Variation of the moment-field with the slab-parameter

λ-value	0	0.2	0.4	0.6	0.8	1.0
Slab moment, m_{ux}, kNm/m	89.14	39.73	26.07	19.53	15.67	13.10
Slab moment, m_{uy}, kNm/m	132.11	58.88	38.64	28.94	23.22	19.41
Beam moment, m_b, kNm	0.00	773.90	1015.76	1141.60	1221.00	1276.00

Table 5.2 postulates various combinations of the slab and beams resisting moments required for supporting a surface load of 10 kN/m^2. Designer can select any suitable value of the moment field depending upon the minimum possible depth of the beam (given constraint) available from the applicable serviceability criterion. In the present case, the

minimum beam depth required for the span of 12.2 m is 850 mm from the deflection consideration and the reinforcement detail for the slab-beam system with $\lambda = 0.8$ is calculated below:

For the slab, 150 mm thick cast in M20 concrete with fe415 grade steel, the steel required along span, L_x of the slab = 10φ 135 mm c/c, and steel required along the short span of the slab (l_y) = 12φ 130 mm c/c. 12-28φ are required at the bottom face and 2-20φ at the top of the supporting beams along with the stirrups of 2 L-8φ 250 mm c/c; thereby giving a moment of resistance of 1345 kKm (> 1221 kNm). Therefore, the total material consumption for the slab-beam system designed using the proposed method:

1) Concrete = 52.25 m^3 **2)** steel = 6145 kg, and **3)** Beam-drop = 700 mm

CASE-2-Slab cast monolithic with the non-yielding supporting beams:

In this case, the supporting beams with dimensions of (300 x 1400 mm) and with a *span/depth* = 10, it will provide a complete non-yielding support to the slab and the slab will act as one-way slab with span of 5.03 m.

Load transferred by the slab = 10 x 5.03 = 50.3 kN/m

Total load acting over the beam including self weight = 60 kN/m

Bending moment for the beam = 1538 kNm, and shear force = 430 kN.

For the slab, 150mm thick cast in M20 concrete with fe415 grade steel, the steel required along span, L_x at the bottom face of the slab @ 12φ 130 mm c/c, and steel required along span, L_x at the top face of the slab @ 12φ 260 mm c/c + 16φ 260 mm c/c (alternate bars). The steel required along the short span, l_y of the slab @ 8φ 250 mm c/c.

And for the supporting beams, 8-28φ are required at the bottom face and 2-20φ at the top face along with stirrups of 2 L-8φ 250 mm c/c to resist the moment of 1538 kNm.

Therefore, the total material consumption for the slab-beam system designed using rigid beams:

1) Concrete = 60 m^3 **2)** steel = 4900 kg, and 3) Beam-drop = 1250 mm.

The comparison of material consumption and the beam-depth required in each case along with the material unit cost is tabulated in Table 5.3.

Table 5.3: Comparison of case 1 and case 2

Case	Material Consumption / m^2		Unit Rate, INR	Total Cost, INR / m^2	Beam Drop, mm
	Concrete	Steel			
1.	0.18	21.30	Concrete: 2500/m^3	1302	700
2.	0.21	17.00	Steel: 40/kg	1205	1250

Table 5.3 shows that the unit material cost for the both cases comes out to be nearly same within ±10% but the beam-drop reduces by 44 % with the use of shallow beams for supporting slabs in comparison to the slabs supported over the rigid beams. Therefore, for a given ceiling height and the beam span, overall building height reduces considerably with the use of shallow- beams or alternatively, beams with longer spans can be used for a given set of design constraint and/or beam depth.

5.6 CLOSURE

- Design equation and procedure have been suggested for proportioning reinforced concrete rectangular slabs cast monolithic with equally spaced internal shallow beams, and resting over simple non-yielding edges on its outer four sides. The results for single panel slab obtained from the suggested procedure compares favorably well with values obtained from well-established literature on the yield line theory.
- A non-dimensional parameter (λ) has been suggested to differentiate the failure mode of the shallow beam supported rectangular slab. If slab has been designed with $\lambda < 1$, it will fail following a global-collapse mechanism otherwise the same slab will collapse in a local-collapse mechanism in which the supporting beams (normally with high steel ratio) will not allow the yield lines to cross over into the adjacent panels. In addition, the slab-beam system will fail with the formation of yield line pattern locally in all panels of the slab at collapse.
- The λ-value can be used very conveniently to control the participation of the supported-slab in load sharing between the supporting beams, and the slab of the slab-beam system. The slab will behave as a single panel slab at zero λ-value and it will be divided into number of smaller rectangular slabs simply resting over the internal beams with discontinuous edges at $\lambda=1$. And for the intermediate λ-values, the slab and supporting beams will share the moment field (m_{ux}, m_b and m_{uy}) induced in a panel of the shallow-beam supported slab in ratio of $1{:}\lambda\alpha_{bc}{:}\ \mu nr$ respectively at collapse.
- An expression for the *k-factor* has been suggested for a multipanel rectangular slab to convert the Nichols moment into the panel-static moment (PSM) that can be distributed among the slab and internal beams in ratio of $1{:}\alpha_b{:}\ \mu nr$ to determine the design moment field in the slab-system.
- Design chart has been suggested that can be used to determine the k-factor for any value of the orthotropy, number of panels and the aspect ratio of the slab-beam system.

- Use of shallow beams in the slab-beam system can results in saving of about 40-50% in the beam drop with the consequential reduction in overall height of the building for same load carrying capacity of the slab in comparison to the slab supported over the non-yielding beams. The overall unit cost of the material consumption remains the same for both the cases.

CHAPTER-6

CONCLUSIONS

6.1 SUMMARY

Slab is the most widely used structural element. It finds application both in the framed as well as in the ordinary load-bearing masonry-structures. It can be viewed as a structural component that transfers the external load to its supports by means of bending, shear and torsion. Because of coupling of these internal force-resultants, the structural behavior of the slabs is very sensitive to the type and the position of support and/or stiffness of the supporting structural members. Any change in the physical parameters of these supporting systems will cause a considerable change in the moment-field induced in the slab under the given set of loading.

The moment coefficients recommended by the design codes are applicable only for the rectangular slabs with various end-restraints and supported over the non-yielding edges on its outer boundary. But in routine design practice, number of case are encountered by designers whereby the beam-drop and the beam-spans are restricted by architects to a level that are not sufficient to provide a non-yielding edge to the slab and as such these coefficients predict the moment-field highly on unsafe side and produce a structurally deficient slab section. This design procedure may be appropriate for many situations, but in many others, it leads to wasteful overdesign or, perhaps worse, underdesigns.

The current state-of-art available for the design of reinforced concrete slab does not satisfactorily address the problem of designing slabs cast monolithic with shallow-beams. Design methods have been suggested based upon the results of an extensive series of tests and well-established performance record of various slab systems. Based upon the results of these tests, empirical relations and some factors have been suggested for apportioning the total static moment to the slab and the supporting beams and/or the column strip for satisfactory performance. Most of the design guidelines recommended by various codes are based upon these empirical results and the performance record of various slab-beam systems. The procedure recommended by most of the design codes has a number of inherent limitations in the form of assumptions, which are mandatory to be satisfied by all

slab panels for the satisfactory performance. It forces the designers to use supporting beams with lesser value of the *span/depth*-ratio that sometimes, fails to meet the architectural and some other design constraints in practice.

In the present research work, an analytical model and design equations has been suggested for proportioning the reinforced concrete rectangular slab cast monolithic along with equally spaced shallow beams and resting over the non-yielding supports at outer boundaries. The use of shallow beams becomes, sometimes, mandatory in buildings due to some architectural constraints (*e.g.* low ceiling height or very long beam spans etc). These design equations can also be used for skew slab resting over the simple supports at its outer edges. The proposed procedure can also be used for multi-bay-multi-panel slab system but it must be supported over the equally spaced shallow beams along the one direction and the non-shallow beams at regular intervals along the other direction of the slab. The slab is subjected to out-of-plane uniform area load over its whole surface.

To validate the analytical results from the proposed analytical model and the design equations, these are compared with the results from the well-established literature on the slab analysis and are found to be in good agreement.

The full-scale slabs designed using the proposed analytical model is experimentally validated to check the hypothetical collapse mechanism and strength of the slab-beam system designed using the proposed model. The actual crack pattern at the collapse load, for the two and three-panel slabs tested in the laboratory, was found to be in good agreement with the analytical results. A non-dimensional parameter called as moment-manipulator, λ (= moment of resistance of beam/moment of resistance of beam required for the simultaneous formation of global and local collapse mechanism) has been proposed to distinguish the nature of the shallow beams. Test slabs designed using the λ-value less than unity failed following a global-collapse mechanism with a load factor of more than 1.40. However, these slabs show more deflection at the design load than the permissible values but selecting a highest possible value of the beam depth satisfying both the serviceability criterion as well as the *span/depth* ratio of the shallow beam can reduce the actual deflection of the slab system under the design load. It is suggested that the actual slab-beam system with shallow beams should never be proportioned with λ-value more than unity as it leads to failure of the slab in a local-collapse mechanism with a reduced load factor.

The test slabs designed for λ-value more than unity and supported over the shallow beams failed following a local-collapse mechanism with a load factor ranging from 1.30

to 1.40, with the formation of negative yield lines near the beam-ends. At the design load, these slabs show a reduced deflection in comparison to the slabs designed for λ-value less than unity but this value of the deflection was more than permitted by the design codes. Therefore, it is suggested that the actual slab-beam system with shallow beams should never be proportioned with λ-value more than or equal to unity.

Working procedure is illustrated with the help of design examples. It is shown that with the use of shallow beam in the slab-beam systems, the unit cost of the material-consumption comes out to be nearly same but the beam-drop of the supporting beams along the short span of the slab-beam system reduces by about 40-50% in comparison to the slabs supported over the non-shallow (rigid) beams.

6.2 CONCLUSIONS

- An analytical model has been suggested for the analysis and design of a laterally loaded rectangular reinforced slab-system resting over the non-yielding edges at its outer boundaries and cast monolithic with the internal equally spaced internal generic beams. These beams can be designed to act as a rigid edge or as a flexible edge. The strength of these beams will dictate the behavior of the slab-system. The results for a single-panel isotropically reinforced square slab obtained from the suggested model compares favorably well with that obtained from the well-established literature on the slab analysis.

- The slab-beam system can fail either globally or locally with the development of a yield line mechanism in the entire slab or in panels of the slab-system respectively depending upon the strength and/or stiffness of the internal supporting beams. The collapse mechanism is called as a global-collapse mechanism if the slab-beam system fails globally; otherwise it is called as a local-collapse mechanism.

- The strength requirement (moment field) in the slab-system and the nature of the failure mode can be determined by selecting a suitable value of the slab-parameter (A) whereas the stiffness of supporting beams and/or slab-system depends entirely upon the *span/depth* ratio. The *span/depth* ratio of less than 12 would initiate a failure of the slab-system in the local-collapse mechanism.

- The slab-beam system sustains the load in the global-collapse mechanism mode only in the narrow range of the slab-parameters, $A_{c1} < A < A_{c2}$ thereby, allowing the designer to proportionate the slab-system with any suitable value of the slab-parameter from this range. The selection of this parameter will greatly control the strength requirement of the

internal beams of the slab-beam system. Low strength supporting-beams are required in the slab-beam system to support the lateral load at the low value of the slab-parameter with a corresponding heavy slab section and vice versa.

- A non-dimensional parameter called as moment-manipulator, λ (= α_b / α_{bc}) has been suggested to classify the slab-system based upon the failure mode at collapse. If it has been designed with $\lambda < 1$, the slab-system would sustain the lateral load in the global-collapse mechanism mode; whereby the supporting-beams of the slab-system can be used very effectively for controlling the load sharing along the components of the slab-system. Otherwise, the same slab (with $\lambda > 1$) will support the external load in the local-collapse mechanism mode and it would be transformed into the slab-beam system consisting of a number of interconnected smaller slabs resting over the internal beams at collapse. The supporting beams of the slab-beam system behave as a shallow-flexible beam if these have been designed with λ-value less than unity. Otherwise, same set of supporting beams would act as shallow-rigid beams.

- The λ-value can be used very conveniently to control the participation of the slab in load sharing along with the beams of the slab-system. The slab-system behaves as a single panel slab at zero λ-value ($A = A_{c1}$) and it is divided into a number of smaller rectangular slabs simply resting over the internal beams at λ=1 ($A = A_{c2}$). The supporting-beams at this λ-value or $A = A_{c2}$ behave similar to the non-yielding beams and/or walls and the slab always fail by the formation of a local-collapse mechanism irrespective of its stiffness. The participation of the slab in the load sharing can be increased by selecting a lower value of the beam-strength parameter, α_b and vice versa.

- The moment field in the slab-system reduces exponentially with the increase of the orthotropy irrespective of the number of panels of a two-way slab-beam system. This rate of reduction becomes almost constant after the $\mu = 3$, and when the slab-beam system has been divided into five or more panels.

- However, this rate of reduction is relatively small and it becomes almost constant (within 5% of the mean value) for the one-way slab-beam systems, when it has been proportioned with the orthotropy of three or more irrespective of the number of panels.

- The strength requirement of the supporting beams increases, when the slab-system has been proportioned with higher value of the orthotropy and it become almost constant after $\mu = 3$, and when the slab-beam system has been divided into five or more panels.

- The moment field in the slab-system reduces with the increase in number of internals panels. The number of panels therefore, should be selected as large as permitted by the architectural constraints and practicability at the site.

- The strength requirement of the supporting beams is insensitive to the increase and/or decrease of the orthotropy for the one-way slabs. It is therefore, suggested that the one-way slab-beam system ($r \leq 0.5$) should be designed without internal beams with short span (l_y) up to the 3.5m and the internal beams should be provided to reduce the slab thickness for higher span (over and above 3.5m).

- The value of the orthotropy should be kept less than unity and as large as permitted by the elastic-distribution of the moment-field for the better performance of the slab-beam system under service load.

- The design moment-field in the slab-system cannot be minimized with respect to the orthotropy. However, selecting the lowest possible of the orthotropy as permitted by the elastic plate theory can help the designer to minimize the design moment field.

- Analytical model predicts the yield line pattern of the slab-system with internal beams and it was found to be in good agreement with the experimental results.

- The proposed procedure can be used for proportioning the total static moment to the slab resting over the non-yielding edges at the outer boundary and its internal monolithic supporting shallow beams and their subsequent design. The total static moment field proportioned using the proposed procedure compares favorably well with the values suggested in the published literature and from a finite element based analysis.

- Internal shallow beams/supports are classified into two categories viz. *shallow-flexible beam* and *shallow-rigid beam*. A beam that leads to the failure of the slab in the global-collapse mechanism is classified as shallow-flexible beam whereas the beam that causes the failure of the slab with the formation of the collapse mechanism, locally and simultaneously, in all panels of the slab is classified as shallow-rigid beam.

- The supporting beam behaves similar to the wall and/or rigid beam; if it has been proportioned with *span/depth* ratio of more than 10. And the same beam acts as a shallow beam if it has been proportioned for *span-depth* ratio more than 12. It can be made to behave as a shallow-rigid or as a shallow-flexible by suitably selecting the slab-parameter or moment-manipulator.

- It was found that orthotropy of 0.7 is the minimum value that will cause failure of the slab-system in the global-collapse mechanism irrespective of number of panels and the beam-strength parameter.

- Design procedure has been proposed for the design of the slab cast monolithic with internal shallow beams. Design Chart has been suggested for proportioning the slab-system. These charts can be used for a single panel as well as multi-bay-multi-panel slab-system failing in the global collapse mechanism and in the local-collapse mechanism.

- The test slabs designed for λ-value less than unity and with the beam depth less than *span/10* failed following the global-collapse mechanism with a load factor of more than 1.40. However, these slabs show more deflection at the design load than the permissible values but selecting a suitable beam depth satisfying both the serviceability criterion as well as the *span/depth* ratio of the shallow beam can reduce the actual deflection of the slab-beam system under the design load. Therefore, it is recommended to use highest possible value of the depth of the supporting shallow beams that satisfies serviceability criterion of the design codes, and simultaneously, facilitates the formation of a global-collapse mechanism in the slab at the ultimate state.

- The test slabs designed for λ-value more than unity, and supported over the shallow beams failed following a local-collapse mechanism with a load factor ranging from 1.30 to 1.40, with the formation of negative yield lines near the beam-ends. At the design load, these slabs show a reduced deflection in comparison to the slabs designed for λ-value less than unity but this value of the deflection was more than permitted by the design codes. Therefore, it is suggested that the actual slab-beam system with shallow beams should never be proportioned with λ-value more than or equal to unity.

- Use of shallow beams in slab-beam system can results in saving of about 40-50% in beam drop with the consequential reduction in overall building height for same load carrying capacity of slab in comparison to the slab supported over non-yielding beams although overall unit cost of material consumption remains same for both cases.

6.3 SCOPE FOR FURTHER STUDY

A) The analytical model can be modified, and extended to take care of the slab-beam system with following design combinations/ constraint:

1. When the shallow beams are used to support the slab along both directions of the column grid. It will produce secondary failure (punching) near the column face at very low beam depth and it would govern the design of the slab-system at zero beam depth.
2. The effect of the pattern loading over the slab-beam system can be considered.
3. The effect of the slab openings on the moment field can be studied.
4. The effect of the column stiffness on the moment field in the slab-beam system.
5. The model can be modified for the analysis of slab-beam system with unequal column spacing along one and/or both directions.
6. The model can be modified to take care of the line load acting over the supporting-beam and/or at any position over the surface of the slab.

B) Deflection, vibration and crack width studies can be carried out on the slab-beam systems designed using the proposed model to check the compliance of the serviceability criterion of the design codes. This can be done for various values of the orthotropy as considerable saving in the strength requirement of system can be made at higher value of orthotropy if permitted by the serviceability criterion of the applicable design code.

C) Experimental studies can be conducted on the slab-beam systems with shallow beams designed using the proposed model at $\lambda \geq 1$ with negative reinforcement provided normal to the internal beams.

REFERENCES

A. Thavalingam, A. Jennings, D. Sloan, J.J. McKeown (1999). Computer-assisted generation of yield-line patterns for uniformly, *Journal of Engineering Structures*, 21: 488-496.

ACI Standard 318 (2008). Building Code Requirements for Reinforced Concrete, American Concrete Institute, Detroit.

A. E. Cardenas, M.A. Sozen (1973). Flexural Yield Capacity of Slabs, *Proc.* ACI, 70: 24-125.

A. Hillerborg (1975). Strip Method of Design, Viewpoint, London.

Alaa Helba and John B. Kennedy (1994). Collapse Load of Continuous skew Composite Bridges, *Journal of Structural Engineering*, 120 (5): 395-1414.

Alaa Helba and John B. Kennedy (1994). Parametric Study on Collapse Load of skew Composite Bridges, *Journal of Structural Engineering*, 120 (5): 1415-1433.

Armand Furst and Peter Marti (1997). Robert Maillart's design Approach for Flat Slabs, *Journal of Structural Engineering*, 123 (8): 1102-1110.

Baker, J. F., Horne, M. R. and Heyman, J. (1961). The Steel Skeleton: Plastic Behaviour and Design, The English Language Book Society, London, pp. 117-128.

Bauer, D. and Redwood, R.G. (1987). Numerical Yield Line Analysis, *Journal of Computer and Structures*, 26 (4): 587-597.

Castro, J. M. et.al (2007) Assessment of Effective Slab Widths in Composite Beams, *Journal of Constructional Steel Research*, 63: 1317-1327.

C.K. Soh, T.K. Chan and S.K. Yu (2001). Numerical Method for Lower-Bound Solution of the Rigid-Plastic Limit Analysis Problem, *Journal of Engineering Mechanics*, 127 (11): 1075-1081.

Clinton O. Rex and W. Samuel Easterling (2000). Behavior and Modeling of Reinforced Concrete Slab in Tension, *Journal of Structural Engineering*, 126 (7): 764-771.

CSA Standard A23.3 (1994). Design of Concrete Structures, Canadian Standards Association, Ontario.

Corley W.G and Jirsa J.O. (1970). Equivalent Frame Analysis for Slab Design, *Journal ACI, Proceeding*, 67 (11): 875-884.

Denton, S. R. (2001). Compatibility Requirements for Yield-Line Mechanisms, *International Journal of Solids and Structures*, 38: 3099-3109.

Famiyesin, O.O.R. et al. (2001). Numerical and Analytical Predictions of the Limit Load of Rectangular Two-Way Slabs, *Journal of Computer and Structures*, 79: 43-52.

Gallanghar, Zienkiewicz (1973). Optimum Structural Design- Theory and Applications, John Wiley and Sons, London.

Gamble W.L. (1972). Moments in Beam Supported Slabs, *Journal ACI, Proceedings*, 69 (3): 149-157.

Gamble W.L, Sozon M.A. and Seiss C.P (1969). Tests on Two-Way Reinforced Concrete Floor Slab, *Proc. ASCE, Journal of Structural Division*, 95 (ST6): 1073-1096.

Hatcher, D.S., Sozen, M.A., and Siess, C.P. (1965). Test of a Reinforced Concrete Flat Plate, *J. Struct. Div., ASCE*, 91 (ST5): 205-231.

Hatcher, D.S., Sozen, M.A., and Siess, C.P. (1969). Test of a Reinforced Concrete Flat Slab, *J. Struct. Div., ASCE*, 95 (ST6): 1051-1072.

Holmes, M and Arnaouti, C (1973). Theoretical Moments at Yield in a Reinforced Concrete Slab, *Building Science*, 8: 363-373.

Islam S, Park R. (1971). Yield Line Analysis of Two-Way Rectangular Slabs with Openings, *Journal Institution of Structural Engineers*, 49 (6): 269-276.

IS 456 (2000). Code of Practice for the Design of Reinforced Concrete Structures, Bureau of Indian Standards, India.

Jain S.C., Kennedy (1973). Yield Criterion for Reinforced Concrete Slabs, *Journal of Structural Division, ASCE*, 100 (ST3): 631-644.

Jain S.C., Kennedy (1973). Yield Criterion for Reinforced Concrete Slabs, *Journal of Structural Division, ASCE*, 100 (ST3): 631-644.

Jennings, A. (1996). On the Identification of Yield-Line Collapse Mechanisms, *Engineering Structures*, 18 (4): 332-337.

Jirsa, J.O., Sozen, M.A., and Siess, C.P. (1966). Test of a Flat Slab Reinforced with Welded Wire Fabric, *J. Struct. Div., ASCE*, 92 (ST3): 199-224.

Johansen K.W. (1967). Yield Line Theory, Cement and Concrete Association, London.

Jones, L. L. (1967). Ultimate Load Analysis of Reinforced and Prestressed Concrete Structures, Chatto and Windus, London.

Jones, L. L and Wood, R. H. (1967). Yield-Line Analysis of Slabs, Thames and Hudson, London.

K. O. Kemp (1965). The yield Criterion for Orthotropically Reinforced Concrete Slabs, *International Journal of Mechanical Science*, 7 (11): 737-746.

Kitjapat Phuvoravan and Elisa D. Sotelino (2005). Nonlinear Finite Element for Reinforced Concrete Slabs, *Journal of Structural Engineering*, 131(4): 643-649.

Kolbjorn Saether (1994). Flat Plates with Regular and Irregular Column Layouts 1: Analysis, *Journal of Structural Engineering*, 120 (5): 1563-1579.

Kowal, Z. and Sawczuk, A. (1976). On the Yield-Line Theory of Plates with Random Plastic Moments, *Engineering Fracture Mechanics*, 8: 275-280.

Kumar, M. S. et.al (2009) Ultimate Strength of Stiffened Plates with a square Opening Under a Axial and Out-of-Plane Loads, *Engineering Structures*, 31: 2568-2579.

Kwiecinski, M.W. (1965). Yield Criterion for an Orthogonally Reinforced Slab, *International Journal of Solids and Structures*, 1: 439-449.

Liu, Y. and Li, R. (2010), "Accurate Bending Analysis of Rectangular Plates with Two Adjacent Edges Free and Others Clamped or Simply Supported based on New Symplectic Approach", *Applied Mathematical Modeling*, 34, 856-865.

Mander, T. J. et.al (2011) Modified Yield Line Theory for Full-Depth Precast Concrete Bridge Deck Overhang Panels, Journal of Bridge Engineering, 16 (1): 12-20.

Maria Anna Polak (1996). Effective Stiffness Model for Reinforced Concrete Slabs, *Journal of Structural Engineering*, 122 (9): 1025-1030.

Mitchell Gohnert (2000). Collapse load analysis of yield-line elements, *Journal of Engineering Structures*, 22: 1048-1054.

Morley, C.T. (1965). On the Yield Criterion of an Orthogonally Reinforced Concrete Slab Element, *J. Mech, Phys. Solids*, 14: 33-47.

Nichols, J. R. (1914). Statical limitations upon the Steel Requirement in Reinforced Concrete Flat Slab Floors', *Transactions, ASCE*, 77: 1670-1736.

P. Adebar, D. Kuchma, M. P. Colins (1990). Strut and Tie Model for the Design of Pile-Cap, An Experimental Study, *ACI Struct. Journal*, 87 (1): 81-92.

Park, R. and Gamble, W. L. (2000). Reinforced Concrete Slabs, John Wiley and Sons, New York.

Park, R. (1971). Further Test on a Reinforced Concrete Floor Designed by Limit Procedures in Cracking, Deflection and Ultimate Load of Concrete Slab Systems, ACI SP-30, American Concrete Institute, Detroit, pp. 251-269.

Park, R. (1968). Limit Design of Beams for Two-Way Reinforced Concrete Slabs, *Journal of Institution of Structure Engineers*, 46 (9): 269-274.

Phillip G. H. (1985). Limit Analysis of Rotationally Symmetric Plates and Shells, PHI, Englewood Cliffs, N.J.

Purushothaman P. (1984). Reinforced Concrete Structural Elements-Behaviour, Analysis and Design, Tata McGraw Hill Publications Co. Ltd., New Delhi.

R. Lenschow and M.A. Sozen (1967). A Yield Criterion for Reinforced Concrete Slabs, *Proc. ACI*, 64: 266-273.

Salvadori M.G. (1979). Spandrel-slab interaction, *Journal of Structural Division, ASCE*, 96 (ST1): 89-106.

Sapountzakis, E.J. and Mokos, V.G. (2008). An Improved Model for the Analysis of Plates Stiffened by Parallel Beams with Deformable Connections, *Computers & Structures*, 86: 2166-2181.

Sapountzakis, E.J. and Mokos, V.G. (2008). An Improved model for the Dynamic Analysis of Plates Stiffened by Parallel Beams, *Engineering Structures*, 30: 1720-1733.

Sawzuak J.J, Winmik C. (1965). Plastic Behavior of simply supported plates at moderately large deflections, *International Journal of Solids and Structures*, 1 (1): 97-111.

S.C. Lin and T.Y. Kam (2000). Probabilistic Failure Analysis of Transversely Loaded laminated Composite Plates Using First-Order Second Moment Method, *Journal of Engineering Mechanics*, 126 (8): 812-820.

Shukla, S. N. (1973). Handbook for Design of Slabs by Yield-line and Strip Methods, Structural Engineering Research Centre Roorkee, India, pp. 17-19.

S. H. Simmonds and S. B. Alexander (1987). Truss Model for Edge Column-Slab Connections, *ACI Struct. Journal*, 84 (4): 296-303.

S. Krenk, L. Dmkilde and O. Hayer (1993). Limit Analysis and Optimal Design of Plates with Equilibrium Elements, *Journal of Engineering Mechanics*, 120 (6): 1237-1254.

Sozon A, Siess C.P. (1963). Investigations of multipanel reinforced concrete floor slabs. Design Methods: their evolution and comparison, *Proceeding ACI*, 60: 999-1028.

Sozen, M. A. and Siess, C. P. (1963). Investigation of Multi-panel Reinforced Concrete Floor Slabs: Design Methods-Their Evolutions and Comparison', *Proc. ACI*, 60: 999-1028.

Szilard R. (1985). Theory and Analysis of Plates-Classical and Numerical Methods, PH, New York.

Tarek Ebeido and John B. Kennedy (1996). Girder Moments in Continuous Skew Composite Bridges, *Journal of Bridge Engineering*, 1 (1): 37-45.

Timoshenko, S. P., Krieger, S. W. (1959). Theory of Plates and Shells, McGraw-Hill Book Company, New Delhi, pp. 113-120.

Quintas, V. (2003). Two Main Methods for Yield Line Analysis of Slabs, *Journal of Engineering Mechanics*, 129 (2): 223-231.

Vanderbilt, M.D., Sozen, M.A., and Siess, C.P. (1969). Tests of a Modified Reinforced Concrete Two-Way Slab, *J. Struct. Div., ASCE*, 95 (ST6): 1097-1116.

Vijayarangan B. (1973). Lower bound Solution for continuous orthotropic slabs, *Journal of Structural Division, ASCE*, 99 (ST3): 443-452.

Wood, R. H. (1961). Plastic and Elastic Design of Slabs and Plates, Thames and Hudson, London.

Wust, J. and Wagner, W. (2008), "Systematic Prediction of Yield-line Configurations for Arbitrary Polygonal Plates", *Engineering Structures*, 30, 2081-2093.

W.S. Hemp (1973). Optimum Structures, Clarendon Press, Oxford.

W. H. Dilger and A. Gali (1981). Shear Reinforcement for Slabs, *Journal of Structural Division, ASCE*, 107 (ST12): 2403-2420.

Y.H.Luo, A.J.Durrani, J.P,Conte (1994). Equivalent Frame Analysis of Flat Plate Buildings For Seismic Loading, *Journal of Structural Engineering*, 120 (7): 2137-2155.

Zienkiewicz O. C. (1977). Finite Element Method, Tata McGraw Hill Publications Co. Ltd., New Delhi.

APPENDIX-A

(Moment-capacity of a skew-slab resting over rigid-edges at outer boundaries)

Consider a reinforced concrete skew slab with skew-angle (θ) failing in the global-collapse mechanism at collapse. The complete yield line pattern of the slab under the uniform area load (w) acting over its top surface at ultimate state is shown in *Figure 3B.1*. The reinforcement in the slab is placed parallel to the outer boundaries.

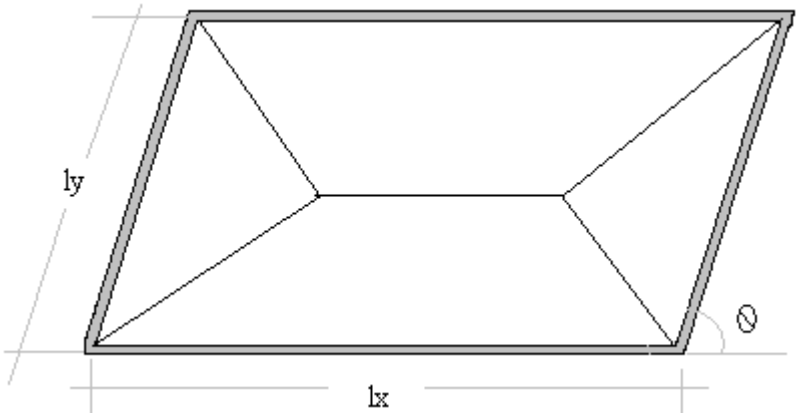

Figure 3B.1: Schematic Diagram of a Skew-Slab along with one possible Yield Line Mechanism

The work done by the uniform area load (w) can be determined by multiplying the total load acting at the center of gravity of corresponding segmental area of the collapse-mechanism by a distance moved in the direction of load due to a kinematically admissible arbitrary displacement (δ) given to the yield line pattern. The external work done by various slab segments are given below:

$$\text{Slab segment - 1} = \frac{\delta \, w \, p \, r \, l_x^2}{6} \tan\frac{\theta}{2} \sin^2\frac{\theta}{2}$$

$$\text{Slab segment - 2} = \frac{\delta \, w \, p \, r \, l_x^2}{6} \tan\frac{\theta}{2} \cos^2\frac{\theta}{2}$$

$$\text{Slab segment - 3} = \frac{\delta \, w \, p \, r \, l_x^2}{12} \tan^2\frac{\theta}{2} \sin\theta$$

$$\text{Slab segment - 4} = \frac{\delta \, w \, p \, r \, l_x^2}{12} \sin\theta$$

$$\text{Slab segment - 5} = \left(1 - p \sec^2\frac{\theta}{2}\right) \frac{\delta \, w \, l_x^2}{4} \sin\theta$$

Therefore, the total external work done, EWD by the applied load can be found by summing up the individual contribution of all collapsed segments of the slab (see *Figure 3B.1*).

$$\text{EWD} = \delta \, \text{r} \sin\theta \, \text{w} \, l_x^2 \left\{ \frac{\text{p} \tan\frac{\theta}{2}}{3\sin\theta} + \frac{1}{2} - \frac{p}{3}\sec^2\frac{\theta}{2} \right\} \qquad \text{3B.1}$$

The internal work performed by the ultimate resisting moments in slab, m_{ux} and m_{uy} at the common edges of adjoining slab segments can be obtained from the work-equation (2.12) *i.e.* $\sum m_{un}\, \theta_n\, l_o = \sum m_{ux}\, \theta_x\, l_y + \sum m_{uy}\, \theta_y\, l_x$. Therefore, total internal work done, IWD by the ultimate positive resisting moments in the slab along yield lines at the edges of all segments of the mechanism can be determined by summing their individual contribution. This is given in equation (3B.2).

$$= 2\left(m_{ux}\theta_x l_y \cos^2\frac{\theta}{2} + m_{uy}\theta_y p l_x \right) + 2\left(m_{ux}\theta_x l_y \sin^2\frac{\theta}{2} + m_{uy}\theta_y p l_x \tan^2\frac{\theta}{2} \right) + 2\left(m_{uy}\theta_y l_x \left(1 - p\sec^2\frac{\theta}{2} \right) \right)$$

$$= 2\left(m_{ux}\theta_x l_y + m_{uy}\theta_y l_x \right)$$

$$= 2\, m_{ux}\delta\, r \left\{ \frac{1}{p\tan\frac{\theta}{2}} + \frac{2\mu}{r^2 \sin\theta} \right\} \qquad \text{(3B.2)}$$

The equilibrium of the skew-slab can be ensured by equating the work done by the external loading (w) with that produced by the internal moment field (m_{ux} and m_{uy}) in the slab in moving through a small virtual kinematically admissible displacement field (δ), *i.e.* by equating equation (3B.1) with equation (3B.4).

$$\Rightarrow \quad \delta \, \text{r} \sin\theta \, \text{w} \, l_x^2 \left\{ \frac{\text{p} \tan\frac{\theta}{2}}{3\sin\theta} + \frac{1}{2} - \frac{p}{3}\sec^2\frac{\theta}{2} \right\} = 2\, m_{ux}\delta\, r \left\{ \frac{1}{p\tan\frac{\theta}{2}} + \frac{2\mu}{r^2 \sin\theta} \right\} \qquad \text{(3B.3)}$$

$$\text{or} \quad m_{ux} = \frac{\left(\frac{p}{3}\tan\frac{\theta}{2} + \frac{\sin\theta}{2} - \frac{p}{3}\sec^2\frac{\theta}{2}\sin\theta \right)}{\left(\frac{1}{p\tan\frac{\theta}{2}} + \frac{2\mu}{r^2 \sin\theta} \right)} \frac{\text{w} \, l_x^2}{2} \qquad \text{(3B.4)}$$

Equation (3B.4) can be simplified to a readily usable form, given in equation (3B.5).

$$m_{ux} = \frac{\left(3\sin\theta - 2p\tan\frac{\theta}{2}\right)}{\left(\frac{1}{p\tan\frac{\theta}{2}} + \frac{2\mu}{r^2\sin\theta}\right)} \frac{w\, l_x^2}{12} \tag{3B.5}$$

Equation (3B.5) will give the maximum value of the positive resisting moment (m_{ux}) only if $\frac{\partial m_{ux}}{\partial p} = 0$ along with negative second derivative of the moment field (m_{ux}). This condition can be achieved if

$$\frac{\frac{\partial}{\partial p}\left(3\sin\theta - 2p\tan\frac{\theta}{2}\right)}{\frac{\partial}{\partial p}\left(\frac{1}{p\tan\frac{\theta}{2}} + \frac{2\mu}{r^2\sin\theta}\right)} = \frac{\left(3\sin\theta - 2p\tan\frac{\theta}{2}\right)}{\left(\frac{1}{p\tan\frac{\theta}{2}} + \frac{2\mu}{r^2\sin\theta}\right)}$$

$$\text{or} \quad \cos^2\frac{\theta}{2}\left(\frac{1}{p}\right)^2 - \frac{2}{3}\left(\frac{1}{p}\right) + \frac{\mu\sec^2\frac{\theta}{2}}{3r^2} = 0 \tag{3B.6}$$

The p-value defining the position of branching point of yield line pattern of the slab at collapse can be calculated by solving the quadratic equation (3B.6).

$$\Rightarrow \quad p = \frac{3\cos^2\frac{\theta}{2}}{\left(1 + \sqrt{1 + \frac{3\mu}{r^2}}\right)} \tag{3B.7}$$

Therefore, the reinforced concrete slab with skew angle (θ) resting over the non yielding edges over its boundary, and subjected to the out-of-plan uniform area load (w) can be designed using equation (3B.5) and equation (3B.7) for any values of orthotropy (μ), and the slab aspect ratio, r (= l_y/l_x).

Equation (3B.7) can be used to determine the moment field in the rectangular slab by taking the skew-angle (θ) of the skew slab as 90^o. The result for a rectangular slab resting over the simple supports matches exactly with the results obtained from equation (3.7). The moment capacity (m_{ux1}) for the rectangular slab is given in equations (3B.8) and (3B.9).

$$m_{ux1} = \frac{3-2p}{\left(\frac{1}{p_1}+\frac{2\mu}{r^2}\right)}\frac{wl_x^2}{12} \tag{3B.8}$$

$$p_1 = \frac{3}{2\left(1+\sqrt{1+\frac{3\mu}{r^2}}\right)} \tag{3B.9}$$

By combining equations (3B.7) and (3B.9), the branching point of the yield line pattern of the skew-slab can be calculated from the equivalent rectangular slab [see equation (3B.10)].

$$p = p_1 \cos^2\frac{\theta}{2} \tag{3B.10}$$

The moment capacity of the skew-slab can be determined from the equivalent rectangular slab by substituting the value of the 'p' from equation (3B.10) into equation (3B.5). The final simplified expression is given in equation (3B.11).

$$m_{ux} = \frac{3-2p}{\left(\frac{1}{p_1}+\frac{2\mu}{r^2}\right)}\frac{wl_x^2}{12}\left(\sin^2\theta\right) \tag{3B.11}$$

By combining equation (3B.8) and equation (3B.11), the moment field in the skew-slab subjected to uniform area load over the whole surface can be determined from the rectangular slab under same set of loading from equation (3B.12).

$$m_{ux} = \left(\sin^2\theta\right)\mathrm{m}_{\mathrm{ux1}} \tag{3B.12}$$

While transforming the moment field of the rectangular slab (m_{ux1}) into the moment field (m_{ux}) of the equivalent skew slab, the aspect ratio (r) of both the slabs must be taken as the ratio of short span and the long span of the skew slab (l_y/l_x).

APPENDIX-B
(Design Illustration)

A typical rectangular slab-system consists of three panels in the two orthogonal directions. The spacing of beams along these two directions is 6m and 7.5m c/c each. Based upon the preliminary estimates, the columns are of size 400mm x *400mm and the beams are of size 400mm* x *550mm. The floor to floor height is 3.5m. Assume a live load of 5kN/m^2 and a finish load of 1 kN/m^2. Determine the design moments for the interior panel of the slab system and compare the results from a finite element analysis.*

Number of panels in each direction of the slab-system = 3

A slab thickness of 180mm will satisfy the deflection criterion of design code.

Therefore, total factored design load = 1.5 (5 + 1 + 0.18x25) = 15.75kN/m^2.

Long span of the slab, L_x = 18m and the short span of the slab, l_y = 7.5m.

Therefore, aspect ratio of the slab-system, r = 7.5/18.0 = 0.4167

The value of the continuity constants *viz:* i_i, i_x and i_y at outer boundary of interior panel and the internal beams are taken as 1.25, 1.333 and 0.0 respectively.

Orthotropy, μ = 1.40 for internal beam *span-depth* ratio of 13.64. [See Appendix-C]

The lower limit of the slab-parameter, A_{c1} = 5.022 [from equation (3.20)]

The upper limit of the slab-parameter, A_{c2} = 6.915 [from equation (3.24)]

The moment field induced in the slab-system is calculated from the proposed model for various values of slab-parameters (A). A comparison of the moment field induced in the slab-system is given in Table B1 against the results obtained from the Direct Design Method prescribed by various design codes and the output of a finite element based software.

Table B1: Comparison of the moment-field at various values of the plate-parameter

λ	$A = \sqrt{\lambda\left(A_{c2}^2 - A_{c1}^2\right) + A_{c1}^2}$	Moment field from design charts (kNm/m and kNm)				
		m_{ux}	m_{uy}	$-m_{ux}$	$-m_{uy}$	m_b
0.0	A_{c1}= 5.022	22.60	31.67	--	42.12	0.0
0.2	5.453	19.68	27.58	24.59	36.68	46.28
0.4	5.893	17.69	24.45	21.81	32.59	106.37
0.6	6.227	15.69	21.99	19.61	29.24	110.78
0.8	6.580	14.26	19.90	17.83	26.58	134.28
1.0	A_{c2} = 6.915	13.08	18.33	16.35	24.44	153.99
Average Moment field		17.15	23.98	21.44	31.94	110.34
Moment field (FEM)		16.47	19.46	24.83	26.57	111.44
Moment field (Direct Design Method)		16.13	19.18	22.02	25.57	128.00

It is indicated in Table B1 that the average value of the moment field in the slab-system compare favorably well with the results obtained from the finite element analysis and direct design method prescribed by the design code. However unlike finite element or design code based solutions, the proposed model gives more flexibility to the designer in

choosing the moment field by varying the value of the moment-manipulator. This would enable the designer to use reinforced concrete slabs, more judicially with a minimum possible thickness, stiffened by a set of equally spaced internal beams with adequate matching strength required for supporting a lateral load in the global-collapse mechanism mode and vice versa. The depth of these internal beams should be selected in a manner that it must satisfy the serviceability conditions of the applicable design code and the depth criterion required for the initiation of a global collapse mechanism in the slab-system.

The strength of the slab materials (reinforcement and concrete) can be utilized to its full allowable capacity by selecting an appropriate value of the slab-parameter (A). Because all design codes restricts the maximum and the minimum spacing of the reinforcement bars in the slab section; thereby, providing some inherent minimum flexural-capacity corresponding to the maximum allowable bar spacing. The designer can choose an appropriate value of the slab-parameter (A) from the valid range of the moment-manipulator ($0 < \lambda < 1$) for the design purpose corresponding to the minimum available flexural capacity of the slab-system; thereby, utilizing the strength of all reinforcement bars to its full allowable capacity, and simultaneously satisfying the detailing-clauses of the design codes.

In the present illustration, *span-depth* ratio of the internal beams along one direction is 10.91 (thereby acting as rigid beams) and along the orthogonal direction, it is 13.64 (< 15 for a continuous outer boundary), thereby producing negative yield lines in the slab along all beams. The maximum slab deflection was found to be 15.60mm and the value of the maximum crack width in the slab section was found to be 0.254mm. These two values are well within the code prescribed safe limits.

APPENDIX-C
(Charts for deciding the value of orthotropy)

The lower and the upper limit of a slab-parameter (A) is a fundamental property of any slab-system. These two limits depend upon the aspect ratio (r), number of panels (n) and orthotropy (μ) of the slab-system. The first two parameters *viz:* aspect ratio (r) and number of panels (n) of the slab-system are independent variables and are, normally, fixed by the architectural constrains in routine design practice whereas, the third parameter namely the orthotropy is a dependent variable. Its value is influenced by the aspect ratio and number of panels of the slab-system in addition to the stiffness of internal beam(s) and it should be very carefully chosen for the design purpose. A large deviation of value of the orthotropy from that required for an elastic distribution of the moment field will cause a significant cracking on tensile face of the in the slab-system. The value of the orthotropy can be taken from Chart C1 for a slab-system with $nr < 2$ and Chart C2 can be used for a slab-system with $nr \geq 2$. These charts have been developed from a parametric study conducted using a finite element based software on a large number of slab specimens by taking aspect ratio, number of panels, and beam depth as variables. However, it is suggested to take the thickness of the slab as per the guidelines prescribed in design codes to satisfy the serviceability requirements or some finite element based software should be used to check the compliance of serviceability clauses of design codes.

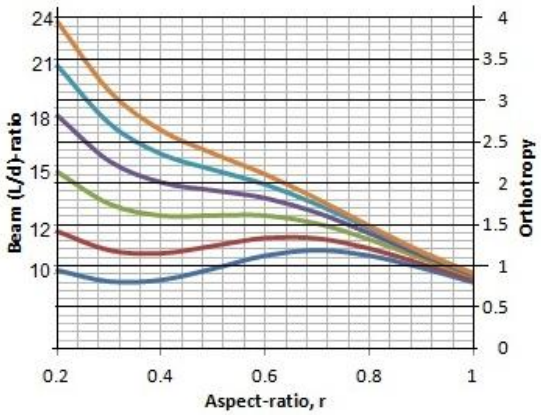

Chart C1: Orthotropy for a slab with $nr < 2$.

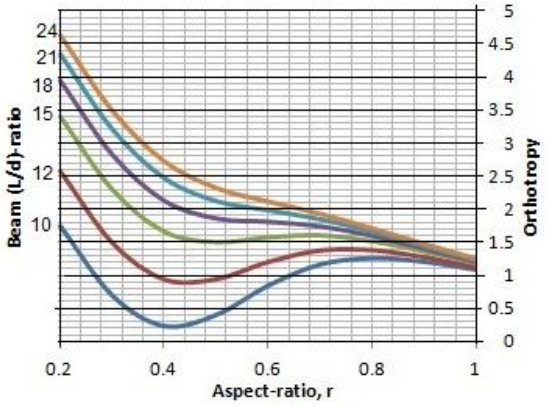

Chart C2: Orthotropy for a slab with $nr \geq 2$.

PATENT AND PUBLICATIONS

List of papers sent to various scientific journals and patent filed from the content of this research work is enumerated below:

Patent:

Patent entitled 'Shallow-Beam Supported Rectangular Reinforced Concrete Slabs' was published on 06/03/2009 in the patent journal no. 10/2009 vide application no. 18/DEL/2009. The provisional patent rights are effective from the date of publication.

Publications:

Following papers are published / accepted in various journals out of this study and some other are communicated for peer review and possible publications:

1. 'Behavior of Shallow-Beam Supported Reinforced Concrete Rectangular Slabs: Analytical and Experimental Investigations' *Advances in Structural Engineering*, Vol.13 (6), pp 1183-1198.
2. 'Prediction of Collapse Load of Three-Side Supported Reinforced Concrete Rectangular Slabs: A Simplified Approach' *Indian Concrete Journal*, Vol. 85 (7), pp 21-28.
3. 'Shallow-Beam Supported Reinforced Concrete Rectangular Slabs: An Alternate Design Procedure' *Emirate Journal of Engineering Research*, Vol.16 (1), pp 53-62.
4. "Laterally Loaded Reinforced Concrete Stiffened-Plates: Analytical Investigations" *Structural Design and Construction* (ASCE), Vol. 17 (1), pp 21-29.
5. **'**Design Charts for RC Rectangular Stiffened plates' under review in Journal *Engineering Structures*.
6. 'Energy-Balance Concept for Design of Laterally Loaded Reinforced Concrete Stiffened-Plates' under review in *ACI Journal of Structural Engineering*.